Hydrogen Bonding Cyclodiphosphazanes: Enantioselective Catalysis

Doctoral thesis

for

the award of the doctoral degree

of the Faculty of Mathematics and Natural Sciences

of the University of Cologne

submitted by

Xiaochen Wang

from Jiangsu, China

accepted in the year 2025

Table of content

0 Abstract

The present work focuses on the design, synthesis, characterization and application of new chiral cyclophosph(V)azanes as hydrogen bond catalysts. Their applications include the catalytic asymmetric Michael additions of different nucleophiles to nitroolefin. In addition, *L*-proline derivatives are explored as a potential chiral scaffold for the catalysts.

In the first part of this work, chiral diaminocyclohexan as a classical chiral scaffold for hydrogen bond catalysts was synthesized according to the literature. Subsequently, a series of six novel chiral cyclophosph(V)azanes as hydrogen bond catalysts, featuring varying amino groups and chalcogen atoms on the phosphorus atom, were designed and synthesized, with yields from 8 to 46%. The new catalysts were identified through different analysis, including ^{31}P-NMR spectrum and X-ray crystal structure.

In the second part of this work, the newly synthesized chiral cyclophosph(V)azane catalysts were employed in catalytic asymmetric Michael additions of different nucleophiles to β-nitrostyrene. After screening the catalysts and condition like solvent and temperature, catalyses of 2-hydroxy-1,4-naphthoquinone gave the bests results, with yields up to 99% and ee-s up to 90%. Among other catalytic additions which only screened the catalysts, catalyses of 4-hydroxycoumarin resulted in yields up to 64% and ee-s up to 17%, addition of Kojic acid chloride gave the yields up to 70% and ee-s up to 80%, and adduct from Meldrum's acid achieved the yields up to 76% and ee-s up to 55%. In the context of reactions involving a single novel catalyst, diethylmalonate and indole exhibited no conversion, acetylacetone yielded a 10% yield, and *N*-Boc-oxindole attained an 84% yield, while its ee-s could not be determined.

In the final part of the work, the synthesis of *L*-proline derivatives was attempted as a chiral scaffold for hydrogen bond catalysts. The 9-step synthetic route with trityl group as the protecting group was conducted, reproducing the literature method. The

desired products were successfully obtained prior to the final step, and for the Mitsunobu reaction on trityl prolinol, as the key step, the configuration of C5 was ascertained through X-ray crystal analysis, aligning with the argument from literature. Subsequently, a novel synthetic route involving the Mitsunobu reaction on methyl prolinol was implemented. The Mitsunobu reaction on methyl prolinol resulted in a ring expansion product, demonstrating the formation of an aziridinium ion intermediate by methyl prolinol. In addition, a nucleophilic attack at C1 position by azide was observed, rather than C5 as seen in trityl prolinol.

1 Introduction

1.1 Enantioselective catalysis

Asymmetric synthesis, also known as chiral synthesis or enantioselective synthesis, is a pivotal branch of organic chemistry dedicated to the controlled production of molecules with a specific chirality and has attracted global attention across the pharmaceutical industry. Chirality refers to the geometric property of molecules or ions that exists in non-superimposable mirror-image forms, even by any combination of rotations, translations, and some conformational changes, and these forms are known as enantiomers. The two enantiomers have the same chemical properties, except when reacting with other chiral compounds. In biochemistry, since a lot of receptors are chiral, enantiomers could have different behaviors in flavor,[1] odor,[2] drug effectiveness[3,4] and even drug safety.[5,6] For Example, *L*-asparagine is tasteless while *D*-asparagine is sweet (Scheme 1.1, a).[1] A more well-known example is thalidomide, whose (*R*)-enantiomer is sedative or “safe” while its (*S*)-enantiomer is teratogenic or “toxic” (Scheme 1.1, b).[7] Insufficiency in knowledge of different behaviors of the two enantiomers of this molecule causes at last one of the biggest scandals in pharmaceutical industry in the late 1950s and early 1960s, with more than 10,000 children born with a range of severe deformities.[8] Increasing demand for enantiomerically pure compounds promotes the development of asymmetric synthesis, which is a new challenge for organic chemists in the 21st century.

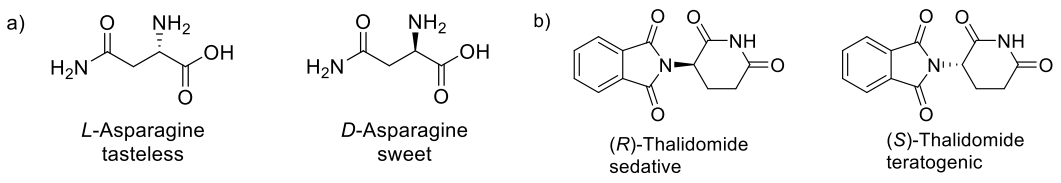

Scheme 1.1: a) The tasteless *L*-asparagine and the sweet *D*-asparagine. b) The sedative (*R*)-thalidomide and the teratogenic (*S*)-thalidomide

The history of asymmetric synthesis can be traced back to the mid-19th century, with early efforts focused on resolving racemic mixtures into their individual enantiomers.

In 1848, Louis Pasteur, considered the pioneer of asymmetric synthesis, firstly separated sodium ammonium tartrate crystals into two distinct forms, showing that they had different optical activities.[9] In 1894, Fischer proposed the lock-and-key model to explain enzyme-substrate interactions, providing a conceptual framework for understanding chirality in biological systems.[10] In early period, crystallization of diastereomeric salts relying on different physical properties of diastereomeric products is the most common method for chiral resolution.[11]

However, the true development of asymmetric synthesis as a systematic and deliberate approach began in the latter half of the 20th century. Inspired by enzymes as nature's asymmetric synthetic machinery, enantioselective catalysis began to be used to facilitate chemical reactions, not only with increasing the reaction rate by lowering the energy barrier, but also with high precision, guiding the formation of chiral products with a desired stereochemistry.[12] In 1960s, Knowles and Noyori independently developed the concept of kinetic resolution using chiral transition metal catalysts, a method to selectively produce one enantiomer from a racemic mixture by exploiting the different rates of reaction between enantiomers, and applied this conception into asymmetric hydrogenation.[13–15] Later in the 1970s and 1980s, Sharpless complemented these reduction reactions by developing a range of asymmetric oxidations.[16–18] During the same time, Corey and Trost introduced the use of chiral auxiliaries, temporary chiral entities attached to a molecule to control the stereochemistry of a reaction.[19,20] These pioneer works led the asymmetric synthesis with chiral catalysts into a golden time. Afterwards, enzymes, as natural chiral catalysts, have been more and more commonly employed for asymmetric synthesis.[21,22] In the 21st century, there has been a significant focus on the development of organocatalysis, where small organic molecules act as chiral catalysts. This has expanded the toolbox of available catalysts, providing more environmentally friendly and cost-effective alternatives.[23]

1.2 Metal–catalysis

The development of metal–catalysis has continued throughout almost the entire history of catalysis. It is evident that the late 19th and early 20th centuries constituted a pivotal era for the advancement of catalysis. The introduction of Sabatier's nickel–catalyzed hydrogenation, the development of the Haber–Bosch process utilizing an iron–based catalyst for ammonia production, and the discovery of the Ziegler–Natta catalyst based on titanium for polymerization, all played a significant role in accelerating industrial growth. The contributions of these chemists were duly recognized with the Nobel Prize.[24,25]

Since the second half of the 20th century, new metal catalysts, especially transition metal catalysts, were found to have good activities in homogeneous catalysis in different types of reactions. As previously mentioned, Noyori and co-workers have been working on metal catalyzed asymmetric hydrogenation based on kinetic resolution since 1960s. In 1987, they applied a Ru (II) catalyst with chiral BINAP in asymmetric hydrogenation of β-Keto carboxylic esters with excellent yields and ee-s, and this catalyst is known today as "Noyori catalyst" (Scheme 1.2.1).[26]

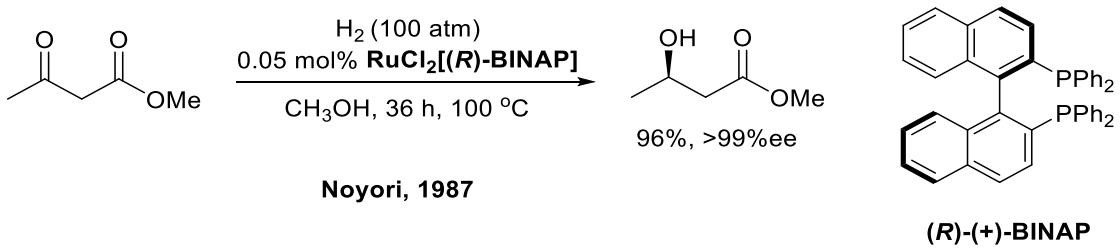

Scheme 1.2.1: Asymmetric hydrogenation of β-Keto carboxylic ester with Noyori catalyst.

Also for Ru(II), in 1992, Grubbs and colleagues commenced investigations into its potential in olefin metathesis.[27] And in 1995, they synthesized the first–generation Grubbs catalyst from $RuCl_2(PPh_3)_3$, phenyldiazomethane, and tricyclohexylphosphine in a one–pot synthesis.[28] Subsequently, they developed the second– and third–generation Grubbs catalyst, as well as the Hoveyda–Grubbs catalyst, which exhibited

enhanced activity and a broader range of applications (Scheme 1.2.2).[29–32]

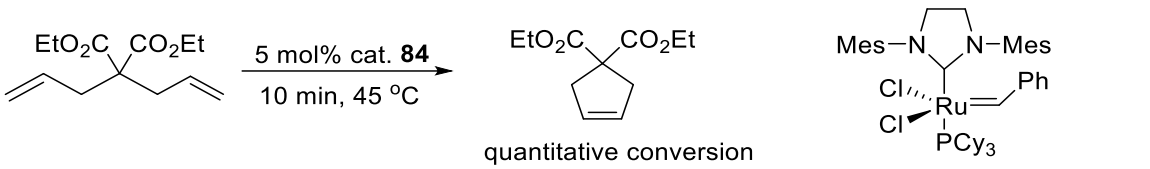

Grubbs, 1999

84
2. generation Grubbs catalyst

Scheme 1.2.2: Ring–closing metathesis with the 2. generation Grubbs catalyst **84**.

For C–C bond forming reaction, Suzuki Coupling has been a prevalent and effective variant since its initial report in 1979 (Scheme 1.2.3). The palladium–catalyzed cross coupling between organoboronic acid and halides necessitates mild reaction conditions and low catalyst loading, exhibits a broad substrate scope and has been employed in a multitude of applications, including pharmaceutical,[33,34] natural product,[35] and polymer synthesis.[36]

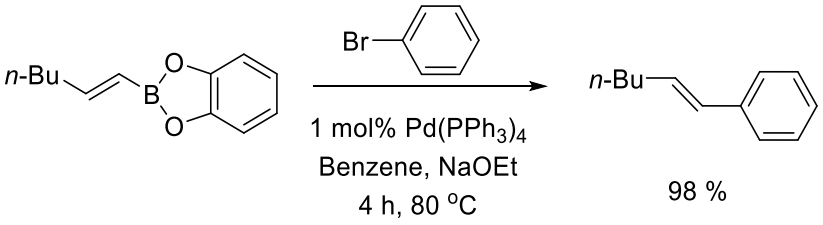

Suzuki, 1979

Scheme 1.2.3: Suzuki coupling between organoboronic acid and halides.

1.3 Organocatalysis

Despite their high efficiency, metal catalysts are frequently identified as hazardous compounds and should, therefore, be carefully eliminated from the final commercialized material. Furthermore, their disposal poses significant issues. They are often not compatible with air or moisture, and therefore require special conditions that can be very expensive and demanding to achieve in industrial plants.[37]

On the other hand, as a significant approach to bioactive compounds, particularly enantio–pure compounds, enzymes are safe for use and work splendidly in a physiological environment. However, they are expensive, do not work well under normal organic conditions of solvent, temperature, and so on, and exhibit high substrate specificity, limiting their scope.[37]

In contrast, in organocatalysis, a purely organic and metal–free small molecule is used to catalyze a chemical reaction. Therefore, they have the advantage of low cost and toxicity, ease of access, secure handling without the need for special equipment or conditions, and the countless new possibilities for modification.[38] Also there were several famous examples in the 20th century, like asymmetric addition of hydrogen cyanide to benzaldehydes catalyzed with chiral cinchona alkaloids,[39] and the Hajos–Parrish–Eder–Sauer–Wiechert reaction catalyzed with *L*-proline.[40–43] The explosive growth of this field began in 2000, with demonstration that small organic molecules can mimic the enzyme–like catalytic activity and mechanism by List,[44] and the conceptualization of the field as organocatalysis and revealed a general activation pattern, which is compatible with several organic transformations by MacMillan.[45] Following this time node, organocatalysis became a subject of increasing interest, as evidenced by the exponential growth in the number of related publications (Figure 1.3).[37] MacMillan and List were also awarded Nobel Prize in Chemistry 2021 for their contributions to asymmetric organocatalysis.

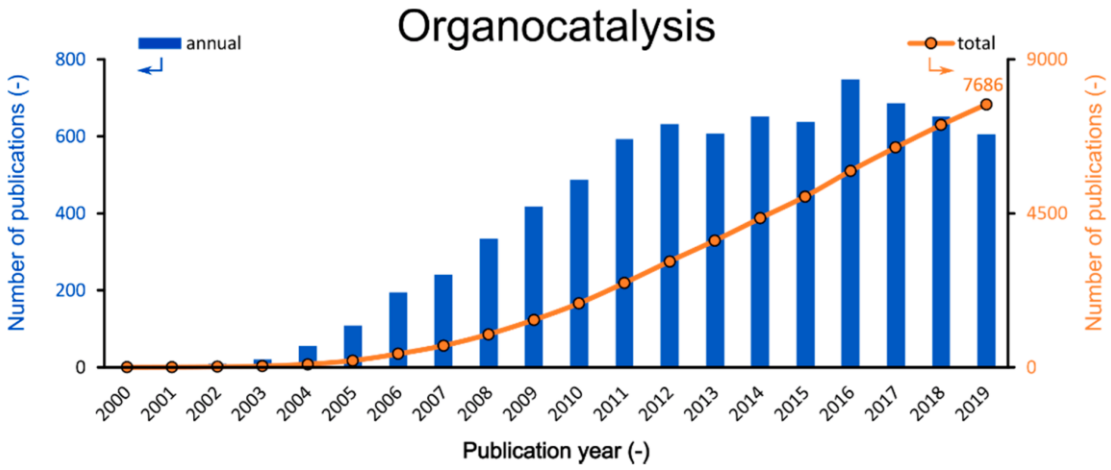

Figure 1.3: Annual (blue) and total (orange) numbers of publications related to organocatalysis.

According to the mechanistic details of individual reaction pathways, organocatalytic reactions proceed either by a much "tighter" or a much "looser" transition state than those mediated by chiral metal complexes. The former class of organocatalysts includes compounds that act as covalently bonded reagents. The latter class induces reactions via non–covalent complexes, and usually via ion pairing as dominant interactions, and encompasses interactions lower than 4 kcal mol^{-1}.[46]

1.3.1 Covalent organocatalysis

Covalent organo–catalysis, also called "primary valence catalysis" before, is a form of catalysis in which the catalyst forms a transient covalent bond with a substrate or an intermediate during the reaction process. This bond formation is crucial for the catalytic mechanism, as it helps lower the activation energy of the reaction, enabling it to proceed more efficiently.[47]

1.3.1.1 Enamine catalysis

Chiral primary or secondary amines, and amino acids have been employed as catalysts for aldol reactions, Mannich–type reactions, and other reactions that proceed through enamine intermediates. Historically, (*S*)-proline derivatives have been used in

stoichiometric asymmetric enamine chemistry since the 1960s.[48,49] These early reactions differed from subsequent catalytic reactions in that they involved the formation and isolation of enamines that were then reacted. In the early 1970s, Hajos and Parrish at Hoffmann–La Roche, and Eder, Sauer, and Wiechert at Schering independently developed a *L*-proline (**38**)–catalyzed intramolecular aldol cyclization of substituted cyclic 1,3-diones toward the corresponding aldol products in quantitative yield and 93% ee (Scheme 1.3.1.1).[40–43] Since their discovery, the scope of this type of amino acid catalysis remained largely unexplored until 2000s.

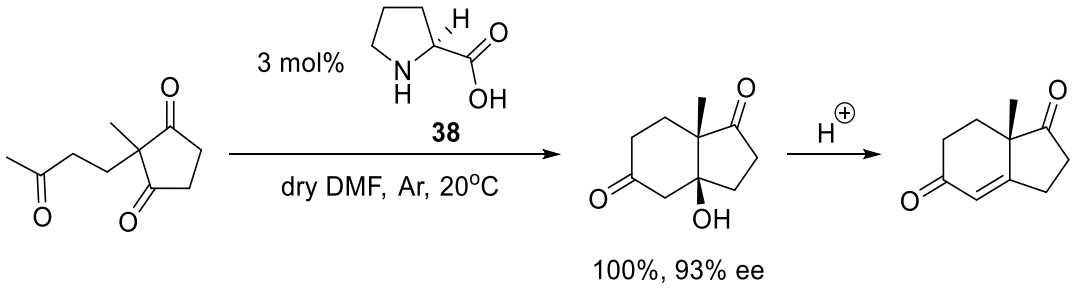

Scheme 1.3.1.1: *L*-Proline **(38)**–catalyzed asymmetric intramolecular aldol reaction and the following elimination (the Hajos–Parrish–Eder–Sauer–Wiechert Reaction).

In 2000, List, Lerner and Barbas began to view *L*-proline (**38**) as the ‘‘elusive’’ open–active site aldolase and emerged it directly in asymmetric aldol reaction between unmodified acetone and a variety of aldehydes resulting in moderate to good yields and enantioselectivities (Scheme 1.3.1.2).[44] They also proposed the reaction mechanism based on enamine formation and the observed stereoselectivity based on the Zimmerman–Traxler model favoring *Re* face approach (Scheme 1.3.1.3).[50] This is the analogous mechanism proposed by Barbas for aldolase antibodies reported by the group in 1995,[51] and in 2003, List, Houk and co-workers successfully conducted computation of the Zimmerman–Traxler six–membered ring chair–like transition state to explain the stereoselectivity of this mechanism, and this transition state began to be named as the “Houk–List transition state”.[52]

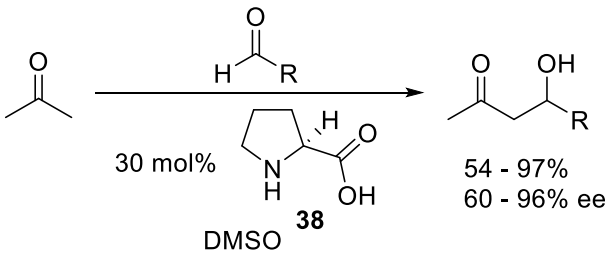

Scheme 1.3.1.2: Proline–catalyzed asymmetric intermolecular aldol reaction, discovered by List, Lerner and Barbas.

Since the discovery by List, *L*-proline has been emerged as an efficient catalyst in asymmetric aldol reactions,[53–55] Mannich reactions,[56–58] (Oxa-)Michael reactions,[59–61] α-aminations,[62–64] and α-halogenations.[65,66] Modifications on the basic proline structure have enabled the expansion of their catalytic applications, like the Enders SAMP/RAMP hydrazone–alkylation reaction,[67] and the Corey–Itsuno reduction with CBS catalyst.[68,69]

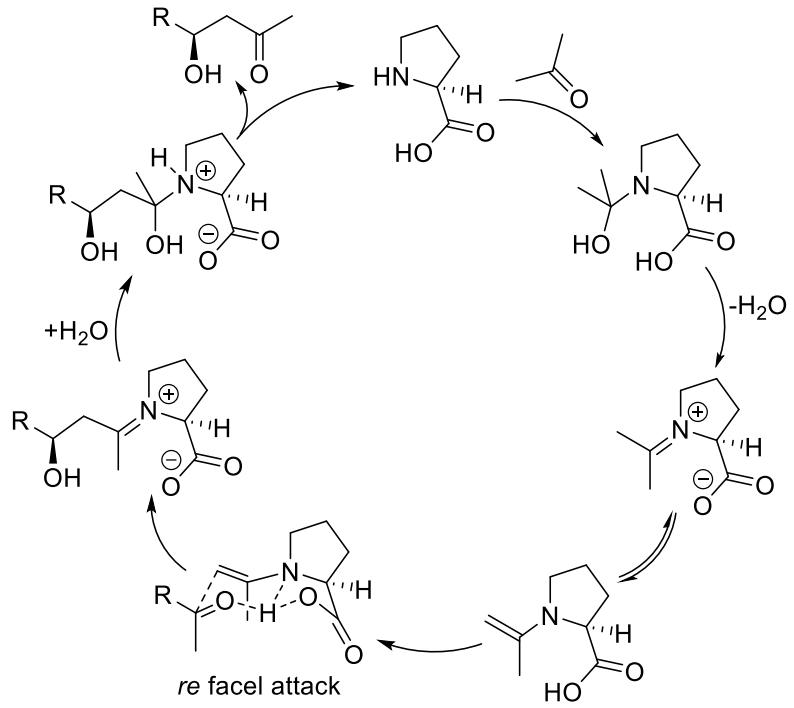

Scheme 1.3.1.3: Mechanism of *L*-proline catalyzed aldol reaction.

1.3.1.2 Iminium catalysis

The formation of iminium ions from the condensation of chiral secondary or primary amines with α,β-unsaturated aldehydes or ketones represents a good activity in a wide variety of catalytic asymmetric cycloaddition and conjugate addition reactions. In 1976, Baum and Viehe firstly discovered that the unsaturated iminium ion derived from the corresponding acetylenic amide could undergo a Diels–Alder reaction with cyclopentadiene (Scheme 1.3.1.4, a).[70] In 1989, Jung and co-workers showed that the chiral iminium ion underwent a smooth Diels–Alder reaction with cyclopentadiene, and the adduct was hydrolyzed to furnish the corresponding amide with high yields and excellent diastereomeric excess.[71] In 1993, Yamaguchi and co-workers represented that the rubidium salt of *L*-proline **85** is an efficient catalyst in asymmetric Michael addition of diisopropyl malonate to a series of α,β-unsaturated aldehydes and ketones (Scheme 1.3.1.4, b).[72] In the following year, Kawara and Taguchi described a similar Michael reaction using *L*-proline derivative as the catalyst.[73]

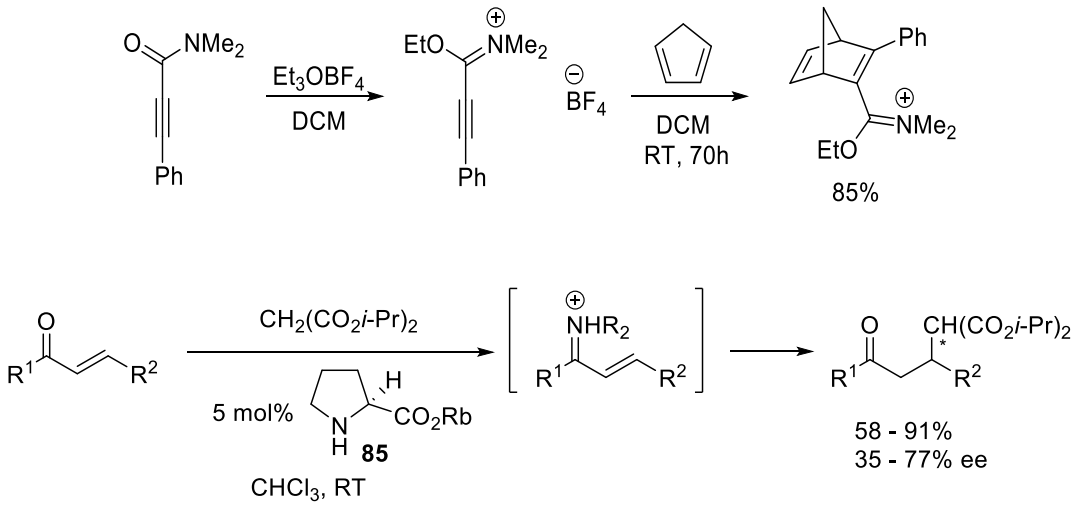

Scheme 1.3.1.4: a) Diels–Alder reaction between unsaturated iminium ion and cyclopentadiene, b) Asymmetric Michael addition of diisopropyl malonate to α,β-unsaturated aldehydes and ketones catalyzed with rubidium salt of *L*-proline **85**.

In 2000, MacMillan, Ahrendt and Borths documented that the chiral imidazolidinone **86** could catalyze the Diels–Alder reaction between α,β-unsaturated aldehydes and

dienes giving excellent yields and ee-s (Scheme 1.3.1.5, a). Based upon design features derived from the area of Lewis acid catalysis, this catalytic concept—termed iminium activation—was founded on the mechanistic postulate that: (i) LUMO–lowering activation and (ii) the kinetic lability toward ligand substitution that enables Lewis acid–catalyst turnover might also be available with a carbogenic system that exists as a rapid equilibrium between an electron–deficient and a relatively electron–rich state (Scheme 1.3.1.5, b). Indeed, they demonstrated that the reversible formation of iminium ions from α,β-unsaturated aldehydes and amines could emulate the equilibrium dynamics and p–orbital electronics that are inherent to Lewis acid catalysis. Of particular significance was the revelation that chiral amines might function as enantioselective catalysts for a diverse array of transformations that traditionally employ metal salts.

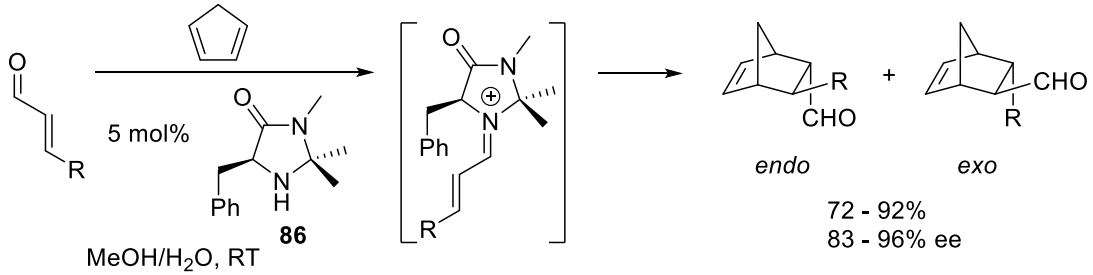

MacMillan, Ahrendt and Borths, 2000

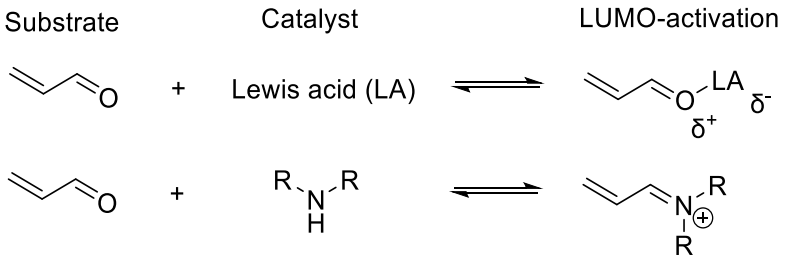

Scheme 1.3.1.5: a) Asymmetric Diels–Alder reaction catalyzed with imidazolidinone **86**, discovered by MacMillan and co-workers, b) LUMO–lowering activation by Lewis acid (LA) and formation of iminium ions.

Computational studies have identified two key stereocontrol elements: (i) the selective formation of the (*E*)-iminium isomer, which avoids nonbonding interactions between the substrate olefin and the geminal methyl substituents; and (ii) the benzyl group on

the catalyst framework, which effectively shields the *re* face of the dienophile, leaving the *si* face exposed to cycloaddition (Scheme 1.3.1.6). It is noteworthy that the catalyst exhibits high levels of organisational control with simple aldehydes, which can be attributed to the geometrical constraints that accompany the formation of the iminium ion π–bond.

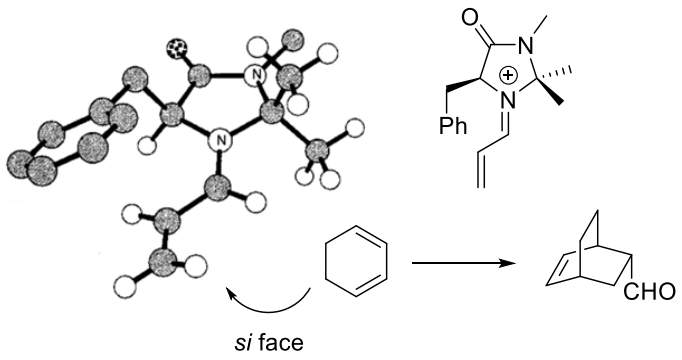

Scheme 1.3.1.6: Stereocontrol by chiral iminium ion intermediate in Diels–Alder reaction.

Since the pioneer work by MacMillan, chiral imidazolidinones were further used as organocatalysts in 1,3-dipolar cycloadditions,[74] Friedel–Crafts reactions,[75] Michael additions,[76] and Mukaiyama−Michael Reactions.[77] Other primary or secondary amine based catalysis with iminium activation modes were also explored, like the chiral diarylprolinol silyl ether based Jørgensen–Hayashi catalyst for asymmetric epoxidation,[78] and the asymmetric Michael addition with chiral *trans*-1,2-diamines based catalysts without the extra addition of strong acids by Goldfuss and co-workers.[79] Notably, in some cases, activation via either an enamine or an iminium is possible.[59]

1.3.1.3 *N*-Heterocyclic carbene (NHC) catalysis

In 1832, Wöhler and Liebig first reported the cyanide–catalyzed coupling of benzaldehyde that became known as the ‘‘benzoin condensation’’.[80] In 1943, Ukai and co-workers first demonstrated that thiazolium salts also surprisingly catalyze the

benzoin condensation, since their original expectation was the addition of thiazolium salt and aldehyde, as an analogue of the addition of pyridinium salt and aldehyde.[81] Later, in 1954, Mizuhara and co-workers recognized that the thiamine (vitamin B_1 (**87**)) –catalyzed decarboxylation of pyruvate and the thiazolium–salt–catalyzed benzoin reaction were chemically similar, as both involved a polarity reversal (umpolung) at the carbonyl center to form an “acyl anion equivalent” (Scheme 1.3.1.7).[82]

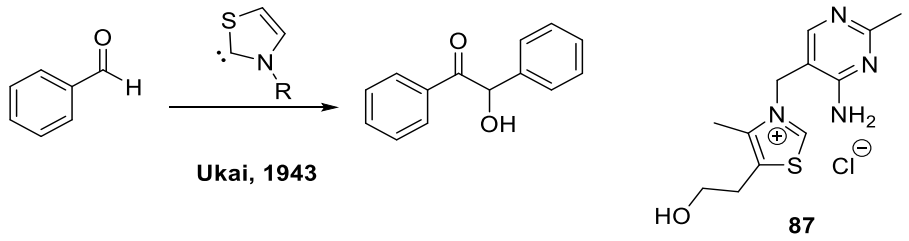

Scheme 1.3.1.7: a) Thiazolium salt catalyzed benzoin condensation, b) Thiamine (vitamin B_1 (**87**)).

In 1958, Ronald Breslow put forth the mechanistic model, postulating that the catalytically active species was thiazolin-2-ylidene, a carbene that would be formed in situ by deprotonation of the thiazolium salt. The resulting heterocyclic carbene couples with an aromatic aldehyde to generate the "active aldehyde," the hydroxy-enamine "Breslow intermediate". This nucleophilic acylation reagent reacts with an electrophilic substrate, such as a second aldehyde molecule, to form the product benzoin, simultaneously regenerating the carbene catalyst (Scheme 1.3.1.8).[83] In 1991, Arduengo and co-workers reported the remarkable isolation of an adamantly–substituted free NHC, which marked the advent of the field now known as NHC–organocatalysis.[84]

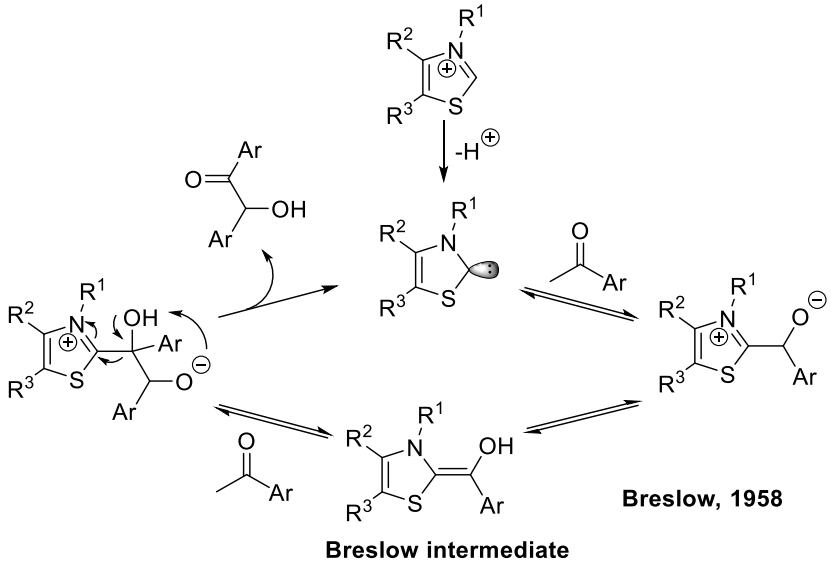

Scheme 1.3.1.8: The catalytic cycle of the NHC catalyzed benzoin condensation including Breslow intermediate, as proposed by Breslow.

In 1976, Stetter successfully investigated the 1,4-addition of aldehydes to α,β-unsaturated carbonyl compounds (Michael acceptors) by activating the aldehyde with thiazolium salt **88** to the Breslow intermediate, known as the "Stetter reaction" (Scheme 1.3.1.9). Notably, as a competing pathway, benzoin condensation is fully reversible and therefore does not interfere with 1,4-adduct formation.[85]

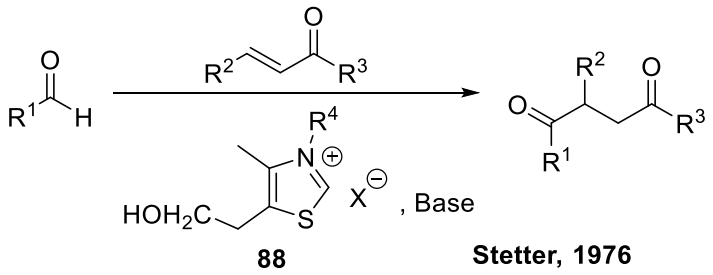

Scheme 1.3.1.9: 1,4-addition of aldehydes to α, β-unsaturated carbonyl compounds catalyzed with thiazolium salt, known as the "Stetter reaction".

In 1995, Enders, Teles and co-workers synthesised triazole–derived NHC scaffolds **89** as the first stable, commercially available NHC catalyst, which could remain stable at temperatures up to 150°C in the absence of air and moisture,[86] and they were later emerged in condensation of formaldehyde to glycolaldehyde (Scheme 1.3.1.10, a).[87]

Simultaneously, they also reported the use of chiral triazolium salts such as compound **90** for the asymmetric benzoin reaction (Scheme 1.3.1.10, b).[88]

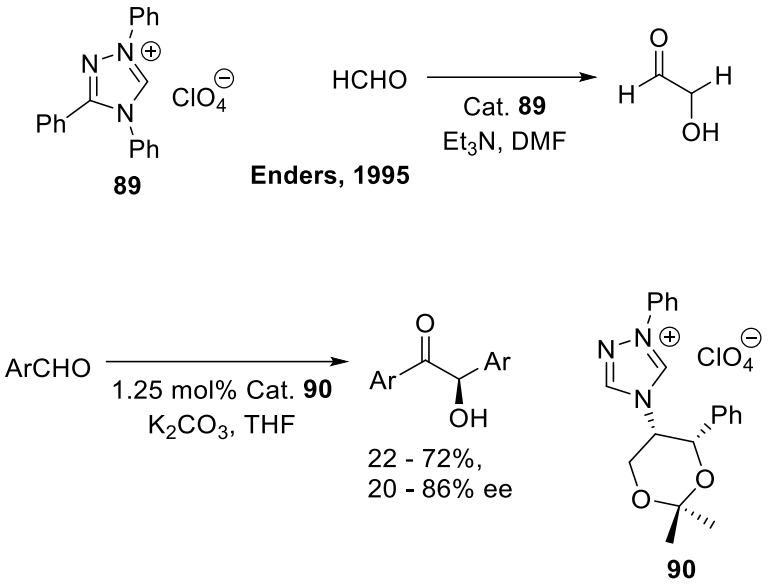

Scheme 1.3.1.10: a) The first stable, commercially available triazole–derived NHC catalyst **89** reported by Enders, Teles and co-workers, emerged in condensation of formaldehyde to glycolaldehyde, b) Chiral triazolium salt **90** for the asymmetric benzoin reaction.

In light of these pioneering studies, further aspects of NHC catalysis have been investigated. These include the noval chiral NHC catalysts based on bicyclic thiazolium salts by Leeper and co-workers[89], the aminoindanol derivatives by Rovis and co-workers,[90] and the newly transferred umpolung based reactivity to the β-position of α,β-unsaturated aldehydes by the Bode and Glorius groups independently.[91,92] In addition, a non–umpolung mode of NHC reactivity was demonstrated by Hein and co-workers,[93] which involves the oxidation of the Breslow intermediate to generate an acylazolium species, thereby maintaining (and in fact, enhancing) the electrophilic character at the carbonyl centre.

1.3.2 Non–covalent organocatalysis

Non–covalent organo–catalysis is a type of catalysis in which the catalyst facilitates a reaction without forming any permanent covalent bonds with the substrate or the reaction intermediate. Instead, the catalyst relies on non–covalent interactions, such as hydrogen bonds, ionic interactions, van der Waals forces, and hydrophobic interactions, to lower the activation energy of the reaction and stabilize reaction intermediates.[47]

1.3.2.1 Asymmetric ion–pairing catalysis

Asymmetric ion–pairing catalysis represents a specific form that occurs with charged intermediates or charged reagents. Notably, the borders between ion pairing and other interactions are not clearly delineated, and other interactions can be overlaid with ion pairing. In Brønsted acid catalysis, for example, some authors may exclude ion pair formation by proton transfer as a form of ion–pairing catalysis, while the Coulombic attraction within the ion pairs may be accompanied by further stabilizing interactions, such as hydrogen bonding, as long as the ionic character of the intermediate does not become negligible.[94]

In one variant of this process, ion–pairing occurs with a charged and chiral catalyst, wherein the charged catalyst can be either cationic or anionic. In early stage, such kind of asymmetric catalysis has been realized in enantioselective phase–transfer catalysis, which is well–established for reactions proceeding via anionic intermediates accompanied by a chiral cation who controls the enantioselectivity. Important chiral cation scaffolds are quaternary ammonium cations and quaternary phosphonium cations.[95] A pioneering study was conducted by a research group at Merck in 1984. Dolling and co-workers employed the cinchonine–derived quaternary ammonium salt **91** as a catalyst for the methylation of a phenylindanone derivative under liquid–liquid phase–transfer conditions (toluene/50% aq. NaOH solution) (Scheme 1.3.2.1). This

resulted in the successful production of the corresponding alkylated product, with an excellent yield and high enantiomeric excess.[96]

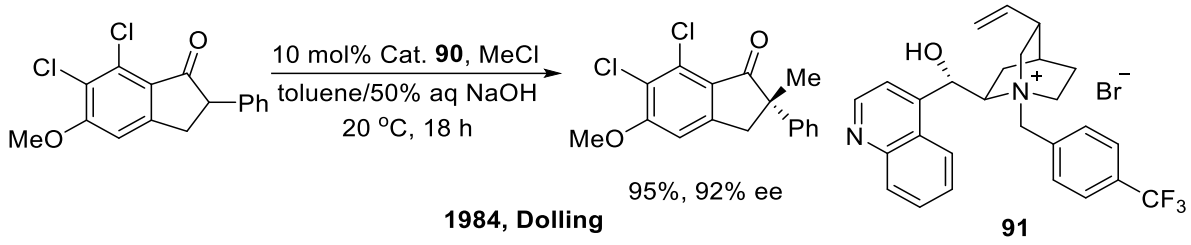

Scheme 1.3.2.1. Methylation of a phenylindanone derivative with the cinchonine–derived quaternary ammonium salt **91** as a catalyst.

In comparison to the early realized efficient asymmetric catalytic transformations involving anionic intermediates with chiral, cationic catalysts, analogous versions of inverse polarity, namely Asymmetric Counteranion–Directed Catalysis (ACDC), have not been achieved with reasonable enantioselectivity until the discovery by List and co-workers. In 2006, they reported the synthesis of a catalytic organic salt comprising an achiral ammonium cation and a chiral phosphate counteranion (TRIP), which catalyzes transfer hydrogenations of aromatic and aliphatic α,β-unsaturated aldehydes with remarkably high enantioselectivities (Scheme 1.3.2.2).[97]

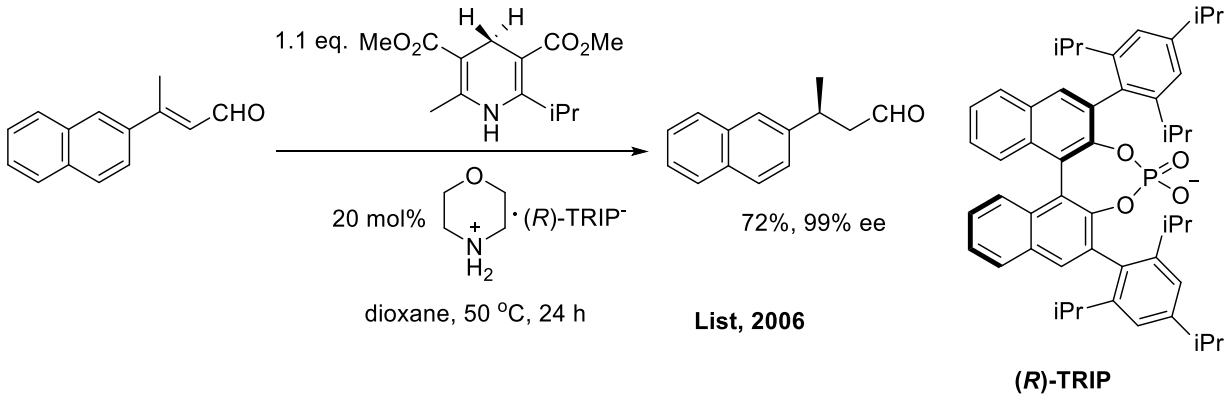

Scheme 1.3.2.2. Asymmetric transfer hydrogenations of α,β-unsaturated aldehydes catalyzed with a salt comprising an achiral ammonium cation and a chiral phosphate counteranion (**TRIP**).

Except for ion–pairing with a charged, chiral catalyst, as previously mentioned,

another asymmetric ion–pairing catalysis approach exists: the noncovalent binding of a chiral, neutral catalyst to the intermediate ion pair.[98] In 2004, based on the bonding activities of ureas and thioureas towards halide–anions, Jacobsen and Taylor discovered that chiral thioureas catalyze the cyclization of indoles onto *N*-acyliminium ions generated in situ by the acylation of imines and this thiourea–catalyzed acyl–Pictet–Spengler reaction is a powerful method for the synthesis of alkaloids.[99] Subsequently, in 2008, asymmetric thiourea–catalyzed addition of silyl ketene acetals to 1-chloroisochromans was achieved, with yields of 70 – 95% and enantioselectivities of 74 – 95% (Scheme 1.3.2.3).[100]

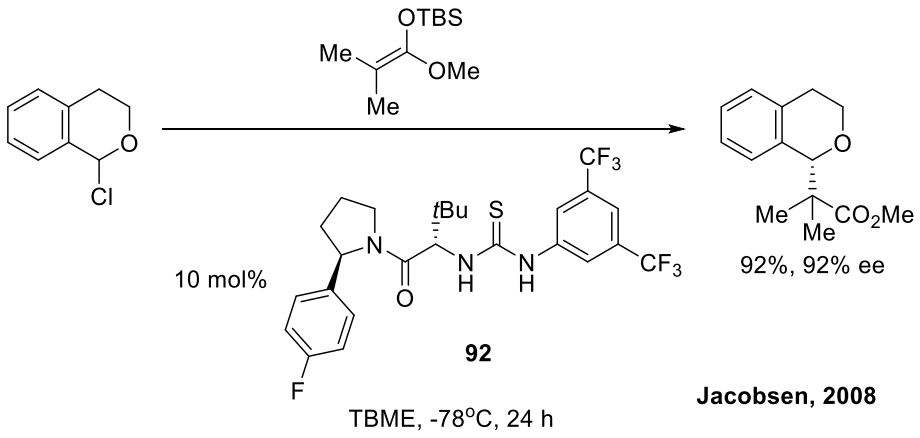

Scheme 1.3.2.3: Asymmetric addition of silyl ketene acetals to 1-chloroisochromans catalyzed with a chiral and neutral thiourea derivative **92**.

In addition to the aforementioned examples, asymmetric ion–pairing catalysis is also employed in a variety of reactions. These include the use of chiral crown ethers as asymmetric phase–transfer catalysts for enantioselective Michael additions,[101] the chiral quaternary phosphonium cations to induce enantioselective Michael and Mannich reactions,[102] and the chiral *N*-triflyl phosphoramide catalyzed asymmetric Diels–Alder reactions.[103]

1.3.2.2 Hydrogen bond catalysis

1.3.2.2.1 Background of hydrogen bonding

The early observations of hydrogen bond (abbreviated as H–bond) dates back to the 19th century. The concept came from the observations of various scientists such as Faraday, Nernst, Lewis and Pauling studying the properties of water and other compounds.[104] A review in 2002 from Steiner gave the H–Bond an appropriate definition:

"An X–H···A interaction is called a 'hydrogen bond', if 1. It constitutes a local bond, and 2. X–H acts as a proton donor to A."[105]

Jeffrey classified the strength of hydrogen bonds as "strong", "moderate", and "weak", primarily determined by geometric parameters.[106] Strong hydrogen bonds are typically described as "mostly covalent" with bond lengths of H···A between 1.2 – 1.5 Å and bond angles of 175 – 180°. Moderate hydrogen bonds are described as "mostly electrostatic", with bond lengths ranging from 1.5 to 2.2 Å and bond angles between 130 and 180°. Weak hydrogen bonds, on the other hand, are described as "electrostatic", with bond lengths ranging from 2.2 to 3.2 Å and bond angles between 90 and 150°. The energies of these bonds can range from 40 kcal/mol for strong bonds to less than 4 kcal/mol for weak hydrogen bonds.[106] According to Morokuma and Stein, the constituent interactions towards the total energy of a hydrogen bond(E_{tot}) could be divided into contributions from electrostatics (E_{el}), polarization (E_{pol}), charge transfer (E_{ct}), dispersion (E_{disp}), and exchange repulsion (E_{er}).[107,108] The constituents' distance and angular characteristics differ significantly. The electrostatic term is directional and has a long range, while the other terms are mainly acting short range roles.[108] The dispersion and exchange repulsion terms are commonly combined into an isotropic "van der Waals" contribution, which is approximately described by the well–known Lennard–Jones potential.[109] In most cases, E_{el} is the dominating term, especially at long distances, and the van der Waals contribution can also not to be ignored. Thus, purely electrostatic and van der Waals models can be

successful for hydrogen bonds of weak to intermediate strengths, despite their simplicity.[110]

1.3.2.2.2 Developments thiourea catalysts

In 1984, Hine and co-workers firstly discovered that 1,8-biphenylenediol could form the cocrystal with phosphoramide, pyridone and pyrone derivative via bidentate H–bonds (Scheme 1.3.2.4, a).[111] Afterwards, since 1988, Etter and co-workers showed that electron–poor diaryl ureas can form double H–bonds and be cocrystallized with a wide range of Lewis bases and was then widely invested in the area of molecular recognition due to their strong hydrogen bonding activity (Scheme 1.3.2.4, b).[112–114] Notably, only the ureas with *meta*-substituted EWGs form the cocrystal, but the effect is neither steric, since $–CF_3$ work but $–CH_3$ do not, nor resonance, since *ortho*- and *para*-substituted EWGs do not induce cocrystal formation but *meta*-substituted EWGs do. Thus, a weak intramolecular hydrogen bond between the weakly acidic *ortho*-C–H protons and the carbonyl oxygen nearby was figured out as a possible factor of forming the cocrystal. Geometry of the cocrystals, including torsion angles of phenyl rings, the H---O distances and the C–H---O angles also trended to prove the existence of such intramolecular hydrogen bond.[112]

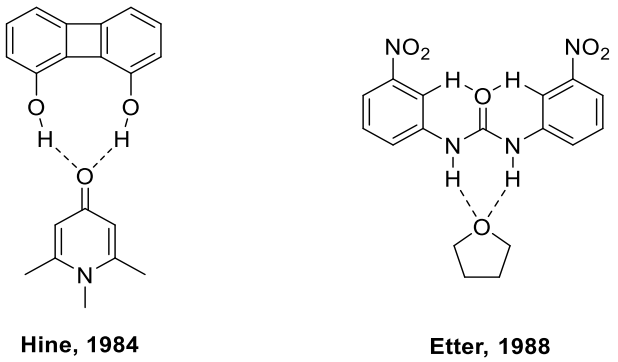

Scheme 1.3.2.4. Cocrystal of a) 1,8-biphenylenediol with 1,2,6-trimethyl-4-pyridone as guest[111] and b) bis-(3-(NO_2)-phenyl)-urea with THF as guest.[112]

The discovery of molecular recognition by hydrogen bond donors inspired people to

explore more applications by their activating effect. In 1990, Kelly and co-workers showed that acidic biphenylenediol **93** could accelerate Diels–Alder reactions by forming complexes with α,β-unsaturated aldehydes as Diels–Alder dienophiles (Scheme 1.3.2.5, a).[115] In 1994, Curran and co-workers firstly designed the electron-poor diaryl urea catalyst **94** and applied it to radical allylations of sulfoxides, with a significant stereoselectivity (Scheme 1.3.2.5, b).[116]

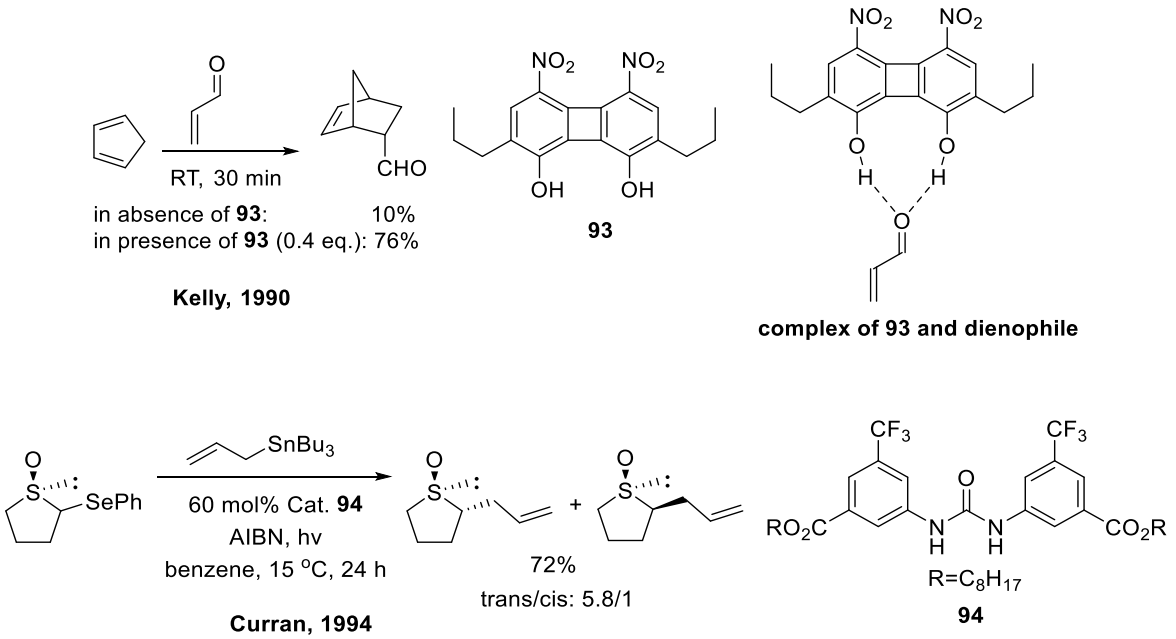

Scheme 1.3.2.5. a) Activation of Diels–Alder reaction by biphenylenediol **93**. b) Diastereoselective allylation of cyclic sulfinyl radicals catalyzed with diaryl urea **94**.

In 1998, Jacobsen firstly reported the enantioselective Strecker reactions catalyzed with thiourea Schiff bases such as **95** (Scheme 1.3.2.6).[117]

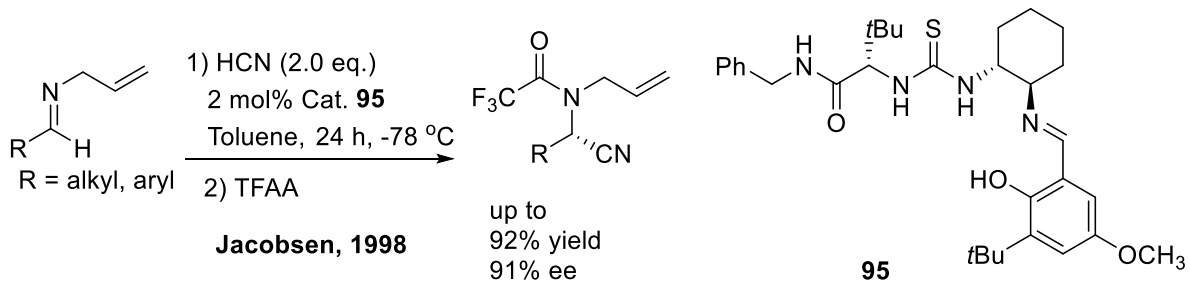

Scheme 1.3.2.6. Enantioselective Strecker reactions catalyzed with thiourea Schiff base **95**.[117]

The Jacobsen's thiourea catalyst was originally designed as a potential Schiff base ligand for Lewis acidic metals. However, the highest enantioselectivity was observed in the absence of metal additives. The following research such as structural modification, NMR, kinetic, and computational studies proved that (Thio)ureas bearing chiral Schiff bases are sufficient to activate the substrate.[118–120]

Since 2002, Schreiner and co-workers reported that they synthesized thioureas with different substituents and applied them to Diels–Alder reactions between cyclopentadiene and different vinyl ketones.[121,122] Among these, the variant with 3,5-bis(trifluoromethyl)phenyl **96** has the best catalytic activity, and is known today as "Schreiner's catalyst" (Scheme 1.3.2.7).

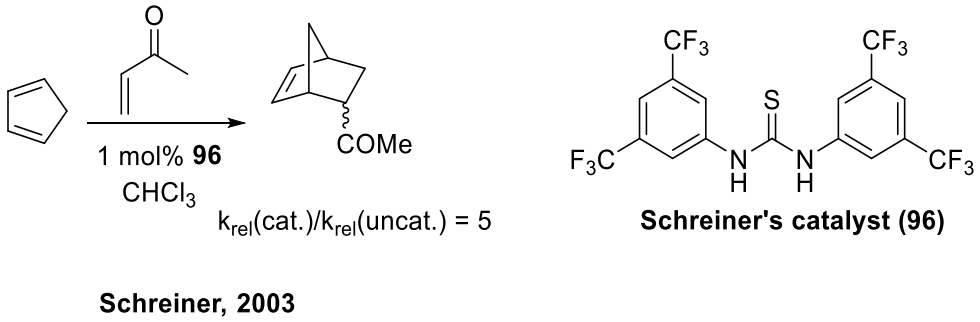

Scheme 1.3.2.7. Diels–Alder reaction catalyzed with Schreiner's catalyst **96**.

The combination of NMR, IR, and ab initio techniques reveals the structural similarities between an exemplary H–bonded complex of an *N*-acyloxazolidinone with an *N*,*N*′-disubstituted electron–poor thiourea and the corresponding Lewis acid complex. Despite the lower H–bond association constant compared to the Lewis acid adduct, Diels−Alder reactions are accelerated and stereochemically altered in a similar fashion to weak Lewis acids.[121] Thioureas are generally stronger hydrogen bond donors than ureas due to the more positive charge of their amino groups.[123] According to quantum chemical analysis, this counterintuitive phenomenon is not explainable by the relative electronegativities of O and S, but rather results from the effective steric size of the chalcogen atoms.[124] Comparable to Etter's results,[112] 3,5-bis(trifluoromethyl)phenyl on thiourea result in the best catalytic activity. In aspect of

electronegativity, the two trifluoromethyl groups on *meta* position as electron–withdrawing groups enhance the acidity of the N–H. In aspect of rigidity, the hydrogen atoms in the *ortho* position are more positively polarized due to the electron–withdrawing groups. These C–H bonds have a small hydrogen bond donor ability, leading to internal interactions between the Lewis–basic sulfur and the *ortho* hydrogen atoms. This interaction hinders the rotation of the phenyl groups, reducing the flexibility of the catalyst, thus minimizing the entropic penalty upon complexation.[122]

Although the Jacobsen's thiourea catalyst is already the pioneer of chiral organo–bifunctional catalysts, their uses are still limited in enantioselective, nucleophilic additions of HCN and ketene silyl acetals to imines.[117–120] As proved by Schreiner, thioureas bearing 3,5-bis(trifluoromethyl)phenyl substitutents possess an efficient activating effect on hydrogen bond acceptors.[121,122] Inspired from these, in 2003, Takemoto and co-workers designed the bifunctional thiourea catalyst **37** combined with 3,5-bis(trifluoromethyl)phenyl and the basic (*R*,*R*)-1,2-cyclohexyldiamine as a chiral scaffold, which is known today as "Takemoto's catalyst", and was successfully employed in enantioselective Michael additions of malonates to nitroolefins (Scheme 1.3.2.8).[125]

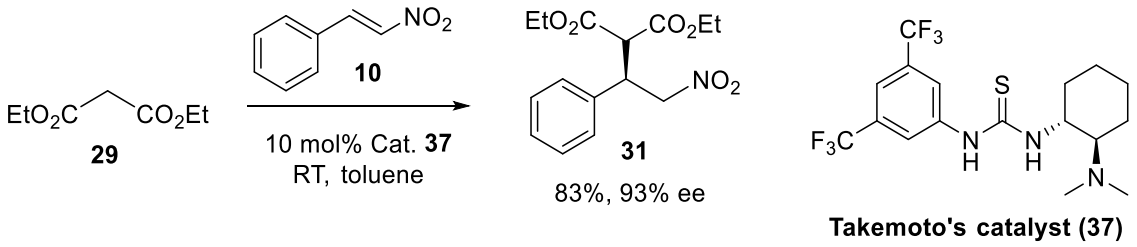

Scheme 1.3.2.8. Enantioselective Michael addition of diethyl malonate to β-nitrostyrene with Takemoto's catalyst **37**.

Since the discovery of the Takemoto's catalyst, various thiourea–based catalysts bearing chiral frameworks have been developed for various synthetically useful enantioselective organic transformations. Examples of these are: Nagasawa's bisthiourea catalyst for Baylis–Hillman reactions,[126] Ricci's chiral thiourea with

additional hydroxy group for Friedel–Crafts alkylations,[127] Soós' thiourea with cinchona alkaloid for the addition of nitroalkanes to chalcones,[128] Berkessel's isophorone diamine–derived bisthiourea catalysts for Morita–Baylis–Hillman reactions,[129] Jacobsen's diphenylphosphinocyclohexane–derived thiourea for imine–allene [3+2] cycloadditions,[130] and Yuan's BINOL–containing thiourea for petasis reactions.[131] Notably, most of these catalysts utilize 3,5-bis(trifluoromethyl)phenyl (Scheme 1.3.2.9).

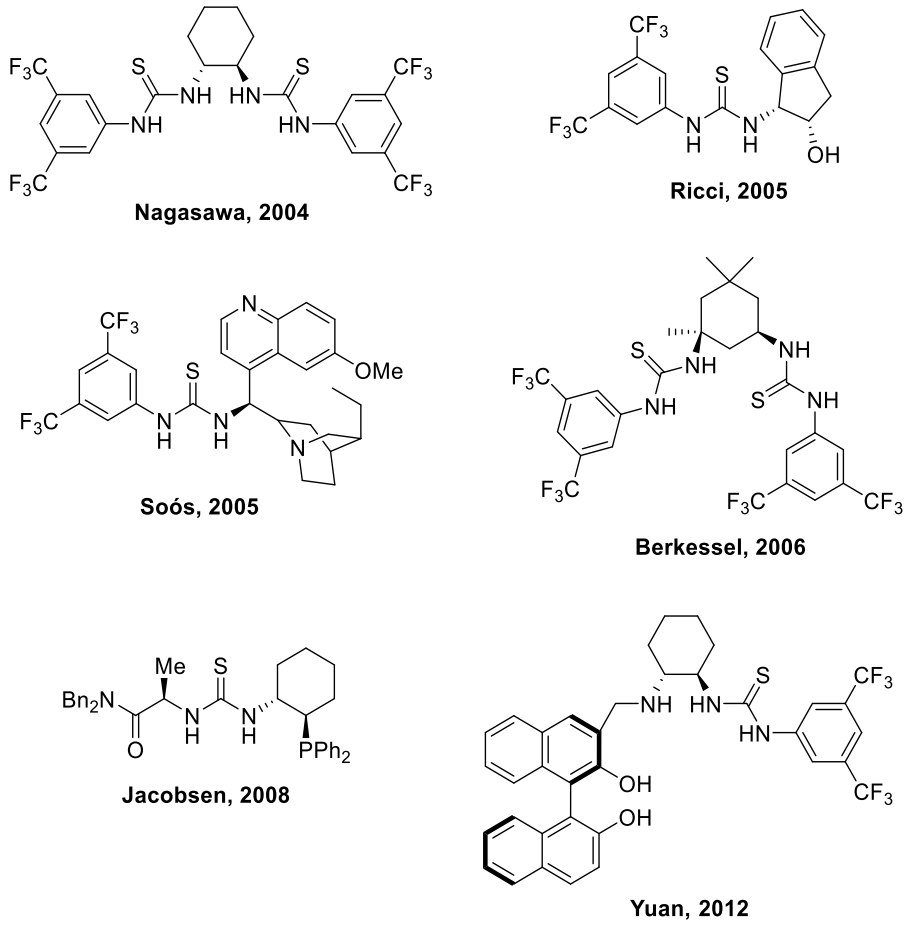

Scheme 1.3.2.9. Various thiourea–based organocatalysts.

1.3.2.2.3 Squaramide catalyst

In 2008, Rawal and co-workers were able to establish another important bidentate structural motif in asymmetric hydrogen bond catalysis: the squaramides derived from

Cinchona alkaloids **97** catalyzes the conjugate addition of acetylacetone (**31**) to β-nitrostyrene (**10**) with excellent yields and enantioselectivities at extremely low catalyst loading (Scheme 1.3.2.10).[132]

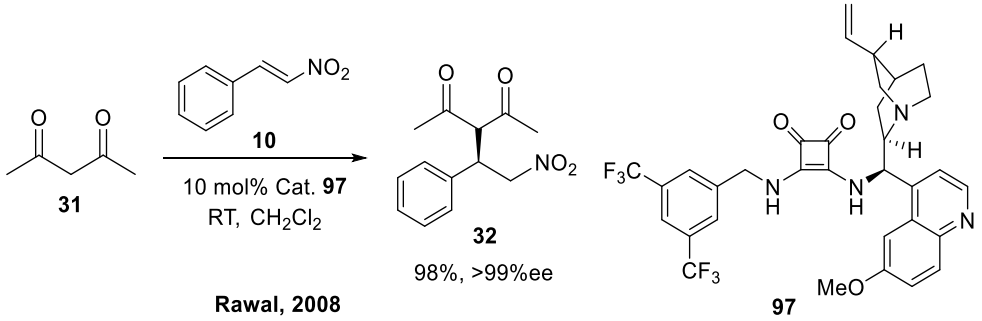

Scheme 1.3.2.10. Enantioselective Michael addition of 2,4-pentanedione to β-nitrostyrene with squaramide catalyst **97**.

Squaramides have emerged as an effective alternative to the (thio)urea catalysts. However, compared to ureas and thioureas, squaramido functionality differs significantly.[133] Firstly, compared with (thio)urea, squaramide shows stronger duality and participates more readily in ditopic binding, and also represents a stronger hydrogen bond acceptor, because of the "increase of the aromatic character" in the four–membered ring upon complexation. Secondly, in both (thio)urea and squaramide, the nitrogen lone pair delocalizes through the carbon–oxygen double bond, but only in squaramides further delocalization can occur through the partially aromatic cyclobutenedione system, thereby restricting the rotation of the C–N bond.[134,135] Thirdly, there is significant difference between thioureas and squaramides in the relative distance between the two NH groups. According to the calculation by Takemoto and Rawal groups,[132,136] the distances for *N*,*N'*-dimethylthiourea and *N*,*N'*-dimethylsquaramidel are approximately 2.13 Å and approximately 2.72 Å, respectively. Fourthly, the "square geometric" structure of the cyclobutenedione ring in squaramides also induces a convergent orientation of the NH groups, canting each by approximately 6°.[132] But such convergent property doesn't appear in the amido/thioamido groups of urea/thiourea. Fifthly, the pK_a values of squaramides are generally lower than those of their thiourea analogues, resulting in a pK_a gap of 0.13–

1.97 units. This difference in acidity suggests that squaramides form stronger hydrogen bonds than their thiourea counterparts, although the magnitude of the pK_a gap sharply depends on the parent structure.[123,137,138]

Following the discovery of Chiral squardamide catalysts in asymmetric Michael additions, they have been widely applied in various of organocatalytic reactions such as the enantioselective aza-Friedel−Crafts reaction of cyclic trifluoromethyl ketimine and naphthol (Scheme 1.3.2.11, a),[139] the kinetic resolution of oxazinones (Scheme 1.3.2.11, b),[140] and the enantioselective Mannich reaction of rhodanines to isatin–derived ketimines (Scheme 1.3.2.11, c).[141]

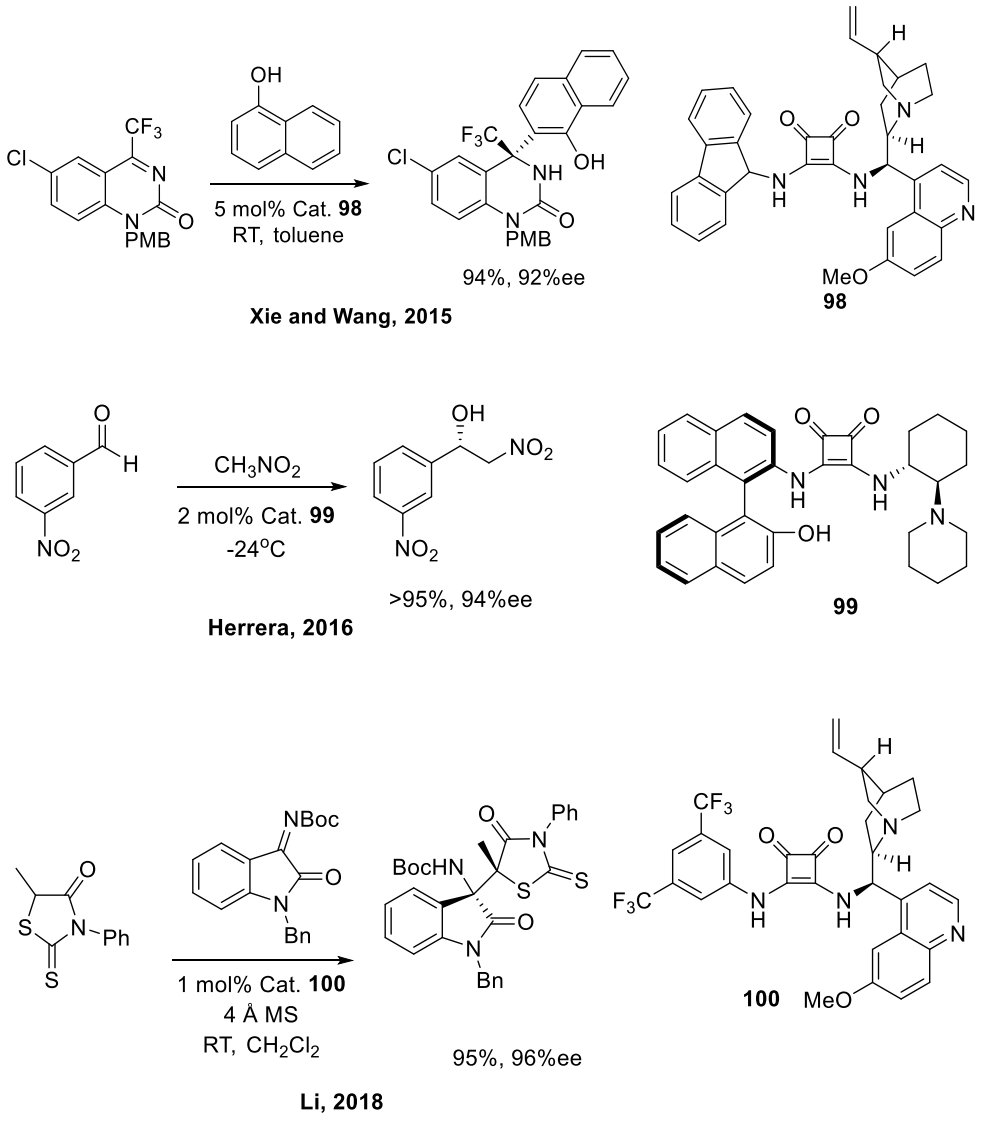

Scheme 1.3.2.11. Various squaramide–based organocatalysts of a) **98**; b) **99** c) **100**.

1.3.2.2.4 (Thio)phosphoric (tri-)amide catalyst

Classic Hydrogen bond motifs like thioureas and squaramides bring success as well as limitation like relatively weak activity and decomposition at a slightly high temperature for thiourea, and incompatible with basic functionality due to increased acidity for guanidinium, quinolinium thioamide, and ammonium. To explore the new neutral alternative, in 2009, Shea and co-workers synthesized sulfamide **101**, phosphoric triamide **102**, and thiophosphoric triamide **103** as candidates for HB catalysts. The compounds demonstrate significant hydrogen bonding in their solid state. Each of the three compound forms demonstrated activity as HB catalysts. Furthermore, the thiophosphoric triamide catalyst **103** showed modest improvements (2.6–fold) in selected Friedel–Crafts reaction when compared to the corresponding thiourea catalyst **96** (Scheme 1.3.2.12, a).[142] In 2013, Nagorny and co-workers combined a Brønsted acid as the catalyst and a hydrogen bond donor as the co-catalyst to catalyze a variety of ionic [2+4] cycloaddition reactions under mild reaction conditions instead of using a highly ionic medium. Remarkably, the thiophosphoramide **103**, which has not been previously utilized for the anion binding, was found to be superior to the standard two–hydrogen bond donors such as thiourea or squaramide (Scheme 1.3.2.12, b).[143]

The (thio)phosphoric triamide motifs combined with chiral scaffolds also present powerful efficiency in asymmetric catalysis. In 2010, Zhou and co-workers screened an asymmetric Strecker reaction of ketimines with TMSCN using different bifunctional catalysts, and their newly developed bifunctional cinchona alkaloid–based phosphinamide catalyst **105** turned out to be the most enantioselective variant (Scheme 1.3.2.12, c).[144] In 2011, Tang and co-workers synthesized the (thio)phosphoric amides bearing (1*R*,2*R*)-*N*,*N*-dimethylcyclohexane-1,2-diamine **106**, and applied them in asymmetric Michael addition of 2-hydroxy-1,4-naphthoquione to nitroolefins, affording the corresponding adducts in high yields with excellent level of enantioselectivities (Scheme 1.3.2.12, d).[145]

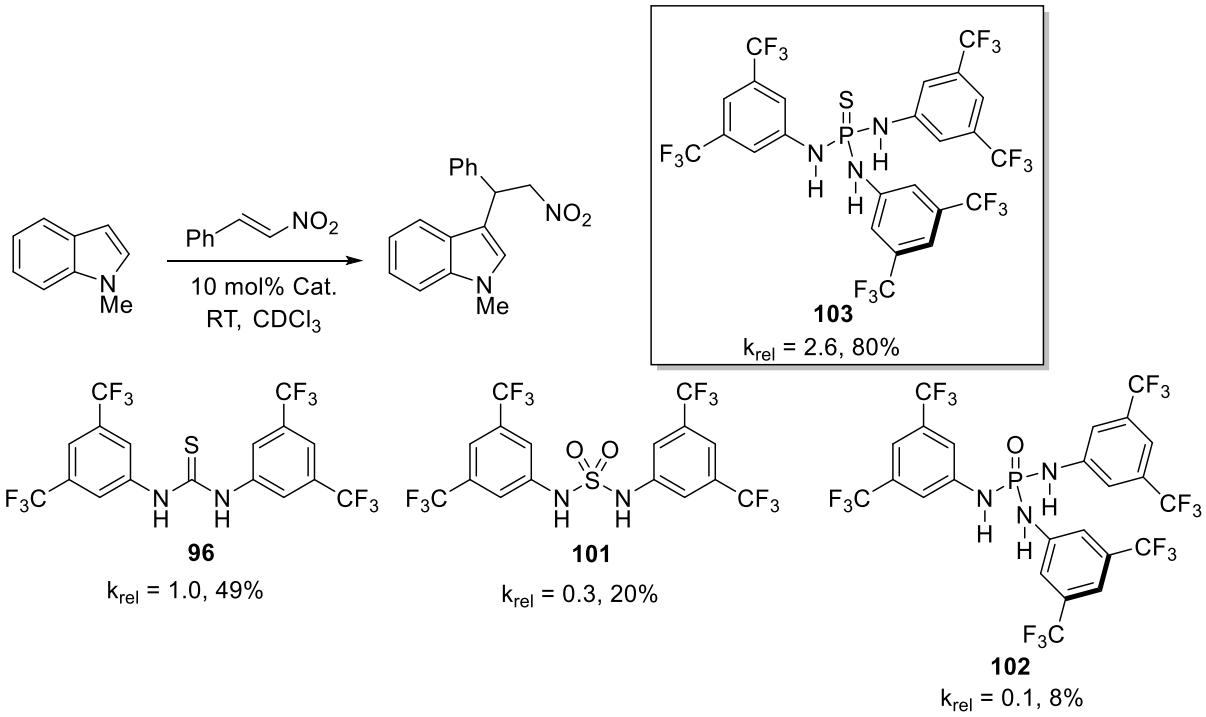

Shea, 2009

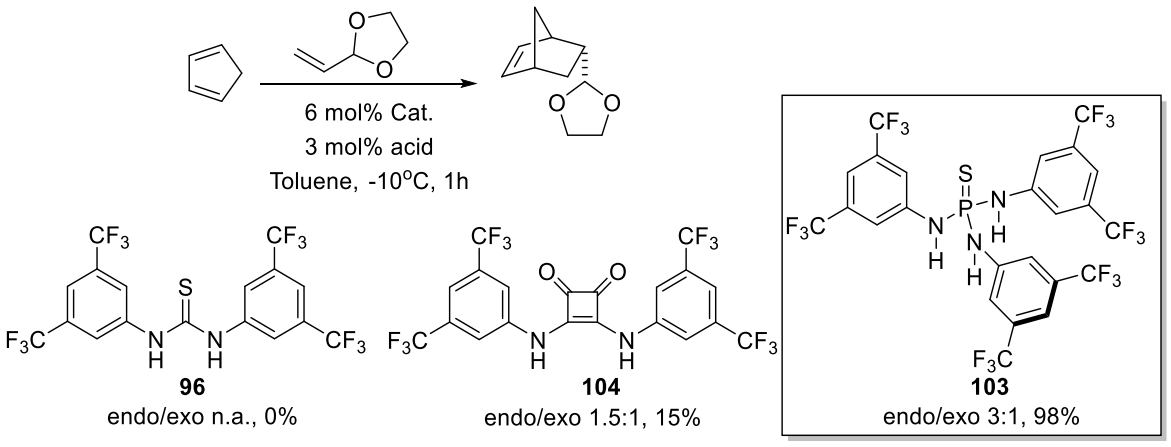

Nagorny, 2013

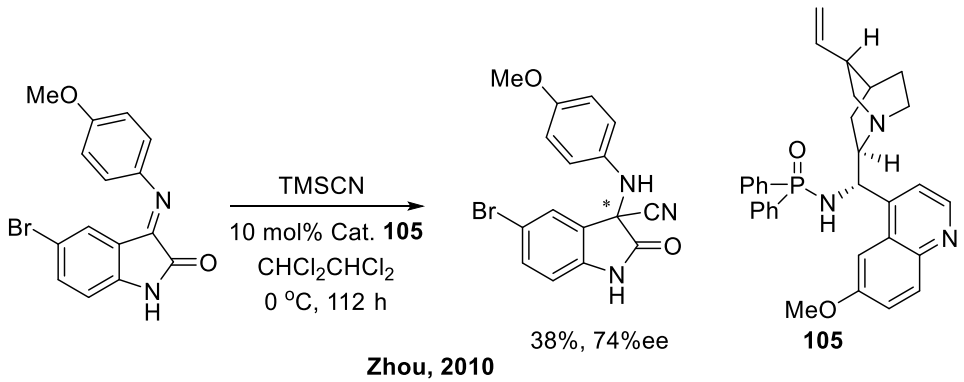

Zhou, 2010

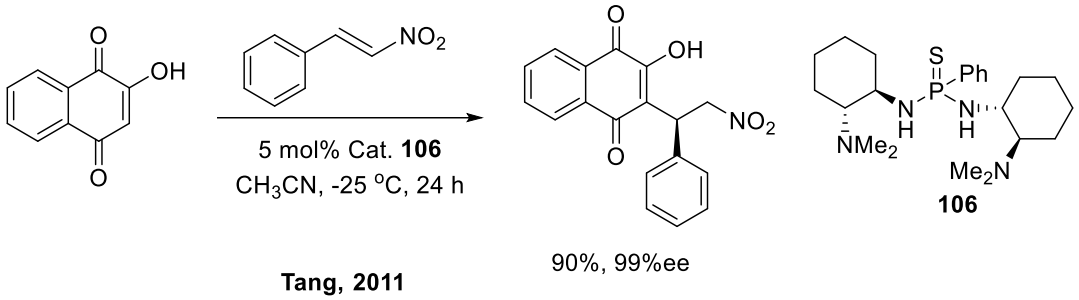

Scheme 1.3.2.12. a) Catalyst comparison for the Friedel–Crafts reaction of *N*-methyl indole with β-nitrostyrene. b) Evaluation of HBD–based cocatalysts of the ionic [2+4] cycloaddition of acrolein acetal and cyclopentadiene. c) Asymmetric Strecker reaction of ketimines with TMSCN with phosphinamide catalyst **105**. d) Asymmetric Michael addition of 2-hydroxy-1,4-naphthoquione to β-nitrostyrene with phosphinamide catalyst **106**.

1.3.2.3 Halogen–bond–based organocatalysis

Halogens, which belong to the 17th group and consist of electronegative elements, exhibit exceptional nucleophilic properties in their anionic state. However, as they transition into a diatomic state through the formation of covalent bonds with more electronegative atoms, this nucleophilicity diminishes. Consequently, an electron–deficient or electrophilic region, known as a σ-hole, emerges.[146] Pioneer theoretical studies were conducted by Politzer and Murray in the 1990s.[147,148] Following this, there was a notable increase in interest in halogen bonds(XB), and in 2013, the International Union for Pure and Applied Chemistry (IUPAC) published a comprehensive introduction to intermolecular interactions involving halogens as electrophilic species.[149] In 2021, the existence of the σ-hole was demonstrated through experiment using Kelvin probe force microscopy, providing tangible evidence for this theory.[150]

In 2008, Bolm and co-workers were the first to propose that halogen bonding interactions play a role in the reduction of quinoline derivatives in the presence of

perfluoroalkyl iodides.[151] In 2011, Huber and co-workers demonstrated the efficacy of achiral cationic and neutral XB–based activating reagents such as **107** in activating benzhydryl bromide in the Ritter reaction through halide abstraction (Scheme 1.3.2.13).[152] The research demonstrated the ability of XB–donor scaffolds to activate the benzhydryl bromide substrate, resulting in the subsequent release of the bromide anion. Notably, this is a stoichiometric reaction since the activation involves both transient (nonstationary) and nontransient halogen bonding.[153]

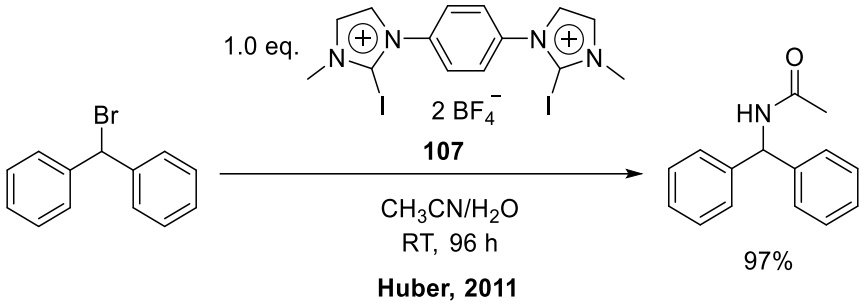

Scheme 1.3.2.13: Reactions of benzhydryl bromide with XB–based activating reagents such as **107** in wet CH_3CN reported by Huber and co-workers.

In 2013, Huber and co-workers discovered the first XB–catalyzed halide abstraction with a silyl enol ether and 1-chloroisochromane as substrate. The reaction resulted in yields up to 91% in the presence of 10 mol% of the neutral multidentate XB donors.[154] 2 years later, in 2015, they observed that preorganisation of the cationic bidentate XB donor **108** significantly enhances the catalytic activity (Scheme 1.3.2.14). Consequently, the *syn*-isomer of **5$^{n\text{-Oct}}$/OTf** could even be used with a loading as low as 0.5 mol%, producing good yields of the isolated product.[155]

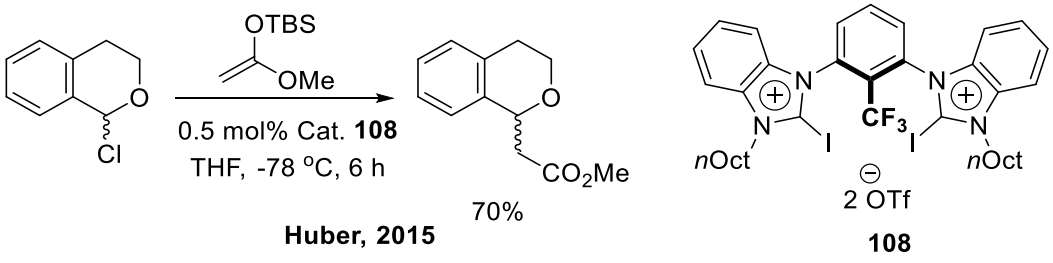

Scheme 1.3.2.14. XB–catalyzed halide abstraction with a silyl enol ether and 1-chloroisochromane.

In 2014, Kee, Tan, and co-workers reported halogenated pentanidiums **109** as phase–transfer catalysts for the asymmetric alkylation of sulfenateanions to various sulfoxides with high enantioselectivities (Scheme 1.3.2.15). Computational studies have proposed the involvement of multiple non–covalent interactions, including halogen bonding, in this process.[156]

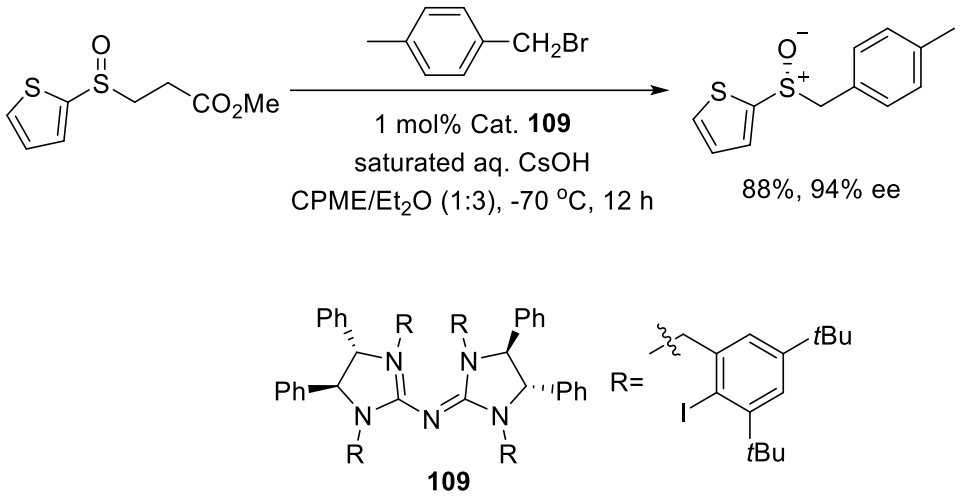

Scheme 1.3.2.15: Asymmetric alkylation of 2-thienyl sulfenate anion catalyzed with iodo-pentanidium **109**.

Subsequently, other XB–based catalysis was discovered, such as the direct dehydroxylative coupling reaction of alcohols with organosilanes,[157] (aza)-Diels–Alder reactions,[158,159] and Michael additions.[160] In addition to the activation through σ-hole, XB catalysis can also be achieved through π−activation.[161]

1.4 Cyclodiphosphazane

1.4.1 Synthesis and characterization

The word phosphoazene refers to the wide variety of molecules containing nitrogen and phosphorus atoms linked by alternating saturated and unsaturated bonds in their backbones, forming either cyclic rings or linear chains.[162] The synthesis of the first

cyclophosphazane, namely hexachlorocyclotriphosphazene, was reported in 1832 by Liebig and co-workers.[163,164] As another major class of the cyclic phosphazane compounds, cyclodiphosphazane, a saturated 4–membered P_2N_2 ring structure, was firstly synthesized in 1894 by Michaelis and Schroeter.[165] Dichlorocyclodiphosphazanes, *cis*-[ClP(μ-NR)]$_2$, are important precursors for the synthesis of a variety of cyclodiphosphazane derivatives through nucleophilic substitutions at the phosphorus atoms (Scheme 1.4.1).[166]

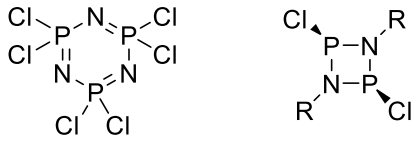

Scheme 1.4.1. hexachlorocyclotriphosphazene and dichlorocyclodiphosphazane.

The conventional method for preparing dichlorocyclodiphosph(III)azane involves the reaction of PCl_3 with primary amines (RNH_2) or with amine hydrochlorides (RNH_3Cl) (Scheme 1.4.2). The formation of different types of cyclophosphazanes is controlled by the stoichiometry, and reaction conditions to a certain extent, but primarily depends on the choice of the primary amine employed in the reaction. The formation of cyclic tetramers and trimers is observed with methyl- and ethylamines, whereas the formation of cyclic dimers, *cis*-[ClP(μ-NR)]$_2$, and, to some extent, monomeric compounds, such as aminobis(phosphanes), is observed exclusively with more sterically demanding primary amines such as $tBuNH_2$ and $ArNH_2$.[167]

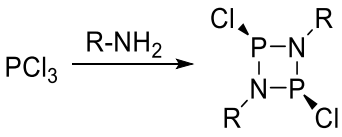

Scheme 1.4.2. Synthesis of dichlorocyclodiphosph(III)azanes from primary amines and PCl_3.

The preference for *cis*/*trans*-isomers does not follow the expected trends based on steric or electronegativity factors. Therefore, it is challenging to predict the outcome. However, there is a clear trend in the ring conformations of these isomers. *Trans*-

isomers exhibit planar or nearly planar $(P–N)_2$ rings, while *cis*-isomers display puckered rings. Keat and co-workers suggested that the source of the puckering is the lone–pair repulsion on adjacent phosphorus and nitrogen atoms, which is decreased for pyramidalized imino-nitrogen atoms.[168] A more recent research showed that for very large ring–substituents, steric effects alone may determine the molecular configuration, and the energy differences between *cis*/*trans*-isomers were small.[169] Despite this complexity, Norman and co-workers summarized a set of empirical rules, which could be simplified as: 1) 2,4-Dihalocyclodiphosph(III)azanes are always *cis*, irrespective of the imino-substituents; 2) 1,3-Diaryl-2,4-bis(amino)cyclodiphosph(III)azanes have the *cis*-geometry as long as at least one of the P-substituents is a primary amine; 3) 1,3-Dialkyl-2,4-bis(amino)cyclodiphosph(III)azanes always exhibit the *cis*-geometry.[170,171]

The first characterization of cyclodiphosphazane dates from 1960s,[172,173] and in 1971 its crystal structure was firstly determined.[174] For dichlorocyclodiphosphazane, chlorine atoms could be substituted with amino groups using either two equivalents of acidic amines, like pyrazoles and aniline, and two equivalents of triethylamine, or with two equivalents of the corresponding lithium amide, affording bis(amino)cyclodiphosph(III)azanes (Scheme 1.4.3).[171]

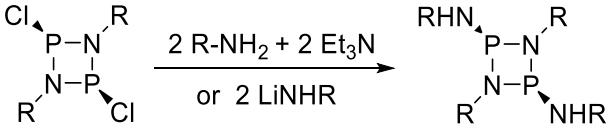

Scheme 1.4.3. Substitution of dichlorocyclodiphosphazane with different nucleophiles.

Although the formation of the ring with phosphorus(V) compounds like $P(X)Cl_3$ or $P(X)(NHR)_3$ (X=O or S) is a more conventional synthetic route,[175–179] it has a good chance of forming the mixture of *trans*- and *cis*-isomers.[180] In contrary, as is summarized, bis(amino)cyclodiphosph(III)azanes bearing alkyl−groups remain in a *cis*-configuation, and could be then oxidized to bis(amino)cyclodiphosph(V)azanes with dimethyl sulphoxide, elemental oxygen, sulfur, selenium, tellurium, alkyl halides

and azides (Scheme 1.4.4).[166,181–184]

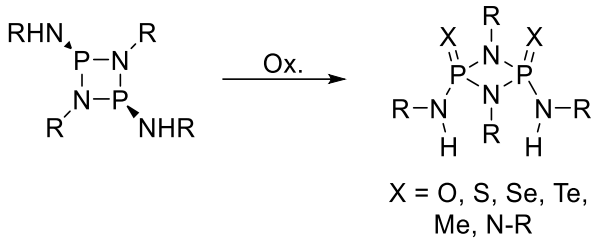

Scheme 1.4.4. Oxidation of bis(amino)cyclodiphosph(III)azanes bearing alkyl−groups.

1.4.2 Cyclodiphosphazane in catalysis

As excellent chelating bis(amide) ligands towards both main group[185–190] and transition elements,[191–193] cyclodiphosph(III)azanes such as **110** are employed for metal catalysis like Polymerization of ethylene (Scheme 1.4.5).[194–198] The catalyst behavior depends on the steric demands of the ligand substituents, and the nature and size of the amido substituents exert a profound influence on the catalytic activity of the investigated metal complexes, as well as on the polymer properties.

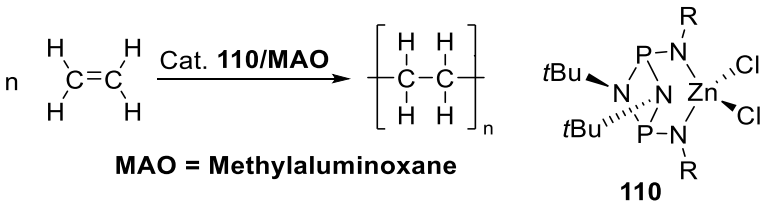

Scheme 1.4.5. Polymerization of ethylene with cyclodiphosph(III)azane **110** as ligand.

Also, for asymmetric catalysis, cyclodiphosph(III)azanes containing chiral R groups are able to act as a perfect chiral ligand for Mori–Tamaru nickel/gold–catalyzed coupling of 1,3-dienes and aldehydes (Scheme 1.4.6).[199] The enantioselectivity is highly dependent on the steric demand of both the bridging scaffold and the amido group on the *ansa*−bridged chiral cyclodiphosph(III)azane ligands such as **111**, and

ee-s up to 84% could be achieved. However, this is the only example for cyclodiphosph(III)azanes acting as a chiral ligand.

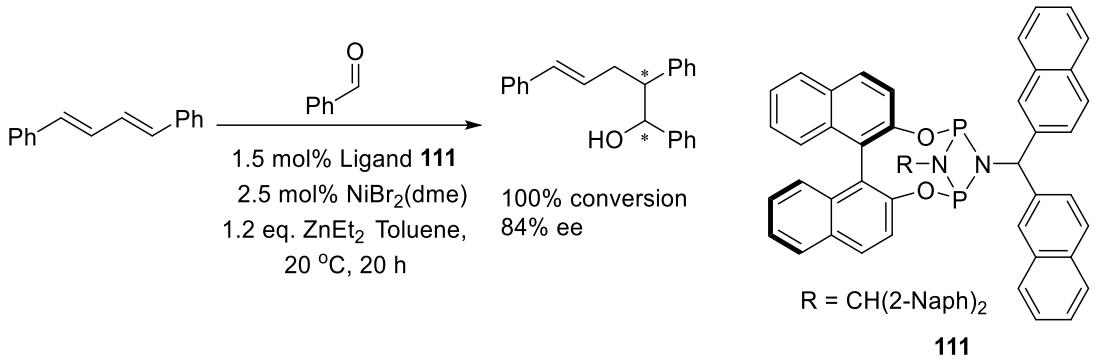

Scheme 1.4.6. Asymmetric catalytic coupling of 1,3-dienes and aldehydes with cyclodiphosph(III)azane **111** as ligand.

Recently, our group explored di-amino substituted cyclodiphosph(V)azanes as hydrogen bond donors and employed them in enantioselective hydrogen bonding catalysis of asymmetric Michael additions (Scheme 1.4.7, a),[180] anion recognition,[200] and counter–ion catalysis of *N*-acyl-Mannich couplings (Scheme 1.4.7, b).[201] The successful results demonstrated that cyclodiphosph(V)azanes are competitive to bidentate anion binding motifs such as (thio)urea and squaramide.

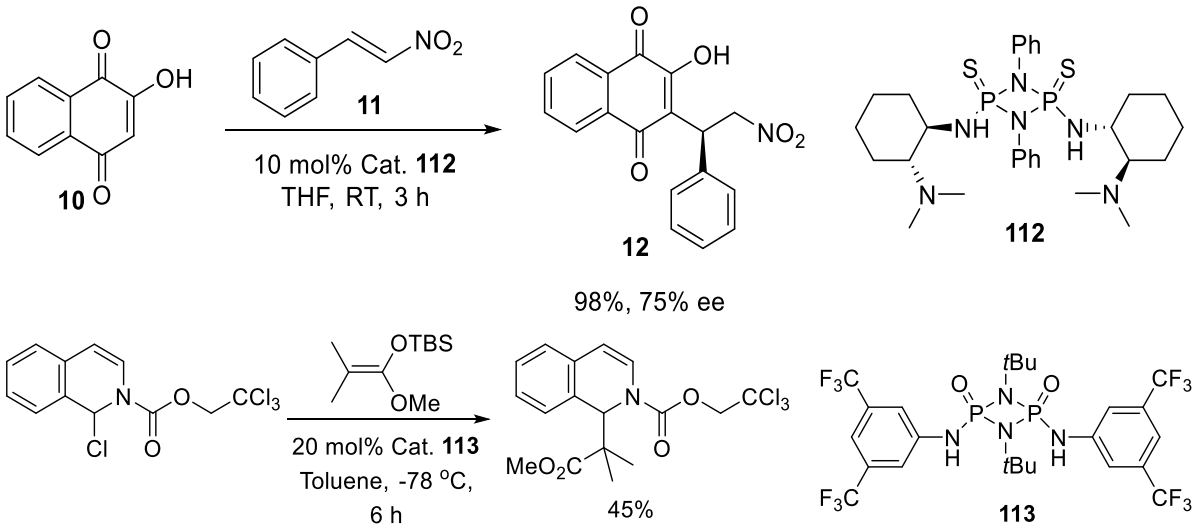

Scheme 1.4.7: a) Asymmetric Michael addition of 2-hydroxy-1,4-naphthoquione to β-nitrostyrene with cyclodiphosph(V)azanes such as **112** as hydrogen bond catalyst. b) Catalyzes of *N*-acyl-Mannich couplings of silyl ketene acetal with cyclodiphosph(V)azanes such as **113** as counter−ion catalyst.

1.5 Michael addition and mechanism

Michael addition is a reaction between a Michael donor (an enolate or other nucleophile) and a Michael acceptor (typically an α,β-unsaturated carbonyl) that results in the formation of a Michael adduct through the creation of a carbon–carbon bond at the acceptor's β-carbon (Scheme 1.5.1). Since their initial discovery by Komnenos in 1883[202] and the subsequent pioneering works of Michael in 1887,[203] the conjugate addition reaction has been the subject of extensive study and has become an invaluable method in organic chemistry for the synthesis of carbon–carbon bonds,[204,205] including many diastereoselective and enantioselective variants.[206,207]

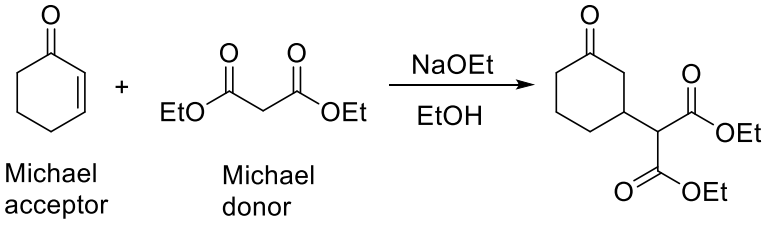

Scheme 1.5.1. Typical Michael addition including a Michael acceptor and a Michael donor.

In terms of the mechanism, the Michael donor is initially deprotonated by a base, resulting in the formation of a carbanion with two enolate ions as resonance structures. The active carbanion, acting as a nucleophile, then attacks the Michael acceptor, forming a new C–C bond and the corresponding new enolate. Following a proton transfer, the ketone is recovered from the enolate as the final product (Scheme 1.5.2). In comparison to with normal alkenes, alkenes conjugated with carbonyl groups become polarized and are thus electrophilic and reactive towards nucleophiles. Since both β-carbon and C=O carbon have large coefficient in the LUMO of Michael acceptor, a competition between 1,4- and 1,2-addition exists. The reaction temperature, nature of Michael acceptor and hard/soft nature of nucleophile could affect this selective.[208]

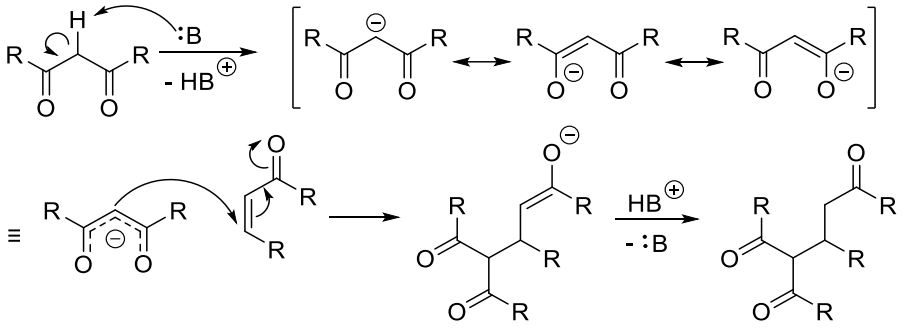

Scheme 1.5.2. Typical mechanism of Michael addition.

In the early stages of development, bifunctional catalysts were employed in heterogeneous catalysis, including hydrogenation and dehydrogenation.[209] Since the discovery of thioureas bearing chiral diamines by Jacobsen, Takemoto and Rawal, as previously discussed, the concept of bifunctional catalysts began to be applied in organocatalysis. In 2013, Tsogoeva and co-workers summarized a comprehensive structural model of bifunctional organocatalyst, including an H–bonding donor for the activation of acceptors/electrophiles, a readily tunable chiral or achiral backbone and a chiral linker with an amine for the activation of donors/nucleophiles (Figure 1.5.1).[210]

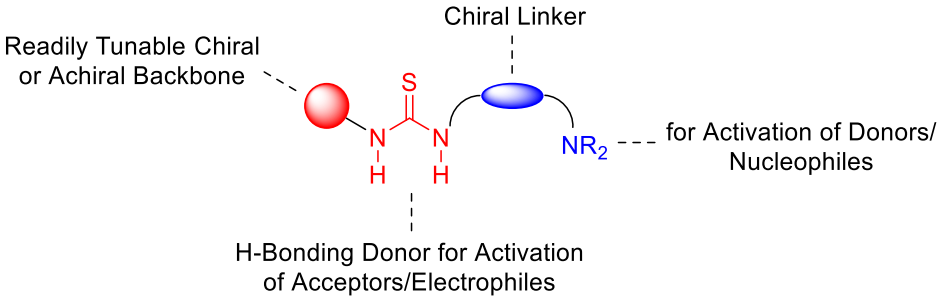

Figure 1.5.1: Structural model bifunctional organocatalyst.

For asymmetric Michael additions, chiral bifunctional organocatalysts are well established due to their dual activation of both electrophile and nucleophile simultaneously, as well as their perfect stereoselectivity. For Mechanism consideration, 3 transition state models are widely accepted. The first mode was suggested by Takemoto and co-workers in 2005, for the Michael addition of diethyl malonate to β-nitrostyrene with Takemoto's catalyst.[136] In this mode, the enolic forms of 1,3-

dicarbonyls are postulated to be deprotonated by the tertiary amine group at first, generating a highly nucleophilic enolate species. The nucleophile coordinates to the protonated amine, while nitroolefins interacts with the thiourea moiety via multiple hydrogen bonds, thereby enhancing the electrophilic character of the reacting carbon center (Figure 1.5.2, a).

In 2006, Pápai and co-workers proposed another route using the same substrates and catalyst as Takemoto's mode.[211] The initial deprotonation of the nucleophile by the tertiary amine group remains unchanged. Then, in contrast to Takemoto's mode, the thiourea moiety coordinates the enolate by forming a bidentate H–bond and the protonated amine interacts with the nitroolefin through a monodentate H–bond (Figure 1.5.2, b). The calculated energy of the ternary complex and the transition state show that this mode is energetically more favored than the Takemoto mode.

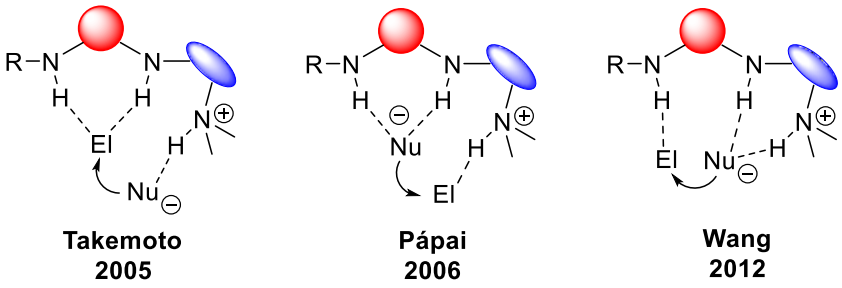

Figure 1.5.2 Transition–state variants of the bifunctional mechanisms, a) Takemoto's Mode. b) Pápai's mode. c) Wang's mode

In 2012, Wang and co-workers found another pathway for the dual activation mechanism on the Michael reaction of α, β-unsaturated γ-butyrolactam (Nu) and chalcone (El) catalyzed with the bifunctional cinchona alkaloid thiourea organocatalys.[212] In this pathway, one N−H group of thiourea and the N−H of the protonated amine simultaneously activate Nu, while the other N−H group activates El (Figure 1.5.2, c). Moreover, they also prognosticated that squaramide–based bi-functional catalysis may preferentially follow this pathway due to the longer distance between the N−H protons in squaramide.

However, in 2014, a joint experimental–theoretical study of a squaramide−amine−catalyzed Michael addition reaction between 1,3-dioxo nucleophiles and nitrostyrene by Soós, Pápai and co-workers demonstrates that Wang's pathway is not applicable to this system, whereas the pathway proposed by Takemoto and Pápai works.[213] Despite the similarity of the geometry and the hydrogen bonding pattern in the transition state of thiourea and squaramide catalysis, the prediction of an optimized hydrogen bonding pattern is difficult due to the significant influence of both the substrate and the catalyst on the reaction pathway.

1.6 *L*-proline derivatives as chiral scaffold

1.6.1 Catalysts and reactions

As mentioned in 1.3.1.1, chiral proline derivatives are widely used in organocatalysis for their activity in forming the enamine−intermediate. In 2006, Tang and co-workers firstly designed the thiourea bifunctional catalyst **77** using *L*-proline derivative as chiral scaffold (Scheme 1.6.1.1). They applied it to the asymmetric Michael reaction of cyclohexanone with both aryl- andalkylnitroolefins, with diastereoselectivity up to 99/1, and enantioselectivity up to 98%.[214]

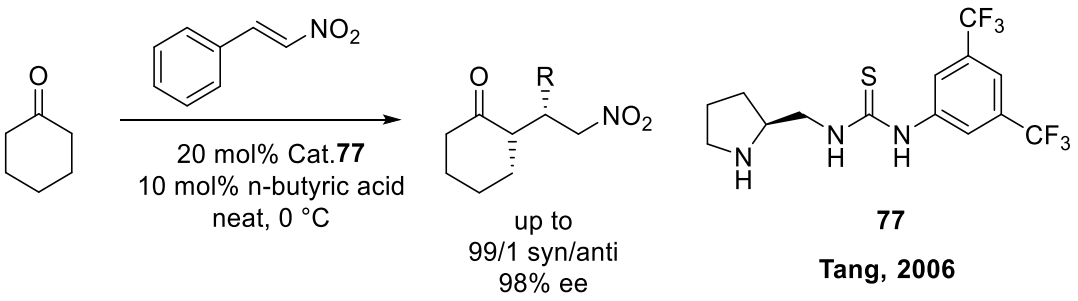

Scheme 1.6.1.1. Asymmetric Michael additions of cyclohexanone to nitroolefins in the presence of organocatalyst **77**.[214]

In 2014, Kesavan and co-workers developed a thiourea based bifunctional

organocatalyst **78** bearing a chiral *L*-proline derived scaffold.[215] The methylated pyrrolidine is a tertiary amine and could thus act as a stronger Lewis base. The newly designed catalyst had an excellent performance on the asymmetric Michael addition of acetylacetone (**31**) to nitrostyrene (**10**) (Scheme 1.6.1.2).

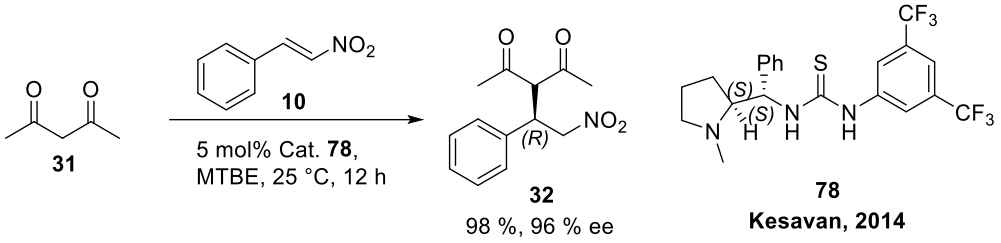

Scheme 1.6.1.2. Asymmetric Michael additions of acetylacetone (**31**) to nitrostyrene (**10**) in the presence of organocatalyst **78**.

Notably they reported the synthesis of catalyst **78** starting from *N*-tritylprolinol **41** via the key intermediate azide **(*S*,*S*)-44**, and they obtained this intermediate **(*S*,*S*)-44** through a Mitsunobu reaction with an inversion of chiral center (Scheme 1.6.1.3).[215] This description sparked an interesting discussion in the near future.

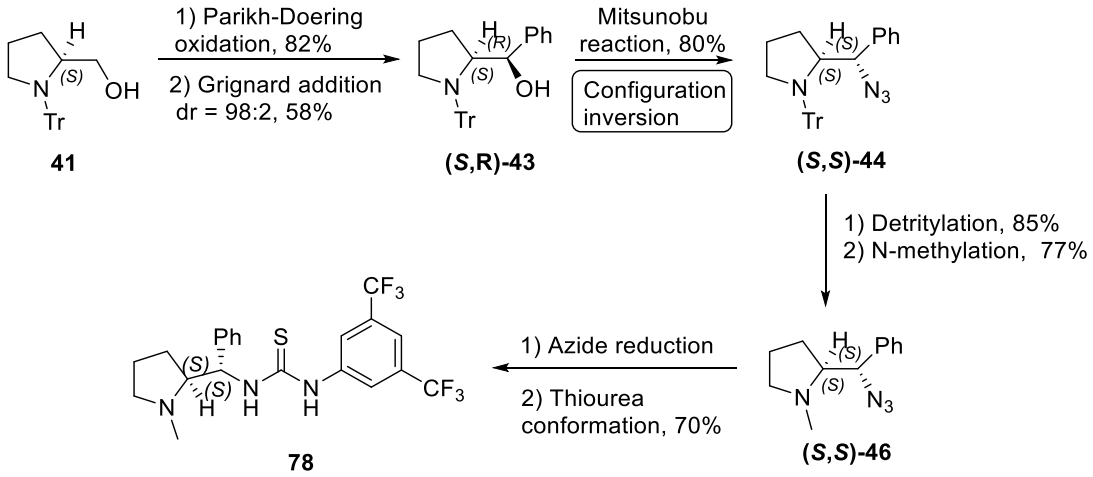

Scheme 1.6.1.3. Synthetic route of bifunctional organocatalyst **78** reported by Kesavan and co-workers.[215]

In 2016, Ryu and co-workers synthesized a series of organocatalysts bearing various proline derivatives as chiral scaffolds, based on (thio)ureas **79** as well as squaramide

80, and applied them to the asymmetric Michael reaction of *S,S'*-diphenyl dithiomalonate and nitrostyrene **10**, with up to 96% yield and 90% ee.[216] Later, they emerged theses catalysts to asymmetric Michael reaction of nitrostyrene **10** and the less reactive ethyl 2-oxochroman-3-carboxylate, and also achieved excellent yields and stereoselectivities (Scheme 1.6.1.4).[217]

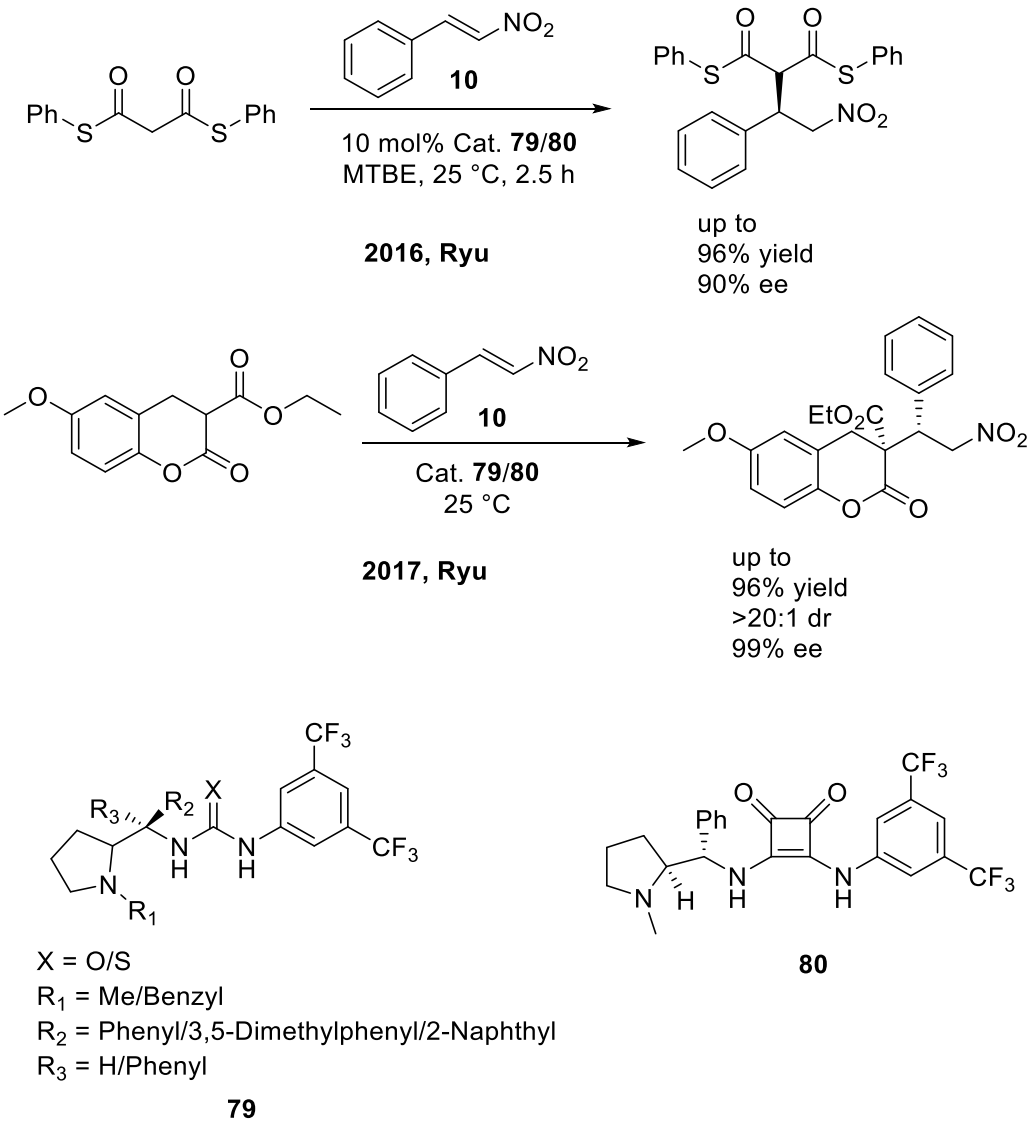

Scheme 1.6.1.4. Asymmetric Michael reaction of nitrostyrene and *S,S'*-diphenyl dithiomalonate/ ethyl 2-oxochroman-3-carboxylate with catalysts **79** and **80**.[216,217]

Later in 2017, Ryu and co-workers noticed an interesting contradiction in determination of configuration of porline derivative between Kesavan's result and Juaristi's,[215,218] and specifically published a paper to illustrate their discovery.[219] For

the preparation of the *N*-benzyl pyrrolidine substituent **(*S,S*)-81**, Kesava and co-workers used phenyl-substituted *N*-tritylprolinol **(*S,R*)-43** as the starting compound. In a Mitsunobu reaction, the hydroxyl group was substituted by an azide group to give key intermediate **(*S,S*)-44**, and conventionally it should be accompanied by an inversion of the configuration. Subsequently, the trityl group at the *N*-terminus was replaced by a benzyl group. This resulted in compound **(*S,S*)-61**, whose measured rotation value $[\alpha]^{25}_{D}$= -105.0° (Scheme 1.6.1.5).[215] It should be noted that the relative configuration of **(S,S)-61** was only determined by NMR spectroscopy.

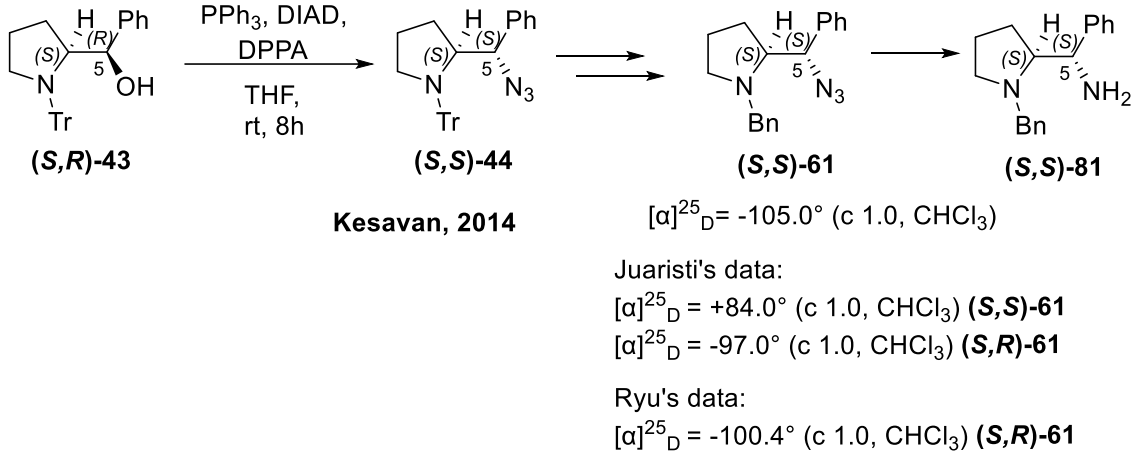

Scheme 1.6.1.5. Kesavan's route for the synthesis of **(*S,S*)-81**.

In contrast, Juaristi and co-workers produced the compound **(*S,S*)-61** and **(*S,R*)-61**, whose absolute configuration was confirmed by crystal structure analysis. A rotation value of $[\alpha]^{25}_{D}$ = +84° was determined for **(*S,S*)-61** and -97° for **(*S,R*)-61**.[218] Ryu and co-workers also prepared **(*S,R*)-61** and obtained $[\alpha]^{25}_{D}$ = −100.4°,[216] which is in accordance with the optical rotation reported by Juaristi and coworkers. The NMR spectra of **(*S,S*)-61** and **(*S,R*)-61** from the Juaristi group are also different. Comparison of the NMR spectra of **(*S,S*)-61** from the Kesava group with the spectra of **(*S,R*)-61** from the Juaristi group shows that they are identical.[215,218] From this it can be concluded that the Kesava working group inadvertently produced **(*S,R*)-44** and subsequently converted it to **(*S,R*)-61**. Ryu and co-workers hypothesized that their Mitsunobu reaction proceeded with retention of configuration at C−5 position, actually

affording azide **(*S,R*)-44** (Scheme 1.6.1.6).[219]

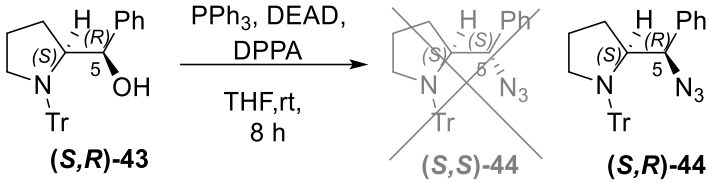

Scheme 1.6.1.6. The actual Mitsunobu reaction pathway of Kesavan's route according Ryu's hypothesis.[219]

1.6.2 Mechanism of retention and inversion in Mitsunobu–reaction

The key step of the synthetic route is the Mitsunobu reaction, firstly reported by Mitsunobu and Yamada in 1967.[220] It allows the conversion of primary and secondary alcohols to esters, phenyl ethers, thioethers and various other compounds under mild conditions (Scheme 1.6.2.1, a). In 1977, Bose and colleagues utilised diphenylphosphoryl azide (DPPA) in the Mitsunobu reaction to enable the azidation of alcohols and phenols in one step. This method is commonly referred to as the "Bose−Mitsunobu method".[221]

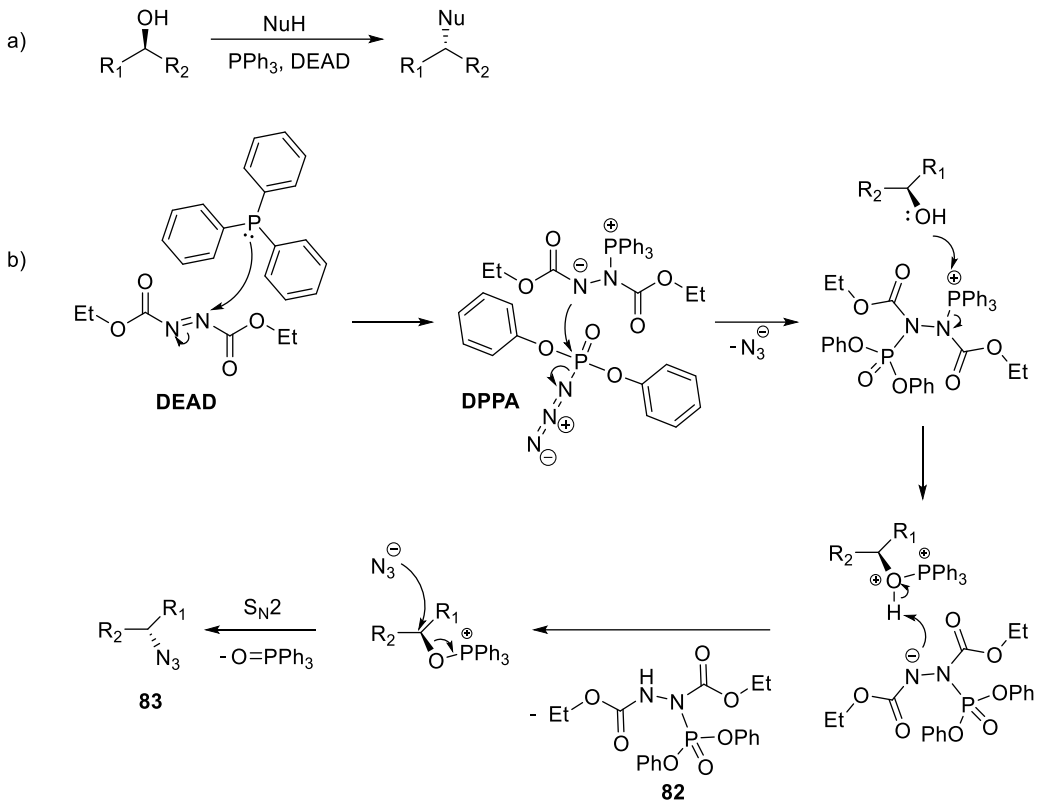

Scheme 1.6.2.1: a) General Mitsunobu−reaction. b) Plausible mechanism of Mitsunobu reaction with DPPA.

Scheme 1.6.2.1 (b) illustrates the plausible mechanism of the Mitsunobu reaction with DPPA. Firstly, the lone pair of phosphine in PPh_3 attacks the N=N bond in DEAD, resulting in an amine anion. This anion is basic enough to undergo nucleophilic attack on the phosphorus atom in DPPA, leading to the separation of the azide group. Subsequently, the positively charged phosphorus group is attacked by the hydroxyl group of the alcohol due to the strong affinity between oxygen and phosphorus. The second resulting amine anion removes the proton of the hydroxyl group, generating the R−O−PPh_3^+ species as the electrophile and by−product **82**. Subsequently, the previous generated nucleophile azide anion attacks the partially positively charged α-carbon of the electrophile through an S_N2 mechanism, yielding the product **83** and by−product triphenylphosphine oxide.

The Mitsunobu reaction conventionally results in a product with inversion of configuration, as the final step involves an S_N2 substitution. However, Ryu and co-

workers have argued that the reaction should result in retention of configuration due to the participation of the neighboring trityl group.[219] This participation could facilitate the formation of an aziridinium ion intermediate **(*S,R*)-53** with configuration inversion, through an intramolecular S_N2, or, S_Ni mechanism. The nucleophilic azide ion attacks the α-carbon through an S_N2 mechanism again, resulting in the Mitsunobu product **(*S,R*)-44**, with retention of configuration due to a doubled configuration inversion.

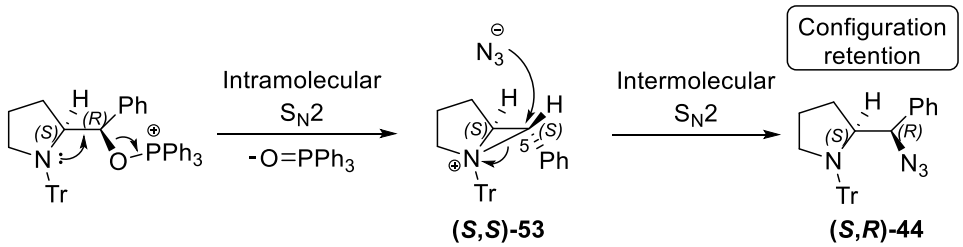

Scheme 1.6.2.2: The plausible mechanism of the doubled S_N2 reaction to compound **(*S,R*)-44**

They also reported that in case of phenyl−substituted *N*-Boc-prolinol **(*S,S*)-56**, the Mitsunobu product **(*S,R*)-57** has an inversion in configuration because the conjugation effect of the amide prevents the formation of aziridinium ion intermediate **(*S,R*)-58** (Scheme 1.6.2.3).[219]

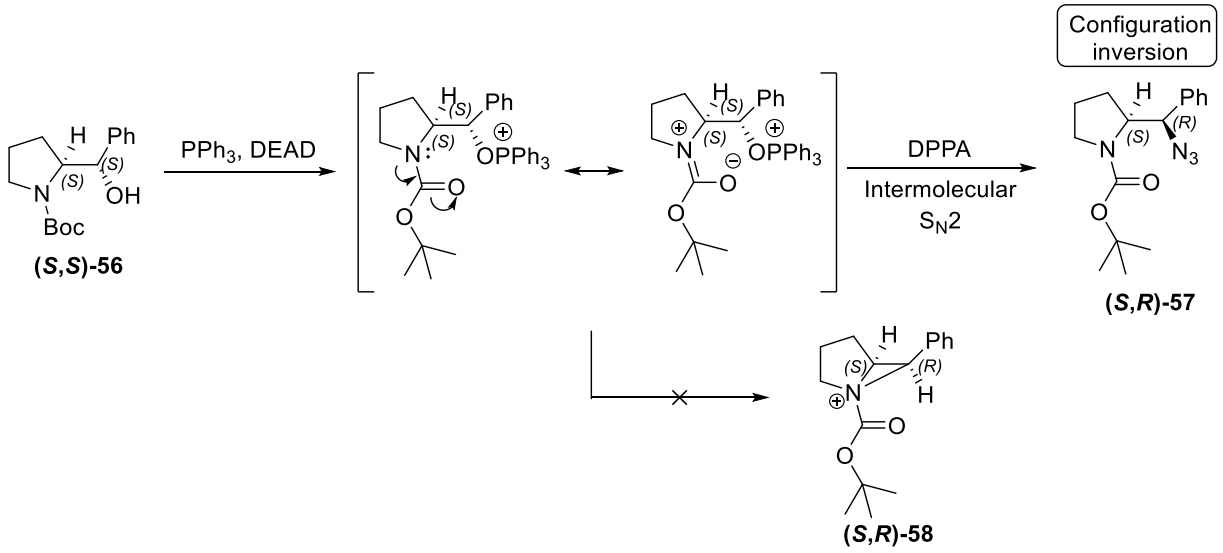

Scheme 1.6.2.3: The conjugation effect of *N*-Boc substituted compound **(*S,R*)-57** on Mitsunobu reaction.[219]

In addition, Yamagiwa and co-workers discovered a more interesting case. They applied the benzyl−protected prolinol **(*R,R*)-59** to the Mitsunobu reaction under identical conditions and obtained products that exhibited configuration inversion (**(*R,S*)-61**) and retention (**(*R,R*)-61**), as well as a ring−expansion product **(*S,S*)-60**. Among these, the inversion product was the major product (Scheme 1.6.2.4). But the ratio of the different products could vary when nucleophiles changed.[222]

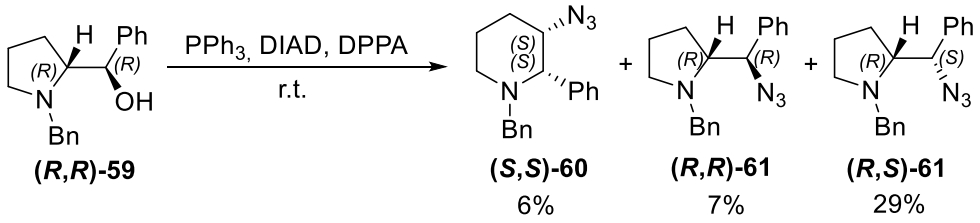

Scheme 1.6.2.4: The Mitsunobu reaction of **(*R,R*)-59** resulted in diverse of products.

Mitsunobu reactions can proceed with retention of configuration via anchimeric assistance of the heterocyclic nitrogen in the substrate.[218,223–225] Except for retention of configuration, this anchimeric assistance could also lead to a rearrangement reaction of piperidine or pyrrolidine derivatives via internal backside nucleophilic substitution (SNib). (Scheme 1.6.2.5).

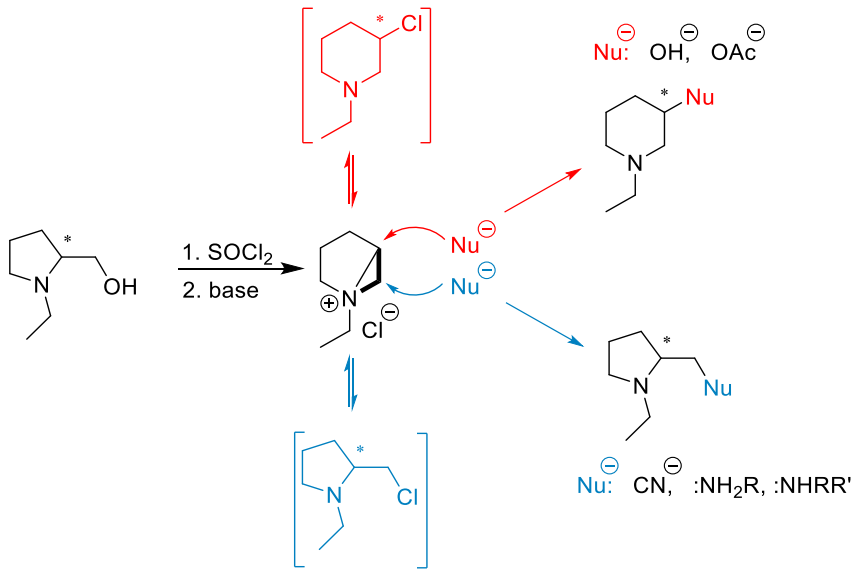

Scheme 1.6.2.5. Mechanism of the nucleophilic displacement reaction on 3-chloromethyl-*N*-ethylpiperidine.[218]

This anchimeric mechanism is well known since 1948.[218,223–227] It was observed that strong nucleophiles such as amines are likely to favor formation of the pyrrolidinic framework, whereas weaker nucleophiles (−OH, −OAc) tend to generate mixtures of 5− and 6−membered ring products. Additionally, it is also worthy to mention that a similar behaviour is observed when linear β-aminoalcohols or polysubstituted pyrrolidinic β-aminoalcohols are used as starting materials in the Mitsunobu reaction.[223,224]

2 Results and discussion

2.1 Chiral cyclodiphosphazane as hydrogen bond catalysts

2.1.1 Motivation

As in Chapter 1.4.2 mentioned, our group employed di-amino substituted cyclodiphosph(V)azanes in hydrogen bonding catalysis,[180] anion recognition,[200] and counter−ion catalysis[201] due to their hydrogen bond donating ability. Compared with other H−bond scaffolds, for binding strength, computation of the interaction between unsubstituted H−bond motifs and nitrobenzene revealed that cyclodiphosph(V)azane has a H−bond length of 2.18 Å (Scheme 2.1.1.1), which is shorter than that of thiourea (2.19 Å) and urea (2.31 Å), but longer than that of squaramide (2.11 Å).[180,228] The computed binding energy is in agreement with the bond length, indicating that cyclodiphosph(V)azane could have a comparable binding ability to that of (thio)urea and squaramide.[229] In terms of binding geometry, the computed distance between the cooperative NH−units of cyclodiphosph(V)azane is 3.2 Å, which is larger than that of thiourea (2.3 Å) and squaramide (3.0 Å), exhibiting a more inward canted directionality.[180]

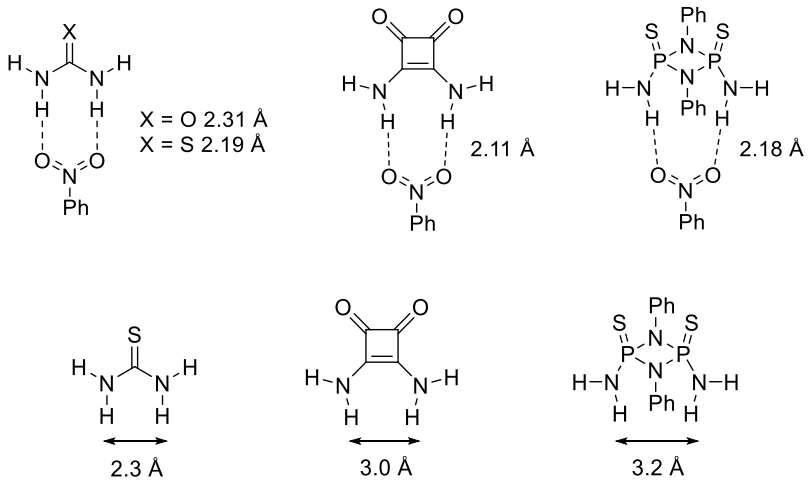

Scheme 2.1.1.1: Computed mean H−bond length of Urea, squaramide and cyclodiphosphazane coordinated to nitrobenzene, and distances between H−atoms.

Specifically, diaminocyclodiphosph(V)azanes have *trans*- and *cis*-isomers, and *cis*-form is able, compared with *trans*-form, to form a stronger hydrogen bond towards acceptors like nitro group, because of its bidentate H−bond ing mechanism. This was demonstrated by a significantly higher enantioselectivity with a *cis*-cyclodiphosph(V)azane bifunctional catalyst (74% ee) compared to a *trans*-form (29% ee) in the reported asymmetric Michael addition. Given the limited number of examples of this species but with good potential, more variations are worth investigating. By design of new cyclodiphosph(V)azane catalysts we focused on the *cis*-form for its good enantioselectivity, fixed the *tert*-butyl group (*t*Bu) on nitrogen of the ring considering its good structural stability[180] and the (*R*,*R*)-diaminocyclohexane as chiral scaffold for its high efficiency,[125] and bring in oxygen or sulfur as chalcogen atoms on phosphorus atom in ring, combining aniline, 3,5-$(CH_3)_2$-aniline or 3,5-$(CF_3)_2$-aniline，which could reduce the flexibility of the catalyst as well as increase the acidity of the N−Hs[122] and thus lead to a stronger catalytic activity.[137] In addition, the diisopropylphenyl group (Dipp) on nitrogen of the ring merits consideration, as it provides steric bulk and compensates for the facile decomposition of the ring with phenyl.[180] Furthermore, it maintains the inductive effect as phenyl compared to *tert*-butyl, which could have a positive effect by increasing the acidity of the N−Hs. Moreover, the newly designed catalysts should also be investigated in asymmetric Michael additions of β-nitrostyrene to different nucleophiles, as asymmetric Michael additions to nitroalkenes have been a powerful tool for the total synthesis of natural and biologically active compounds (2.1.1.2).[230]

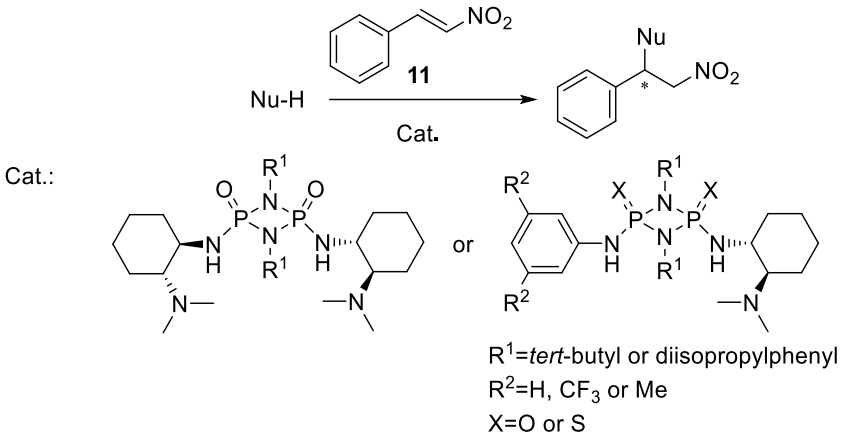

Scheme 2.1.1.2: Asymmetric Michael additions of β-nitrostyrene to different nucleophiles with different newly designed cyclodiphosph(V)azane catalysts as aim of the work.

2.1.2 Synthesis of (1*R*,2*R*)-*N*1,*N*1-dimethylcyclohexane-1,2-diamine as chiral scaffold

The synthesis of (1*R*,2*R*)-*N*1,*N*1-dimethylcyclohexane-1,2-diamine **(1)** was conducted in accordance with the established methodology originally described by Gandelman and co-workers,[231] while some of the procedures are modified in order to simplifying the work.

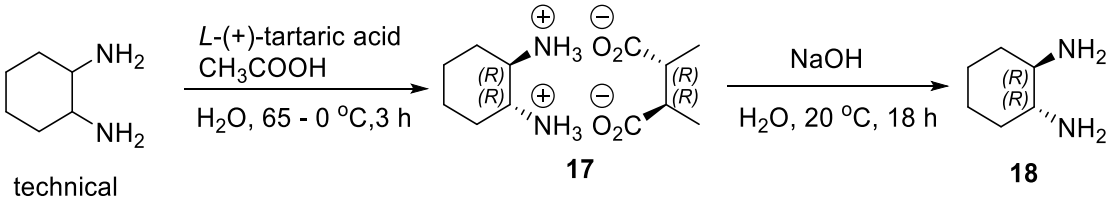

Scheme 2.1.2.1: Synthesis of (1*R*,2*R*)-diaminocyclohexane **18** via chiral resolution of technical diaminocyclohexane

First of all, (1*R*,2*R*)-diaminocyclohexane **18** is synthesised via chiral resolution of technical diaminocyclohexane which contains *rac*-diaminocyclohexane with *L*-(+)-tartaric acid. The classical reaction was carried out according to Klare's doctoral

thesis,[232] with the formation of amine tartrate salt **17** at first, and then the alkalization to release the free amine (Scheme 2.1.2.1). Notably, by concentration in vacuum after the extraction in the alkalization step, the solvent should be carefully evaporated by rotary evaporator in reduced pressure under the water bath at room temperature instead of 40 °C for the easily volatilization of the product, and the crude product as a yellow oil containing trace of DCM will be directly taken into the next step. The conversion of alkalization is established to be quantitative for its simple acid−base reaction property, and the stoichiometry calculation of the reagents as well as the yield for the following steps are based on the amount of the used amine tartrate salt.

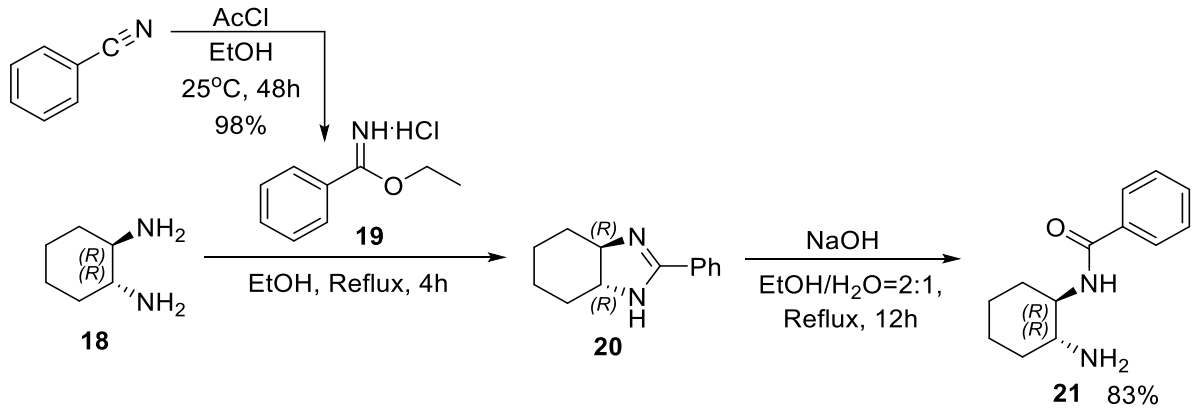

Scheme 2.1.2.2: Synthesis of N-((1*R*,2*R*)-2-aminocyclohexyl)benzamide (**21**) starting from (1*R*,2*R*)-diaminocyclohexane **18**.

Subsequently, mono−functionalized diamine compound **21** was produced via a two−step process starting from compound **18** with ethyl benzimidate hydrochloride **19** (Scheme 2.1.2.2). Ethyl benzimidate hydrochloride was synthesized following the literature procedure by Yadav and co-workers.[233] The ethyl benzimidate salt **19** reacted the with *trans*-diaminecyclohexane **18** to the imidazoline **20** as the ring−closed product. As the conversion is almost complete according to the TLC, the crude product without any purification would be further invested for the subsequent ring−opening reaction under basic condition. A simplified purification of washing the crude product with cold DCM instead of column chromatography gave a pure product with a good yield of 83% relating to the amount of the used amine tartrate salt.

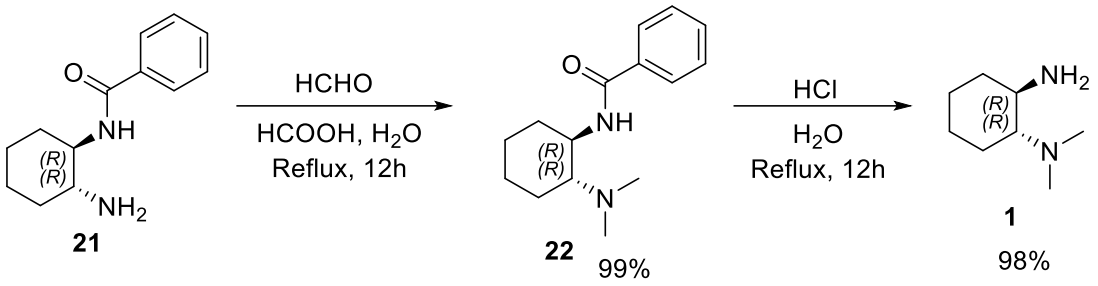

Scheme 2.1.2.3: Synthesis of (1*R*,2*R*)-*N*1,*N*1-dimethylcyclohexane-1,2-diamine (**1**) starting from *N*-((1*R*,2*R*)-2-aminocyclohexyl)benzamide (**21**).

The next step is methylation by the Eschweiler−Clarke reaction of amide **21** with water, formaldehyde, and formic acid. Under standard conditions, the reaction resulted in complete conversion. TLC and NMR analysis indicated a pure dimethylated product without any purification, so the crude product could be used directly in the next step. In the final step, the methyl amide **22** was deprotected through acid−catalyzed hydrolysis, which also resulted in excellent conversion to the diamine **1** and the crude product could be directly invested in the next step (Scheme 2.1.2.3). It is noteworthy that the final product **1**, as a yellow oil, decomposes more readily in the ambient atmosphere than the protected compound **1**, as a white solid. It is therefore recommended that methyl amide **22** could be stored for a long time, while product **1** should be freshly synthesised shortly before use.

2.1.3 Synthesis and characterization of chiral cyclodiphosphazanes

2.1.3.1 Synthesis of precursor *cis*-[*t*-BuNPCl]$_2$

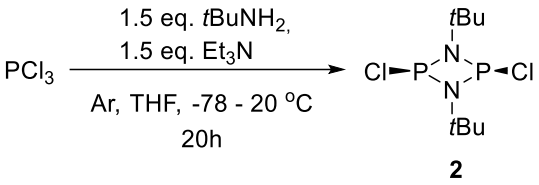

Scheme 2.1.3.1: Synthesis of *cis*-dichlorocyclodiphosph(III)azanes with *t*-Bu (*cis*-[*t*-BuNPCl]$_2$) as precursor **2**.

The *cis*-dichlorocyclodiphosph(III)azanes with *t*-Bu (*cis*-[*t*-BuNPCl]$_2$) as precursor **2** is readily prepared by the reaction of PCl_3 with *t*$BuNH_2$ according to the reported method by Wright and co-workers.[234] For stoichiometric settlement, either PCl_3:*t*$BuNH_2$ = 1:3 or PCl_3:*t*$BuNH_2$:Et_3N = 2:3:3 is suitable for the reaction, because the amount of *t*$BuNH_2$ involved in building the product is only 1 equivalent while the excess of amine serves as a Brønsted base for the HCl generated in the reaction (Scheme 2.1.3.2).[171,234]

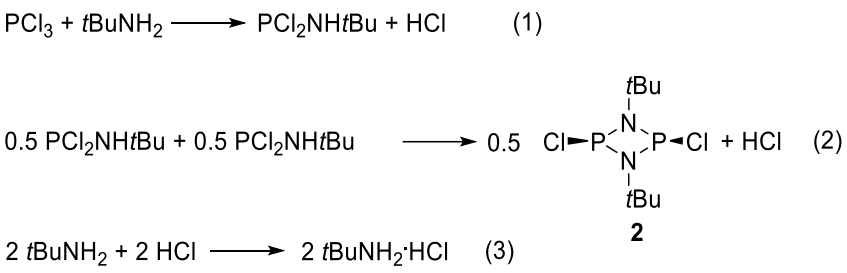

Scheme 2.1.3.2: Plausible reaction process by synthesis of precursor **2**.

The reaction resulted in a low yield of around 35%, after a distillation under an inert condition as the product hydrolysis easily in ambient atmosphere, and the distillation should be conducted not with cooling water, but with regular slight heating on the condenser, since the product **2** rapidly solidifies. This could lead to the decrease of yield, but ensured the purity of the desired product, as the existance of the side reaction brings in the by−product, as well as decreases the yield.

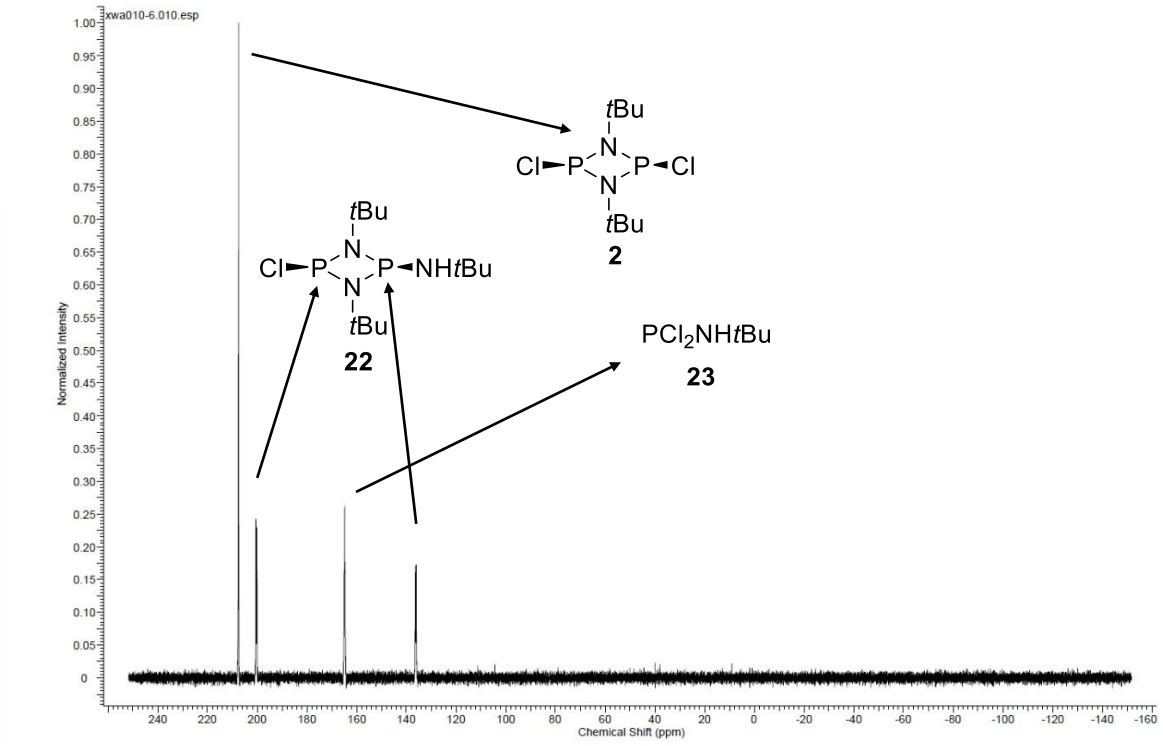

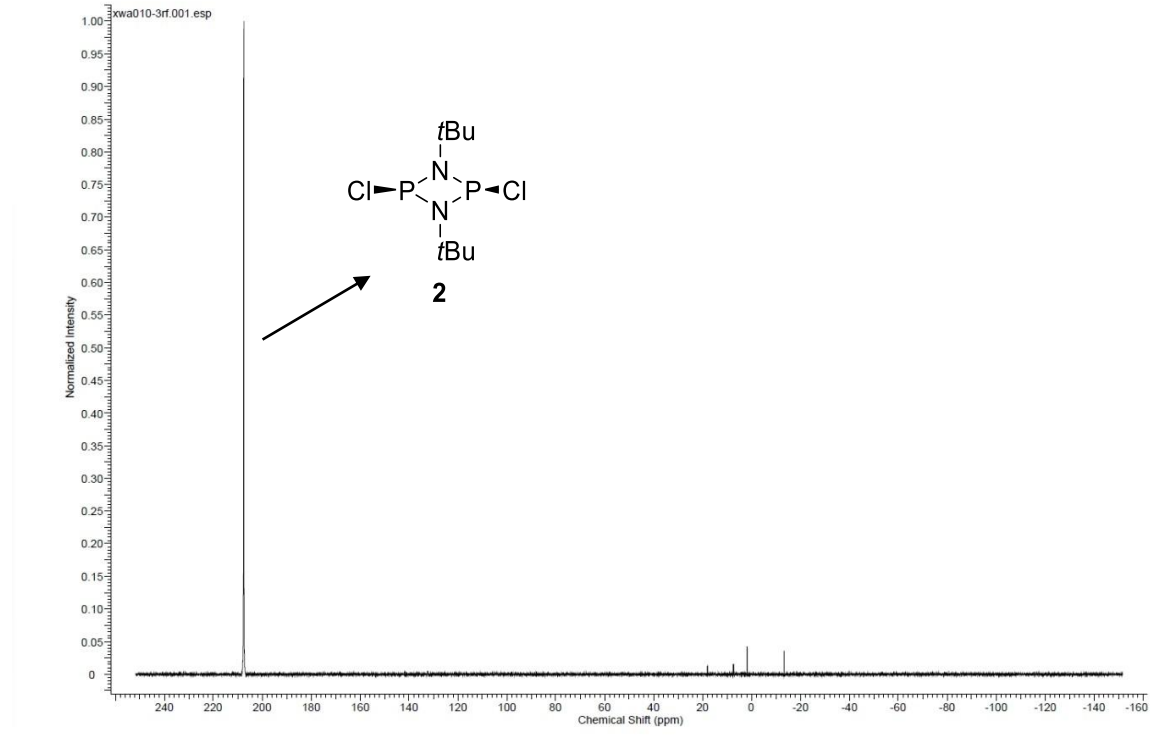

Figure 2.1: a) ^{31}P-NMR spectrum of crude product of *cis*-[*t*-BuNPCl]$_2$, b) ^{31}P-NMR spectrum of pruified product of *cis*-[*t*-BuNPCl]$_2$.

^{31}P-NMR analysis helps for a better understanding of the reaction. Figure 2.1 (a) is the ^{31}P-NMR spectrum of the crude product without distillation, and it shows not only the

target molecule **2** (207.50 ppm), but also the *t*BuNH-chlorocyclodiphosph(III)azane **22** (200.51 ppm, 136.41 ppm) and the intermediate **23** (164.83 ppm) as by−products.[235] However, after the distillation, as in Figure 2.1 (b) shows, the peaks of by−products disappear.

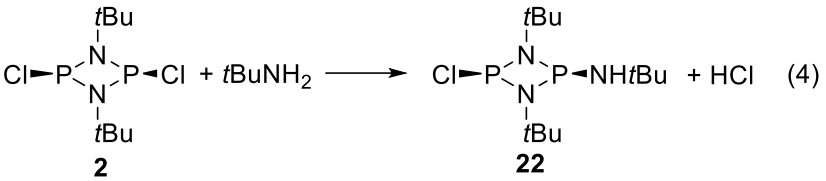

Scheme 2.1.3.3: Plausible side reaction to form the by−product **22**.

The side reaction in Scheme 2.1.3.3 may provide an explanation for the formation of by−products. With the adding of the *t*BuNH$_2$ into the reaction mixture, it has a chance to react with the newly formed product **2**, generating the new aminochlorocyclodiphosph(III)azane **22**. As the subsequent substitution with primary amine occurs under a similar condition (See Chapter 1.4.1), the chemoselectivity between PCl_3 and product **2** exists, but differs not that much, which means that the side reaction could not be avoided.[235] Since the total added amine is a 3−fold excess, this side reaction would consume the *t*BuNH$_2$ which initially participated in forming the product x, and thus lead to an excess of the unreacted intermediate **23**, as another by−product, because a lack of the Brønsted base for the HCl generated in the reaction. According to this consideration, it is reasonable to infer that the product is always accompanied with by−product of **22** and intermediate **23**, and the ratio of **22** and **23** should be approximately 1:1.

2.1.3.2 Synthesis of precursor *cis*-[DippNPCl]$_2$

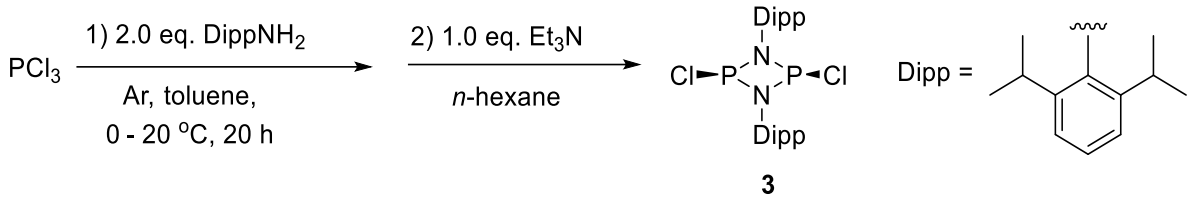

3

Scheme 2.1.3.4: *cis*-dichlorocyclodiphosph(III)azanes with Dipp (*cis*-[DippNPCl]$_2$) as precursor **3**.

The *cis*-dichlorocyclodiphosph(III)azane with Dipp (*cis*-[DippNPCl]$_2$) (Dipp = diisopropylphenyl) as precursor **3** is readily prepared through the reaction of PCl_3 with $DippNH_2$ according to the reported method by Burford and co-workers (Scheme 2.1.3.4).[236] The reaction shares the same principle of the synthesis of *cis*-[*t*-BuNPCl]$_2$ (**2**), and differs sightly in the procedure of working up. Instead of an inert distillation, an inert crystallisation−filtration−washing working up procedure gave a pure product of *cis*-**1**. The *cis*-[DippNPCl]$_2$ (**3**) is more stable than the *cis*-[*t*-BuNPCl]$_2$ (**2**), since it remains unchanged under a longer time of storage, occasionally. The synthesis resulted in a yield of 58%, which is even higher than the literature value, possibly because the amount of *n*-hexane for re−dissolving of the residue after the first round of filtration is higher than the amount of the literature procedure.[236]

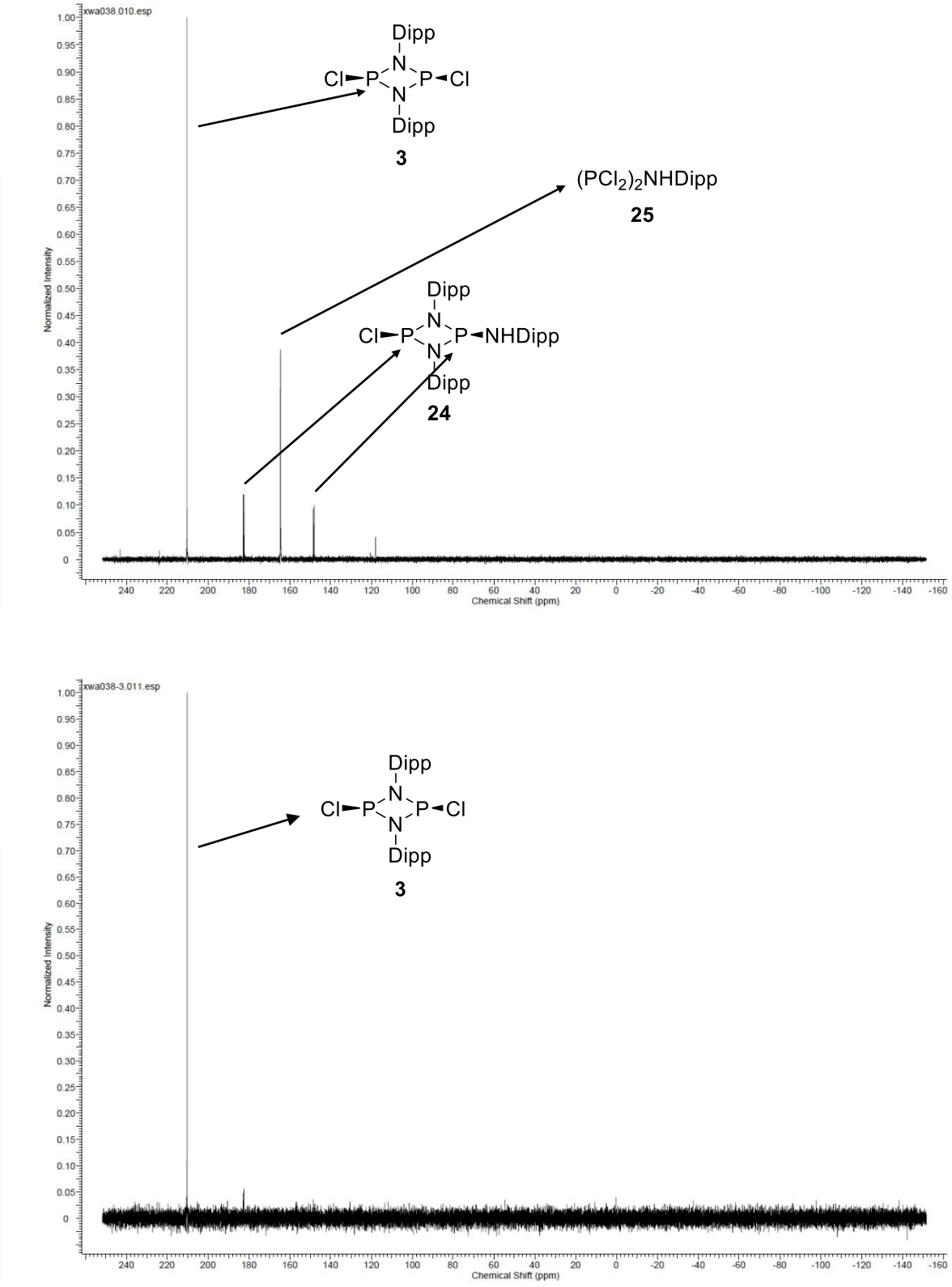

Figure 2.2: a) ^{31}P-NMR spectrum of the crude product of *cis*-[DippNPCl]$_2$, b) ^{31}P-NMR spectrum of the pruified product of *cis*-[DippNPCl]$_2$.

Similar to the synthesis of *cis*-[*t*-BuNPCl]$_2$ (**2**), ^{31}P-NMR spectrum of the crude product, Figure 2.2 (a), shows the target molecule **3** (210.25 ppm) as well as the by−products of DippNH-chlorocyclodiphosph(III)azane **24** (182.72 ppm, 148.50 ppm) and **25** (164.57 ppm).[236] For the purified product **3**, as in Figure 2.2 (b) shows, the peaks of by−products disappear.

$$2PCl_3 + DippNH_2 \longrightarrow \underset{\mathbf{25}}{(PCl_2)_2NDipp} + 2HCl \qquad (1)$$

Scheme 2.1.3.5: Plausible side reaction to form the by−product **25**.

The reasoning of forming the by−product **24** is similar to the case of *cis*-[*t*-BuNPCl]$_2$, but by−product of **25** is formed from the side reaction of PCl_3 and $DippNH_2$ in 2:1, which differs the case of *cis*-[*t*-BuNPCl]$_2$ (**2**) (Scheme 2.1.3.5).

As previously mentioned, compared to *cis*-[*t*-BuNPCl]$_2$ (**2**), *cis*-[DippNPCl]$_2$ (**3**) doesn't decompose so readily even when it was shortly exposed in ambient atmosphere. Its single crystal was then obtained and analyzed.

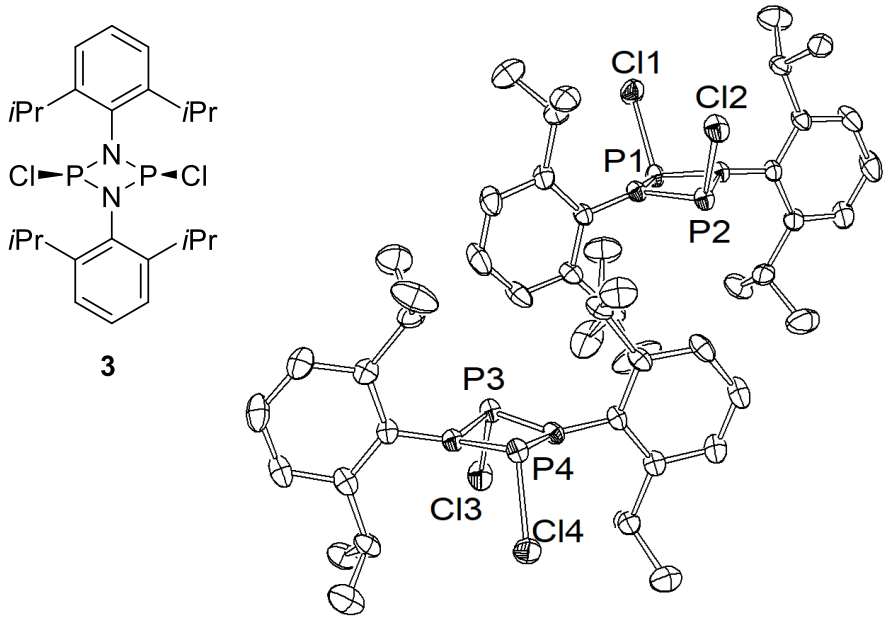

Figure 2.3: X−ray crystal structure of two crystallographic independent molecules of *cis*-[DippNPCl]$_2$ (**3**) with thermal ellipsoids at the 50% probability level; protons are omitted for clarity.

The crystal structure exhibits a *cis*-conformation of the both chlorine atom (Figure 2.3). Moreover, the P_2N_2 ring was shielded well by the 2 isopropylphenyl group, which could explain the good stability of the molecule. And this steric bulk, on the one hand, enhances the stability of the ring and protects it from ring opening or hydrolysis; however, on the other hand, it might increase the difficulty of nucleophilic substitution, for example, with amine.

2.1.3.3 Synthesis of chiral cyclodiphosphazanes

2.1.3.3.1 Synthesis of chiral *t*-Bu-cyclodiphosph(V)azane catalysts

The Synthesis of new cyclodiphosph(V)azane catalysts **4** − **9** (Scheme 2.1.3.6) followed the previously published method.

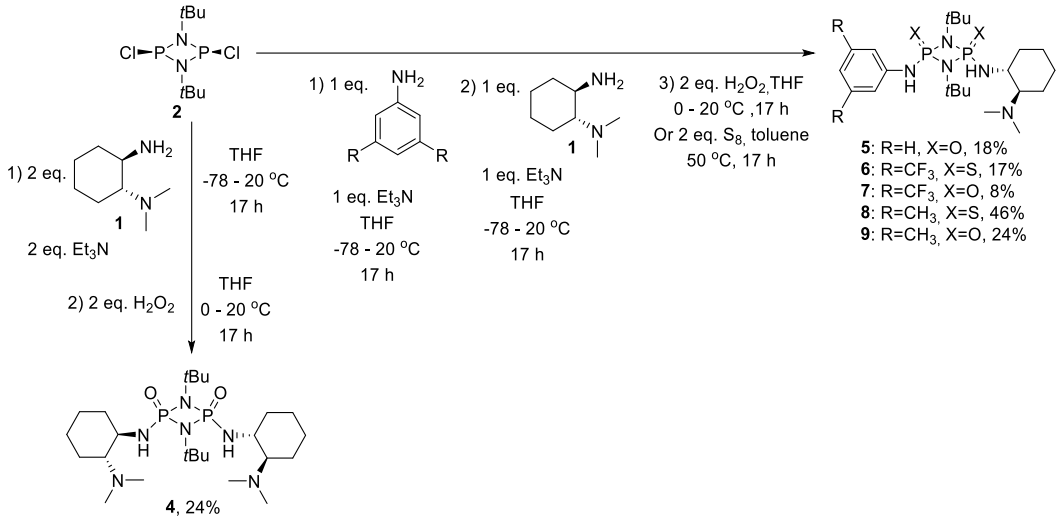

Scheme. 2.1.3.6: Synthesis of novel chiral cyclodiphosph(V)azane catalysts.

Starting from precursor *cis*-[*t*-BuNPCl]$_2$ (**2**), substitution with the respective amine derivatives and Et_3N as the base, and the subsequent oxidations with H_2O_2 or elemental sulfur gave the desired products, with low up to moderate yields. (Scheme 2.1.3.6).

Notably, by synthesis of the asymmetric catalysts from **5** to **9**, 1 equivalent of aniline derivative was added into the solution of precursor, with an intention of

monochlorcyclodiphosphazane as intermediate. But purification using flash column chromatography after the last step of oxidation always gave not only the desired asymmetric compound, but also the symmetric compounds with aniline derivative or (*R,R*)-diaminocyclohexane on both sides of the catalyst, indicating a not exclusive selectivity in the first step of substitution of aniline derivative onto mono- and dichlorcyclodiphoshpazane. Since only 1 equivalent of aniline derivative was added, building of diphenylaminocyclodiphosphazane consumed extra aniline derivative, resulting the unsubstituted dichlorcyclodiphosph(V)azane, which would be further substituted with (*R,R*)-diaminocyclohexane **1** (Scheme 2.1.3.7).

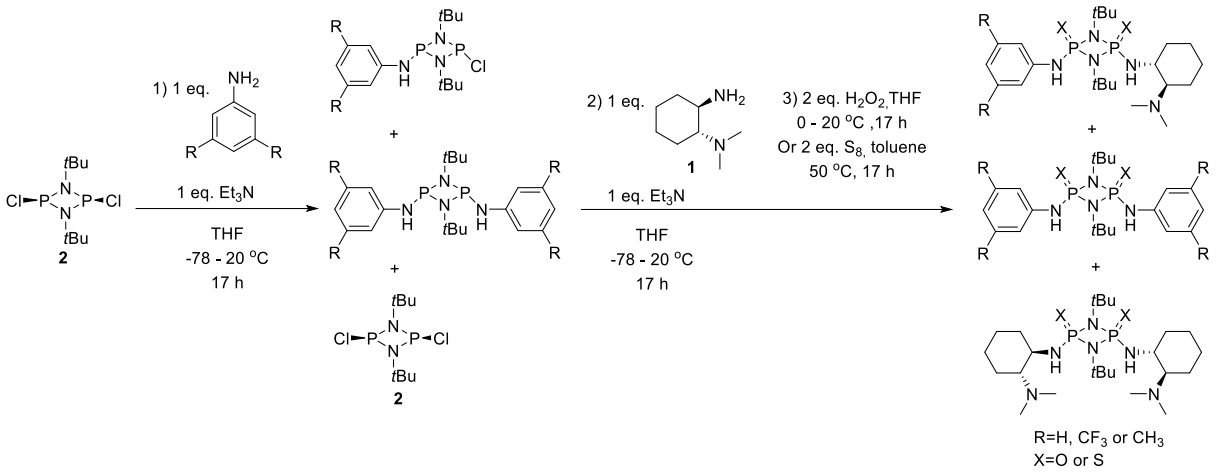

Scheme 2.1.3.7: Plausible reaction process by synthesis of novel chiral cyclodiphosphazane catalysts with formation of by−products.

Thus, freshly purified precursor and amine were required, since trace of impurity could lead to an absence of the desired product. Also, the synthesis before the last oxidation should be kept in inert atmosphere without the purification of intermediate, considering the instability of mono- and dichlorcyclodiphosph(III)azane.

In addition, for oxidation with oxygen, unlike the reported method,[180,200,201] 2 equivalent of H_2O_2 instead of an excess amount were used, because excessive H_2O_2 oxidated the nitrogen of the tertial amine of the (*R,R*)-diaminocyclohexane by synthesis of Cat. 5 and 7, and formed the oxidized by−products **75** and **76** (Scheme 2.1.3.8). By synthesis of Cat. **9**, 2 equivalent of H_2O_2 was used and no oxidized

by−products was observed.

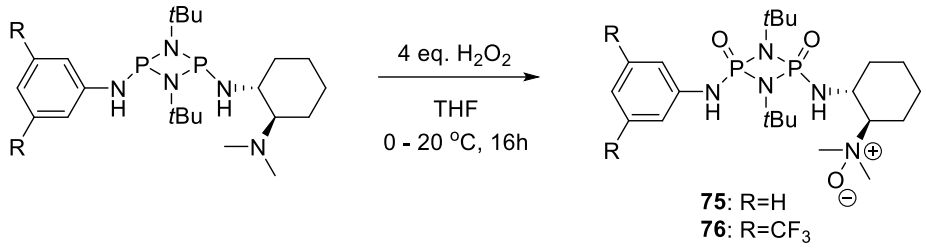

Scheme 2.1.3.8: Oxidation of nitrogen of the tertial amine as side reactions by synthesis of Cat. **5** and **7** forming the by−products **75** and **76**

$^{31}P\{^{1}H\}$-NMR analysis shows the difference between catalyst **4** and the others. The singlet of catalyst **4** represents a magnetically equivalent of the 2 phosphorus atoms, which revealed a C_2−symmetry in the molecule (Figure 2.4, a). For the other forms, magnetically difference in the 2 phosphorus atoms leads to two doublets, with identical J_{PP} constants, like 52.4 Hz for example for catalyst **5** (Figure 2.4, b).

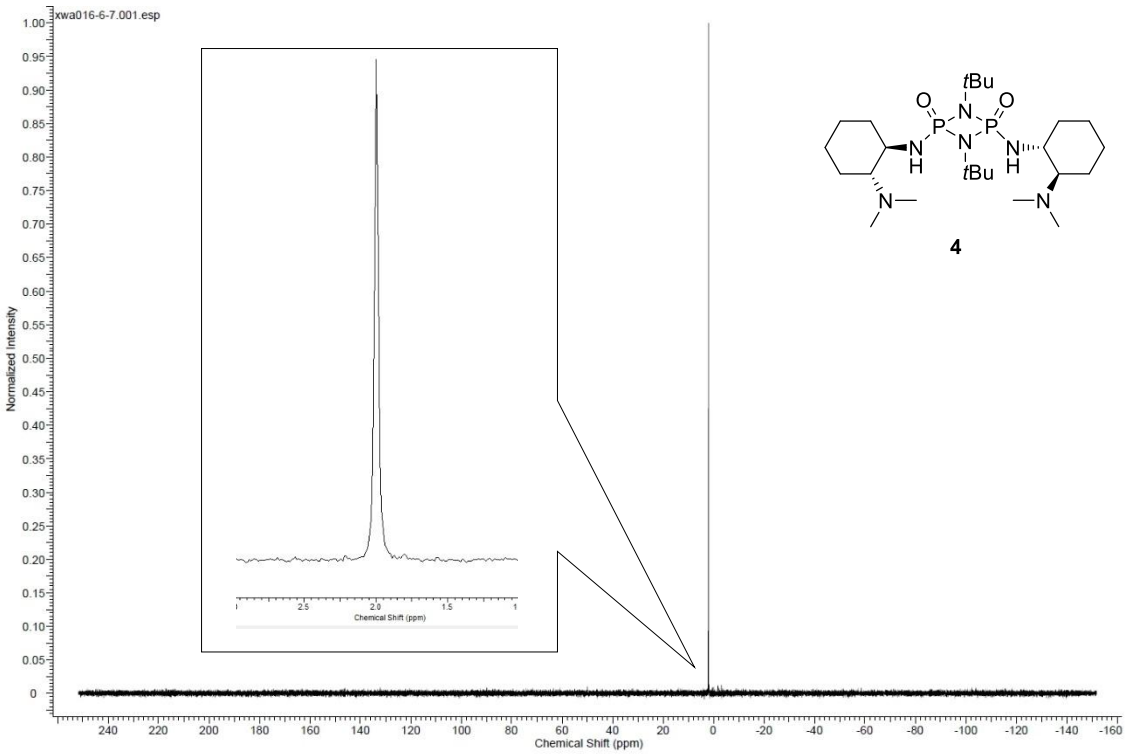

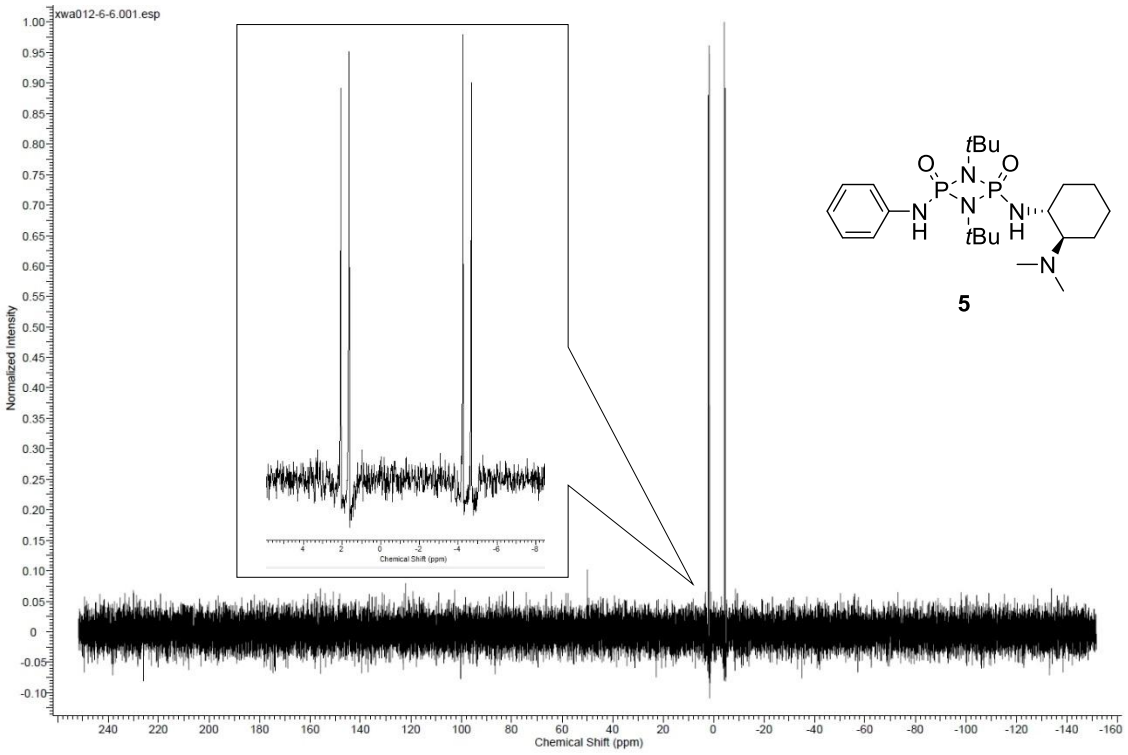

Figure 2.4: $^{31}P\{^{1}H\}$-NMR spectra of catalyst a) **4** and b) **5**.

The X−ray crystal structure of newly synthesized cyclodiphosph(V)azane catalysts were obtained except for **6** (Figure 2.5). Among these, most of the catalysts exhibit a NH−in−out−conformation, which is favored in energy according to the DFT−computation,[200] with exception of **4** and **7**. Unlike the NH−in−out form with sufur, the symmetric compound **4** and **7** with Oxygen has a NH−in−in−conformation, which could be attributed to a stronger intermolecular hydrogen bond between the corporative NH and O=P(NR_3) moieties.[201] The rest asymmetric structures all have a NH−in−out−conformation, while the “out” side are all orientated to the more acidic aryl-NH side, which could be attributed to another pattern of intermolecular hydrogen bond, forming dimer as a beneficial form. Unfortunately, no cocrystal of H−bond acceptor and cyclodiphosph(V)azane catalysts, especially the catalysts bearing CF_3, could be obtained. Thus, no NH−in−in−conformation with intramolecular hydrogen bond between the weakly acidic *ortho*-C−H on phenyl and the oxygen on phosphorus atom could be observed or analyzed.

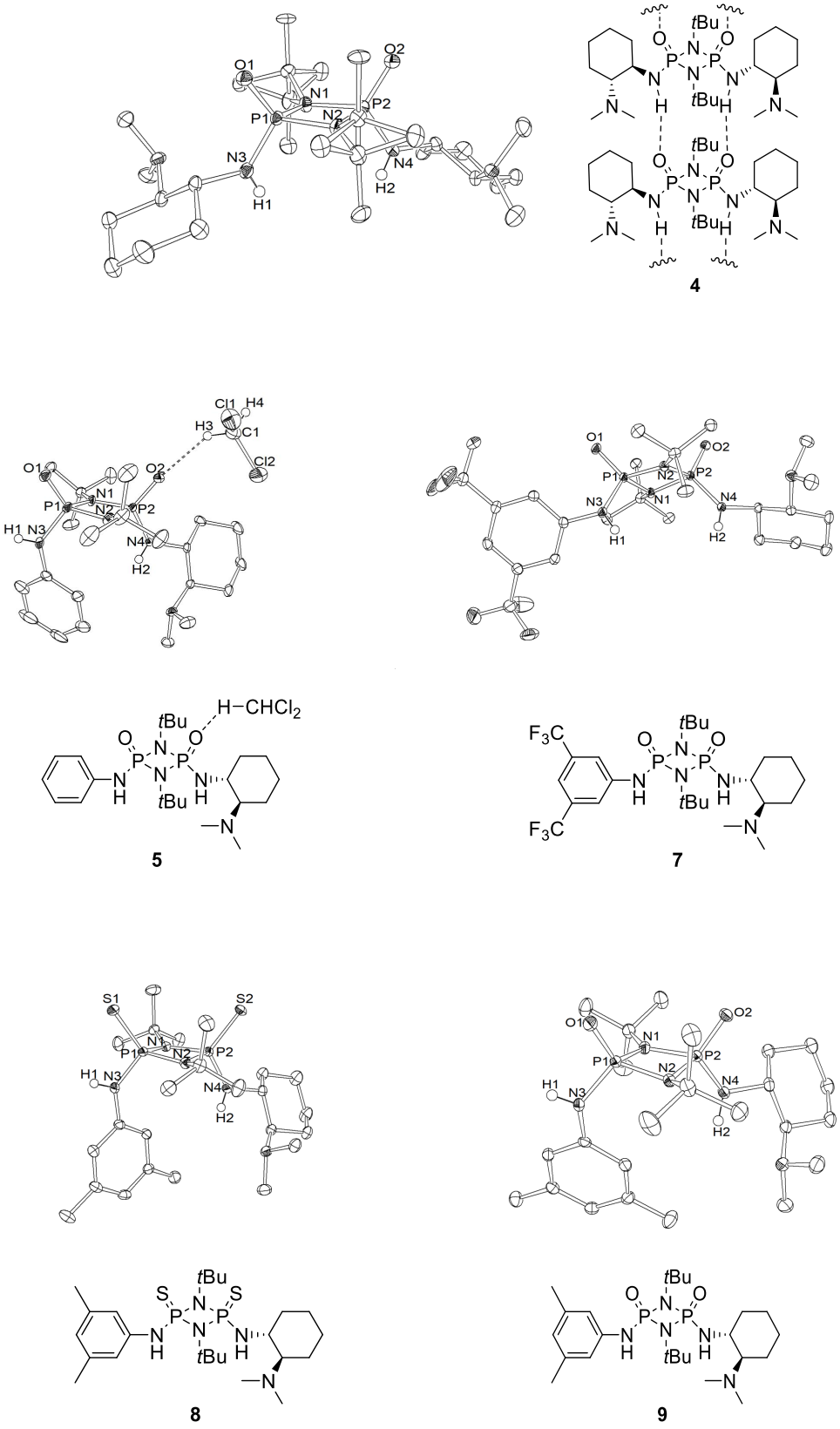

Figure 2.5: X−ray crystal structure of cyclodiphosph(V)azane **4**, **5**, **7**, **8** and **9** with thermal ellipsoids at the 50% probability level; protons except NHs are omitted for clarity

All of the cyclodiphospazane ring are slightly distorted. The dihedral angle between the two [NPN] planes of catalyst **4** and **5** are 5.5° and 4.9° respectively, while the structures with substitution groups on phenyl are more puckered, leading to the angles of 8.7°, 7.8° and 10.3° for catalyst **7**, **8** and **9**. Most angular sums around N3/N4 of the catalysts are close to 360° (**4**: 359.9°/359.9°, **5**: 356.6°/354.9°, **7**: 355.9°/359.7°, **8**: 359.7°/352.1°, **9**: 352.1°/344.0°), which indicates a higher tendency of sp^2−hybridization of the ring nitrogen against sp^3.

2.1.3.3.2 Synthesis of chiral Dipp-cyclodiphosph(V)azane catalysts

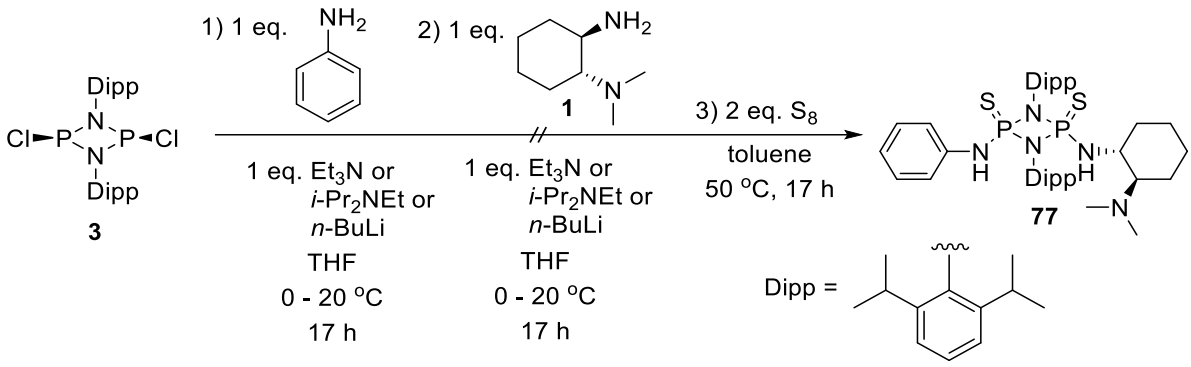

Scheme 2.1.3.9: Attempts to synthesize the new chiral cyclodiphosph(V)azane **77** bearing diisopropylphenyl group (*cis*-[DippNPCl]$_2$).

Synthesis of the chiral Dipp-cyclodiphosph(V)azane catalyst **77** was unsuccessful (Scheme 2.1.3.9). Starting from the precursor of *cis*-[DippNPCl]$_2$ (**3**), after addition of 1 eq. aniline, 1 eq. chiral cyclohexane diamine and elemental sulfur in sequence, multiple spots could be observed in TLC. Through column chromatography, some fraction could be isolated, and after a test of ^{1}H- and ^{31}P-NMR, no corrected product could be determined, with lack of either the correct doublets at a chemical shift of approximately 38 − 46 ppm in ^{31}P-NMR, or the peaks of chiral cyclohexane diamine in ^{1}H-NMR. This failure to isolate the correct product was observed to be consistent, even after changing the helping base into a stronger variant, like *i*-Pr$_2$NEt, or *n*-BuLi.

To understand the reaction better, ^{31}P-NMR of intermediate after the addition of aniline was tested (Scheme 2.1.3.10).

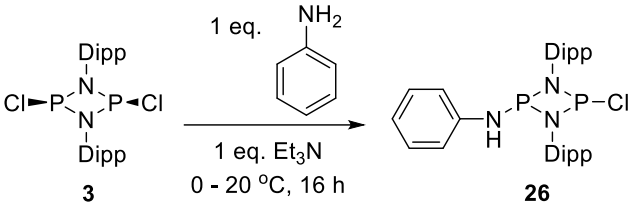

Scheme 2.1.3.10: Substitution of precursor **3** with aniline forming the intermediate **26**.

Examines of the ^{31}P-NMR for intermediates of two repeated reactions under the same conditions were conducted, solely changing the scale slightly, without the purification of the intermediates.

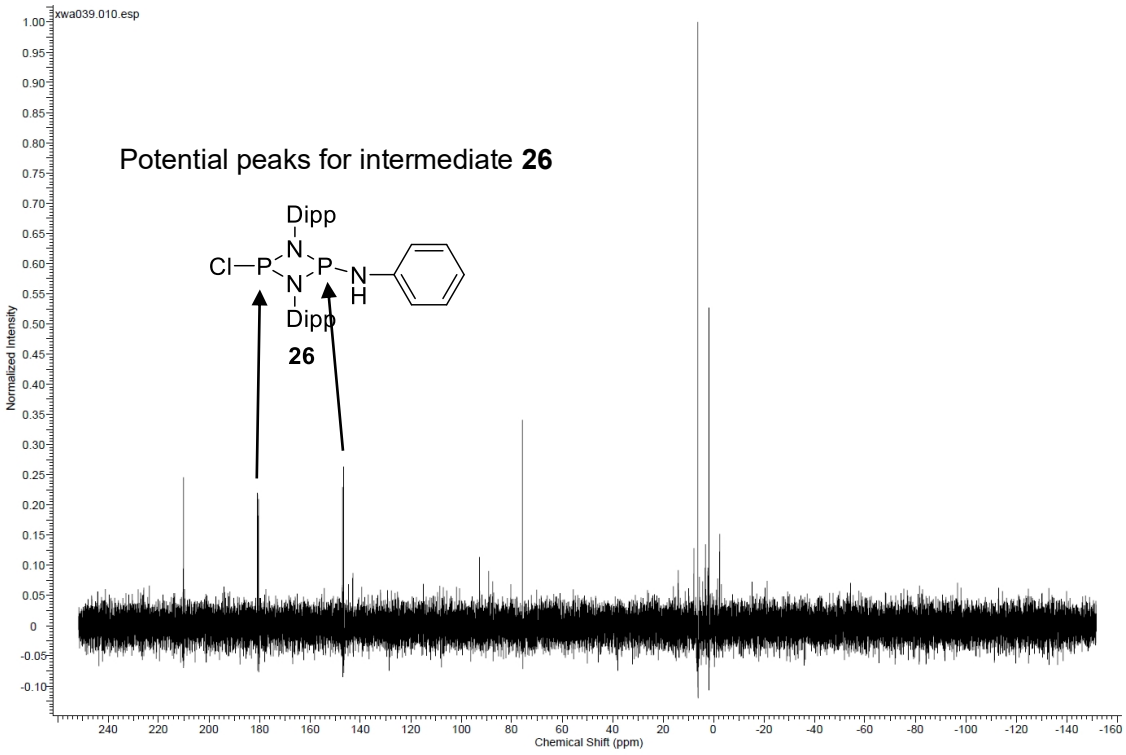

Figure 2.6: ^{31}P-NMR spectrum of the 1. sample of the reaction mixture after the substitution of precursor **3** with aniline.

For the ^{31}P-NMR spectrum of the first sample (Figure 2.6), except for the peaks of the

unreacted precursor **3** (210 ppm) and the hydrolyzed/oxidized impurities with P=O at approximately 0 ppm, two doublets at 146.69 ppm and 180.37 ppm, with J_{PP} constants of 48.1 Hz for each, has a good potential being that of the intermediates **26**.[236]

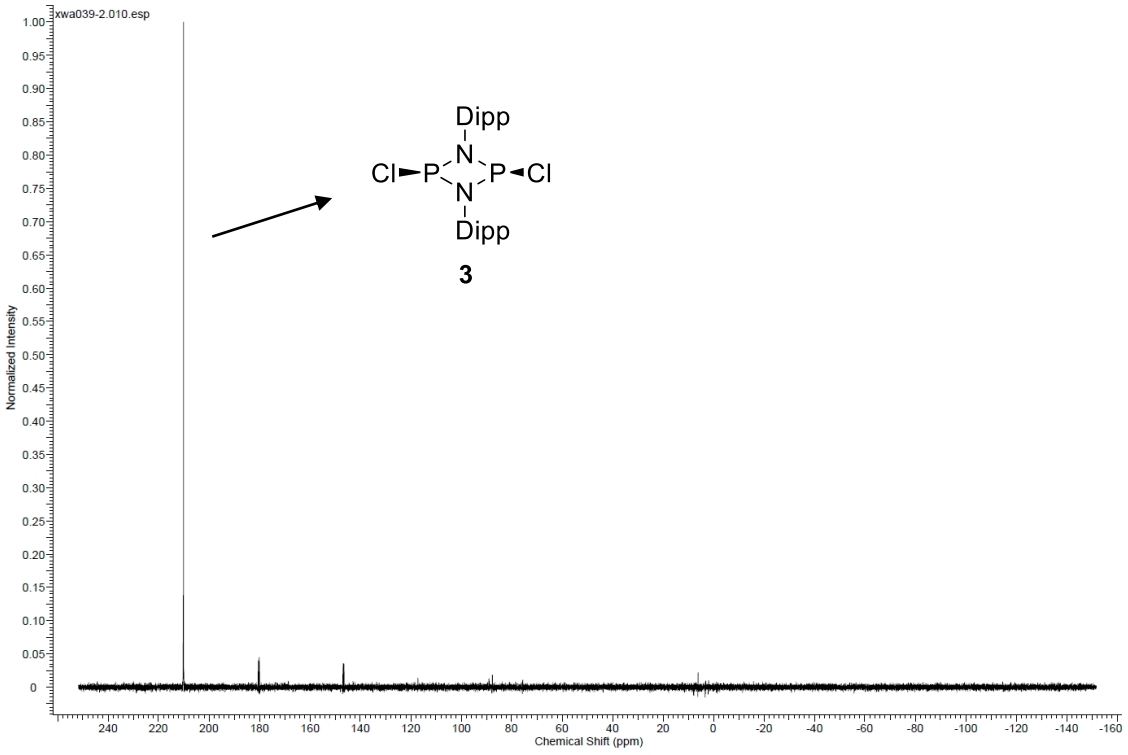

Figure 2.7: ^{31}P-NMR spectrum of the 2. sample of the reaction mixture after the substitution of **3** with aniline.

For the ^{31}P-NMR spectrum of the second tested sample (Figure 2.7), almost only the peak of the precursor **3** (210 ppm) could be observed, indicating minimum conversion took place in this trial.

Complexity of forming the intermediate might be attributed to the difficulty of the nucleophilic attack of amines onto the P_2N_2 because of the bulk generated by the diisopropyl group.

2.1.4 Asymmetric Michael addition of *trans*-β-nitrostyrene(10) to various nucleophiles with chiral cyclodiphosph(V)azanes as enantioselective catalysts

2.1.4.1 Catalysis with 2-hydroxy-1,4-naphthoquinone (11)

Quinones and naphthoquinones are important basement for many nature products, and their derivatives exhibit good bioactivity, especially antitumor effects, like ametantrone,[237] doxorubicin[238] and mitoxantrone.[239] In this work, 2-hydroxy-1,4-naphthoquinone (**11**) is selected in priority since it was already tested by our group for asymmetric Michael addition to β-nitrostyrene (**10**) with excellent yield (98%) and modest enantiomeric excess (75% ee), performed by cyclodiphosph(V)azane catalyst with sulfur- and phenyl-substitution on the ring.[180] Nevertheless, the performance of sulfur- and *t*-Bu substituted form *all-cis*-**16** is more interesting for us, for its slightly lowered but still modest enantiomeric excess (67% ee) and also excellent yield (95%), but higher stability against decomposition.[180]

Table 2.1.1: Cyclodiphosph(V)azanes catalyzed Michael addition of 2-hydroxy-1,4-naphthoquinone (**11**) to β-nitrostyrene (**10**).

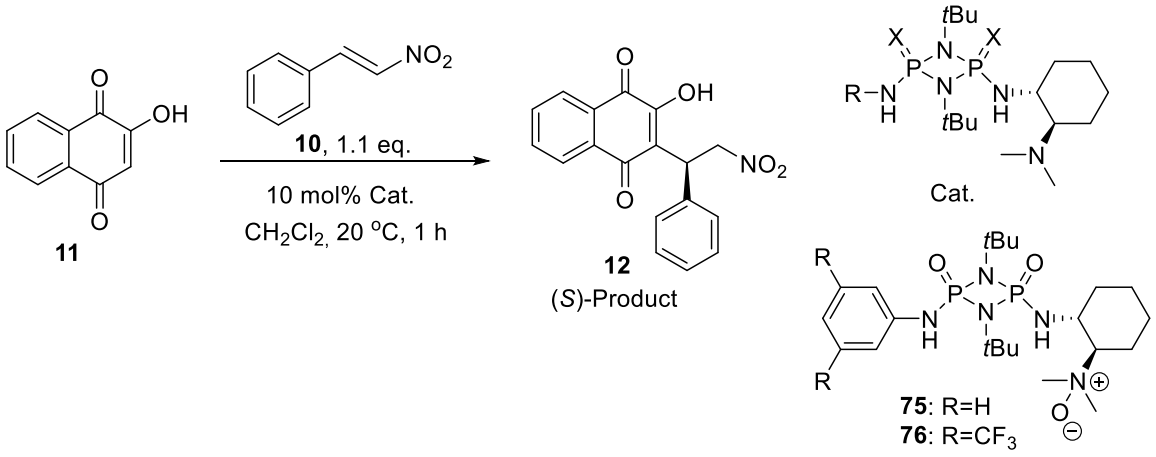

Catalyst	R of catalyst	X of catalyst	Yield(%)[a]	ee(%)[b]
None(30h)	/	/	0	/
Et_3N	/	/	84	*rac*
***all-cis*-15** [c]	(*R,R*)-*N*,*N*-DMDACH	S	83	*rac*
***all-cis*-16 (3h)**[c]	Ph	S	72	61(*S*)
4	(*R,R*)-*N*,*N*-DMDACH	O	82	53(*S*)
5	Ph	O	98	65(*S*)
6	m-$(CF_3)_2$-C_6H_3	S	94	55(*S*)
7	m-$(CF_3)_2$-C_6H_3	O	98	61(*S*)
8	m-$(CH_3)_2$-C_6H_3	S	85	62(*S*)
9	m-$(CH_3)_2$-C_6H_3	O	80	56(*S*)
75+Et_3N	Ph	O	75	*rac*
76+Et_3N	m-$(CF_3)_2$-C_6H_3	O	79	8(S)

[a]Isolated yields. [b]Chiral HPLC Daicel OJ, hexane/iPrOH 60:40, 0.7 mL/min, 254 nm, 25 °C, (*S*)-enantiomer 30.2 min, (*R*)-enantiomer: 87.3 min. [c]Reaction was reproduced according to the Literature's condition with reported catalyst *all-cis*-**15** and *all-cis*-**16**.[180]

The previous published *tert*-butyl substituted catalyst (***all-cis*-15** and ***all-cis*-16**) were firstly reproduced in this work, obtaining the product **12** with a yield of 83% as racemic by *all-cis*-**15**, which is higher than the literature value (69% yield, *rac*), and a yield of 72% with an ee of 61% by *all-cis*-**16**, which are worse than the literature value (95% yield, 67% ee),[180] but as they are not significantly deviated, we still regard them as

comparable results. Hence, we fixed the reaction condition and tested the reaction with all of the newly synthesized cyclodiphosph(V)azane catalysts (Table 2.1.1), including without any catalyst and with Et_3N as contrast group. Among these, there is no conversion without catalyst even after 30 h, and with Et_3N there is product with a good yield of 84%. For reaction with chiral catalysts, all of them give good till excellent yield ranging 80 − 98% and moderate enantiomeric excess ranging 53 − 65%, with the same major stereoisomer. Although the differences of the results are not extraordinarily remarkable, we still make some summary from them: 1. Catalysts with (*R.R*)-diaminocyclohexane on both sides are always worse than that with one side (*R,R*)-diaminocyclohexane and another side phenyl derivatives in enantiomeric excess (Cat. **4** vs. Cat. **5**, **7** and **9**, and *all-cis*-**15** vs. *all-cis*-**16**[180] and **8**); 2. For catalysts with (*R,R*)-diaminocyclohexane on both sides, or CF_3 substituted phenyl, the catalyst with oxygen are better than that with sulfur in enantiomeric excess (Cat. **7** vs. Cat. **6,** Cat. **4** vs. *all-cis*-**15**), but for methyl substituted catalysts, the form with sulfur is better than oxygen in enantiomeric excess (Cat. **8** vs Cat. **9**); 3. Trifluoromethyl or methyl substituted phenyl in this case have similar, or worse effects compared to unsubstituted phenyl in enantiomeric excess (Cat. **7**/Cat. **9** vs. Cat. **5**, and Cat. **6**/Cat. **8** vs. *all-cis*-**16**), and this result concurred with Hydrogen bond length between the oxygen of DMSO and the N−H of different cyclodiphosph(V)azanes from X−ray crystal structure.[200] In addition, oxidized by products **75** and **76** were also tested for the catalysis accompanied with additional Et_3N considering the lowered basicity on the oxidized tertial amine of catalyst. Reaction with both by−products resulted in good yields of 75% and 79%, and **76** with Et_3N even led to an ee of 8%, which could be well attributed to the steric bulk by their co-catalysis pathway. Among these, the reaction with catalyst **5** has the best yield (98%) and best enantiomeric excess (65% ee) and was hence chosen as the catalyst for further screening of reaction conditions.

For further optimization of the catalysis condition, we screened the solvent, catalyst loading and temperature (Table 2.1.2).

Table 2.1.2: Screening of solvent, catalyst loading and temperature of the asymmetric Michael addition of 2-hydroxy-1,4-naphthoquinone (**11**) to β-nitrostyrene (**10**) with catalyst **5**.

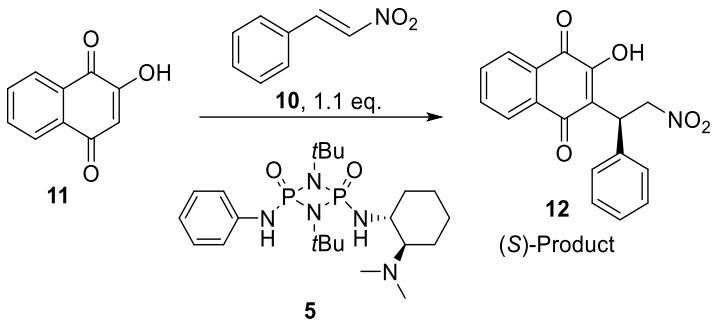

Reaction time(h)	Solvent	Cat. loading (mol%)	Temperature (°C)	Yield (%)[a]	ee (%)[b]
1	DCM	10	20	98	65(*S*)
1	1,4-Dioxane	10	20	90	60(*S*)
1	MeCN	10	20	79	36(*S*)
1	Toluene	10	20	84	72(*S*)
1	THF	10	20	83	54(*S*)
168	Toluene	1	20	99	77(*S*)
24	Toluene	1	20	94	76(*S*)
1	Toluene	5	20	48	75(*S*)
6	Toluene	5	10	90	80(*S*)
1	Toluene	10	10	42	80(*S*)
1	Toluene	10	0	27	82(*S*)
24	Toluene	10	0	84	84(*S*)
1	Toluene	10	-20	trace	n.d.
24	Toluene	10	-20	48	88(*S*)
120	Toluene	5	-20	75	90(*S*)

[a]Isolated yields. [b]Chiral HPLC Daicel OJ, *n*-hexane/*i*PrOH 60:40, 0.7 mL/min, 254 nm, 25 °C, (*S*)-enantiomer 30.2 min, (*R*)-enantiomer: 87.3 min.

For solvent, we tested some aprotic solvent since for this substrate, protic solvent like methanol has negative effect on catalysis for their competitive hydrogen bond interaction with the organocatalyst or the substrate.[125] All the solvents gave good yields (79% till 90%), while 1,4-dioxane and THF gave modest enantiomeric excess (60% and 54%), which are similar to dichloromethane. Acetonitrile gave the worst yield (79%) and enantioselectivity (36% ee), and toluene gave a good yield (84%) and

the best enantioselectivity (72% ee) and was thus identified as the optimal solvent for this reaction. For catalyst loading, we tested the lowered amount of 5% and 1% and found, that a lower catalyst loading could only slightly increase the enantioselectivity (up to 77% ee), but dramatically decrease the reaction rate, so that a much longer reaction time is needed for a good conversion of the reaction. For temperature, a lowered temperature has an obviously positive effective on the enantioselectivity as well as a hindering of the reaction rate. Reduction of temperature from 20 to 10 and 0 °C could increase the enantioselectivity from 72% ee to 80% ee and 82% ee, but also decrease the yield from 84% to 42% and 27%. For a trial of extreme condition, we set up the reaction with 5 mol% of catalyst under -20 °C, and with a reaction time of 5 days we got the yield of 75%, and the enantiomeric excess of 90% ee.

2.1.4.2 Catalysis with 4-hydroxycoumarin (27)

Coumarin scaffolds, expecially 3-substituted-4-hydroxycoumarins are frequently identified in a variety of natural products, and show significant biological properties, like anti−HIV,[240,241] antibacterial,[242] antimalarial[243], and the well-known anticoagulant named after warfarin.[244] In this work, 4-hydroxycoumarin (**27**) was selected as the subsequent nucleophile for testing in the catalytic Michael reaction with β-nitrostyrene (**10**), since chiral squaramide catalysts have been well established in this reaction by our group.[245]

Table 2.1.3: Cyclodiphosph(V)azanes catalyzed Michael addition of 4-hydroxycoumarin (**27**) to β-nitrostyrene (**10**).

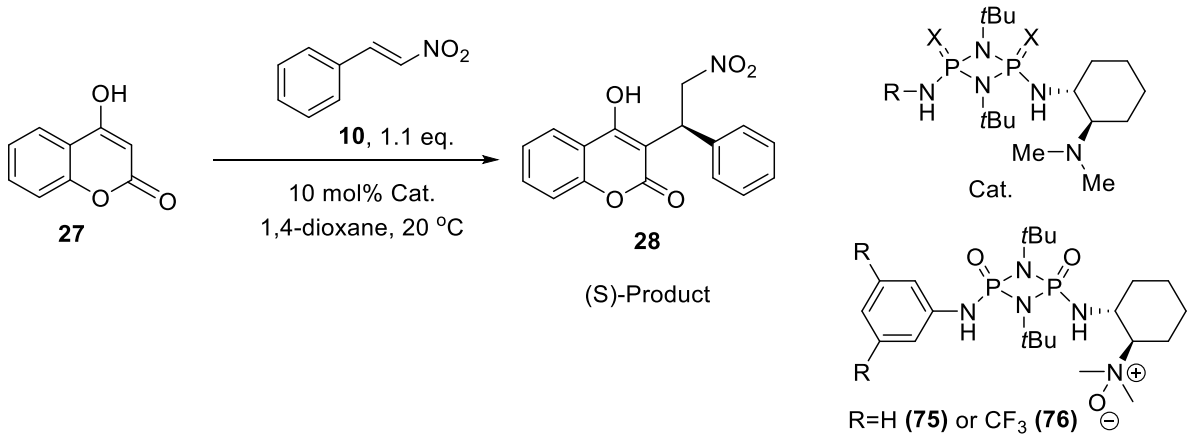

catalyst	R of catalyst	X of catalyst	%Yield[a]	% ee[b]
Et_3N (4h)	/	/	47	*rac*
***all-cis*-15**	(*R,R*)-*N*,*N*-DMDACH	S	54	6(R)
***all-cis*-16**	Ph	S	62	13(S)
4	(*R,R*)-*N*,*N*-DMDACH	O	56	2(S)
5	Ph	O	51	17(S)
6	m-$(CF_3)_2$-C_6H_3	S	63	7(S)
7	m-$(CF_3)_2$-C_6H_3	O	59	7(S)
75+Et_3N	6h	O	64	3(S)
76+Et_3N	6h	O	21	*rac*
5[c] (120 h)	5d	O	13	28(S)

[a]Isolated yields. [b]Chiral HPLC Chiralpak AD-H, sample with additional 0.1% TFA (but eluent not!), *n*-hexane/*i*PrOH 85:15, 1.0 mL/min, 254 nm, 18 °C, (*S*)-enantiomer 11.5 min, (*R*)-enantiomer: 16.4 min. [c]Reaction conducted at -20 ° C in toluene.

The reactions were conducted under constant temperature, solvent and catalyst loading conditions, with the catalysts being the variable factor (Table 2.1.3). Compared to squaramides,[245] cyclodiphosph(V)azane catalysts lead to slightly lower yields (51 − 63%), and sharp decreased ee-s (2 − 17%). Trial with toluene and Cat. **5** under -20 °C serves an improved ee of 28%, but much lower yield of 13%, ever with a longer reaction time of 120 h. As results under a mild condition are close to that of Et_3N, it could be inferred that the reaction of 4-hydroxycoumarin (**27**) and cyclodiphosph(V)azane catalysts undergoes a Brønsted base catalysis pathway prior

to a bifunctional catalysis pathway. Similar to reactions of 2-hydroxy-1,4-naphthoquinone (**11**), discrepancies between the results are not notably remarkable, and a brief summary is nevertheless proposed: 1, Catalysts carrying oxygen are in most cases better than that with sulfur in ee% (Cat. **5** vs. *all-cis*-**16**, and compared to Cat. **4**, the Major product from *all-cis*-**15** is even a (*R*)-isomer), while Cat. **7** and Cat. **6** led to the same ee-s; 2, Trifluoromethyl substituted phenyl in this case have a worse effect than that of unsubstituted phenyl in ee-s. (Cat. **6** vs. *all-cis*-**16**, Cat. **7** vs. Cat. **5**); 3, Catalysts with (*R,R*)-*N*,*N*-DMDACH on both sides performe always worse than that with one side DMDACH and another side phenyl in ee-s. (*all-cis*-**15** vs. *all-cis*-**16**, Cat. **4** vs. Cat. **5**).

2.1.4.3 Catalysis with diethyl malonate (29), acetylacetone (31), indole (33) and *N*-Boc-oxindole (35)

As in Chapter 1.3.2.2 mentioned, diethyl malonate (**29**) and acetylacetone (**31**) are suitable nucleophiles for catalytic asymmetric Michael additions to nitrostyrenes with chiral thioureas and squaramides.[132,136] In addition, indole (**33**) has also been well established in 1,4-addition to nitrostyrene not only with H−bond donors bearing hydroxy group,[127] but also with bifunctional catalysts.[246] Thus, these 3 compounds were tested for 1,4-addition to nitrostyrene fixing the condition with cyclodiphosph(V)azane catalyst **5** in toluene at 20 °C and varying the reaction time (Scheme 2.1.4.1).

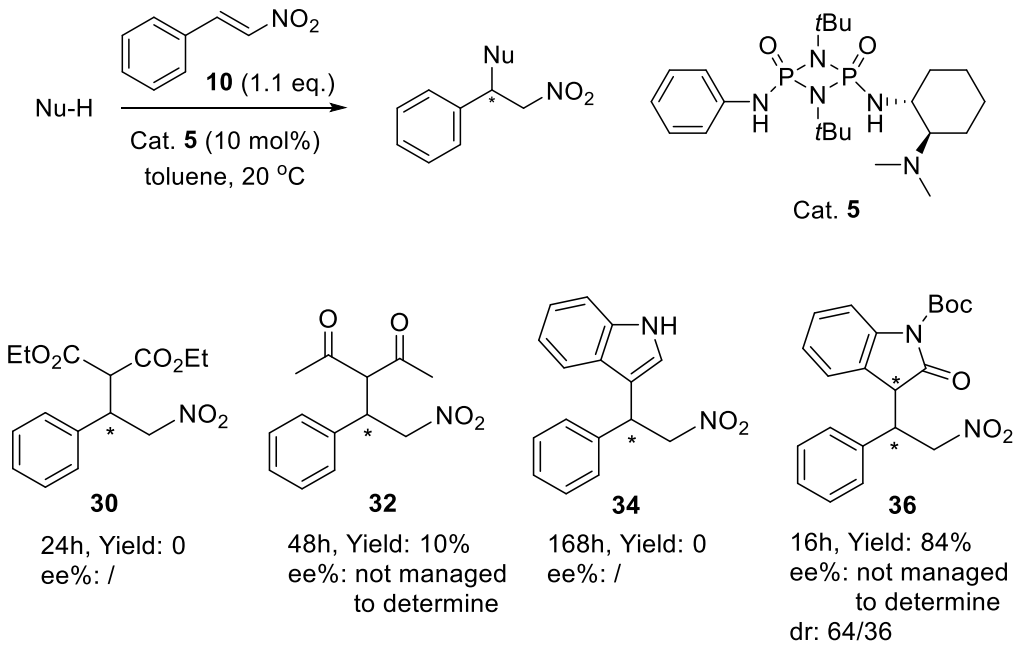

Scheme 2.1.4.1: 1, 4-additions of β-nitrostyrene to various nucleophiles fixing the condition with chiral cyclodiphosph(V)azane catalyst **5** in toluene at 20 °C and varying the reaction time.

However, there was no conversion for diethylmalonate (**29**) after 24 h, only 10% yield for acetylacetone (**31**) after 48 h, and no conversion for Indole (**33**) after 168 h. The underlying reasons for the failure of these trials to yield expected results remain unclear, but the complexity in prediction of an optimized hydrogen bonding pattern could be the prior potential explanation due to the significant influence of both the substrate and the catalyst on the reaction pathway. However, a preliminary tendency can be postulated when comparing 2-hydroxy-1,4-naphthoquinone (**11**) and 4-hydroxycoumarin (**27**) as the relative "active" nucleophiles. According to the predicted pK_a value by Scifinder, nucleophiles with lower pK_a values (2-hydroxy-1,4-naphthoquin one (**11**): 4.31; 4-hydroxycoumarin (**27**): 4.50 (literature: 4.10)[247]), namely with higher acidities, appear to be more "active" than those with higher pK_a values (diethyl malonate (**29**): 11.84; acetylacetone (**31**): 8.94; indole (**33**): 17.00).

Based on this cursory prediction, N-Boc-oxindole (**35**) was selected then as the next potential nucleophile for its predicted high acidity (pK_a: -0.59), and its catalytic 1, 4-addition to nitrostyrene with diaminonitroethylene as bifunctional hydrogen bonding catalyst was reported.[248] With the same reaction condition for diethylmalonate (**29**),

acetylacetone (**31**) and indole (**33**), a product **36** with a yield of 84% was achieved after 16 h, accompanied with a dr of 64/36. However, the ee could not be determined after multiple trials of chiral HPLC test with chiral HPLC column available in the working group. The only literature reporting the chiral HPLC condition tests the corresponding deprotected product with the chiral HPLC column which is not available in the working group.[249]

2.1.4.4 Catalysis with Kojic acid chloride (15)

As a relatively novel compound, Kojic acid derivatives have demonstrated notable bioactivities.[250–253] A recent study has revealed their efficacy in 1,4-addition to nitroolefins in the presence of squaramide catalysts.[254] Among these derivatives, Kojic acid chloride has a predicted pK_a value of 7.80 (according to Scifinder), suggesting its potential for H−bond ing catalysis by cyclodiphosph(V)azanes. Consequently, asymmetric Michael addition of β-nitrostyrene (**10**) to Kojic acid chloride (**15**) with a fixed, mild reaction condition and different cyclodiphosph(V)azanes catalysts were tested (Table 2.1.4).

Table 2.1.4: Cyclodiphosph(V)azanes catalyzed Michael addition of Kojic acid chloride (**15**) to β-nitrostyrene (**10**).

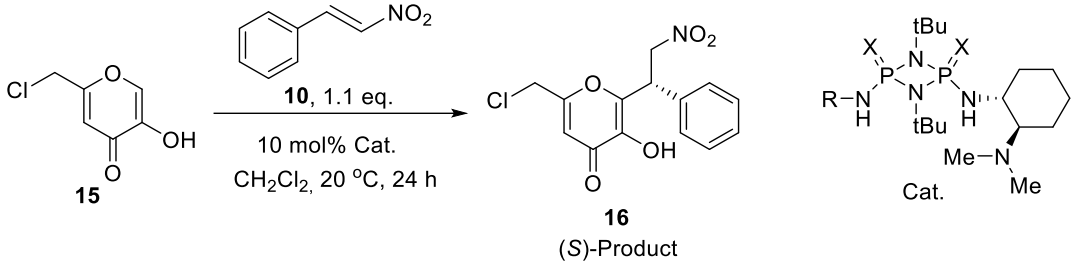

catalyst	R of Catalyst	X of Catalyst	Yield(%)[a]	ee(%)[b]
4	(*R,R*)-*N*,*N*-DMDACH	O	41	17(*S*)
5	Ph	O	54	78(*S*)
6	m-$(CF_3)_2$-C_6H_3	S	66	74(*S*)
7	m-$(CF_3)_2$-C_6H_3	O	60	75(*S*)
8	m-$(CH_3)_2$-C_6H_3	S	70	80(*S*)
9	m-$(CH_3)_2$-C_6H_3	O	63	70(*S*)

[a]Isolated yields. [b]Chiral HPLC Chiralpak OJ-H, *n*-hexane/*i*PrOH 50:50, 0.5 mL/min, 254 nm, 25 °C, (*S*)-enantiomer 46.0 min, (*R*)-enantiomer: 111.3 min.

Kojic acid chloride (**15**) was synthesized by Dr. rer. nat. Denis Sartakov according to the reported method.[255] Almost all the new catalysts gave moderate yields of product **16**, ranging 41 − 70%, and good enantiomeric excess ranging 70 – 80%, except for Cat. **4** with a much lower ee of 17%. For this reaction, the catalysts performed differently in the tendency compared with 2-hydroxy-1,4-naphthoquinone (**11**): 1, Catalysts with sulfur have better enantiomeric excess than that with Oxygen (Cat. **6** vs. Cat. **7**, Cat. **8** vs Cat. **9**); 2, Catalysts with CH_3 performed better than that with CF_3 or without substitution group on phenyl, and catalyst with CH_3 and sulfur has the best ee, and catalyst with unsubstituted phenyl performed still very well.

Notably, we observed an enantioenrichment in solution of product under crystallization. Normally we prepared an original solution of a certain product from a catalyzed reaction with a certain chiral catalyst with enantiomeric excess as the sample for chiral

HPLC, and test its ee. Occasionally we stored a sample of **16** for overnight and a crystallization of product took place, we tested then the ee of the solution part again and found surprisedly a significant rising of the ee. For a further test, we prepared the solution of the product **16** of catalysis with catalyst **9**, tested the ee and got the value of 70%. Then we stored the solution and it formed the crystal, and we separated the solution and the crystal and tested the ee for each, and got 85% from the solution part, and 44% from the crystal part (Figure x).

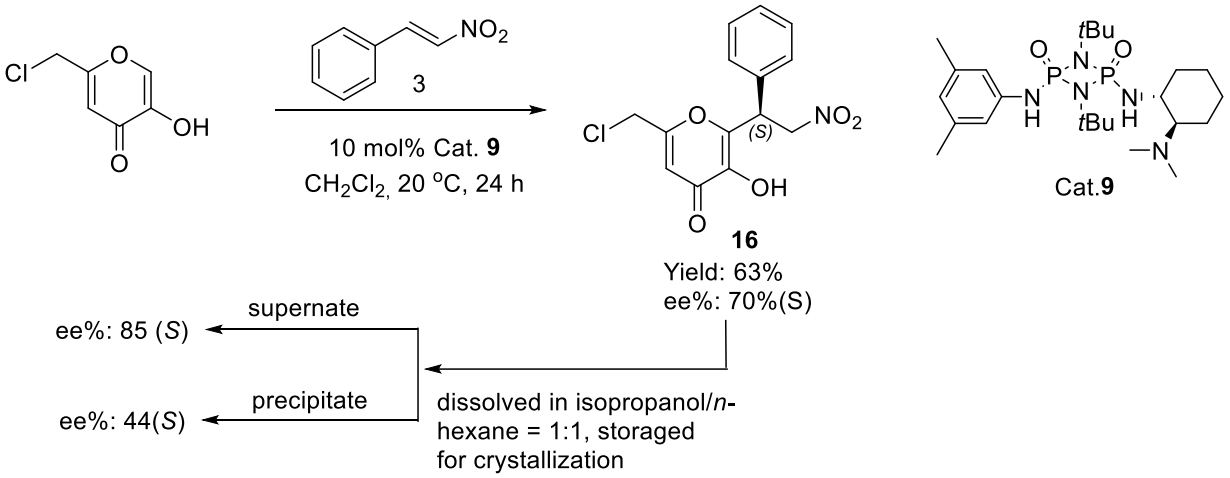

Scheme 2.1.4.2: Test of enantioenrichment in solution of product **16**.

Solely with this result, it's still insufficient to imply to which form of crystalline racemate our product belongs to, according to Roozeboom's definition,[256] but it's still obvious that it belongs to the form whose melting point of racemate is lower than that of enantiomer.

2.1.4.5 Catalysis with Meldrum's acid (13)

As a dicarbonyl compound, Meldrum's acid (**13**) is well known for its high acidity (pK_a: 4.83[257]) even without a carboxylic acid group. Takemoto successfully invested it for the thiourea catalyzed asymmetric Michael addition with nitroolefin in his early study,[136] and the reaction turned out to be a key step for enantioselective synthesis to (*S*)-pregabalin, an anticonvulsant, analgesic, and anxiolytic amino acid medication.[258]

Thus, it was tested for asymmetric Michael addition to β-nitrostyrene (**10**) with a fixed, mild reaction condition and different cyclodiphosph(V)azanes catalysts, as well as the Takemoto's catalyst (**37**) for a comparison purpose (Table 2.1.5).

Table 2.1.5. Cyclodiphosph(V)azanes catalyzed Michael addition of Meldrum's acid (**13**) to β-nitrostyrene (**10**)

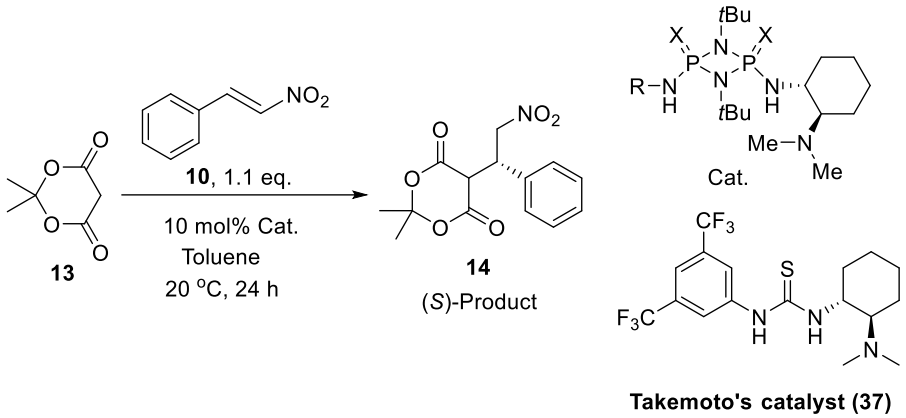

catalyst	R of Catalyst	X of Catalyst	Yield(%)[a]	ee(%)[b]
4	(*R,R*)-*N,N*-DMDACH	O	59	22(*S*)
5	Ph	O	76	55(*S*)
6	m-$(CF_3)_2$-C_6H_3	S	45	15(*S*)
7	m-$(CF_3)_2$-C_6H_3	O	69	38(*S*)
8	m-$(CH_3)_2$-C_6H_3	S	63	15(*S*)
8[c]	m-$(CH_3)_2$-C_6H_3	S	63	*rac*
9	m-$(CH_3)_2$-C_6H_3	O	72	46(*S*)
37	/	/	74	48(*S*)

[a]Isolated yields. [b]Chiral HPLC Chiralpak AD-H after chemical correlation to diethylmalonate adduct, *n*-hexane/*i*PrOH 90:10, 1.0 mL/min, 210 nm, 25 °C, (*S*)-enantiomer 17.4 min, (*R*)-enantiomer: 49.0 min. [c]Meldrum's acid: 2.0 eq, Solvent: Toluene(0.4mL).

It was firstly carried out under literature's condition (0.4 mL solvent, 2.0 eq. *β*-nitrostyrene (**10**))[136] and our previous condition (1.2 mL solvent, 1.1 eq *β*-nitrostyrene (**10**)) with catalyst **8**, and it surprisedly exhibits that the solvent amount and equivalent

of substrate significantly affect the ee of product **14**, and our previous condition has a better ee. Then we fixed mild reaction condition as our previous condition, and screened different catalysts (Table 3). All the new catalysts gave moderate till good yields ranging 45 − 76%, and low till moderate enantiomeric excess ranging 15 − 55%. As the catalyst **5** has a higher enantiomeric excess than that of Takemoto's catalyst with literature's condition (46% ee),[136] which is also till now the best ee for product **14**, we reproduced this reaction with Takemoto's catalyst (**37**) under our condition, leading to a similar performance. For this reaction, yields and enantiomeric excess has notable positive correlation. The performance of catalysts has similar substitution group related tendency, compared with 2-hydroxy-1,4-naphthoquinone (**11**): 1, Catalysts with sulfur have worse performance than that with Oxygen (Cat. **6** vs. Cat. **7**, Cat. **8** vs Cat. **9**); 2, Catalysts with CF_3 performed not better than that with CH_3 (Cat. **6** vs. Cat. **8**, Cat. **7** vs Cat. **9**), but unsubstituted form (Cat. **5**) is the best, even better than that of Takemoto's catalyst. For the generally low ee-s by this substrate, Takemoto made a plausible reasoning for the missing of a cyclic enol form of 1,3-dicarbonyl compounds, which might be crucial for a good enantioselectivity.[136]

2.2 *L*-proline derivatives as chiral scaffold

2.2.1 Motivation

As mentioned in Chapter 1.6.1, *N*-substituted-*L*-proline derived chiral diamines have been demonstrated to be powerful chiral scaffolds for H−bond catalysts based on thiourea and squaramide motifs and were well established in asymmetric Michael additions.[214,215,217] Due to the catalytic potential of the cyclodiphosphazane catalysts with (*R*,*R*)-diaminocyclohexane as chiral scaffold discovered by our group,[180] it is logical to explore the variation of the chiral diamino scaffold into *N*-substituted-*L*-proline−derived chiral diamines and to assess their catalytic activities.

Aiming at this target, a reproducing of the 9−step synthesis to (*S*)-2-((*R*)-aminophenylmethyl)-1-methylpyrrolidine **((*S,R*)-47)** via a trityl protected intermediate **(*S,R*)-43** involving a Mitsunobu reaction as the key step should be a realistic plan (Scheme 2.2.1.1, a), with a configuration retention at the C5 atom.[215] If the newly synthesised diamine is in sufficient quantity, the subsequent synthesis of new chiral cyclodiphosphazane catalysts like Cat. **48** can be attempted (Scheme 2.2.1.1, b).

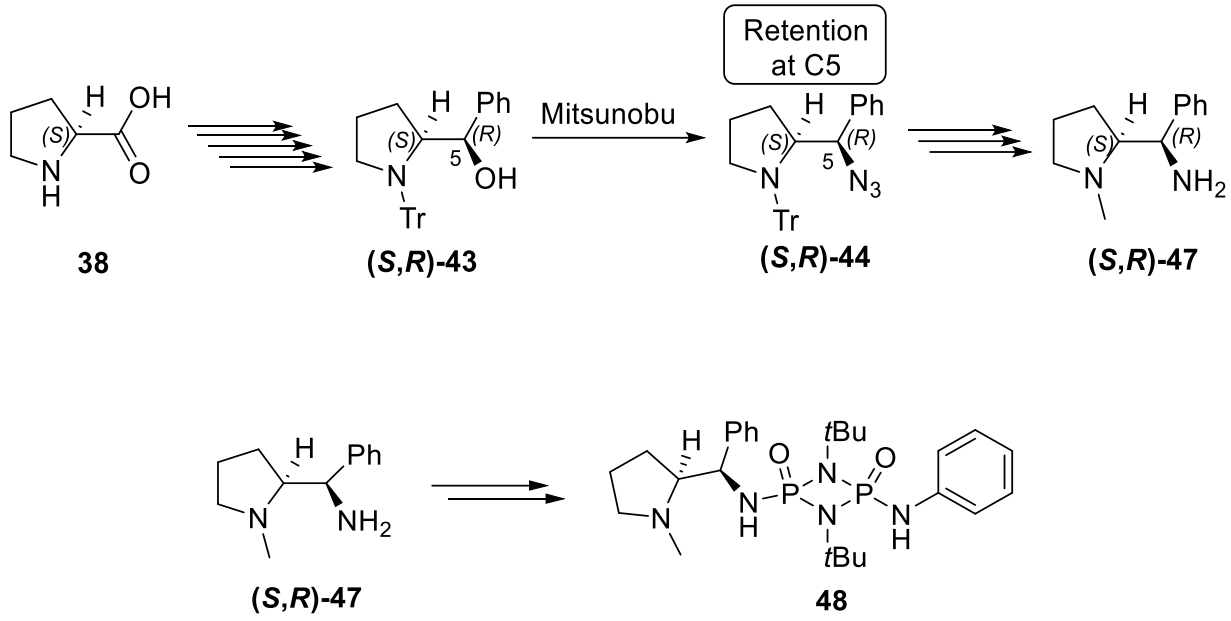

Scheme 2.2.1.1: a) 9−step synthetic route to methyl-*L*-proline derivative **(*S,R*)-47** via trityl protected intermediate **(*S,R*)-43**. b) Synthesis of new chiral cyclodiphosphazane **48** with **(*S,R*)-47**.

In addition, the effect of the neighboring group on Mitsunobu reaction of *N*-substituted−prolinols remains to be further explored. For example, it would be interesting to test the Mitsunobu reaction of *N*-methyl-prolinol **(*S,S*)-51** since methyl, as a less bulky and more electron−donating group on prolinol, has never been tested for its neighboring group effect (Scheme 2.2.1.2).

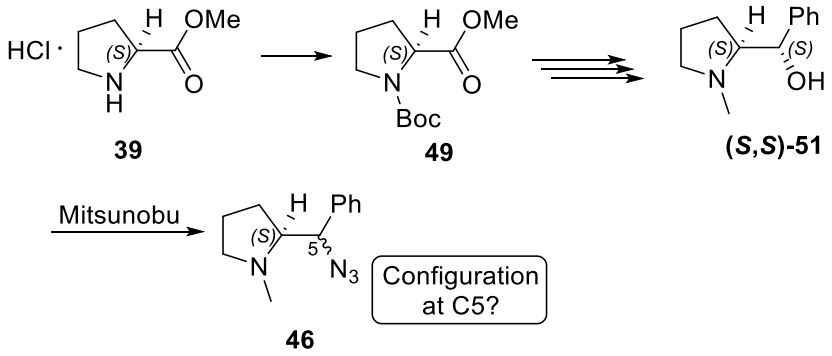

Scheme 2.2.1.2: Synthesis of *N*-methyl-prolinol **(*S,S*)-51** and its Mitsunobu reaction.

2.2.2 Synthesis and characterization of trityl substituted *L*-proline derivatives

The synthesis of trityl substituted *L*-proline derivatives was conducted in accordance with the established methodology originally described by Chemla and co-workers,[259] and Kesavan and co-workers,[215] and most of the synthesis works were carried out in cooperation with B. Sc. student Ioannis Panagiotidis.

2.2.2.1 Synthesis of *N*-trityl-(*S*)-proline methyl ester (40)

In the first synthesis step, the carboxylic acid function of *L*-proline (**38**) was esterified with methanol. For this purpose, the hydroxyl group was converted to an acyl chloride by adding thionyl chloride ($SOCl_2$). The solvent methanol (MeOH) acted as a nucleophile, which then attacked the carbonyl of the acyl chloride. By splitting off HCl, *L*-proline methyl ester **39** in salt form was obtained (Scheme 2.2.2.1). Therefore, the crude product without purification would be further invested for the following step, involving the introduction of a trityl protecting group at the N terminus of the pyrrolidine ring of proline ester **39** (Scheme 2.2.2.1).

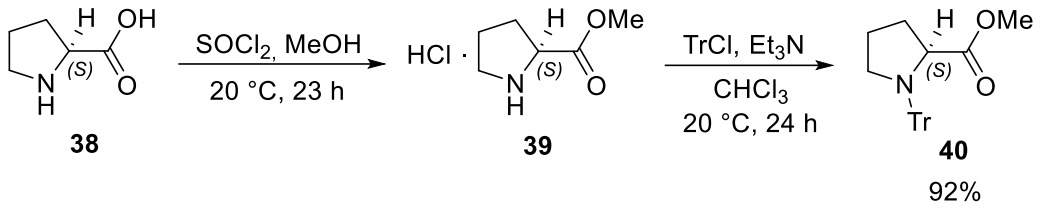

Scheme 2.2.2.1: Synthesis of *N*-tritylprolineester **40** from *L*-proline (**38**).

After the addition of triphenyl methyl chloride (trityl chloride: TrCl), its methine group is nucleophilically attacked by the free electron pair of the N atom, and HCl is eliminated by the added triethylamine (Et_3N), promoting the conversion of the reaction. *N*-tritylprolineester **40** was obtained in a yield of 92% after recrystallization, remaining traces of chloroform and diethyl ether according to the ^{1}H-NMR.

2.2.2.2 Synthesis of *N*-trityl-(*S*)-prolinal (42)

The next synthesis involves the reduction of prolineester **40** to the prolinol **41** via $LiAlH_4$, followed by a Swern oxidation to form the corresponding aldehyde **42** (Scheme 2.2.2.2).

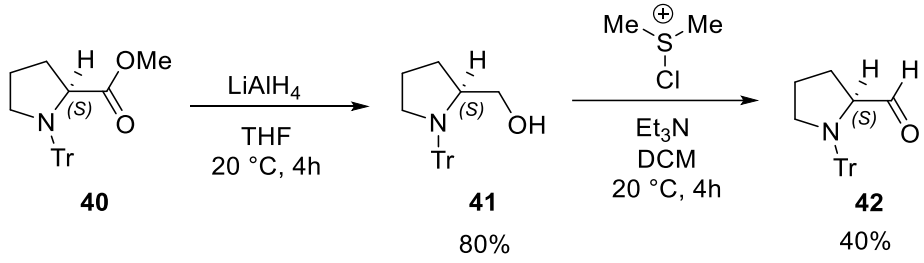

Scheme 2.2.2.2: Synthesis of *N*-tritylprolinal **42** from *N*-tritylprolineester **40**.

The reduction from **40** to **41** undergoes a cascade mechanism. First, a hydride anion is added to the carbonyl function of the ester, releasing a tetrahedral intermediate. By eliminating an alcoholate, an aldehyde is formed. This aldehyde is further hydrogenated and forms an aluminium alcoholate. After subsequent hydrolysis with

sodium potassium tartrate, *N*-tritylprolinol (**41**) was obtained with a yield of 80% (lit. 97%).[259] Apart from traces of THF, no traces of reactant or other impurities were present in the ^{1}H-NMR spectrum even without further purification. Due to the good miscibility of water and THF, there were problems during extraction with DCM. As a result, quantities of product remained in the aqueous phase and yields were lost.

Then, the preparation of *N*-tritylprolinal **42** proceeded via a Swern oxidation with DMSO, oxalyl chloride $(COCl)_2$ and Et_3N. In the first step, DMSO reacts with $(COCl)_2$ to form a chlorosulfonium ion (Scheme 2.2.2.3).

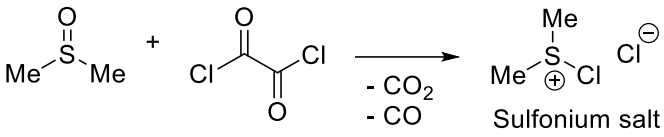

Scheme 2.2.2.3: Formation of the active sulfonium intermediate.

This then reacts with compound **41** to form a sulfonium salt. The addition of Et_3N results in the release of compound **42** in a yield of 40%, after recrystallization. One reason for the low yield may be the slight decomposition of $(COCl)_2$. As a result, the oxidizing agent DMSO was not fully activated, which led to incomplete conversion of compound **42**. Furthermore, residue of product in mother liquid by recrystallization could also result in a decrease of yield.

2.2.2.3 Synthesis of (*R*)-phenyl-((*S*)-1-tritylpyrrolidin-2-yl)methanol ((*S*,*R*)-43)

In the next synthesis step, a phenyl group is introduced through a Grignard reaction with stereoselectivity. The newly built *R*-configuration is necessary for the following Mitsunobu reaction (Scheme 2.2.2.4).

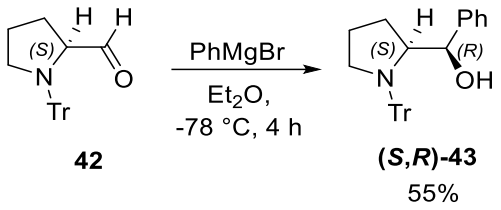

42 **(*S*,*R*)-43** 55%

Scheme 2.2.2.4: Synthesis of *N*-tritylprolinol **(*S*,*R*)-43** from *N*-tritylprolinal **42**.

Chemla and co-workers were able to achieve a dr of >98:2 in the conversion of *N*-tritylprolinal **42** to compound **(*S*,*R*)-43** in a Grignard reaction with phenylmagnesium bromide.[259] The reaction was carried out at -78 °C in order to control it thermodynamically. In this work, compound **(*S*,*R*)-43** was obtained in a yield of 55% after purification with column chromatography, which is significantly lower than Chemla's yield (90%),[259] but similar to that of Kesavan (58%).[215] Loss of yield occurs either due to a potential accumulation of moisture in the diethyl ether which could cause the hydrolysis of Grignard reagent, or an incomplete conversion to the Grignard reagent. The ^{1}H-NMR spectrum shows approximately only one diastereomer, and the rotation value was determined as $[\alpha]_D^{20}$ = -77.20, which are both in agreement with the literature,[215] demonstrating an excellent stereoselectivity of this reaction.

The decisive factor for the selectivity is that the carbonyl function of the *N*-tritylprolinal **42** is in a pseudoaxial position and the trityl group is in the *trans* position to the carbonyl group. According to the reported PM3 calculations,[259] this results in two possible conformations that can influence the selectivity: In the first conformation (**C1**), the oxygen of the carbonyl function lies across the five−membered ring, the Si side of which is sterically blocked by the trityl group. This results in a nucleophilic attack on the Re side of the carbonyl function (TS1), which leads to the main product 6 (Scheme 2.2.2.5, a).

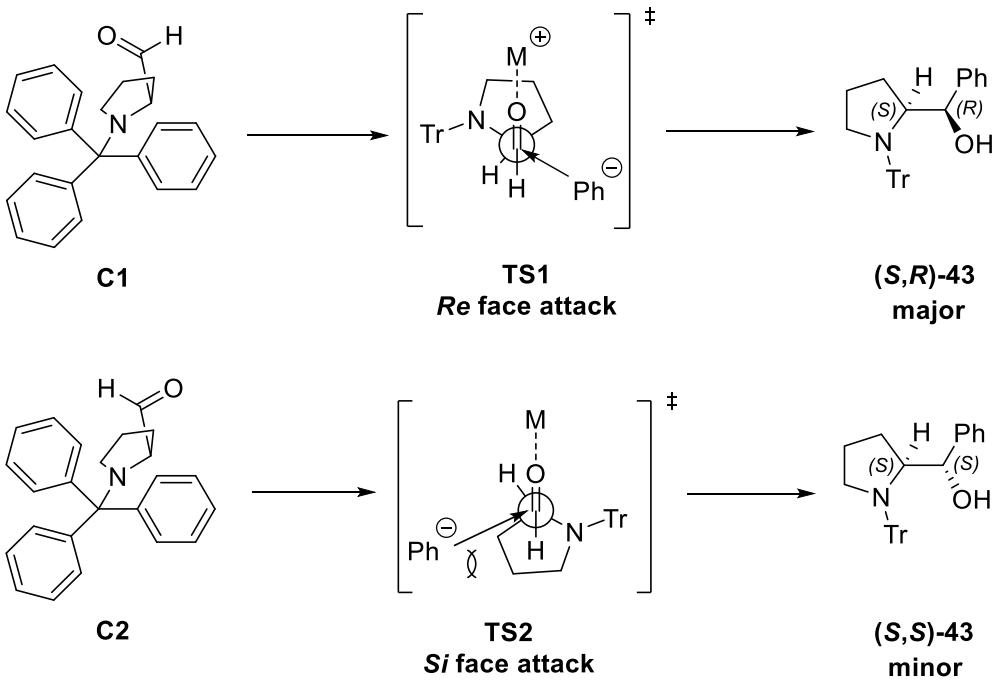

Scheme 2.2.2.5: Transition states of a) *Re* and b) *Si* face attack to *N*-tritylprolinal **42** by Grignard reagent.[259]

In the possible second conformation (**C2**), the carbonyl oxygen is outside the five−membered pyrrolidine ring. In this case, the trityl group blocks the Re side (**TS2**) and the nucleophilic attack on the Si side is energetically favored (Scheme 2.2.2.5, b). However, Si side attack of the organometallic species in TS2 is hindered by the pyrrolidine ring, leading to a higher energy compared to TS1, and the corresponding product is thus a minor isomer.

2.2.2.4 Synthesis and characterization of (*S*)-2-((*R*)-azido(phenyl)methyl)-1-tritylpyrrolidine ((*S*,*R*)-44)

From the next step, the further syntheses for the preparation of compound **(*S*,*R*)-44** were carried out as described by Kesavan and co-workers (Scheme 2.2.2.6).[215] In this step, the hydroxyl group was substituted by an azide group using the Mitsunobu reaction explained in Chapter 1.6.2 while retaining the configuration.

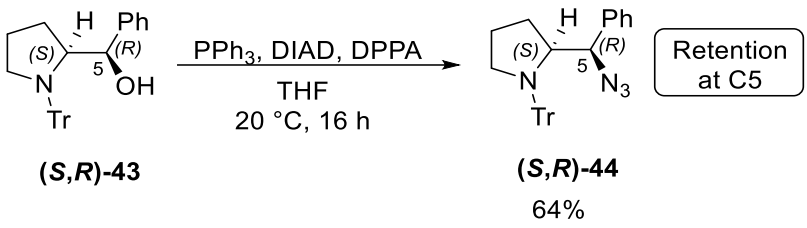

(*S*,*R*)-43 **(*S*,*R*)-44** 64%

Scheme 2.2.2.6: Mitsunobu reaction of *N*-tritylprolinol **(*S*,*R*)-43** to azido-*N*-tritylproline **(*S*,*R*)-44**.

In this work, diisopropylazodicarboxlate (DIAD) was chosen as the starting reagent instead of DEAD. Compound **(*S*,*R*)-44** was obtained in a yield of 64% (lit. 80%). Loss of yield is possible due to the formation of by−products. It is possible that reactions with an inversion at the C5 atom occurred and small amounts of epimer **(*S*,*S*)-44** were formed, and by column chromatography it was separated and disposed. The analytical data (^{1}H-NMR, ^{13}C-NMR, ESI-MS) agree with those from the literature. A rotation value of $[\alpha]_D^{20}$= -70.19 was determined for the product, which deviates slightly from the literature value (lit.: $[\alpha]_D^{20}$ = -93.5).[216] With this value, it could be concluded that an **(*S*,*R*)-44** instead of **(*S*,*S*)-44** was achieved, since the rotation value of the subsequently synthesised Bn−protected variant based on this diastereomer by Kesavan and co-workers is in agreement with Juaristi's **(*S*,*R*)-61**.[218]

The absolute configuration together with the molecular structure of compound **(*S*,*R*)-44** was confirmed by crystal structure analysis (Figure 2.8). Single crystal was obtained by B. Sc. Ioannis Panagiotidis.

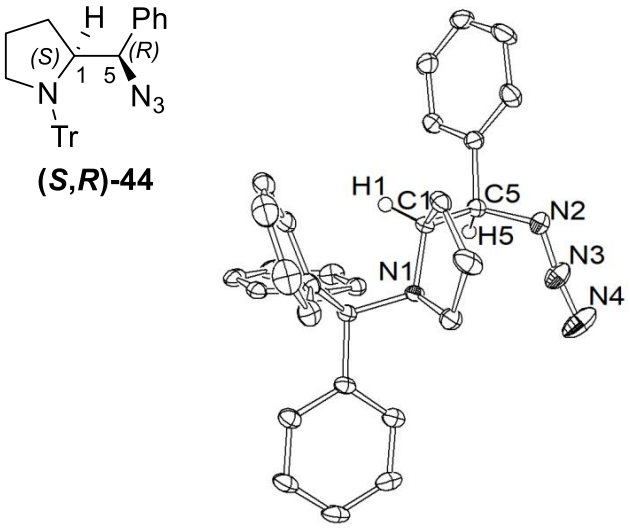

Figure 2.8: Crystal structure of **(*S,R*)-44** with thermal ellipsoids at the 50% probability level; protons except C1−H and C5−H are omitted for clarity.

The crystal structure analysis exhibits an *R*-configuration at the C5 atom, demonstrates the retention at this position, and thus indicates the formation of an aziridinium ion intermediate via participation of the neighboring group during the Mitsunobu reaction, as discussed in Chapter 1.6.2 (Scheme 2.2.2.7).

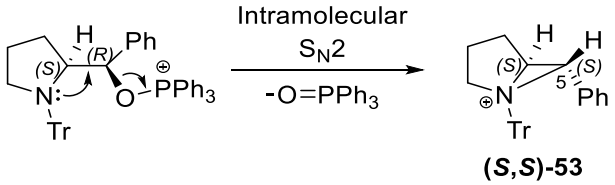

Scheme 2.2.2.7: Formation of aziridinium ion intermediate **(*S,S*)-53** via participation of the neighboring group with trityl.

Brief DFT computations (b97d3/6-31G(d)) was carried out by Professor Dr. Bernd Goldfuss, showing two possible competing transition states (**TS-*Re*** & **TS-*Si***) which are possible in the azide substitution of the aziridinium intermediate **(*S,S*)-53** (Figure 2.9). The Gibbs free energy of both states was calculated. The azide substitution in **TS-*Re*** leads to a *Re* side attack on the C5 atom and thus to an *R*-configuration at this

position, while the **TS-*Si*** variant leads to an *S*-configuration at the C5 atom. The calculated energy of **TS-*Re*** is 1.76 kcal/mol lower than **TS-*Si***, and therefore **TS-*Re*** should be more favored. Based on a neighboring group effect that leads to the *R*-configuration at the C5 atom, the theoretical calculations agree with the experimentally determined configuration.

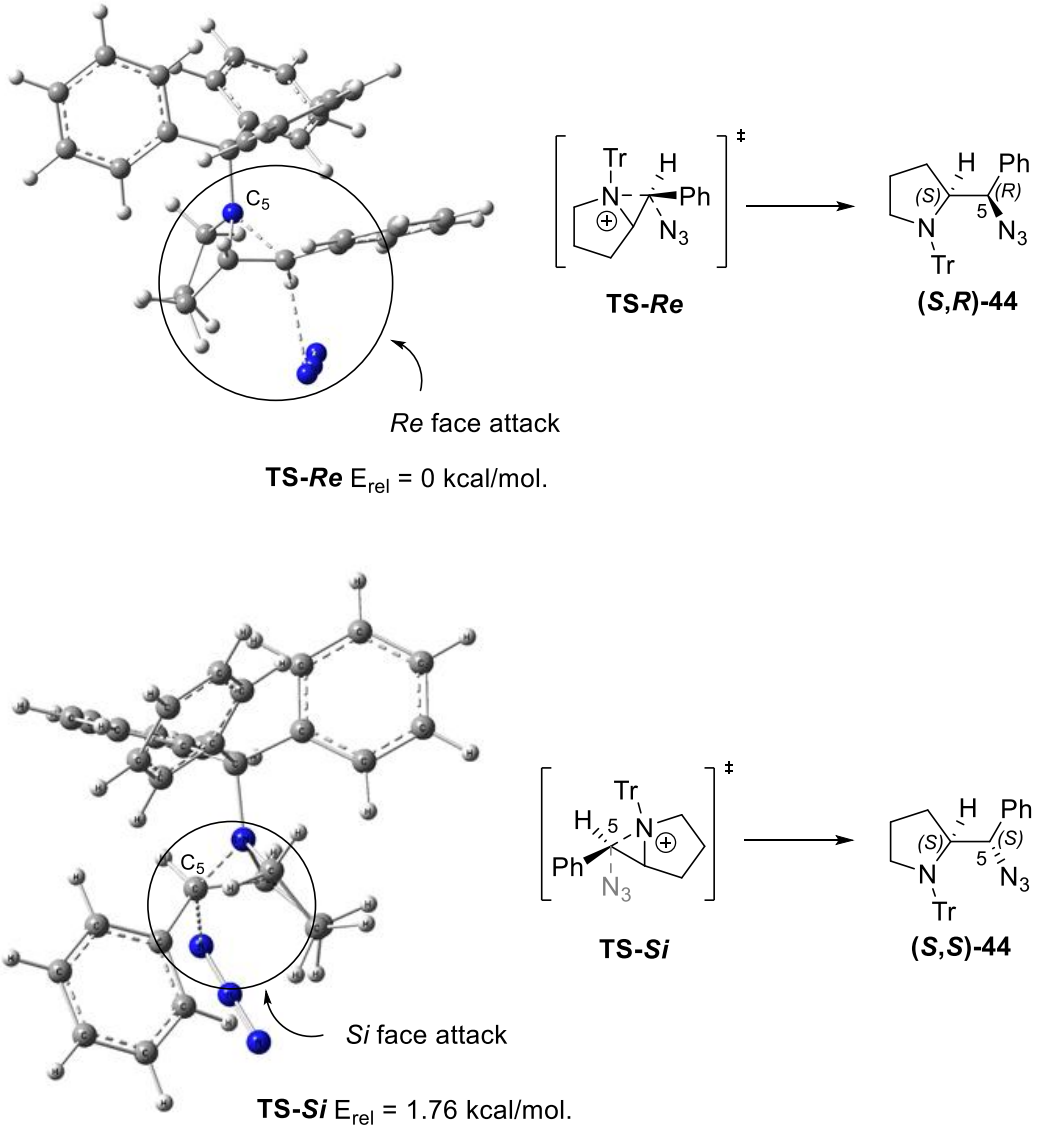

Figure 2.9: Two competing transition states of a) *Re* and b) *Si* face attack at C5 atom of the aziridinium intermediate **(*S,S*)-53** according to DFT computations, b97d3/6-31G(d).

2.2.2.5 Synthesis of (*S*)-2-((*R*)-azido(phenyl)methyl)-1-methylpyrrolidine (46)

The next synthesis steps involved the removal of the trityl protecting group. For this purpose, compound **(*S,R*)-44** was hydrolyzed with hydrochloric acid (HCl) and then worked up (Scheme 2.2.2.8). Without further purification and without further analysis of compound **45**, this was used for the further conversion.

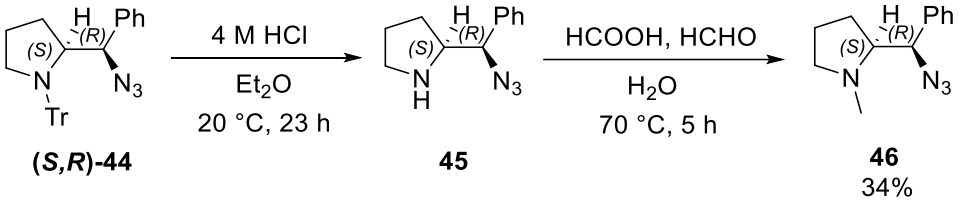

Scheme 2.2.2.8: Synthesis of azido-*N*-methylproline **46** from azido-*N*tritylproline **(*S,R*)-44**.

The secondary amine in the pyrrolidine ring of compound **45** was then converted in an Eschweiler−Clarke methylation. The methylation reagent used is formaldehyde, which is used in excess together with excess formic acid.

The yield starting from compound **(*S,R*)-44** was 34% (lit. 52%).[215] Yield losses were caused possibly by a lack of purification like column chromatography, despite the good conversion according to TLC. It should also be mentioned that the conversion of compound **45** to **46** was not complete according to TLC, even with an expanded reaction time.

2.2.2.6 Attempt to Synthesize (*S*)-2-((*R*)-amino(phenyl)methyl)-1-methylpyrrolidine ((*S,R*)-47)

In the final synthesis step, the azide group of compound **46** was to be reduced with $LiAlH_4$ to a primary amine to obtain the target compound **(*S,R*)-47** (Scheme 2.2.2.9).

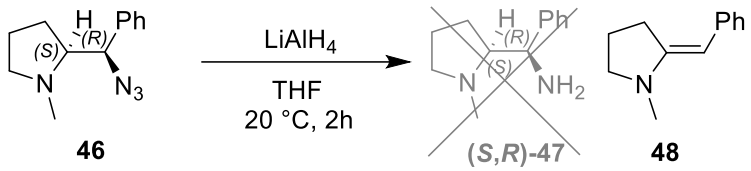

Scheme 2.2.2.9: Attempt to Synthesize the of *N*-methylprolinediamine **(*S,R*)-47** from azido-*N*-methylproline **46**, resulting in an elimination product **48**.

Low scale of starting material (0.83 mmol) was invested in the reaction as this was the last step with accumulated loses of yields in previous steps. Despite column chromatographic purification after the reaction, signals from an unidentifiable by−product and cyclohexane were present in the ^{1}H-NMR spectrum. Different eluents were tested in the TLC to separate the impurity from the product. However, only one component could be detected on all TLC plates and, after it was isolated, it turned out to be in a very low yield of less than 10 mg. The characterization of compound **(*S,R*)-47** proved to be problematic. Firstly, no single crystal could be obtained for crystal structure analysis as the product is present as an oil. For this reason, only a ^{1}H-NMR, ^{13}C-NMR and an ESI-MS were recorded. The chemical shifts and the calculated integrals of the ^{1}H-NMR spectrum do not match the target molecule, and show many impurities, which make the exact determination of yield impossible. In the ^{13}C-NMR spectrum, the signals could not be assigned because of a lot of impurities. The ESI-MS spectrum could not detect a signal matching the molar mass of the target compound. Instead, a signal was present at 174 m/z (100%). This agrees with the molecular formula $[C_{12}H_{16}N + H]^{+}$. This molecular formula is in accordance with the Hoffman elimination's product **48** of the target molecule **(*S,R*)-47** (Scheme 2.2.2.10). Some of the signals of the ^{1}H-NMR spectrum could be assigned to compound **48**. Since there was no starting material left, further tests of this reaction were not conducted.

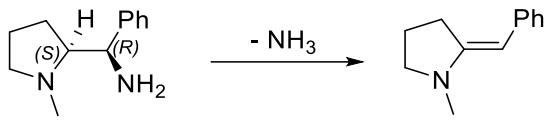

(*S,R*)-47
Molar mass: 190 g/mol

48
Molar mass: 173 g/mol

Scheme 2.2.2.10: Plausible elimination from **(*S*,*R*)-47** to **48** as the side reaction.

2.2.3 Synthesis and characterization of methyl substituted *L*-proline derivatives

N-methyl-*L*-prolinol was synthesised in this work, starting with the Boc protection, followed by one−pot ester reduction/alkylation, and the direct exchange from Boc to methyl. Afterwards, the Mitsunobu reaction on *N*-methyl-*L*-prolinol was tested. Most of the synthesis works were carried out in cooperation with M. Sc. student Yinyu Sun.

2.2.3.1 Synthesis of *tert*-butyl (*S*)-2-((*S*)-hydroxy(phenyl)methyl)pyrrolidine-1-carboxylate (*S,S*)-50

The protection of amine with Boc group was conducted following the method from Nelson, Marsden and co-workers,[260] and the subsequent one−pot ester reduction/alkylation reaction was conducted following the method from Rye and co-workers (Scheme 2.2.3.1).[216]

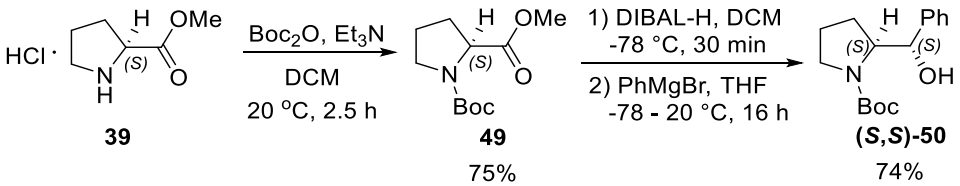

39

49
75%

(*S,S*)-50
74%

Scheme 2.2.3.1: Synthesis of *N*-Bocprolinol **(*S,S*)-50** from *L*-prolineester **39**.

The optimized synthetic route to Mitsunobu substrate **(*S*,*S*)-51** is shown in Scheme 2.2.1.2. Starting from **39**, the first step is the Boc protection of the amine using di-*tert*-butyldicarbonate (Boc_2O) and Et_3N, to prevent the lone pair on the secondary amine on the pyrrolidine ring from undergoing nucleophilic interaction with subsequent reagents. Apart from Boc protection, other protecting groups of amines include benzyl (Bn), trityl (Tr) and tosyl (Ts). Boc was selected for its potential to undergo direct conversion to methyl. The Boc-protected product **49** was obtained in yield of 75% (lit.: 99%)[260] after column chromatography. The resulting product was determined by the ^{1}H-NMR spectroscopy.

In the second step, the methyl ester **49** was transformed directly to phenyl prolinol derivative **(*S*,*S*)-50** in a one−pot ester reduction/alkylation reaction with 74% yield (lit.: 74%).[216] The reactant was treated with DIBAL-H followed by the addition of PhMgBr. The mechanism involving the stereoselectivity at the C5 position was shown in Scheme 2.2.3.2.[225] The ester oxygen atom first attacks the Al atom and the hydrogen atom in return attacks the carbonyl group, which leads to two possible intermediates **49a** and **49b.** In the presence of the Boc group, the aluminium atom coordinates to both two ester oxygen atoms, which results in the aluminoxyacetal structure. The excellent diastereoselectivity is achieved by the epimerization from **49a** to **49b**, since **49b** is more stable than **49a**, which was verified via calculation.[261] Without the formation of the aldehyde, **49b** reacts with the Grignard reagent BrMgPh through an S_Ni mechanism and yields prolinol **(*S*,*S*)-50** with configuration retention.[225] The resulting product was determined by the NMR spectroscopy.

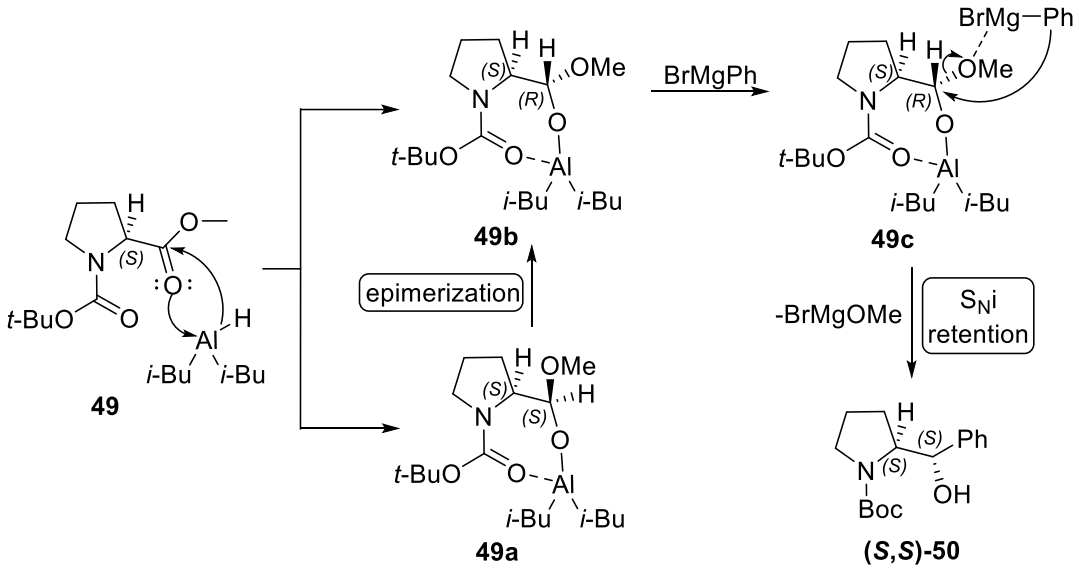

Scheme. 2.2.3.2: Plausible mechanism of amino ester reduction/alkylation from **49** to **(*S*,*S*)-50**.

2.2.3.2 Synthesis of (*S*)-((*S*)-1-methylpyrrolidin-2-yl)(phenyl)methanol ((*S*,*S*)-51)

According to the reported method by Yeung and co-worker,[262] the following conversion from *N*-Boc-prolinol **(*S*,*S*)-50** to the *N*-methyl-prolinol **(*S*,*S*)-51** was conducted in the presence of $LiAlH_4$ with a yield of 46% (Scheme 2.2.3.3).

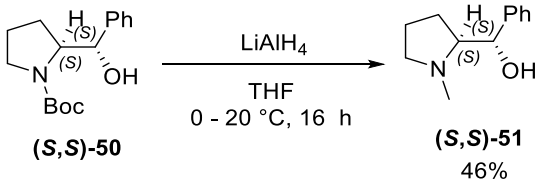

Scheme 2.2.3.3: Synthesis of *N*-methylprolinol **(*S*,*S*)-51** from *N*-Boc-prolinol **(*S*,*S*)-50**.

For the mechanism consideration, the reductant $LiAlH_4$ attacks *N*-carbon for three times and generates twice the leaving groups of *t*-butoxide anion and $[OAlH_3]^{2-}$ anion (Scheme 2.2.3.4).[208] The product **(*S*,*S*)-51** was confirmed by the NMR spectroscopy. The relatively low yield is probably due to the insufficient quality of the reductant. As

this direct transformation has a strict requirement on the quality of $LiAlH_4$, separated deprotection and methylation could serve as a viable alternative synthetic route.

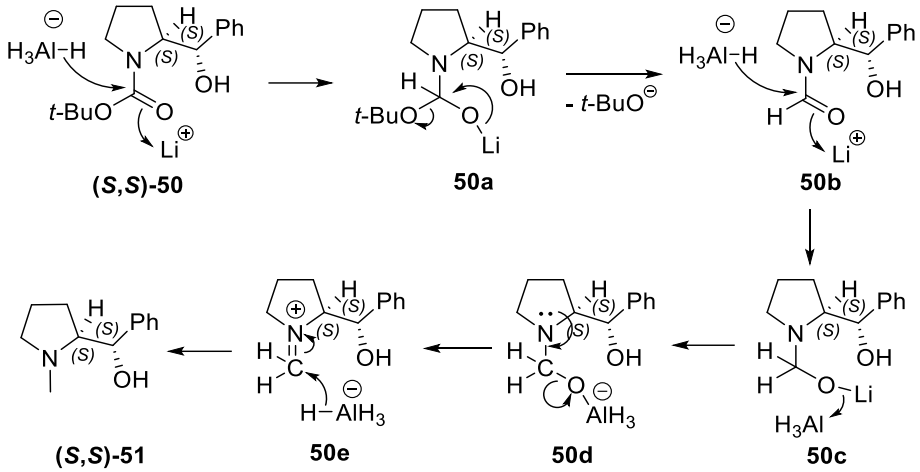

Scheme 2.2.3.4: Mechanism of transformation from *N*-Boc-prolinol **(*S,S*)-50** to *N*-methyl-prolinol **(*S,S*)-51**.

2.2.3.3 Mitsunobu reaction of prolinol (*R,R*)-52

The Mitsunobu reaction with the same condition as Chapter 2.2.2.4 was conducted on the *N*-methylprolinol **(*S,S*)-51** (Scheme 2.2.3.4).

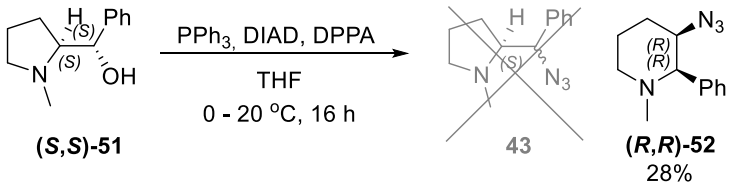

Scheme 2.2.3.5: Mitsunobu reaction of *N*-methylprolinol **(*S,S*)-51** to piperidine **(*R,R*)-52**.

The result of the final Mitsunobu reaction has been shown differently from the expectation. After comparison with relevant literatures, [218,263] it could be inferred that it is the ring−expansion product, namely piperidine **(*R,R*)-52** (with the yield of 28%) rather than the predicted pyrrolidine product azide **43** that was generated. Since

(*R*,*R*)-52 is a new compound, the constructure of the product could be indirectly determined based on the facts: 1) ESI-MS shows a signal at 217 m/z, which agrees with the molecular formula $[C_{12}H_{16}N_4 + H]^+$ and demonstrates the successful substitution of the azide−group; 2) According to the literatures, neither the ^{1}H-NMR of the inversion's product **(*S,R*)-43**[216] nor that of the retention's product **(*S,S*)-43**[219] agrees with the synthesized product (Figure 2.10); 3) For the azide-C hydrogen peak as the characteristic peak in ^{1}H-NMR, the newly synthesized compound has a chemical shift at 3.62 ppm (Figure 2.10), which shifts significantly towards low−field, compared to that of the inversion's (4.70 ppm) and the retentions product (4.33 ppm). This low−field shifting effect works similarly on the azide-C hydrogen of *N*-Bn-piperidine,[218] and on the hydroxy-C hydrogen of *N*-methyl-piperidine,[263] compared to their corresponding pyrrolidine derivatives. For the purpose of a more precise analysis, 2D-NMR like HMBC and HSQC could be introduced.

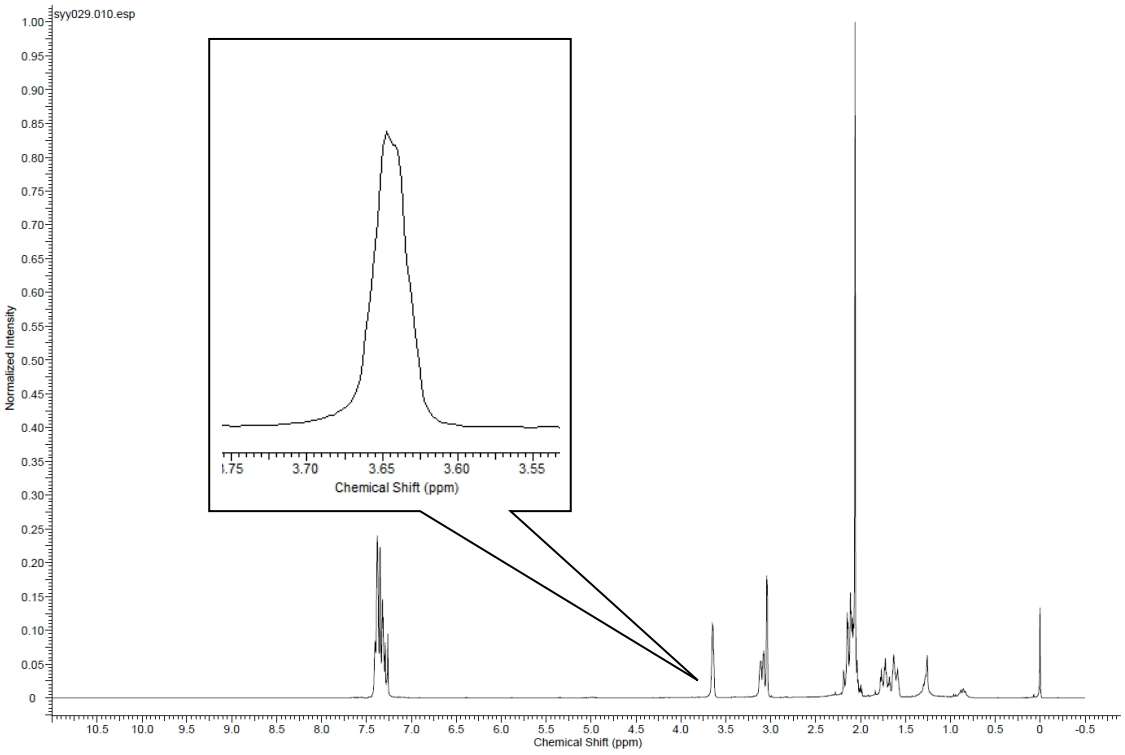

Figure 2.10. ^{1}H-NMR spectrum of the piperidine **(*R*,*R*)-52**.

The formation of the ring expansion product could be attributed to the anchimeric mechanism as outlined in Chapter 1.6.2 (Scheme 2.2.3.6). The aziridinium ion

intermediate **(*S,R*)-54** is formed as in argument reported by Ryu and co-workers.[219] However, the azide anion undergoes nucleophilic attack to the C1 position resulting in the formation of piperidine **(*R,R*)-52**. As the intermediate in this case is a (*S*,*R*)-form, it is not reasonable to compare it directly with the *N*-Tr-intermediate **(*S,S*)-53** (See Scheme 1.6.2.2 in Chapter 1.6.2) since that is an (*S*,*S*)-form. Therefore, an (*S*,*R*)-N-Tr-prolinol is worth being synthesized and tested for the Mitsunobu reaction via an (*S*,*R*)-aziridinium ion intermediate.

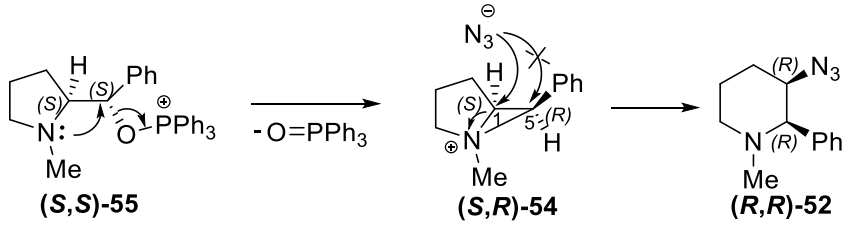

Scheme 2.2.3.6: Plausible mechanism of Mitsunobu ring expansion to piperidine **(*R,R*)-52**.

It is also remarkable that compared to the substrate prolinol **(*S,S*)-51**, the configuration of the two stereocenters in the product should be fully inversed to **(*R,R*)-52**, because the two S_N2 processes took place in different carbon atoms. Furthermore, given the comparatively low yield, it appears reasonable to hypothesize the existence of undetected five−membered ring products. In analogous cases, piperidine and pyrrolidine products have been detected concurrently,[218,263] thereby demonstrating that multiple mechanisms are engaged during the reaction, as opposed to a singular pathway.

To make a unified summary of the neighboring group effect of Mitsunobu reaction on methyl proline derivative in this work and other proline derivatives with different protecting group is not feasible, since some reaction were conducted on (*S*,*S*)-prolinols while some were on (*S*,*R*)-types. Nevertheless, an attempt can be made to summarize certain laws that pertain to analogous conditions: 1), For Mitsunobu reaction on (*S*,*S*)-prolinols (or (*R*,*R*)-Prolinol), *N*-Me-prolinol **(*S,S*)-51** has a tendency of forming aziridinium ion intermediate **(*S,R*)-54**, while the *N*-Boc- prolinol **(*S,S*)-56**[219] and *N*-Bn-prolinol **(*R,R*)-59**[222] preferred not forming such intermediate (Scheme

2.2.3.7, summarized with Scheme 1.6.2.3 and Scheme 1.6.2.4 in Chapter 1.6.2);

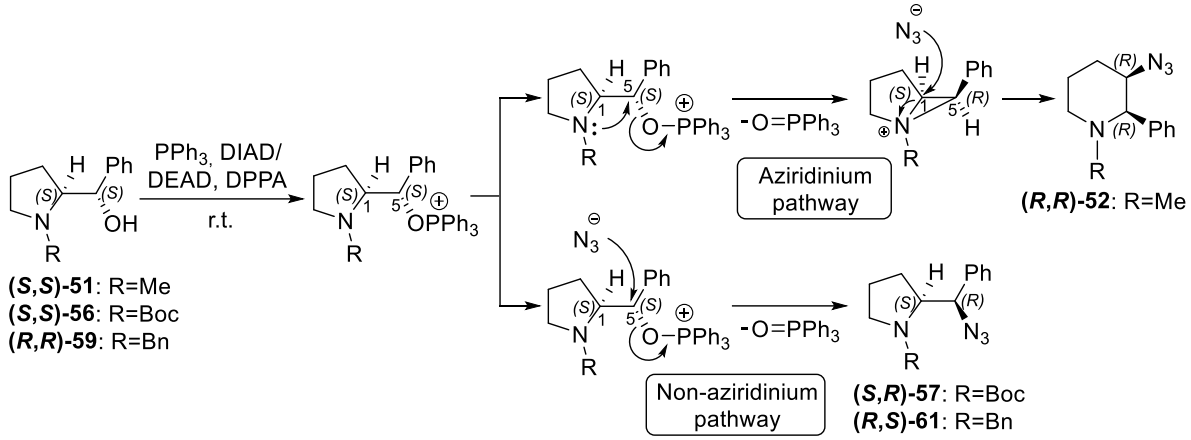

Scheme 2.2.3.7: Competition Mitsunobu pathways on prolinols with different protecting groups.

2), For nucleophilic attack by azide to aziridinium ion intermediate, (*S*,*R*)-*N*-Me-intermediate **(*S,R*)-54** has a tendency to be attacked to its C1 position, while (*S*,*S*)-*N*-Tr-intermediate **(*S,S*)-53**[219] preferred to be attacked to its C5 position (Scheme 2.2.3.8, summarized with Scheme 1.6.2.2 in Chapter 1.6.2).

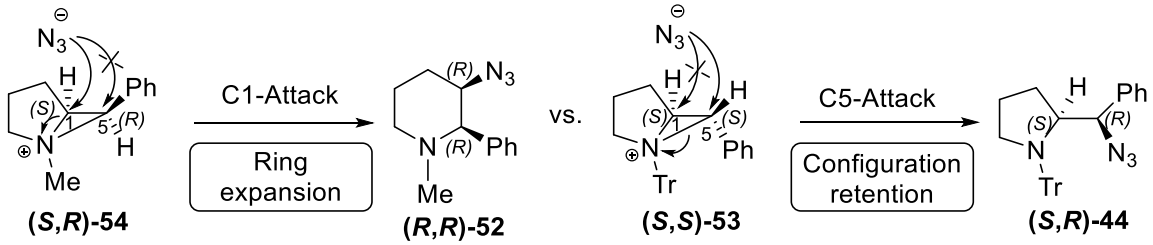

Scheme 2.2.3.8: Competition nucleophilic attack pathways on aziridinium ions with different protecting groups.

3 Summary

3.1 Synthesis and characterization of chiral cyclodiphosphazanes

In the first part of this work, 6 newly designed chiral cyclodiphosphazanes were synthesized. In priority, (1*R*,2*R*)-*N*1,*N*1-dimethylcyclohexane-1,2-diamine as the chiral scaffold for the catalyst was synthesized according to the reported method, whereas some procedures were simplified. Starting with kinetic resolution of technical diaminocyclohexane, followed by alkalization, ring closing and opening, methylation and at last the deprotection, the target molecule **1** was obtained with a total yield of 81%, with economic materials, and the whole synthesis was conducted without column chromatography (Scheme 3.1.1).

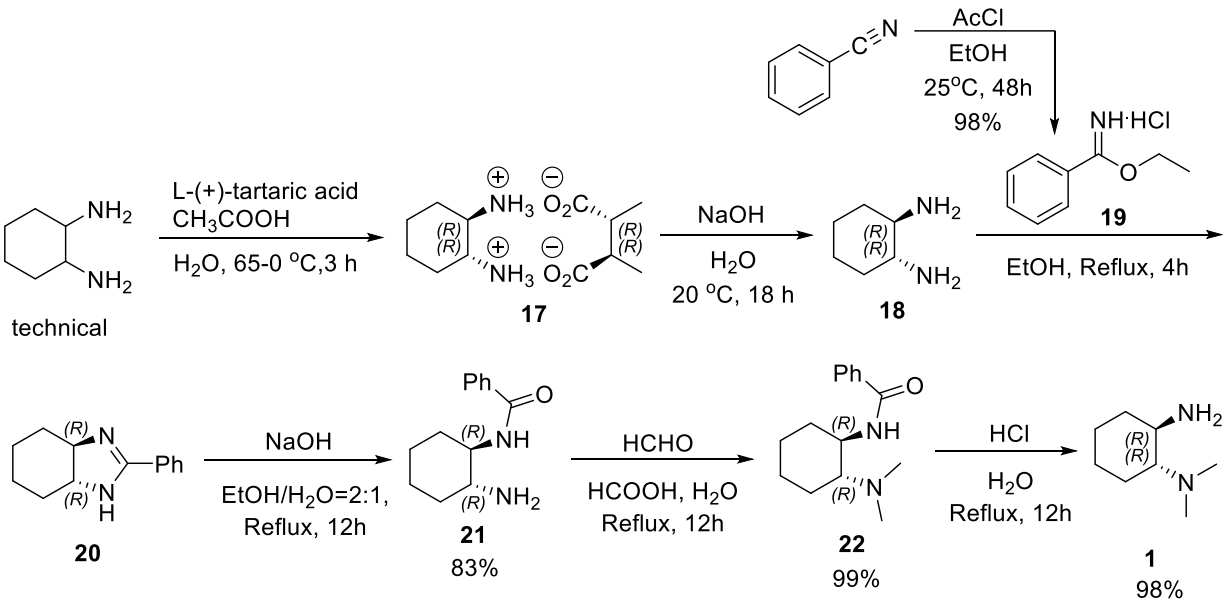

Scheme 3.1.1: 6−step synthesis of (1*R*,2*R*)-*N*1,*N*1-dimethylcyclohexane-1,2-diamine **1** starting from technical diaminocyclohexane.

Newly designed cyclodiphosph(V)azane catalysts **4** − **9** bearing *tert*-butyl group with (1*R*,2*R*)-*N*1,*N*1-dimethylcyclohexane-1,2-diamine as the chiral scaffold were then

synthesized (Scheme 3.1.2). The synthetic route began with the preparation of *cis*-dichlorocyclodiphosphazane x as precursor with PCl_3 and *t*$BuNH_2$ according to the reported method. Corresponding amines were then substituted onto the phosphazane ring in sequence with presence of helping base. Finally, with oxidation with H_2O_2 or elemental sufur, the catalysts were obtained with low (8%) to moderate (46%) yields. All steps should be stoichiometrically controlled, otherwise side reaction could take place and bring by−products.

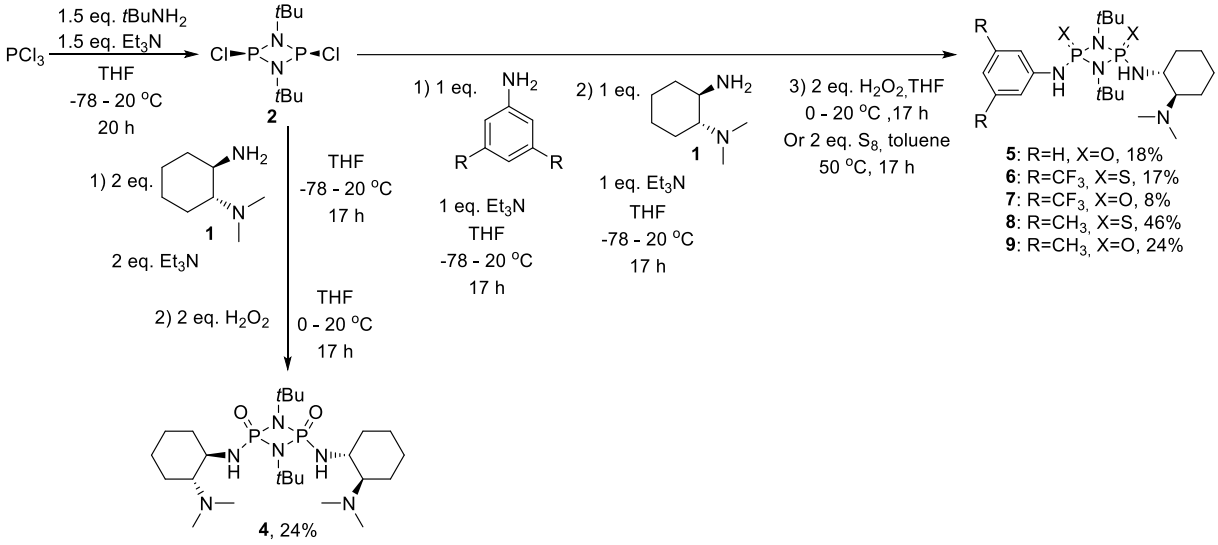

Scheme 3.1.2: Newly synthesized chiral cyclodiphosph(V)azanes **4** − **9** as catalysts

Analysis including ^{31}P-NMR spectrum demonstrated the desired phosphorus containing compounds. The X−ray crystal structures of newly synthesized catalysts **4** − **9** were obtained except for **6** (Figure 3.1).

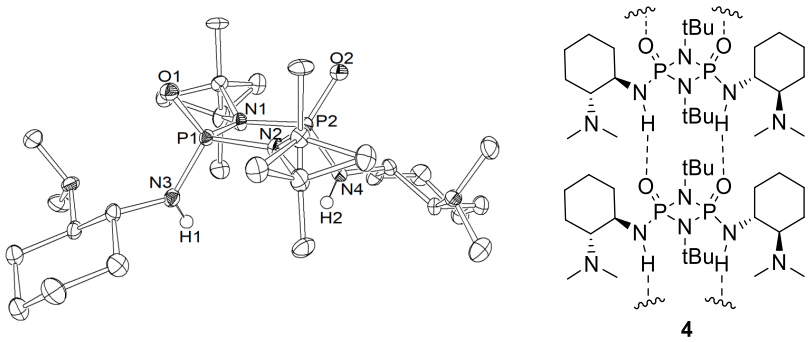

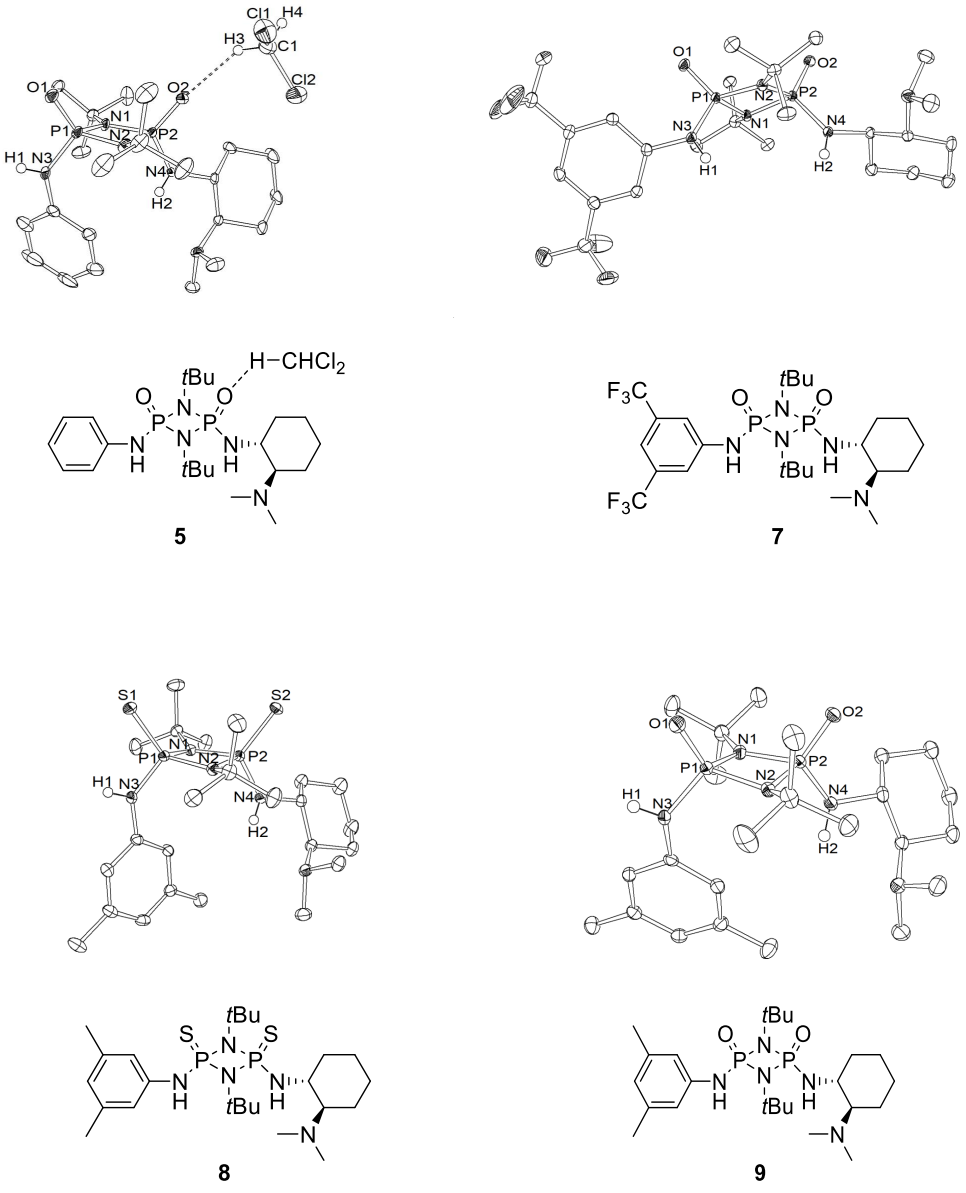

Figure 3.1: X−ray crystal structure of cyclodiphosph(V)azane **4**, **5**, **7**, **8** and **9** with thermal ellipsoids at the 50% probability level; protons except NHs are omitted for clarity

Synthesis of cyclodiphosph(V)azane catalyst **114** bearing diisopropylphenyl group with (1*R*,2*R*)-*N*1,*N*1-dimethylcyclohexane-1,2-diamine as the chiral scaffold was also attempted (Scheme 3.1.3). The *cis*-dichlorocyclodiphosph(III)azane precursor **3** is successfully synthesized through the reaction of PCl_3 with $DippNH_2$ according to the reported method. But the following synthesis including substitution with amines and oxidation with elemental sulfur didn't result in the target molecule even with stronger

helping bases.

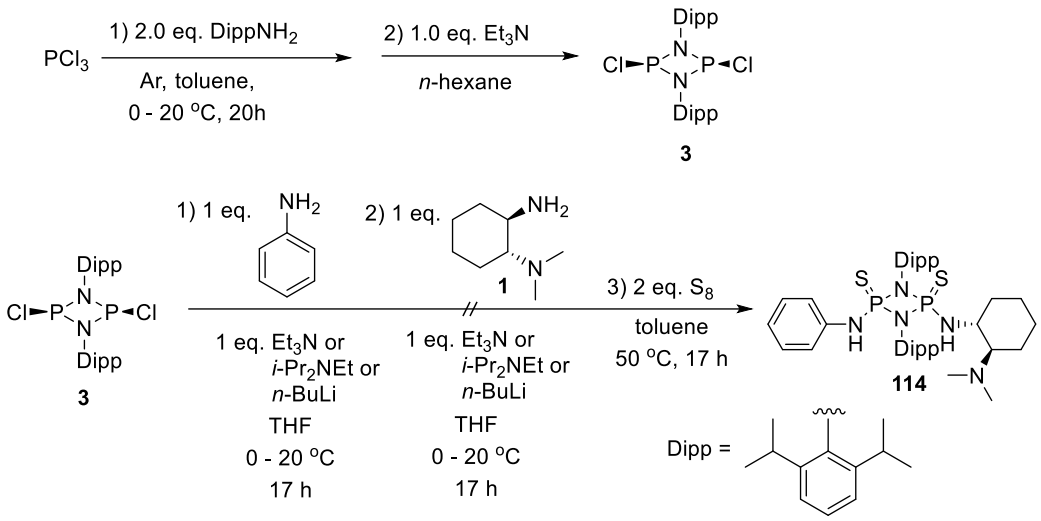

Scheme 3.1.3: Attempts to synthesize new chiral cyclodiphosph(V)azane **114** bearing diisopropylphenyl group.

3.2 Enantioselective catalysis with chiral cyclodiphosph(V)azanes

The newly designed and synthesized chiral cyclodiphosph(V)azane catalysts (**4** − **9**) were investigated in asymmetric Michael additions of β-nitrostyrene to various nucleophiles. In addition, reported cyclodiphosph(V)azane catalysts (*all-cis*-**15**/**16**) and by−products (**75**/**76**) were also tested in some reactions for comparative purposes (Scheme 3.2.1).

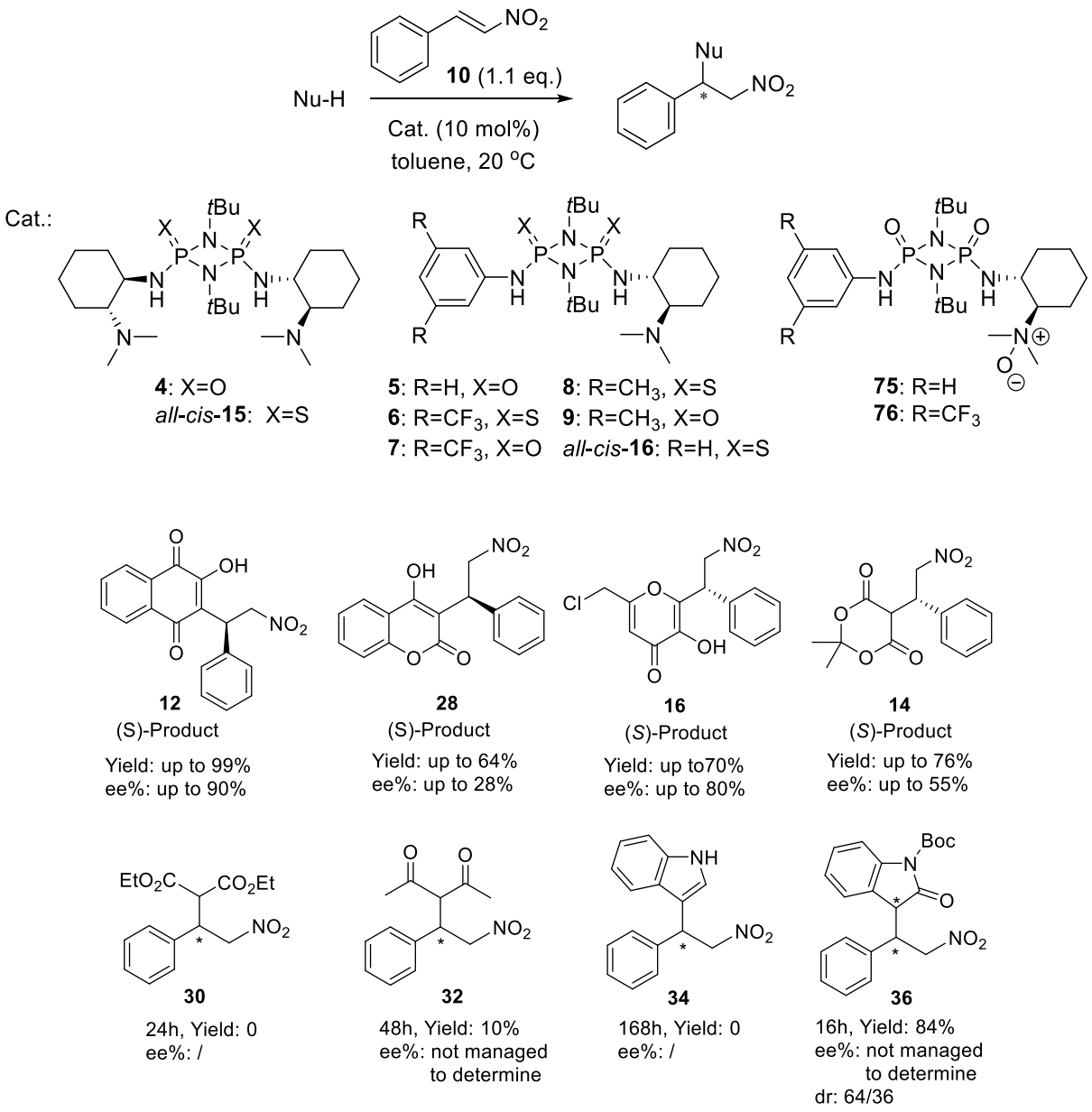

Scheme 3.2.1: Michael additions of β-nitrostyrene (**10**) to various nucleophiles with chiral cyclodiphosph(V)azane catalysts.

Among the results, adducts from 2-hydroxy-1,4-naphthoquinone (**11**) exhibited good to excellent yields of up to 99% under mild conditions, and after screening of the conditions such as solvents and temperatures, catalyses with catalyst **5** serve improved ee-s of up to 90%. Catalyses with 4-hydroxycoumarin (**27**) resulted in moderate yields of up to 64%, accompanied by low ee-s of up to 17% under mild conditions, and an improved ee of 28% under a lowered temperature of -20 °C in toluene, with catalyst **5**. Catalyses with Kojic acid chloride (**15**) yielded moderate

results, with the best yield of 70% and the best ee of 80% achieved with catalyst **8** simultaneously. Adducts from Meldrum's acid (**13**) exhibited moderate yields and low to moderate yields, with catalyst **5** achieving the peak value for both involving yield of 76% and ee of 55%. Reactions of diethylmalonate (**29**), acetylacetone (**31**) and indole (**33**) with catalyst **5** resulted in no conversion or low yield, after at least 24 h. Catalysis of *N*-Boc-oxindole (**35**) with catalyst **5** exhibited good yield of 84% and dr of 64/36, while ee could not be determined.

3.3 Synthesis and characterization of *L*-proline derivatives

In the first part of this work, the 9−step synthesis of *L*-proline derivative **(*S*,*R*)-47** was undertaken according to the reported method in cooperation with B. Sc. Ioannis Panagiotidis (Scheme 3.3.1). The synthetic route began with the esterification of *L*-proline (**38**), followed by the introduction of a trityl group, yielding a 92% yield. Subsequently, the ester function was transferred into aldehyde through a reduction with $LiAlH_4$ and a Swern oxidation in sequence, followed by the stereoselective introduction of a phenyl group through a Grignard reaction, yielding a total of 32%. The subsequent Mitsunobu reaction, as the key step, substituted the hydroxy group with an azide, with a retention at the C5 position, as evidenced by X−ray crystal analysis. Subsequent deprotection and methylation on amine yielded methylated intermediate **46**, with a total yield of 34%. Following the final reduction with $LiAlH_4$, the elimination product **48** was obtained, rather than the desired primary amine. As starting material **46** of this reaction was consumed, no further attempts were made to retry the reaction.

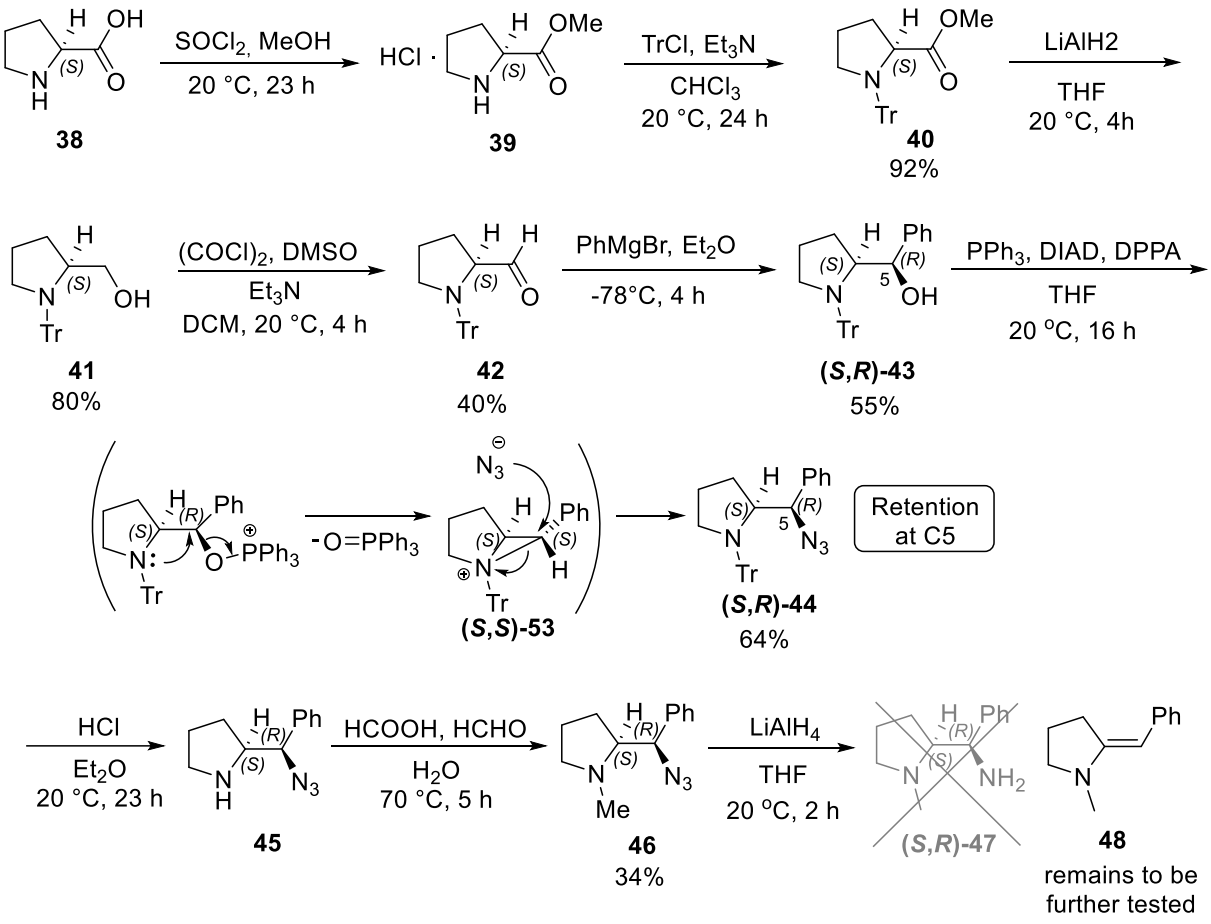

Scheme 3.3.1: Attempt to synthesize *L*-proline derivative **(*S*,*R*)-47** in 9 steps involving the Mitsunobu reaction

In the second part of this work, the neighboring group effect with methyl was explored for the Mitsunobu reaction on *L*-proline derivative in cooperation with M. Sc. student Yinyu Sun (Scheme 3.3.2). Firstly, *L*-proline ester **39** was protected with Boc, followed by the one−pot ester reduction/alkylation with DIBAL-H and Grignard reagent, so that the phenyl group was stereoselectively introduced, with a total yield of 56%. Afterwards, a one−step transfer from Boc to methyl was executed with $LiAlH_4$, yielding 46%. Finally, Mitsunobu reaction was carried out on the methyl prolinol **(*S*,*S*)-51**, resulting 28% of a ring expansion product **52**, instead of the anticipated pyrrolidine derivative **43**. This demonstrated the forming of aziridinium ion as the intermediate by the neighboring group effect of methyl, and a changed attack position at C1 by azide instead of C5 in the case of trityl prolinol.

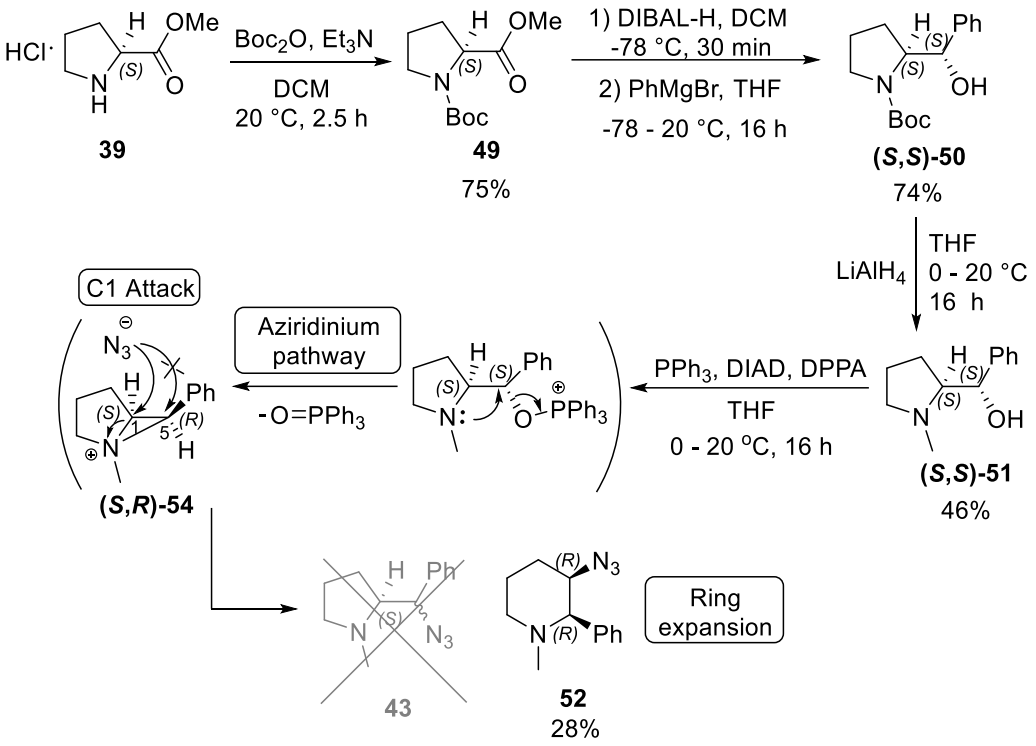

Scheme 3.3.2: Exploring of neighboring group effect of methyl for the Mitsunobu reaction on *L*-proline derivative **(*S*,*S*)-51**.

4 Outlook

In the interest of optimization, further exploration is warranted into the potential of novel cyclodiphosph(V)azane catalysts bearing the diisopropylphenyl (Dipp) group. As previously mentioned in Chapter 1.4.2 (Scheme 1.4.2.3, a), a comparison of the catalytic activity of chiral cyclodiphosph(V)azane catalysts reveals that those bearing a phenyl group exhibit superior activity compared to their *tert*-butyl group counterparts. This observation can be attributed to the enhanced inductive effect provided by the phenyl group (pK_a of aniline: 4.6[264]) compared to *tert*-butyl (pK_a of *tert*-butylamine: 10.6[265]), which results in a higher acidity of N−Hs. However, cyclodiphosph(V)azane bearing a phenyl group also exhibits a higher propensity for decomposition compared to the *tert*-butyl variant,[180] potentially due to a deficiency in steric bulk provided by the phenyl group. Consequently, as discussed in Chapter 2.1.1, the cyclodiphosph(V)azane diisopropylphenyl group (Dipp) was selected as the motif due to its advantageous combination of enhanced acidity of N−Hs (pK_a of 2,6-diisopropylaniline: 4.2 predicted by Scifinder), akin to phenyl, and notable stability, similar to *tert*-butyl.

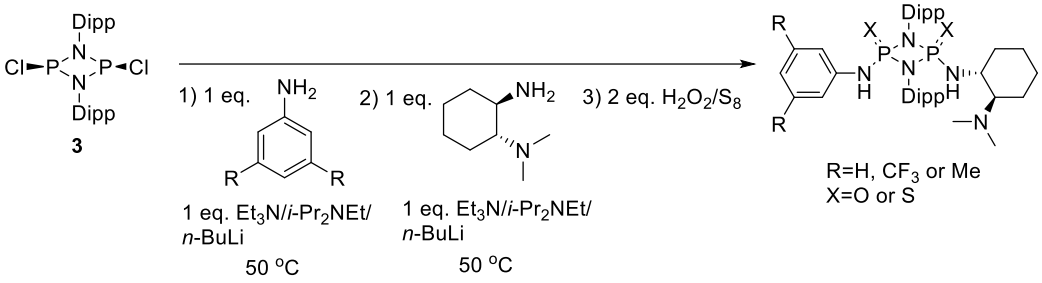

Scheme 4.1: Proposed synthesis of new chiral cyclodiphosph(V)azane catalysts bearing Dipp

Despite the failure in synthesis of the catalysts with Dipp, further experimentation is warranted, such as the raise of the temperature (Scheme 4.1), since the dichlorcyclodiphosph(V)azane with Dipp is bulky, the substitution with amine might necessitate an increased energy.

In the field of asymmetric Michael additions, the application of Michael donors and

Michael acceptors has expanded to include additional substrates. For Michael donors, the use of cyclodiphosph(V)azane catalysts is particularly effective when the substrates exhibit high acidity. Therefore, compounds such as barbituric acid (**62**) and dimedone (**63**) are promising candidates for testing in this context.[266] For Michael acceptors, the screening of different substituted β-nitrostyrenes **64** − **68**, 2-furanyl/thienyl nitroolefins **69** and **70**, and chalcones **72** are worth being tested.[267]

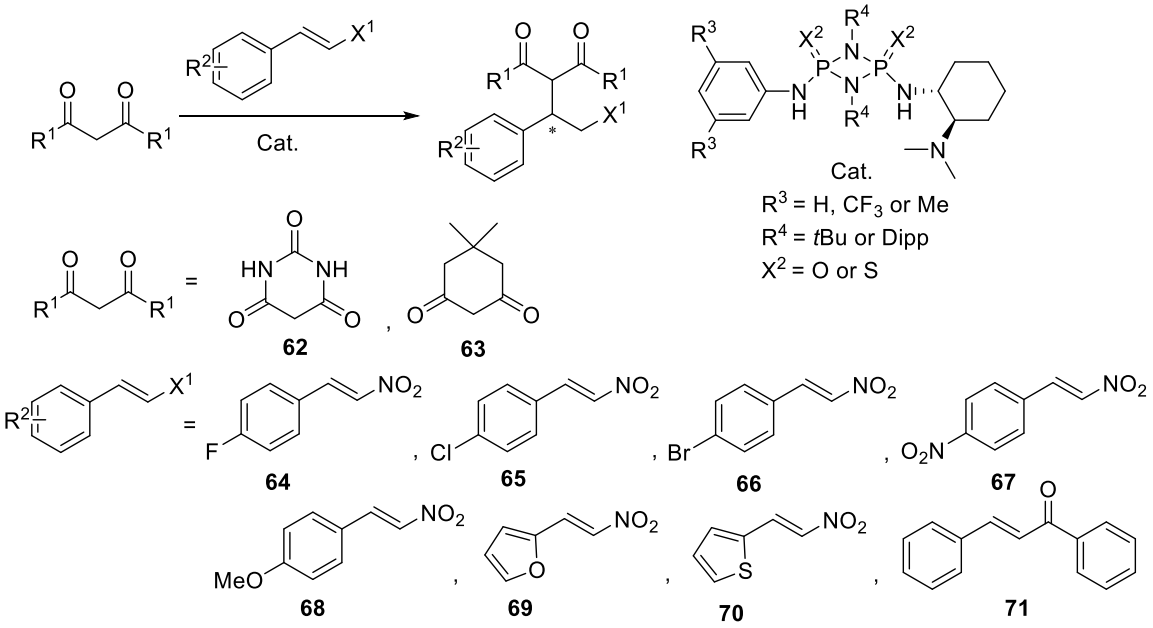

Scheme 4.2: Proposed asymmetric Michael additions of different Michael donors to different Michael acceptors with chiral cyclodiphosph(V)azane catalysts.

In the case of proline derivatives, it is imperative to conduct a re−examination of the Mitsunobu reaction of both *N*-trityl prolinol **(*S*,*R*)-43** and *N*-methyl prolinol **(*S*,*S*)-51** to determine the precise ratio of different products. Moreover, the following reduction on the major compounds **46** and **(*R*,*R*)-52** to the respective primary amines **(*S*,*R*)-47** and **(*R*,*R*)-72** should be conducted again. Finally, the pyrrolidine product and the piperidine product could be used in the construction of cyclodiphosph(V)azane catalysts **73** and **74**, as both are pure chiral scaffolds and should have good enantioselectivity in bifunctional catalysis. Notably, piperidine diamine **(*R*,*R*)-72** could be a valuable unit in squaramide catalysts such as **116**, as it was already emerged in thiourea catalysis (Cat. **115**),[268] but not reported yet in squaramide catalysis.

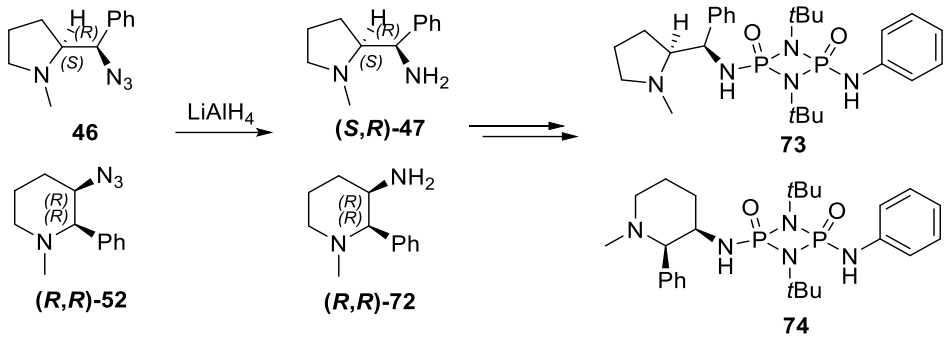

Scheme 4.3: Proposed reduction to chiral diamine **(*S*,*R*)-47** and **(*R*,*R*)-72** and the corresponding cyclodiphosph(V)azane catalysts **73** and **74** bearing them

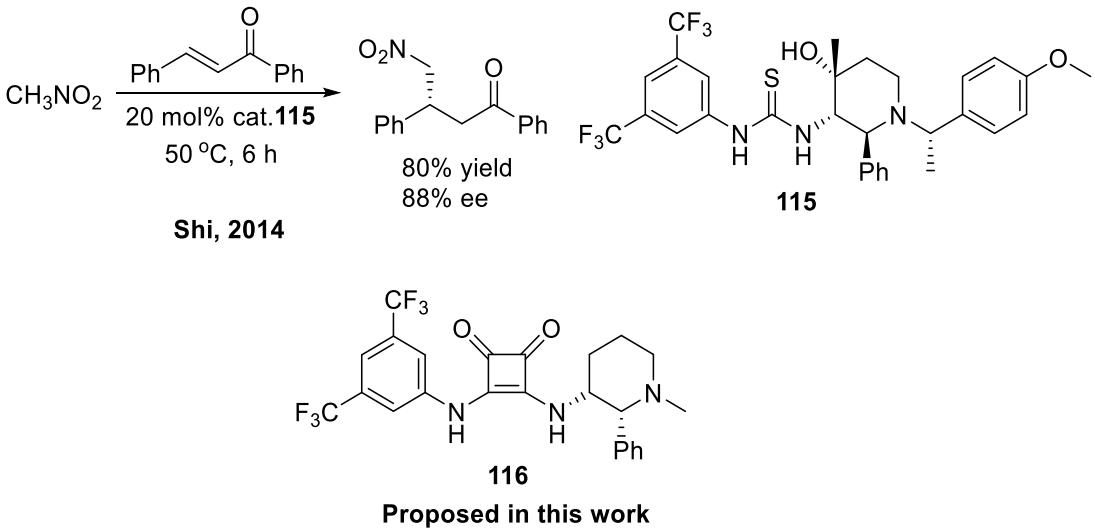

Scheme 4.4: Reported thiourea catalysis **115** with chiral piperidine and the proposed squaramide **116** bearing **(*R*,*R*)-72**.

5 Experimental part

5.1 Working techniques

5.1.1 General methods

All reactions with air− and/or moisture−sensitive substances were carried out in evacuated, heated and septum−sealed Schlenk flasks under an argon atmosphere, unless otherwise stated. Liquid reactants and solvents were added using plastic or Hamilton syringes with steel cannulas. Solids were decanted in the argon countercurrent.

Solvents were dried according to standard methods. Tetrahydrofuran, diethyl ether, triethylamine and *n*-hexane were dried over sodium and distilled before use. Dichloromethane were dried over phosphorus pentoxide and distilled before use. Other solvents were purchased directly from the distributor in high purity and dryness, usually sealed with a septum and stored via molecular sieve (3 or 4 Å).

Reactions at low temperatures were carried out using either isopropanol/dry ice (-78 °C) or water/ice (0 °C). Water (30 − 40 °C) or oil baths (>40 °C) were used to heat reactions.

Thin−layer chromatography was performed over silica gel plates from *Merck* with the designation "DC Kieselgel 60 F254". Observed substances were visualized by irradiation with UV light (254 nm) or staining with a $KMnO_4$ solution.

"Silica gel 60" (0.035 − 0.070 mm) from *Acros Organics* was used for flash chromatography, while the solvent mixtures used were indicated in volume percentages (v/v).

All substances were concentrated through removing the solvent by using a rotary evaporator at a maximum of 40 °C and then dried in an oil pump vacuum at <0.1 mbar.

5.1.2 Reagents

All chemicals used were purchased from the following companies and, unless otherwise stated, were used without further purification: *Acros Organics*, *Alfa−Aesar*, *Merck*, *Sigma−Aldrich*, *TCI, Carbolution*.

5.1.3 Analysis

Melting points

Melting points were determined in open capillary tubes on an SMP3 device from Stuart Scientific.

NMR spectroscopy

NMR were recorded using Bruker DPX, AV and AV II devices (300, 400, 500 and 600 MHz). Measurements were performed at room temperature unless otherwise stated. The chemical shift was indicated in the ^{1}H-NMR and ^{13}C-NMR spectra relative to the resonance of tetramethylsilane (TMS), in the ^{19}F-NMR spectra relative to the resonance of trichlorofluoromethane, with the solvent as internal standard. In the case of the ^{31}P-NMR spectra, 85% phosphoric acid in D_2O was used as the external standard. In all cases, deuterated solvents from Deutero and Eurisotop were used. NMR peak multiplicities were abbreviated by "s" for singlet, "d" for doublet, "t" for triplet, "q" for quartet and "quin" for quintet, "sep" for septet, "m" for multiplet and "br" for broad. A double splitting was indicated by writing the splitting patterns one behind the other, e.g. the doublet of a triplet as "dt".

Crystal structure analysis

Crystal structure analysis was performed on a Bruker D8 Venture with Kappa geometry with a copper microfocus source. The structures were solved with SHELXS-97 and SHELXL-97. Unless otherwise indicated, structures shown are ellipsoids with 50% probability of residence.

IR analysis

IR spectra were recorded on a Perkin−Elmer Paragon 1000 FT−IR spectrometer. The substances dissolved in diethyl ether were measured as dark films. Wavenumbers are given in [cm^{-1}]. Very intense bands are labeled with "s" (strong), bands of medium intensity with "m" (medium) and weak bands with "w" (weak). Exceptionally broad bands are indicated with "b" (broad).

High−resolution mass spectroscopy

HR−MS spectra were prepared on a Thermo LTQ Orbitrap XL instrument from Thermo Fisher Scientific. The measured substances were ionized by electron spray ionization.

HPLC analysis

HPLC analysis were performed with the complete Elite LaChrom system from VWR, consisting of the components Hitachi Pump L-2130 and UV detector L2400. In addition, a Chromaster 5310 column thermostat, also from VWR, was used. The temperature was kept constant at 25 °C for the measurements, unless otherwise stated. Columns of the type "Chiralcel OJ", "Chiralpak AD-H" and "Chiralcel OJ-H" with a length of 25 cm from Daicel were used. The solvents used were purchased in HPLC grade quality from Fisher Scientific.

5.2 Synthesis

5.2.1 Synthesis of (1*R*,2*R*)-*N*1,*N*1-dimethylcyclohexane-1,2-diamine (DMDACH)

5.2.1.1 Synthesis of *L*-(+)-tartaric salt of cyclohexane-1,2-diamine (DACH)

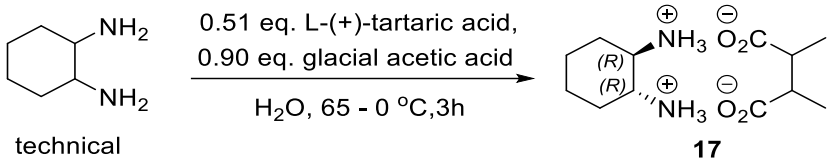

The synthesis was carried out according to the procedure by Klare's doctoral thesis.[232] The *L*-(+)-tartaric acid (75 g, 0.50 mol, 0.51 eq.) in distilled water (200 mL) was added to *rac*-1,2-diaminocyclohexane (120 mL, 115 g, 0.97 mol, 1.00 eq.) with stirring at 65 °C. After that, glacial acetic acid (50 mL, 52.5 g, 0.88 mol, 0.90 eq.) was dropwise added and heated for 2 h. The temperature did not exceed 75 °C. The reaction mixture was cooled down to room temperature, and then, further to 0 °C for 1 h in an ice bath. The reaction mixture was filtered, the filter cake was washed with cold distilled water (1x50 mL), and methanol (6x50 mL), and then dried in vacuo. 71.8g (0.276 mol) of tartrate salt as the colorless solid was obtained and would be invested into the next step without further purification.

5.2.1.2 Synthesis of (1*R*,2*R*)-cyclohexane-1,2-diamine

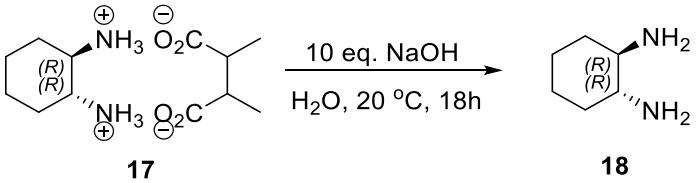

The synthesis was carried out according to the procedure by Klare's doctoral thesis.[232] 25 g of the obtained amine tartrate salt **17** (96 mmol) was suspended in DCM (125 mL), and the solution of 10% NaOH (37.5 g, 960 mmol, 10 eq.) in distilled water (100 mL) was added and stirred at 20 °C for 18 h. The mixture solution was extracted with DCM (3X35 mL). The combined organic phase was dried over $MgSO_4$ and concentrated in vacuum. The solvent should be carefully evaporated under the water bath at room temperature for the easily volatilization of the product and the crude product as a yellow oil containing trace of DCM will be directly taken into the next step, and the conversion is established to be quantitative for the stoichiometry calculation of the following step.

^{1}H-NMR: (300 MHz, $CDCl_3$) δ [ppm] = 2.32 – 2.17 (m, 1H), 1.82 (d, J = 13.1 Hz, 1H), 1.68 (s, 3H), 1.17 (dt, J = 41.5, 9.2 Hz, 2H)

^{13}C-NMR: (75 MHz, $CDCl_3$) δ [ppm] = 57.3, 35.2, 25.1

To determine the enantiomeric excess, a small portion of the product **18** was converted to the corresponding diimine by reaction with benzaldehyde in ethanol according to Terence and co-workers:[269] (1*R*,2*R*)-cyclohexane-1,2-diamine (114 mg, 1 mmol) and benzaldehyde (212 g, 2 mmol) were combined in ethanol (1.3 mL). After stirring for 0.5 h at 20 °C, a precipitate was collected and dried under rotary evaporator. The subsequent washing with cold ethanol (0.4 mL) yielded 1a as a white, analytically pure crystalline solid (234 mg, 81% yield). The enantiomeric excess was then determined by chiral HPLC. The ee was 99.9%.

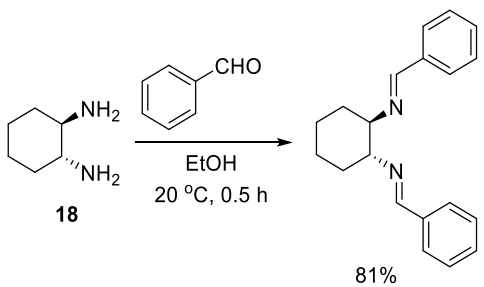

Chirale HPLC: Daicel OD-H, *n*-Hex:2-propanol 90:10, flow 1.0 mL/min, λ = 254 nm,

25 °C, t_R = 4.4 min, 27.4 min

5.2.1.3 Synthesis of ethyl benzimidate hydrochloride

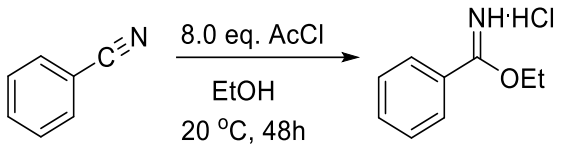

19

The synthesis was carried out according to the procedure by Yadav and co-workers.[233] 285 mL of AcCl (4.0 mol, 8.0 eq.) was added to a stirred solution of a 52 mL of 99% benzonitrile (0.5 mol, 1.0 eq.) and 350 mL of EtOH (6 mol, 12.0 eq.). The solution was stirred in a flask at 20 °C. After the reaction was complete by TLC after 48 h, the volatiles were removed under reduced pressure to purify the benzimidate hydrochloride. 86.048 g of ethyl benzimidate hydrochloride as colorless solid was obtained with yield of 98%.

^{1}H-NMR: (300 MHz, $CDCl_3$) δ [ppm] = 7.67 (d, J = 7.1 Hz, 2H), 7.42- 7.30 (m, 3H), 4.31-4.21 (q, J = 7.1 Hz, 2H), 1.36 (t, J = 7.1 Hz, 3H)

5.2.1.4 Synthesis of (3a*R*,7a*R*)-2-phenyl-3a,4,5,6,7,7a-hexahydro-1H-benzo[d]imidazole

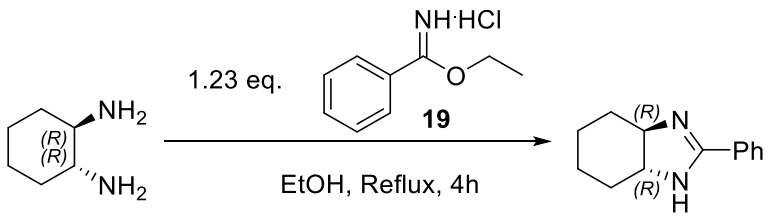

18 **20**

The synthesis was carried out according to the procedure by Gandelman and co-workers.[231] Ethyl benzimidate hydrochloride **19** (21.86 g, 118 mmol, 1.23 eq.) and ethanol (100 mL) were added to compound **18** (96 mmol, calculated according to the applied amine tartrate salt **17** in previous step) and heated to reflux for 4 h. To remove hydrochloride which is attached to the produced compound, 1M NaOH (5.2 g NaOH in 130 mL distilled water) was added and the solution turned to be clear. Aqueous layer was extracted with 5% CH_3OH in DCM (CH_2Cl_2/MeOH 95:5, 3X50 mL) and dried with over Na_2SO_4. The solvent was evaporated, and the crude product 20 can be obtained as a pale yellow solid. The crude product was direct taken into the next step without being purified, and the conversion is established to be quantitative for the stoichiometry calculation of the following step. This reaction was repeated again on a small scale (7.4 mmol of compound **18**) for the purpose of analysis, and the crude product was purified by column chromatography over silica (CH_2Cl_2, then CH_2Cl_2/MeOH/25% aq. NH_4OH 90:10:1) yielding 85% (1.2677 g, 6.3 mmol) of product as a colorless solid.

^{1}H-NMR: (300 MHz, $CDCl_3$) δ [ppm] = 7.89 – 7.59 (m, 2H), 7.39 (q, J = 6.7, 6.2 Hz, 3H), 3.16 – 3.07 (m, 1H), 2.29 (d, J = 11.9 Hz, 1H), 2.07 – 1.68 (m, 2H), 1.68 – 1.46 (m, 1H), 1.45 – 1.26 (m, 1H)

5.2.1.5 Synthesis of *N*-((1*R*,2*R*)-2-aminocyclohexyl)benzamide

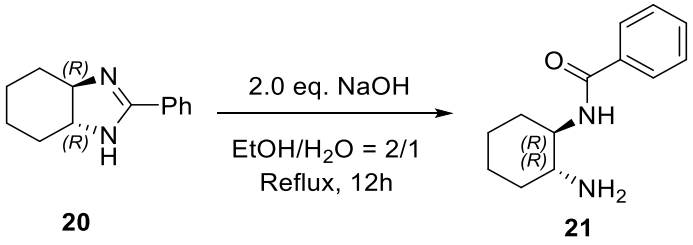

20 **21**

The synthesis was carried out according to a modified procedure by Gandelman and co-workers.[231] 5% NaOH (8.1 g NaOH, 203 mmol, 2.1 eq., in 162 mL distilled water)

and mixture of ethanol and H_2O (EtOH:H_2O ratio 2:1, total 354 mL) were added to compound **20** (ca. 96 mmol) in a flask and was refluxed overnight. After cooling down to room temperature, ethanol was removed by evaporation, and aqueous layer was extracted with DCM (3X100 mL), dried with over $MgSO_4$, filtered and concentrated in vacuum again. The product **21** was purified through washing with cold DCM (1X50 mL) instead of column chromatography for a purpose of simplify. After drying under rotary evaporator, 17.3640 g of product (79.6 mmol) as colorless solid was obtained with yields of 83% (based on the amount of used amine tartrate salt **17** (96 mmol)).

^{1}H-NMR: (300 MHz, $CDCl_3$) δ [ppm] = 7.78 (d, J = 6.8 Hz, 1H), 7.46 (dq, J = 14.3, 7.1, 6.7 Hz, 2H), 6.14 (d, J = 8.1 Hz, 1H), 3.85 – 3.57 (m, 1H), 2.49 (td, J = 10.3, 4.0 Hz, 1H), 2.25 – 1.87 (m, 1H), 1.75 (d, J = 8.8 Hz, 1H), 1.55 – 1.00 (m, 3H)

5.2.1.6 Synthesis of *N*-((1*R*,2*R*)-2-(dimethylamino)cyclohexyl)benzamide

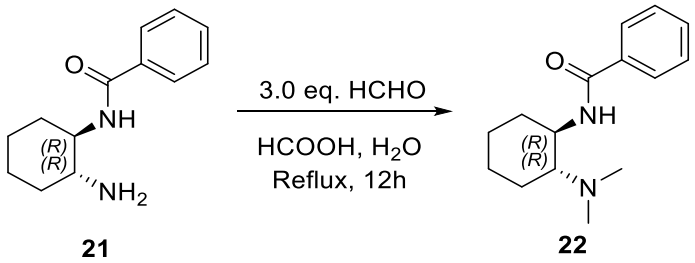

21 **22**

The synthesis was carried out according to the procedure by Gandelman and co-workers.[231] Distilled water (42 mL), formic acid (18.32 g, 398.2 mmol, 15 mL, 5 eq.) and 37 wt.% formaldehyde solution in H_2O (20.05 g in total, containing formaldehyde: 7.42g, 274 mmol, 3.44 eq.) were added into **21** (17.3604 g, 79.63 mmol) and heated to reflux overnight. After cooling to room temperature, 2M NaOH was added until the pH equaled around 11 and the aqueous phase was extracted with DCM (3X100 mL). The combined organic phase was dried with over $MgSO_4$, and the solvent was then evaporated under reduced pressure. Since TLC indicated a complete conversion,

19.43 g of product was obtained as colorless solid with a yield of 99% without any purification.

^{1}H-NMR: (300 MHz, $CDCl_3$) δ [ppm] = 7.78 (d, J = 6.6 Hz, 1H), 7.45 (dq, J = 14.0, 7.0, 6.6 Hz, 2H), 3.58 (d, J = 3.9 Hz, 0H), 2.72 (d, J = 11.9 Hz, 0H), 2.40 (t, J = 9.4 Hz, 1H), 1.97 – 1.79 (m, 1H), 1.71 (d, J = 12.9 Hz, 1H), 1.24 (tt, J = 37.5, 11.4 Hz, 2H)

5.2.1.7 Synthesis of (1*R*,2*R*)-*N*1,*N*1-dimethylcyclohexane-1,2-diamine

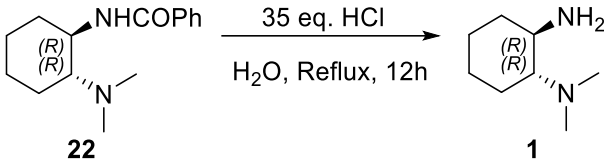

The synthesis was carried out according to the procedure by Gandelman and co-workers.[231] 6 mL of concentrated 12M HCl with distilled water (HCl:H_2O ratio 1:1) was added to the compound **22** (0.2410 g, 0.980 mmol), and the mixture was heated to reflux for 12 h, then cooled down to room temperature, and added with 10% NaOH and stirred until the insoluble residue disappeared and the pH equaled around 11. The aqueous layer was extracted with DCM (3X20 mL) and the combined organic phase was dried over $MgSO_4$. After being concentrated in vacuum, 0,1359 g product (0.956 mmol) as yellow oil was obtained, with the yield of 97.6%. The product without purification was pure enough according the NMR analysis, and should be immediately used in the next step.

^{1}H-NMR: (300 MHz, $CDCl_3$) δ [ppm] = 2.57 (td, J = 10.1, 4.1 Hz, 1H), 2.23 (s, 4H), 2.02 (td, J = 11.0, 10.5, 3.3 Hz, 1H), 1.93 (s, 2H), 1.82 – 1.58 (m, 3H), 1.27 – 1.00 (m, 3H)

^{13}C-NMR: (75 MHz, $CDCl_3$) δ [ppm] = 69.50, 51.24, 39.98, 34.87, 25.38, 24.87, 20.41

5.2.2 Synthesis of precursors of cyclodiphosph(V)azane catalysts

The precursors were synthesized, purified and stored under Argon atmosphere.

5.2.2.1 Synthesis of *cis*-1,3-di-*tert*-butyl-2,4-dichloro-1,3,2,4-diazadiphosphetidine

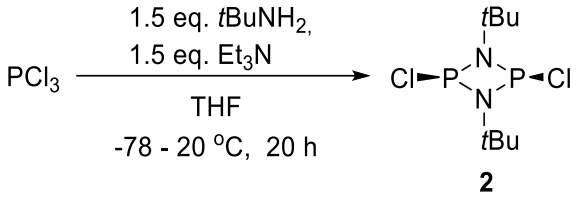

2

The synthesis was carried out according to a modified procedure by Wright and co-workers.[234] Under an argon atmosphere PCl_3 (13.18 g, 96 mmol, 1.0 eq.) was added to a solution of triethylamine (14.57 g, 144 mmol, 1.5 eq.) in 90 mL dry tetrahydrofuran. After cooling to -78 °C *tert*-butylamine (10.53 g, 144 mmol, 1.5 eq.) dissolved in 90 mL tetrahydrofuran was dropwise added. After stirring at this temperature for 4h, the mixture was allowed to warm to 20 °C and stirred for further 16 h. The resulting suspension was filtered, and the residue was washed with *n*-pentane. The solvent was removed under reduced pressure and the obtained crude product was purified via distillation. Since the product rapidly solidifies, the condenser should not be cooled, and regularly heated with heat gun if necessary (bp: 86 °C, p = 0.5 mbar). The product **2** was obtained as colorless crystals (4.66 g, 16.9 mmol, 35%).

$^{31}P\{^1H\}$-NMR: (122 MHz, $CDCl_3$) δ [ppm] = 207.64

The analytical data are in agreement with the literature data.[234]

5.2.2.2 Synthesis of *cis*-2,4-dichloro-1,3-bis(2,6-diisopropylphenyl)-1,3,2,4-diazadiphosphetidine

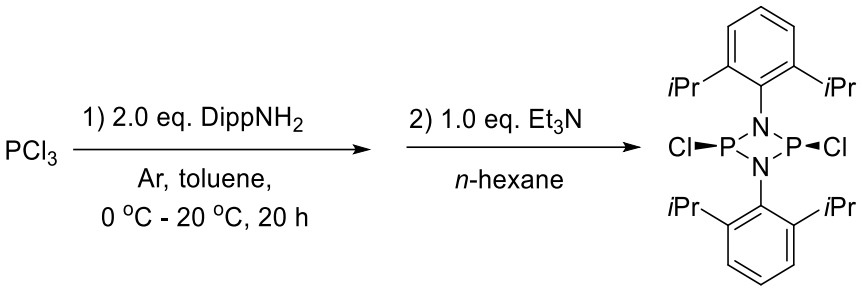

3

The synthesis was carried out according to a modified procedure by Burford and co-workers.[236] Under an argon atmosphere a solution of $DippNH_2$ (10 mL, 53 mmol, 2.0 eq.) in toluene (20 mL) was dropwise added into a solution of a solution of PCl_3 (2.3 mL, 26 mmol, 1.0 eq.) in toluene (15 mL) at 0°C with intensive stirring. The solution was allowed to warm to 20 °C and a white precipitate formed. After stirring for further 16 h, the mixture was stirred for 4 h at -78 °C and then overnight at 20 °C. The resulting suspension was filtered, Toluene in filtrate was removed in vacuo and the and the resulting oil was dissolved in *n*-hexane (50 mL) to promote precipitation. The mixture was filtered and NEt_3 (3.7 mL, 26 mmol, 1.0 eq.) was added to filtrate, with the immediate production of a yellow solution and white precipitate. The mixture was filtered again and the solvent of filtrate was slowly removed to give large white crystals, which were washed with fresh hexane. The product **3** was obtained as colorless crystals (3.61g, 7.5 mmol, 58%)

$^{31}P\{^1H\}$-NMR: (122 MHz, $CDCl_3$) δ [ppm] = 210.25

The analytical data are in agreement with the literature data.[236]

5.2.3 Synthesis of bis(amino)cyclodiphosph(V)azane catalysts

For the synthesis of bis(amino)cyclodiphosph(V)azane, by oxo-variant, the reactions were carried out under argon atmosphere until the step before the oxidation with H_2O_2 is finish, and by thio-variant, the reactions were carried out under argon atmosphere until the oxidation with elemental sulfur is finish.

5.2.3.1 Synthesis of 1,3-di-*tert*-butyl-2,4-bis(((1*R*,2*R*)-2-(dimethylamino)cyclohexyl)amino)-1,3,2,4-diazadiphosphetidine 2,4-dioxide

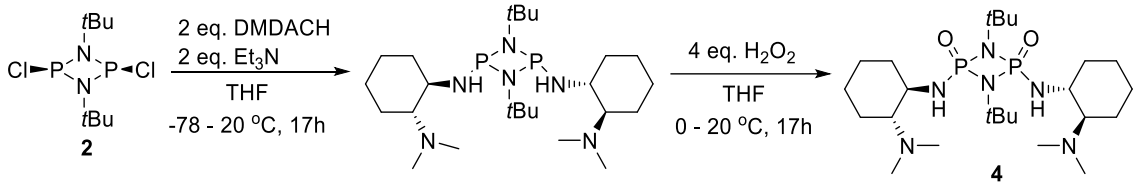

A solution of (*R*,*R*)-N,N'-dimethyl-cyclohexane-1,2-diamine (**1**) (1.994 g, 14.0 mmol, 4.0 eq.) and Et_3N (1.417 g, 14.0 mmol, 4.0 eq.) in THF (20 mL) was added dropwise to a solution of freshly synthesized and distilled *cis*-(*t*BuNPCl)$_2$ (**2**) (1.926 g, 7.0 mmol) in THF (40 mL) at -78 °C. After stirring at this temperature for 1 h, the mixture was allowed to warm to 20 °C and stirred for further 16 h. The resulting suspension was filtered and the filtrate was diluted with 150 mL THF. 5.5 mL (64.0 mmol, 4.0 eq.) of 35% stabilized aqueous H_2O_2-solution was added at 0 °C, and the solution was stirred at this temperature for 1 h and then allowed to warm to 20 °C and stirred for further 17 h. Solvent was removed in vacuo and the crude product was purified by column chromatography over silica (CH_2Cl_2/MeOH/25% aq. NH_4OH 100:10:1) yielding 24% (870 mg, 1.68 mmol) of **4** as a colorless solid.

^{1}H-NMR: (300 MHz, $CDCl_3$) δ [ppm] = 4.04 (br. s., 2 H), 3.12 − 2.88 (m, 2 H), 2.77 − 2.63 (m, 2 H), 2.23 (s, 12 H), 2.18 − 2.09 (m, 2 H), 1.86 − 1.78 (m, 4 H), 1.74 − 1.64 (m, 2 H), 1.49 − 1.42 (m, 18 H), 1.28 − 1.16 (m, 8 H)

^{13}C-NMR: (75 MHz, $CDCl_3$) δ [ppm] = 68.4(t, J_{PC} = 6.1 Hz), 54.1, 53.3, 40.4, 33.8, 30.4(t, J_{PC} = 4.4 Hz), 25.3, 24.4, 21.1

^{31}P{^{1}H}-NMR: (122 MHz, $CDCl_3$) δ [ppm] = 2.00

HRMS: ESI$^+$ (m/z) [M + H]$^+$ calcd. for $C_{24}H_{53}O_2N_6P_2$: 519.36997; found: 519.36989

5.2.3.2 General procedure for Synthesis of oxodiaminocyclodiphosph(V)azanes

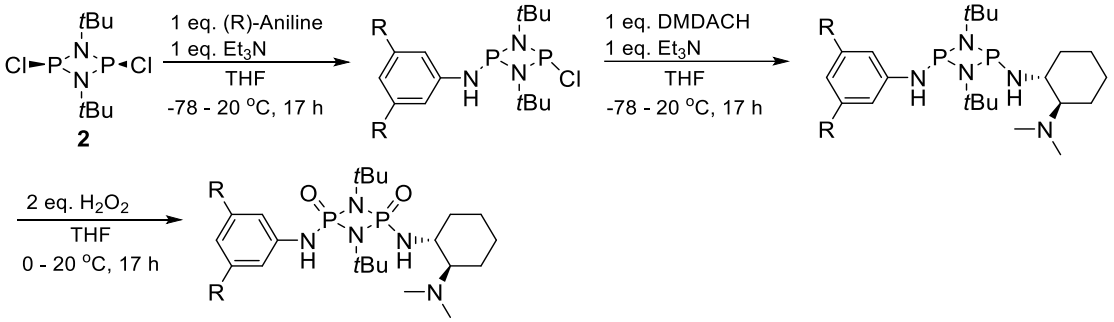

A solution of aniline (0.926 g, 9.92 mmol, 1.0 eq.) and Et_3N (1.100 g, 10.91 mmol, 1.1 eq.) in THF (30 mL) was added dropwise to a solution of freshly synthesized and distilled *cis*-(tBuNPCl)$_2$ (**2**) (2.730 g, 9.92 mmol) in THF (50 mL) at -78 °C. After stirring at this temperature for 1 h, the mixture was allowed to warm to 20 °C and stirred for further 16 h. To the suspension was then added a solution of (*R*,*R*)-*N*,*N'*-dimethyl-cyclohexan-1,2-diamin (**1**) (1.409 g, 9.92 mmol, 1.0 eq.) and Et_3N (1.100 g, 10.91 mmol, 1.1 eq.) in THF (15 mL) at -78 °C. After 0.5 h the mixture was allowed to warm to 20 °C and stirred stirred for further 16 h. The Suspension was filtrated and the filtrate was diluted with 200 mL THF. 5.4 mL (63.0 mmol, 4.0 eq.) of 35% stabilized aqueous H_2O_2-solution was added at 0 °C and the solution was stirred at this temperature for 1 h and then allowed to warm to 20 °C and stirred for further 17 h. Solvent was removed in vacuo and the crude product was purified by column chromatography over silica (CH_2Cl_2/MeOH/25% aq. NH_4OH 1000:10:1 − 200:10:1,

ratio could vary by different catalysts) yielding 18% (852 mg, 1.82 mmol) of **5** as a colorless solid.

It is noteworthy that the scale for synthesizing each catalyst exhibits slight variations, as the synthesis commenced directly after the collection of the precursor **2** in a Schlenk flask, which had been previously weighed. The amount of substance of the precursor **2**, differs slightly for each time, was then calculated and completely invested for the subsequent synthesis without being transferred to any other apparatus. The scale of the subsequent reagents was then calculated. The yield of the final product was then calculated based on the amount of the invested precursor **2**.

5.2.3.2.1 1,3-di-*tert*-butyl-2-(((1*R*,2*R*)-2-(dimethylamino)cyclohexyl)amino)-4-(phenylamino)-1,3,2,4-diazadiphosphetidine 2,4-dioxide

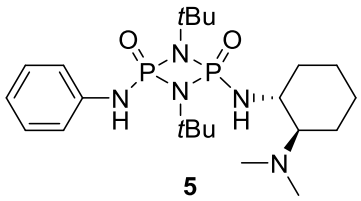

5

The product is colorless solid yielding 18%.

^{1}H-NMR: (300 MHz, $CDCl_3$) δ [ppm] = 7.31 − 7.36 (m, 2 H), 7.14 − 7.22 (m, 2 H), 7.07 (t, J = 7.4 Hz, 1 H), 5.09 (d, J_{PH} = 6.8 Hz, 1 H), 4.12 (d, J_{PH} = 10.8 Hz, 1 H), 2.78 − 2.90 (m, 1 H), 2.25 (s, 7 H), 2.10 − 2.21 (m, 1 H), 1.78 − 1.91 (m, 2 H), 1.61 − 1.72 (m, 1 H), 1.43 (s, 9 H), 1.41 (s, 9 H), 1.14 − 1.32 (m, 4 H)

^{13}C-NMR: (75 MHz, $CDCl_3$) δ [ppm] = 140.9, 129.2, 122.0, 119.2 (d, J_{PC} = 6.63 Hz), 68.7 (d, J_{PC} = 11.06 Hz), 54.9, 54.3, 53.8, 40.6, 34.7, 30.2, 25.4, 24.5, 21.1

^{31}P{^{1}H}-NMR: (122 MHz, $CDCl_3$) δ [ppm] = 1.86 (d, J_{PP} = 52.4 Hz), -4.46 (d, J_{PP} = 52.4 Hz)

HRMS: ESI$^+$ (m/z) [M + H]$^+$ calcd. for $C_{22}H_{42}O_2N_5P_2$: 470.28083; found: 470.28039

5.2.3.2.2 2-((3,5-bis(trifluoromethyl)phenyl)amino)-1,3-di-*tert*-butyl-4-(((1*R*,2*R*)-2-(dimethylamino)cyclohexyl)amino)-1,3,2,4-diazadiphosphetidine 2,4-dioxide

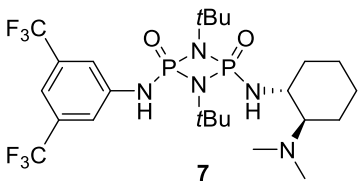

7

The product is colorless solid yielding 8%.

^{1}H-NMR: (300 MHz, $CDCl_3$) δ [ppm] = 8.84 (s, 1 H), 7.83 (s, 2 H), 7.47 (s, 1 H), 3.86 (s, 1 H), 3.19 − 3.36 (m, 1 H), 2.53 − 2.72 (m, 1 H), 2.09 − 2.32 (m, 7 H), 1.77 − 1.93 (m, 2 H), 1.64 − 1.75 (m, 1 H), 1.44 (s, 9 H), 1.39 (s, 9 H), 1.13 − 1.33 (m, 4 H)

^{13}C-NMR: (126 MHz, $CDCl_3$) δ [ppm] = 142.6, 132.6 (q, J_{FC} = 33.2 Hz), 123.3 (q, J_{FC} = 272.9 Hz), 117.7, 114.9, 67.7(d, J_{PC} = 10.5 Hz), 55.8, 54.8, 54.2, 35.3, 30.1 (t, J_{PC} = 4.3 Hz), 29.9 (t, J_{PC} = 4.5 Hz), 25.3, 24.6, 21.3

^{31}P{^{1}H}-NMR: (122 MHz, $CDCl_3$) δ [ppm] = 2.29 (d, J_{PP} = 52.4 Hz), -5.26 (d, J_{PP} = 52.4 Hz)

HRMS: ESI$^+$ (m/z) [M + H]$^+$ calcd. for $C_{24}H_{40}O_2N_5F_6P_2$: 606.25559; found: 606.25509

5.2.3.2.3 1,3-di-*tert*-butyl-2-(((1*R*,2*R*)-2-(dimethylamino)cyclohexyl)amino)-4-((3,5-dimethylphenyl)amino)-1,3,2,4-diazadiphosphetidine 2,4-dioxide

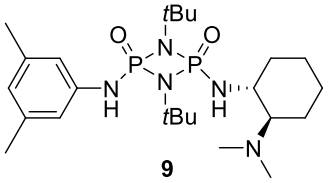

9

The product is colorless solid yielding 24%.

^{1}H-NMR: (500 MHz, $CDCl_3$) δ [ppm] = 6.93 (s, 2 H), 6.84 (br. s, 1 H), 6.65 (s, 1 H), 3.70 (s, 1 H), 3.18 − 3.27 (m, 1 H), 2.66 − 2.75 (m, 1 H), 2.31 (s, 6 H), 2.10 − 2.24 (m, 7 H), 1.76 − 1.89 (m, 2 H), 1.64 − 1.71 (m, 1 H), 1.47 (s, 9 H), 1.37 (s, 9 H), 1.14 − 1.29 (m, 4 H)

^{13}C-NMR: (75 MHz, $CDCl_3$) δ [ppm] = 140.3, 138.8, 123.9, 116.8 (d, J_{PC} = 6.6 Hz), 68.5 (d, J_{PC} = 11.1 Hz), 55.2, 54.4, 53.9, 40.6, 35.5, 30.2 (t, J_{PC} = 4.4 Hz), 25.3, 24.7, 21.5, 21.2

^{31}P{^{1}H}-NMR: (202 MHz, $CDCl_3$) δ [ppm] = 2.22 (d, J_{PP} = 52.2 Hz), -4.41 (d, J_{PP} = 52.2 Hz)

HRMS: ESI$^+$ (m/z) [M + H]$^+$ calcd. for $C_{24}H_{46}O_2N_5P_2$: 498.31213; found: 498.31136

5.2.3.3 General procedure for synthesis of thiodiaminocyclodiphosph(V)azanes

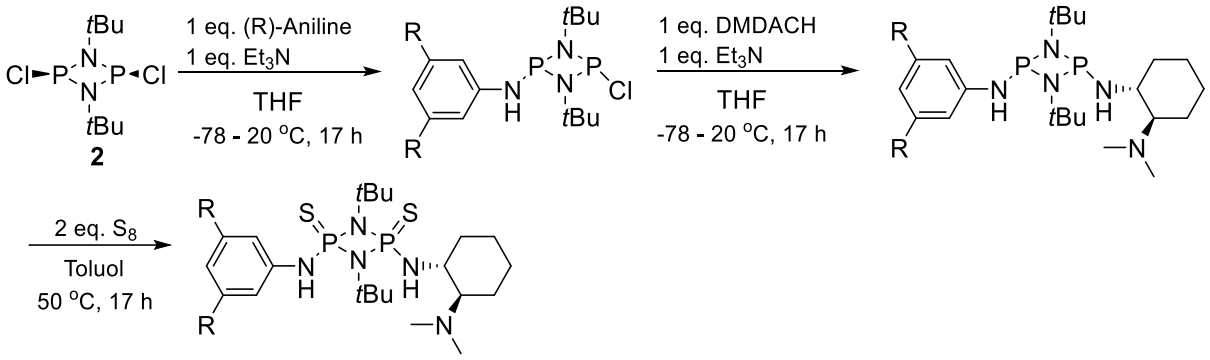

A solution of 3,5-dimethylaniline (0.691 g, 5.70 mmol, 1.0 eq.) and Et_3N (0.635 g, 6.27 mmol, 1.1 eq.) in THF (18 mL) was added dropwise to a solution of freshly synthesized and distilled *cis*-(*t*BuNPCl)$_2$ (**2**) (1.568 g, 5.70 mmol) in THF (30 mL) at -78 °C. After stirring at this temperature for 1h, the mixture was allowed to warm to 20 °C and stirred for further 16 h. To the suspension was then added a solution of (*R*,*R*)-*N*,*N'*-dimethyl-cyclohexane-1,2-diamine (**1**) (0.810 g, 5.7 mmol, 1.0 eq.) and Et_3N (0.635 g, 6.27 mmol, 1.1 eq.) in THF (10 mL) at -78 °C. After 0.5 h the mixture was allowed to warm to 20 °C and stirred for further 16 h. The Suspension was filtrated under inert condition with a Schlenk−frit and the filtrate was concentrated in vacuo. The residue was redissolved in toluene (50 mL), elemental sulfur was added (0.400g, 12.5 mmol, 2.2 eq.) and stirred for 16 h at 50 °C. Solvent was removed in vacuo and the crude product was purified by column chromatography over silica (CH_2Cl_2/MeOH/25% aq. NH_4OH 1000:10:1 - 200:10:1, ratio could vary by different catalysts) yielding 46% (1.378 g, 2.60 mmol) of **8** as a colorless solid.

5.2.3.3.1 2-((3,5-bis(trifluoromethyl)phenyl)amino)-1,3-di-*tert*-butyl-4-(((1*R*,2*R*)-2-(dimethylamino)cyclohexyl)amino)-1,3,2,4-diazadiphosphetidine 2,4-disulfide

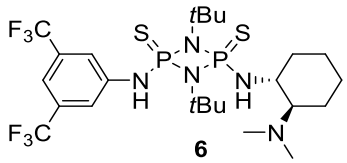

6

The product is colorless solid yielding 17%.

^{1}H-NMR: (300 MHz, $CDCl_3$) δ [ppm] = 7.78 (s, 2 H) 7.58 (s, 1 H) 6.12 (br. s, 1 H) 4.09 (br. s, 1 H) 3.18 − 3.38 (m, 1 H) 2.61 − 2.84 (m, 1 H) 2.19 − 2.35 (m, 1 H) 2.08 (s, 6 H) 1.84 (m, 2 H) 1.59 − 1.72 (m, 10 H) 1.54 (s, 9 H) 1.12 − 1.31 (m, 4 H)

^{13}C-NMR: (75 MHz, $CDCl_3$) δ [ppm] = 141.3 (d, J_{PC} = 5.53 Hz), 132.8 (q, J_{FC} = 33.40 Hz), 123.1 (q, J_{FC} = 273.10 Hz), 119.3, 116.4, 66.9 (d, J_{PC} = 10.70 Hz), 57.9, 57.2, 55.8, 40.7, 35.1, 30.0 (t, J_{PC} = 4.40 Hz), 29.5 (t, J_{PC} = 4.42 Hz), 25.2, 24.5, 21.6

^{31}P{^{1}H}-NMR: (121 MHz, $CDCl_3$) δ [ppm] = 50.06 (d, J_{PP} = 35.9 Hz), 38.01 (d, J_{PP} = 35.9 Hz)

HRMS: ESI^+ (m/z) $[M + H]^+$ calcd. for $C_{24}H_{40}N_5F_6P_2S_2$: 638.20991; found: 638.20952

5.2.3.3.2 1,3-di-*tert*-butyl-2-(((1*R*,2*R*)-2-(dimethylamino)cyclohexyl)amino)-4-((3,5-dimethylphenyl)amino)-1,3,2,4-diazadiphosphetidine 2,4-disulfide

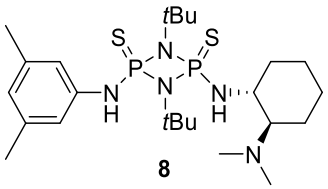

8

The product is colorless solid yielding 46%.

^{1}H-NMR: (500 MHz, $CDCl_3$) δ [ppm] = 6.81 (s, 2 H), 6.67 (s, 1 H), 5.28 (d, J = 12.8 Hz, 1 H), 3.82 (s, 1 H), 3.28 − 3.13 (m, 1 H), 2.68 (d, J = 10.4 Hz, 1 H), 2.25 (s, 6 H), 2.08 − 2.02 (m, 1 H), 1.99 (s, 6 H), 1.71 (m, 2 H), 1.58 (s, 9 H), 1.43 (s, 9 H), 1.23 − 1.01 (m, 4 H)

^{13}C-NMR: (126 MHz, $CDCl_3$) δ [ppm] = 139.5 (d, J_{PC} = 6.81 Hz), 138.9, 125.3, 118.35 (d, J_{PC} = 5.45 Hz), 67.94 (d, J_{PC} = 10.90 Hz), 57.3, 56.7, 55.1, 35.5, 29.9 (t, J_{PC} = 4.30 Hz) 29.59 (t, J_{PC} = 4.31 Hz) 25.2, 24.5, 21.7, 21.6

^{31}P{^{1}H}-NMR: (122 MHz, $CDCl_3$) δ [ppm] = 48.78 (d, J_{PP} = 35.90 Hz), 38.92 (d, J_{PP} = 35.90 Hz)

HRMS: ESI$^+$ (m/z) [M + H]$^+$ calcd. for $C_{24}H_{46}N_5P_2S_2$: 530.26644; found: 530.26571

5.2.4 Synthesis of 1-(3,5-bis(trifluoromethyl)phenyl)-3-((*R*,*R*)-2-(dimethylamino)cyclohexyl)thiourea (Takemoto's catalyst)

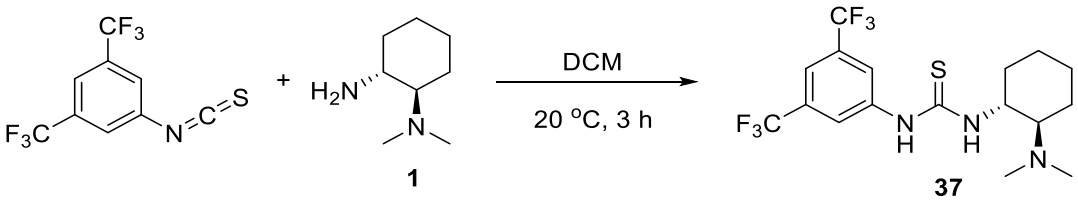

The synthesis was carried out according to the procedure by Takemoto and co-workers.[125] Under an argon atmosphere 3,5-bis(trifluoromethyl)phenylisothiocyanate (11) (1.023 g, 3.78 mmol, 1.25 eq.) was dissolved in 12 mL dry dichloromethane and (*R*,*R*)-*N*,*N*-dimethylcyclohexane-1,2-diamine (**1**) (430.30 mg, 3.02 mmol, 1 eq.) was added dropwise. The mixture was stirred for 3 h at 20 °C and the solvent was removed in vacuo. The crude product was purified by column chromatography over silica (CH_2Cl_2/MeOH/25% aq. NH_4OH 200:10:1). The product was obtained as colorless solid (534 mg, 43%).

^{1}H-NMR: (300 MHz, $CDCl_3$) δ [ppm] = 7.88 (s, 2 H), 7.64 (s, 1 H), 3.90 (br. s, 1 H), 2.55 (m, 2 H), 2.38 (s, 6 H), 1.83 − 2.05 (m, 2 H), 1.78 (m, 1 H), 1.08 − 1.47 (m, 4 H)

The analytical data are in agreement with the literature data.[270]

5.2.5 Synthesis of *N*-(*tert*-Butoxycarbonyl)-2-indolinone

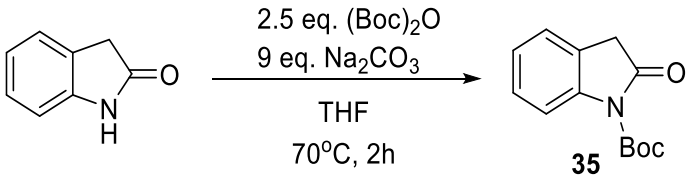

35

The synthesis was carried out according to the procedure by Cativiela and Ordóñez.[271] 2-indolinone (0.50 g, 3.75 mmol), di-*tert*-butyl dicarbonate (2.05 g, 9.40 mmol, 2.5 eq.) and sodium carbonate (3.60 g, 33.75 mmol, 9 eq.) were added to THF (15 mL) and heated at 70 °C for 12 h. The solid was filtered off and the solvent was removed in vacuo. Purification by column chromatography over silica (EtOAc/cyclohexane 1:9) afforded **35** as a colorless solid (0.7218 g, 3.10 mmol, 83% yield).

^{1}H-NMR: (300 MHz, $CDCl_3$) δ [ppm] = 7.79 (d, J = 8.2 Hz, 1 H), 7.27 − 7.34 (m, 1 H), 7.21 − 7.26 (m, 1 H), 7.14 (t, J = 7.6 Hz, 1 H), 3.65 (s, 2 H), 1.65 ppm (s, 9 H)

The analytical data are in agreement with the literature data.[271]

5.2.6 General procedure for the Michael addition of Nucleophiles to *trans*-β-nitrostyrene

To a stirred mixture of 2-hydroxy-1,4-naphthoquinone (**11**) (34.8 mg, 0.2 mmol) and

trans-β-nitrostyrene (**10**) (32.8 mg, 0.22 mmol) in dry DCM (1.2 mL) was added catalyst **5** (9.40 mg, 0.02 mmol) and stirred for 1 h at room temperature. After completion of the reaction the solvent was removed in vacuo and the obtained residue was purified by column chromatography over silica (EtOAc/cyclohexane in different ratio with different product) to afford the corresponding Michael adduct as a red solid in 98% yield. The product is a known compound and its data are identical to those reported in literature hitherto. Et_3N instead of chiral catalysts was used for praparation of racemic products of Michael addition.

5.2.6.1 (*S*)-2-hydroxy-3-(2-nitro-1-phenylethyl)naphthalene-1,4-dione

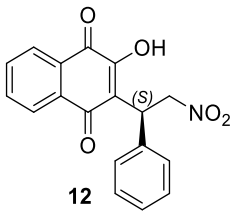

12

Purification by column chromatography over silica (EtOAc/cyclohexane 1:3) afforded **12** as a red solid.

^{1}H-NMR: (300 MHz, $CDCl_3$) δ [ppm] = 8.12 (dd, J=14.3, 7.3 Hz, 2 H), 7.67 − 7.86 (m, 3 H), 7.49 (d, J = 7.0 Hz, 2 H), 7.29 − 7.40 (m, 3 H), 5.51 (dd, J = 12.9, 8.8 Hz, 1 H), 5.28 − 5.39 (m, 1 H), 5.17 ppm (dd, J = 12.9, 6.4 Hz, 1 H)

Chiral HPLC: Daicel OJ, *n*-hexane/*i*PrOH 60:40, 0.7 mL/min, 254 nm, 25 °C, (*S*)-enantiomer 30.2 min, (*R*)-enantiomer: 87.3 min.

The analytical data are in agreement with the literature data.[272]

5.2.6.2 (*S*)-4-hydroxy-3-(2-nitro-1-phenylethyl)-2H-chromen-2-one

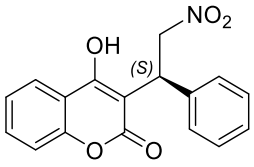

28

Purification by column chromatography over silica (EtOAc/cyclohexane 1:1) afforded **28** as a colorless solid.

^{1}H-NMR: (300 MHz, $CDCl_3$) δ [ppm] = 7.76 − 7.84 (m, 1 H), 7.59 (td, J = 7.8, 1.2 Hz, 1 H), 7.44 − 7.51 (m, 2 H), 7.29 − 7.43 (m, 5 H), 5.39 − 5.55 (m, 1 H), 5.15 − 5.30 (m, 2 H)

Chiral HPLC: Chiralpak AD-H, sample with additional 0.1% TFA (but eluent not!), *n*-hexane/*i*PrOH 85:15, 1.0 mL/min, 254 nm, 18 °C, (*S*)-enantiomer 11.5 min, (*R*)-enantiomer: 16.4 min.

The analytical data are in agreement with the literature data.[245]

5.2.6.3 (*S*)-6-(chloromethyl)-3-hydroxy-2-(2-nitro-1-phenylethyl)-4H-pyran-4-one

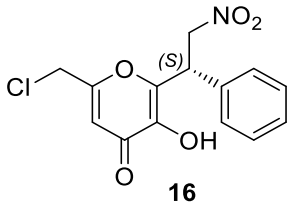

16

Purification by column chromatography over silica (EtOAc/cyclohexane 1:3) afforded **16** as a red solid.

^{1}H-NMR: (500 MHz, $(CD_3)_2SO$) δ [ppm] = 9.57 (s, 1 H), 7.29 − 7.43 (m, 5 H), 6.55 (s, 1 H), 5.33 (dd, *J* = 14.3, 9.2 Hz, 1 H), 5.18 (dd, *J* = 14.3, 6.7 Hz, 1 H), 5.09 (dd, *J* = 9.2, 6.7 Hz, 1 H), 4.70 (s, 2 H)

Chiral HPLC: Chiralpak OJ-H, *n*-hexane/*i*PrOH 50:50, 0.5 mL/min, 254 nm, 25 °C, (*S*)-enantiomer 46.0 min, (*R*)-enantiomer: 111.3 min.

The analytical data are in agreement with the literature data.[273]

5.2.6.4 (*S*)-2,2-dimethyl-5-(2-nitro-1-phenylethyl)-1,3-dioxane-4,6-dione

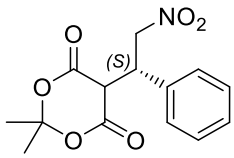

14

Purification by column chromatography over silica (EtOAc/cyclohexane 1:1) afforded **14** as a yellow oil.

^{1}H-NMR: (300 MHz, $CDCl_3$) δ [ppm] = 7.29 − 7.39 (m, 5 H), 5.43 (dd, *J* = 14.0, 9.4 Hz, 1 H), 5.01 (dd, *J* = 14.0, 6.4 Hz, 1 H), 4.65 (ddd, *J* = 9.4, 6.4, 2.9 Hz, 1 H), 4.03 (d, *J* = 2.9 Hz, 1 H), 1.72 (s, 3 H), 1.39 ppm (s, 3 H)

The analytical data are in agreement with the literature data.[274]

To determine the enantiomeric excess, the product was converted to the corresponding malonate derivative according to Takemoto and co-workers: To a solution of **14** (42 mg, 0.143 mmol) in EtOH (1.5 mL), conc. H_2SO_4 (25 µL, 3.2 eq.) was added, and then heated at reflux for 16 h. The mixture was then diluted with EtOAc, washed with aq. sat. $NaHCO_3$, dried over $MgSO_4$, and concentrated in vacuo.

The residue was purified by column chromatography over silica (EtOAc/cyclohexane 1:10) affording **117** as a colorless oil (28.6 mg, 0.093 mmol, 65% yield).

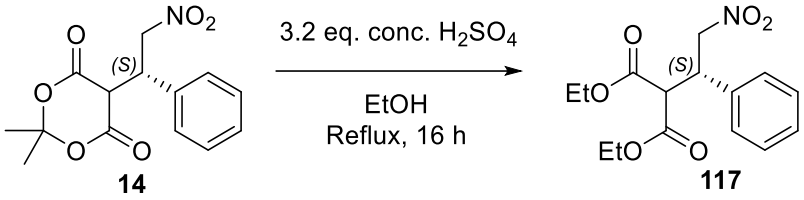

^{1}H-NMR: (300 MHz, $CDCl_3$) δ [ppm] = 7.21 − 7.39 (m, 5 H), 4.95 (dd, J = 12.9, 5.3 Hz, 1 H), 4.88 (dd, J = 13.4, 9.4 Hz, 1 H), 4.18 − 4.32 (m, 3 H), 4.03 (q, J = 7.0 Hz, 2 H), 3.84 (d, J = 9.4 Hz, 1 H), 1.28 (t, J = 7.3 Hz, 3 H), 1.07 (t, J = 7.0 Hz, 3 H)

Chiral HPLC: Chiralpak AD-H after chemical correlation to diethylmalonate adduct, *n*-hexane/*i*PrOH 90:10, 1.0 mL/min, 210 nm, 25 °C, (*S*)-enantiomer 17.4 min, (*R*)-enantiomer: 49.0 min.

The analytical data are in agreement with the literature data.[125]

5.2.6.5 *tert*-butyl 3-(2-nitro-1-phenylethyl)-2-oxoindoline-1-carboxylate

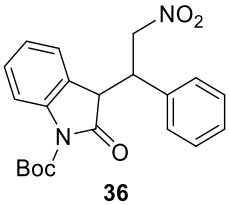

Purification by column chromatography over silica (EtOAc/cyclohexane 1:20) afforded **36** as a pale red solid.

^{1}H-NMR: (300 MHz, $CDCl_3$) δ [ppm] = 7.58 (d, J = 7.6 Hz, 1 H), 7.01 − 7.36 (m, 9 H), 5.34 (dd, J =13.9, 7.2 Hz, 1 H), 5.13 (dd, J =13.7, 7.9 Hz, 1 H), 4.26 (m, 1 H), 3.93 (d,

J = 3.5 Hz, 1 H), 1.60 (s, 9 H) The NMR data were described to major diastereomer.

The analytical data are in agreement with the literature data.[248]

5.2.6.6 3-(2-nitro-1-phenylethyl)pentane-2,4-dione

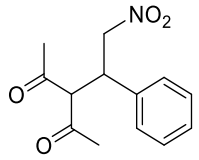

32

Purification by column chromatography over silica (EtOAc/cyclohexane 1:5) afforded **32** as a colorless solid.

^{1}H-NMR: (300 MHz, $CDCl_3$) δ [ppm] = 7.28 − 7.38 (m, 3 H), 7.15 − 7.23 (m, 2 H), 4.57 − 4.70 (m, 2 H), 4.38 (d, J = 10.5 Hz, 1 H), 4.18 − 4.31 (m, 1 H), 2.30 (s, 3 H), 1.94 (s, 3 H)

The analytical data are in agreement with the literature data.[136]

5.2.7 Synthesis of *L*-proline derivatives

5.2.7.1 Synthesis of methyl *L*-prolinate hydrochloride

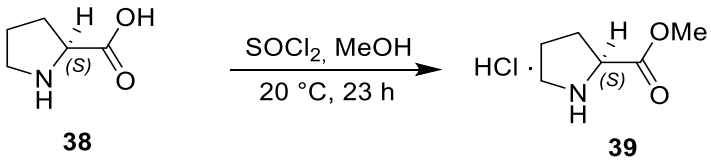

38 **39**

The synthesis was carried out according to the procedure by Chemla and co-workers.[259] 11.55 g (100 mmol, 1.0 eq.) *L*-proline (**38**) was dissolved in 100 mL

methanol. 14.5 mL (200 mmol, 2 eq.) thionyl chloride was slowly added to the solution at 0 °C. The solution was then warmed to 20 °C and stirred overnight. Solvent and other volatile compounds was removed in vacuo and the crude product was obtained as a yellowish oil with a yield of 12.98 g (100 mmol, 100%). The ^{1}H-NMR of the crude product shows a complete conversion with traces of solvent, and the product **39** was therefore used in the next step without further purification.

^{1}H-NMR: (300 MHz, $CDCl_3$) δ [ppm] = 4.50 (m, 1H), 3.85 (s, 3H), 3.56 (m, 2H), 2.43, 2.20 (m, 2H), 2.11 (m, 2H)

^{13}C-NMR: (50 MHz, $CDCl_3$) δ [ppm] = 169.2, 59.2, 53.5, 45.9, 28.7, 23.6

5.2.7.2 Synthesis of methyl trityl-*L*-prolinate

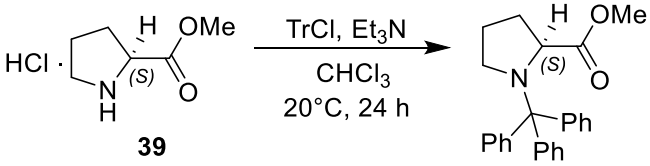

The synthesis was carried out according to the procedure by Chemla and co-workers.[259] 12.98 g (100 mmol, 1 eq.) of compound **39** was dissolved in 120 mL chloroform ($CHCl_3$). After addition of 41.85 mL (300 mmol, 3 eq.) of triethylamine (Et_3N), 30.66 g (110 mmol, 1.1 eq.) of trityl chloride dissolved in 60 mL of $CHCl_3$ was slowly added to the reaction mixture and stirred at 20 °C overnight. The reaction mixture was hydrolyzed with a mixture of saturated NH_4Cl- and 30% NH_3 solution (in a ratio of 2:1) and separated from the aqueous phase. The aqueous phase was extracted three times with 30 mL DCM for each. The combined organic phases were dried over $MgSO_4$ and the solvent was removed in vacuo. The crude product was recrystallized in Et_2O. The product **40** was obtained as a white crystalline solid in a yield of 32.21 g (92 mmol, 92%).

m.p.: 123.7 − 124.7 °C

^{1}H-NMR: (300 MHz, $CDCl_3$) δ [ppm] = 7.65 – 7.53 (m, 6H), 7.32 – 7.22 (m, 6H), 7.22 – 7.14 (m, 3H), 3.92 (dd, J = 9.1, 2.5 Hz, 1H), 3.71 (s, 3H), 3.44 (ddd, J = 11.1, 7.8, 5.3 Hz, 1H), 2.96 – 2.78 (m, 1H), 1.67 – 1.47 (m, 2H), 1.14 – 0.89 (m, 2H)

^{13}C-NMR: (75 MHz, $CDCl_3$) δ [ppm] = 177.2, 144.7, 129.3, 127.6, 126.2, 62.8, 49.9, 31.2, 24.3

The analytical data are in agreement with the literature data.[259]

5.2.7.3 Synthesis of (*S*)-(1-tritylpyrrolidin-2-yl)methanol

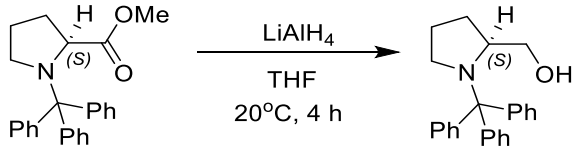

40 **41**

The synthesis was carried out according to the procedure by Chemla and co-workers.[259] 1.21 g (32 mmol, 0.8 eq.) of $LiAlH_4$ was added to 30 mL of dry THF under argon atmosphere. Then 14.84 g (40 mmol, 1 eq.) of compound **40** was dissolved in 50 mL of dry THF and slowly added to the $LiAlH_4$ suspension. After 4 h stirring at 20 °C, the conversion to product 4 completed, monitored by TLC. The reaction mixture was hydrolyzed with 50 mL (1M) sodium tartrate−solution, and then mixed with 50 mL Et_2O. The organic phase was separated from the aqueous phase. The aqueous phase was extracted three times with 50 mL DCM for each. The combined organic phases were dried over $MgSO_4$ and solvents were removed in vacuo. Product **41** was obtained as a white foam in a yield of 12.32 g (32 mmol, 80%). The product contains only traces of solvents and was therefore used in the next step without further purification.

^{1}H-NMR: (300 MHz, $CDCl_3$) δ [ppm] = 7.59 (dd, J = 7.4, 1.8 Hz, 6H), 7.28 (t, J = 7.5 Hz, 6H), 7.20 (t, 3H), 3.82 – 3.72 (m, 1H), 3.69 – 3.58 (m, 1H), 3.51 (ddd, J = 11.0, 5.6, 2.2 Hz, 1H), 3.21 (dt, J = 12.5, 7.9 Hz, 1H), 3.00 (ddd, J = 12.4, 8.3, 3.8 Hz, 1H), 2.25 (bs, 1H), 1.50 – 1.33 (m, 1H), 1.08 – 0.89 (m, 1H), 0.69 – 0.52 (m, 2H)

The analytical data are in agreement with the literature data.[259]

5.2.7.4 Synthesis of (*S*)-1-tritylpyrrolidine-2-carbaldehyde

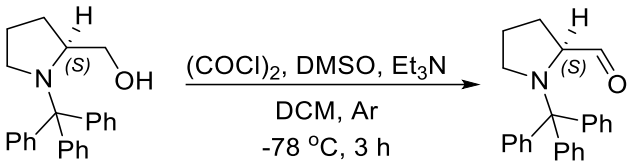

The synthesis was carried out according to the procedure by Chemla and co-workers.[259] 5.6 mL (79.46 mmol, 2.2 eq.) of DMSO dissolved in 15 mL of dry DCM was slowly added to a pre−dissolved solution of 3.4 mL (39.73 mmol, 1.1 eq.) of oxalyl chloride ($(COCl)_2$) in 35 mL of dry DCM at about -78°C under argon atmosphere. Subsequently, 12.32 g (36.12 mmol, 1.0 eq.) of compound **41** was dissolved in 35 mL of dry DCM and slowly added to the reaction mixture. After stirring for 1.5 h at -78 °C, 22.5 mL Et_3N was added and stirred for a further 1.5 h at the same temperature. The reaction mixture was hydrolyzed with a mixture of saturated NH_4Cl and 30% NH_3 solution (in a ratio of 2:1). The aqueous phase was separated and extracted three times with 30 mL DCM for each. The combined organic phases were dried over $MgSO_4$ and the solvent was removed in vacuo. The crude product was dissolved in 150 mL THF and filtered off from the insoluble residue. The solvent was removed in vacuo again and recrystallized in Et_2O. Product **42** was obtained as a white solid in a yield of 5.34 g (14.76 mmol, 40%).

m.p.: 137.7 °C

^{1}H-NMR: (300 MHz, $CDCl_3$) δ [ppm] = 9.87 (d, J = 2.8 Hz, 1H), 7.62 – 7.53 (m, 6H), 7.34 – 7.24 (m, 6H), 7.24 – 7.15 (m, 3H), 3.78 (dt, J = 9.2, 3.3 Hz, 1H), 3.30 (dt, J = 11.7, 7.1 Hz, 1H), 2.94 (ddd, J = 11.7, 7.7, 5.7 Hz, 1H), 1.69 – 1.57 (m, 1H), 1.44 (tt, J = 13.4, 7.6 Hz, 1H), 1.14 (ddd, J = 12.6, 6.4, 2.7 Hz, 1H), 0.90 – 0.75 (m, 1H)

The analytical data are in agreement with the literature data.[259]

5.2.7.5 Synthesis of (*R*)-phenyl((*S*)-1-tritylpyrrolidin-2-yl)methanol

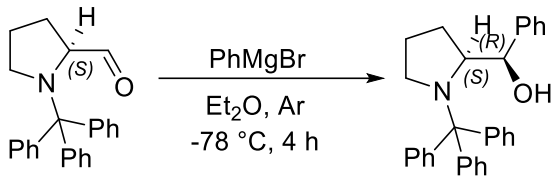

42 **(*S*,*R*)-43**

The synthesis was carried out according to the procedure by Kesavan and co-workers.[215] 0.58 g (23.85 mmol, 2.4 eq.) magnesium turnings was added to 15 mL dry Et_2O. 2.09 mL (20 mmol, 2 eq.) phenyl bromide was dropwise added under argon atmosphere and allowed to stir at 20 °C for 30 min. In a separate flask, 3.4 g (10 mmol, 1 eq.) compound **42** was added separately to 100 mL dry Et_2O under argon. The Grignard reagent (phenylmagnesium bromide) prepared in situ was now slowly added to the solution via a syringe at approx. -78 °C. After 4 h the conversion to product 6 was completed, monitored by TLC. The reaction mixture was hydrolyzed with a mixture of saturated NH_4Cl and 30% NH_3 solution (in a ratio of 2:1). The aqueous phase was separated and extracted three times with 30 mL DCM for each. The combined organic phases were dried over $MgSO_4$ and the solvent was removed in vacuo. The crude product was purified by column chromatography over silica (*c*-Hex/EtOAc/Et_3N 100:5:1). Product **(*S*,*R*)-43** was obtained as a white powder in 55% yield of 2.39 g (5.5 mmol, 55%).

Rotational value: $[\alpha]_D^{20}$ = - 77.20° (c = 1.0, $CHCl_3$) (Lit.:[259] $[\alpha]_D^{20}$ = - 77.8° (c = 2.29,

$CHCl_3$))

^{1}H-NMR: (300 MHz, $CDCl_3$) δ [ppm] = 7.62 (d, J = 7.1 Hz, 6H), 7.35 – 7.17 (m, 12H), 7.11 (d, J = 6.9 Hz, 2H), 5.13 (d, J = 3.4 Hz, 1H), 3.75 (ddd, J = 8.8, 5.3, 3.5 Hz, 1H), 3.31 (ddd, J = 12.0, 9.1, 6.8 Hz, 1H), 3.07 (ddd, J = 11.6, 7.8, 3.4 Hz, 1H), 1.53 – 1.41 (m, 1H), 1.40 – 1.27 (m, 1H), 0.82 (dtd, J = 12.6, 8.8, 8.4, 4.4 Hz, 1H), 0.31 – 0.15 (m, 1H)

^{13}C-NMR: (75 MHz, $CDCl_3$) δ [ppm] = 144.5, 129.9, 128.0, 127.6, 126.5, 126.4, 125.4, 77.0, 75.5, 66.0, 53.3, 26.9, 25.8, 24.8

HRMS: ESI^+ (m/z) $[M + 2H - H_2O]^{2+}$ calcd. for $C_{11}H_{14}N$: 160.11208; found: 160.11205

The analytical data are in agreement with the literature data.[215]

5.2.7.6 Synthesis of (*S*)-2-((*R*)-azido(phenyl)methyl)-1-tritylpyrrolidine

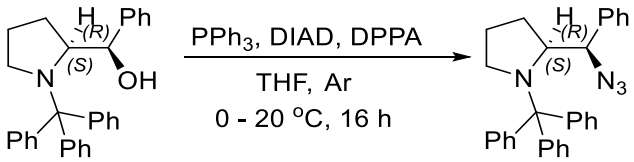

(*S*,*R*)-43 **(*S*,*R*)-44**

The synthesis was carried out according to the procedure by Kesavan and co-workers.[215] 2.0 g (4.77 mmol, 1 eq.) of compound **(*S*,*R*)-43** and 2.5 g (9.54 mmol, 2 eq.) of triphenylphospine (PPh_3) were added to 21 mL of dry THF under argon atmosphere. Subsequently, 1.5 mL (7.64 mmol, 1.6 eq.) of diisopropylazodicarboxylic acid ester (DIAD) was slowly added to the solution at 0 °C, followed by a similar addition of 1.4 mL (6.20 mmol, 1.3 eq.) of diphenylphosporyl azide (DPPA) and the mixture was allowed to warm to room temperature and stirred overnight. The reaction

mixture was separated from volatile compounds under reduced pressure and 30 mL of distilled water was added. The aqueous phase was separated and extracted three times with 20 mL EtOAc for each. The organic phase was then dried over Na_2SO_4 and the solvent was removed in vacuo. The crude product was purified by column chromatography over silica (*n*-Hex/EtOAc/Et_3N 400:10:1). Product **(*S*,*R*)-44** was obtained as a white crystalline solid in a yield of 1.38 g (3.10 mmol, 64%).

Rotational value: $[\alpha]_D^{20}$ = -70.91 (c = 1.0, $CHCl_3$) (Lit.:[216] $[\alpha]_D^{20}$ = -93.5° (c = 1.0, $CHCl_3$))

^{1}H-NMR: (300 MHz, $CDCl_3$) δ [ppm] = 7.64 (d, J = 7.8 Hz, 6H), 7.38 – 7.27 (m, 6H), 7.27 – 7.18 (m, 6H), 6.89 (d, J = 7.9 Hz, 2H), 5.30 (s, 1H), 3.84 – 3.76 (m, 1H), 3.52 – 3.36 (m, 1H), 3.09 (ddd, J = 12.2, 7.0, 4.4 Hz, 1H), 1.55 – 1.37 (m, 1H), 0.96 – 0.80 (m, 1H), 0.32 – 0.07 (m, 1H)

^{13}C-NMR: (75 MHz, $CDCl_3$) δ [ppm] = 144.8, 129.9, 128.3, 127.7, 127.1, 126.3, 126.1, 70.9, 67.3, 52.0, 25.5, 24.9

HRMS: ESI$^+$ (m/z) $[M + H - N_3]^+$ calcd. for $C_{11}H_{14}N$: 160.11208; found: 160.11205

The analytical data are in agreement with the literature data.[215]

5.2.7.7 Synthesis of (*S*)-2-((*R*)-azido(phenyl)methyl)-1-methylpyrrolidine

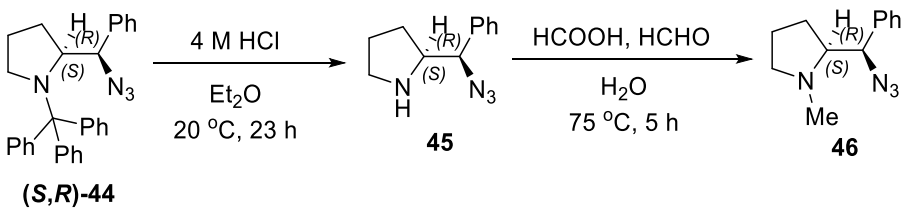

The synthesis was carried out according to the procedure by Kesavan and co-workers.[215] 1.08 g (2.42 mmol, 1 eq.) of compound **(*S*,*R*)-44** was added to 12 mL Et_2O. To the solution, 12 mL of a 4M HCl solution was added and stirred for 23 h at 20 °C. The reaction mixture was then washed three times with 20 mL Et_2O for each. The aqueous phase was slowly alkalinized with concentrated NaOH solution at 0 °C and extracted three times with 30 mL DCM for each. The combined organic phases were dried over Na_2SO_4 and the solvent was removed in vacuo. Without further purification, the crude product **45** was diluted with 2 mL distilled water, followed by addition of 1 mL 98% HCOOH (26.0 mmol) and 1.6 mL aq. 37% HCHO solution (21.5 mmol). The reaction mixture was heated to 75 °C and refluxed for 5 h, then cooled, alkalized with concentrated sodium hydroxide solution and extracted three times with 30 mL DCM for each. The combined organic phases were dried over Na_2SO_4 and the solvent was removed under reduced pressure. The crude product 9 was purified by column chromatography over silica (*n*-Hex/EtOAc 92:8) In a yield of 180 mg (0.83 mmol, 34%), compound **46** was obtained as a yellowish oil.

^{1}H-NMR: (300 MHz, $CDCl_3$) δ [ppm] = 7.43 – 7.35 (m, 2H), 7.35 – 7.27 (m, 3H), 4.72 (d, J = 3.9 Hz, 1H), 3.15 (ddd, J = 9.5, 7.3, 1.9 Hz, 1H), 2.51 (ddd, J = 8.3, 6.3, 3.9 Hz, 1H), 2.36 (s, 3H), 2.25 (ddd, J = 10.0, 9.0, 6.7 Hz, 1H), 1.99 – 1.87 (m, 1H), 1.87 – 1.75 (m, 1H), 1.68 (m, 1H), 1.63 – 1.55 (m, 1H)

^{13}C-NMR: (75 MHz, $CDCl_3$) δ [ppm] = 138.4, 71.0, 66.60, 57.50, 41.0, 29.7, 25.9, 22.8

The analytical data are in agreement with the literature data.[215]

5.2.7.8 Synthesis of 1-(*tert*-butyl) 2-methyl (*S*)-pyrrolidine-1,2-dicarboxylate

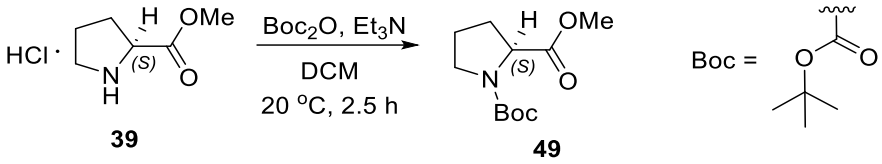

The synthesis was carried out according to the procedure by Nelson, Marsden and co-workers.[260] Under argon atmosphere, 0.808 g (4.88 mmol, 1.0 eq.) of prolinate **39** and ca.1 g of $MgSO_4$ were dissolved in 60 mL of DCM, then 1.27 g (5.61 mmol, 1.15 eq.) of Boc_2O and 1.97 mL (14.15 mmol, 2.9 eq.) of Et_3N were added to the solution. The mixture was stirred at 20 °C for 2.5 h under argon atmosphere. Next, the by−product solid was filtered under reduced pressure and the organic phase was washed by 2x130 mL of 1N HCl and once by 130 mL of saturated Na_2CO_3 solution. The combined organic layers were dried over Na_2SO_4, then filtered over celite, and the solvents were removed. The crude product was purified by column chromatography over silica (*n*-Hex/ EtOAc/Et_3N 15:1:1, then *n*-Hex/EtOAc 4:1). The product dicarboxylate **49** was obtained as a white solid in a yield of 0.8391 g (3.66 mmol, 75%).

^{1}H-NMR: (300 MHz, $CDCl_3$) δ [ppm] = 4.32 (dd, J = 8.3, 3.0 Hz, 0.35H), 4.22 (dd, J = 8.4, 4.1 Hz, 0.58H), 3.72 (s, 3H), 3.60 – 3.34 (m, 2H), 2.29 – 2.11 (m, 1H), 2.04 – 1.80 (m, 3H), 1.46 (s, 3.5H), 1.41 (s, 5.5H)

The analytical data are in agreement with the literature data.[260]

5.2.7.8 Synthesis of *tert*-butyl (*S*)-2-((*S*)-hydroxy(phenyl)methyl)pyrrolidine-1-carboxylate

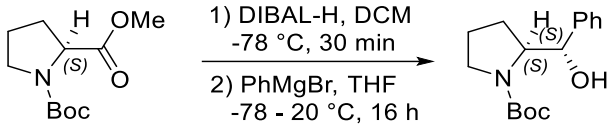

49 **(*S*,*S*)-50**

The synthesis was carried out according to the procedure by Rye and co-workers.[216] Under argon atmosphere, 5.22 mL (1.0 M in hexane, 5.22 mmol, 1.2 eq.) of DIBAL-H was dropwise added to a solution of 1.00 g (4.36 mmol, 1.0 eq.) of dicarboxylate **49** in 20 mL of dry DCM at -78 °C. The mixture was stirred for 30 min.

In another 100 mL Schlenk flask, 0.380 g (15.62 mmol, 3.6 eq.) of Mg turnings was suspended in 13 mL of THF, and 1.40 mL (13.33 mmol, 3.0 eq.) of PhBr was added dropwise under argon atmosphere at 20 °C. The reaction mixture was stirred for 30 min. Subsquently, the newly prepared PhMgBr solution was added dropwise into the substrate solution and the reaction mixture was warmed to 20 °C and stirred overnight.

After that, the reaction was quenched by 20 mL of saturated NH_4Cl solution and 20 mL of sodium tartrate solution and the mixture was stirred for another 30 min at 20 °C. The aqueous layer was extracted by 3x30 mL of DCM. The combined organic layers were dried over Na_2SO_4 and concentrated in vacuo. The crude product was purified by column chromatography over silica gel (EtOAc/n-Hex 1:5), yielding alcohol **(*S*,*S*)-50** as a colorless oil in a yield of 0.8496g (3.23 mmol, 74%).

^{1}H-NMR: (300 MHz, $CDCl_3$) δ [ppm] = 7.44 – 7.19 (m, 5H), 5.83 (br, 1H), 4.53 (d, J = 8.3 Hz, 1H), 4.17 – 4.02 (m, 1H), 3.47 (dt, J = 10.8, 7.6 Hz, 1H), 3.37 (d, J = 4.2 Hz, 1H), 1.82 – 1.58 (m, 4H), 1.52 (s, 9H)

The analytical data are in agreement with the literature data.[216]

5.2.7.9 Synthesis of (*S*)-((*S*)-1-methylpyrrolidin-2-yl)(phenyl)methanol

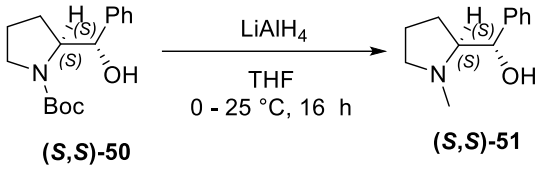

(*S*,*S*)-50 (*S*,*S*)-51

The synthesis was carried out according to a modified procedure by Yeung and co-worker.[262] To a solution of 2.3731 g (8.56 mmol, 1.0 eq.) of alcohol **(*S*,*S*)-50** in 20 mL of dry THF under argon atmosphere, 0.975 g (25.68 mmol, 3.0 eq.) of $LiAlH_4$ was added at 0 °C. The reaction mixture was warmed to 25 °C and stirred overnight. Subsquently, the mixture was cooled to 0 °C and quenched with 1.7 mL of water, 1.7 mL of 15% NaOH aqueous solution and another 2.8 mL of water, respectively. After being stirred for 30 min, the mixture was diluted by 50 mL of EtOAc and the aqueous phase was extracted by 3x50 mL of DCM. The combined organic phase was dried over anhydrous Na_2SO_4, then they were filtered and concentrated under vacuum. The crude product was purified by column chromatography over silica (DCM/MeOH/25% aq. NH_4OH 100:10:1), yielding 0.7517 g alcohol **(*S*,*S*)-51** (3.93 mmol, 46%) as a pale yellow oil.

Rotational value: $[\alpha]_D^{20}$ = + 25.70° (c = 0.95, MeOH).

^{1}H-NMR: (300 MHz, $CDCl_3$) δ [ppm] = 7.45 – 7.16 (m, 5H), 4.40 (d, J = 5.3 Hz, 1H), 3.96 (br, 1H), 3.21 – 3.09 (m, 1H), 2.79 (m, 1H), 2.51 – 2.34 (m, 1H), 2.27 (s, 3H), 1.99 – 1.65 (m, 4H)

The analytical data are in agreement with the literature data.[262]

5.2.7.10 Synthesis of (2*R*,3*R*)-3-azido-1-methyl-2-phenylpiperidine

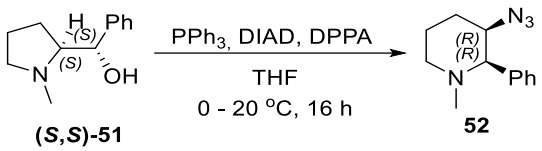

(*S*,*S*)-51 **52**

To a solution of 0.300 g (1.568 mmol, 1.0 eq.) of alcohol **(*S*,*S*)-51** in 6.9 mL of dry THF under argon atmosphere, 0.823 g (3.136 mmol, 2.0 eq.) of PPh_3 were added at 20 °C, then 0.507 mL (2.509 mmol, 1.6 eq.) of DIAD and 0.46 mL (2.038 mmol, 1.3 eq.) of DPPA were added to the solution dropwise at 0 °C. The mixture was then warmed to 20 °C and stirred overnight. 9.8 mL of distilled water was added to quench the reaction. The aqueous layer was extracted by 3 × 6 mL of EtOAc. The combined organic layers were dried over $MgSO_4$, then filtered and concentrated under vacuum. The crude product was purified by column chromatography over silica (EtOAc/*c*-Hex 1:3), yielding 0.094 g piperidine azide **52** (0.433 mmol, 28%) as a yellow oil.

^{1}H-NMR: (300 MHz, $CDCl_3$) δ [ppm] = 7.43 – 7.25 (m, 5H), 3.69 – 3.62 (m, 1H), 3.08 (m, 1H), 3.04 (d, J = 2.1 Hz, 1H), 2.20 – 2.07 (m, 3H), 2.06 (s, 3H), 1.81 – 1.55 (m, 2H)

^{13}C-NMR: (75 MHz, $CDCl_3$) δ [ppm] = 140.0, 128.6, 128.3, 127.6, 72.6, 63.2, 57.1, 44.6, 29.4, 20.6

FT-IR: (ATR) $\tilde{\nu}$ [cm^{-1}] = 2944 (m), 2849 (m), 2782 (m), 2724 (w), 2103 (s), 1720 (w), 1493 (m), 1452 (m), 1357 (m), 1331 (m), 1288 (s), 1202 (m), 1176 (m), 1124 (s), 1080 (m), 1032 (m), 959 (m), 882 (w), 757 (m), 702 (s), 611 (w), 539 (m)

HRMS: ESI^+ (m/z) $[M + H]^+$ calcd. for $C_{12}H_{17}N_4$: 127.14477; found: 127.14445

6. References

[1] J. Gal, *Chirality* **2012**, *24*, 959–976.
[2] T. J. Leitereg, D. G. Guadagni, Jean. Harris, T. R. Mon, Roy. Teranishi, *J. Agric. Food Chem.* **1971**, *19*, 785–787.
[3] J. Hyttel, K. P. Bøgesø, J. Perregaard, C. Sánchez, *J. Neural Transm. Gen. Sect. JNT* **1992**, *88*, 157–160.
[4] U. Lepola, A. Wade, H. F. Andersen, *Int. Clin. Psychopharmacol.* **2004**, *19*, 149.
[5] I. A. Jaffe, K. Altman, P. Merryman, *J. Clin. Invest.* **1964**, *43*, 1869–1873.
[6] S. W. Smith, *Toxicol. Sci.* **2009**, *110*, 4–30.
[7] S. Gao, S. Wang, R. Fan, J. Hu, *Biomed. Pharmacother.* **2020**, *127*, 110114.
[8] J. H. Kim, A. R. Scialli, *Toxicol. Sci.* **2011**, *122*, 1–6.
[9] J. Gal, *Chirality* **2011**, *23*, 1–16.
[10] E. Fischer, *Berichte Dtsch. Chem. Ges.* **1894**, *27*, 3189–3232.
[11] M. B. Smith, J. March, *March's Advanced Organic Chemistry: Reactions, Mechanisms, and Structure*, Wiley, **2006**.
[12] B. M. Trost, *Proc. Natl. Acad. Sci.* **2004**, *101*, 5348–5355.
[13] W. S. Knowles, M. J. Sabacky, *Chem. Commun. Lond.* **1968**, 1445–1446.
[14] H. Nozaki, H. Takaya, S. Moriuti, R. Noyori, *Tetrahedron* **1968**, *24*, 3655–3669.
[15] M. Kitamura, I. Kasahara, K. Manabe, R. Noyori, H. Takaya, *J. Org. Chem.* **1988**, *53*, 708–710.
[16] K. B. Sharpless, D. W. Patrick, L. K. Truesdale, S. A. Biller, *J. Am. Chem. Soc.* **1975**, *97*, 2305–2307.
[17] T. Katsuki, K. B. Sharpless, *J. Am. Chem. Soc.* **1980**, *102*, 5974–5976.
[18] E. N. Jacobsen, Istvan. Marko, W. S. Mungall, Georg. Schroeder, K. Barry. Sharpless, *J. Am. Chem. Soc.* **1988**, *110*, 1968–1970.
[19] E. J. Corey, H. E. Ensley, *J. Am. Chem. Soc.* **1975**, *97*, 6908–6909.
[20] B. M. Trost, D. O'Krongly, J. L. Belletire, *J. Am. Chem. Soc.* **1980**, *102*, 7595–7596.
[21] F. S. Sariaslani, J. P. N. Rosazza, *Enzyme Microb. Technol.* **1984**, *6*, 242–253.
[22] C. Wandrey, A. Liese, D. Kihumbu, *Org. Process Res. Dev.* **2000**, *4*, 286–290.
[23] D. W. C. MacMillan, *Nature* **2008**, *455*, 304–308.
[24] J. Wisniak, *Educ. Quím.* **2010**, *21*, 60–69.
[25] P. C. J. Kamer, D. Vogt, J. Thybaut, *Contemporary Catalysis: Science, Technology, and Applications*, Royal Society of Chemistry, **2017**.
[26] R. Noyori, T. Ohkuma, M. Kitamura, H. Takaya, N. Sayo, H. Kumobayashi, S. Akutagawa, *J. Am. Chem. Soc.* **1987**, *109*, 5856–5858.
[27] S. T. Nguyen, L. K. Johnson, R. H. Grubbs, J. W. Ziller, *J. Am. Chem. Soc.* **1992**, *114*, 3974–3975.
[28] P. Schwab, M. B. France, J. W. Ziller, R. H. Grubbs, *Angew. Chem. Int. Ed. Engl.* **1995**, *34*, 2039–2041.
[29] J. S. Kingsbury, J. P. A. Harrity, P. J. Bonitatebus, A. H. Hoveyda, *J. Am. Chem. Soc.* **1999**, *121*, 791–799.
[30] M. Scholl, S. Ding, C. W. Lee, R. H. Grubbs, *Org. Lett.* **1999**, *1*, 953–956.

[31] S. B. Garber, J. S. Kingsbury, B. L. Gray, A. H. Hoveyda, *J. Am. Chem. Soc.* **2000**, *122*, 8168–8179.
[32] J. A. Love, J. P. Morgan, T. M. Trnka, R. H. Grubbs, *Angew. Chem. Int. Ed.* **2002**, *41*, 4035–4037.
[33] J. Magano, J. R. Dunetz, *Chem. Rev.* **2011**, *111*, 2177–2250.
[34] J. Boström, D. G. Brown, R. J. Young, G. M. Keserü, *Nat. Rev. Drug Discov.* **2018**, *17*, 709–727.
[35] A. Taheri Kal Koshvandi, M. M. Heravi, T. Momeni, *Appl. Organomet. Chem.* **2018**, *32*, e4210.
[36] M. V. Bautista, A. J. Varni, J. Ayuso-Carrillo, M. C. Carson, K. J. T. Noonan, *Polym. Chem.* **2021**, *12*, 1404–1414.
[37] P. Kisszékelyi, S. Nagy, Z. Fehér, P. Huszthy, J. Kupai, *Chemistry* **2020**, *2*, 742–758.
[38] E. Reyes, L. Prieto, A. Milelli, *Molecules* **2023**, *28*, 271.
[38] G. Bredig, P. Fiske, *Biochem. Z.* **1912**, *46*, 7–23.
[39] Z. G. Hajos, D. R. Parrish, Deutsches Patent DE 21022623,**1971**
[40] U. Eder, G. R. Sauer, R. Wiechert, Deutsches Patent DE 2014757, **1971**
[42] U. Eder, G. Sauer, R. Wiechert, *Angew. Chem. Int. Ed. Engl.* **1971**, *10*, 496–497.
[43] Z. G. Hajos, D. R. Parrish, *J. Org. Chem.* **1974**, *39*, 1615–1621.
[44] B. List, R. A. Lerner, C. F. Barbas, *J. Am. Chem. Soc.* **2000**, *122*, 2395–2396.
[45] K. A. Ahrendt, C. J. Borths, D. W. C. MacMillan, *J. Am. Chem. Soc.* **2000**, *122*, 4243–4244.
[46] P. I. Dalko, L. Moisan, *Angew. Chem. Int. Ed.* **2004**, *43*, 5138–5175.
[47] A. Berkessel, H. Gröger, *Asymmetric Organocatalysis: From Biomimetic Concepts to Applications in Asymmetric Synthesis*, Wiley, **2005**.
[48] S. Yamada, K. Hiroi, K. Achiwa, *Tetrahedron Lett.* **1969**, *10*, 4233–4236.
[49] S. Yamada, G. Otani, *Tetrahedron Lett.* **1969**, *10*, 4237–4240.
[50] H. E. Zimmerman, M. D. Traxler, *J. Am. Chem. Soc.* **1957**, *79*, 1920–1923.
[51] J. Wagner, R. A. Lerner, C. F. Barbas, *Science* **1995**, *270*, 1797–1800.
[52] S. Bahmanyar, K. N. Houk, H. J. Martin, B. List, *J. Am. Chem. Soc.* **2003**, *125*, 2475–2479.
[53] W. Notz, B. List, *J. Am. Chem. Soc.* **2000**, *122*, 7386–7387.
[54] B. List, P. Pojarliev, C. Castello, *Org. Lett.* **2001**, *3*, 573–575.
[55] A. B. Northrup, D. W. C. MacMillan, *J. Am. Chem. Soc.* **2002**, *124*, 6798–6799.
[56] B. List, P. Pojarliev, W. T. Biller, H. J. Martin, *J. Am. Chem. Soc.* **2002**, *124*, 827–833.
[57] A. Córdova, S. Watanabe, F. Tanaka, W. Notz, C. F. Barbas, *J. Am. Chem. Soc.* **2002**, *124*, 1866–1867.
[58] M. M. B. Marques, *Angew. Chem. Int. Ed.* **2006**, *45*, 348–352.
[59] B. List, P. Pojarliev, H. J. Martin, *Org. Lett.* **2001**, *3*, 2423–2425.
[60] B. List, C. Castello, *Synlett* **2001**, *2001*, 1687–1689.
[61] B.-C. Hong, P. Kotame, C.-W. Tsai, J.-H. Liao, *Org. Lett.* **2010**, *12*, 776–779.
[62] B. List, *J. Am. Chem. Soc.* **2002**, *124*, 5656–5657.
[63] N. Kumaragurubaran, K. Juhl, W. Zhuang, A. Bøgevig, K. A. Jørgensen, *J. Am. Chem. Soc.* **2002**, *124*, 6254–6255.

[64] P. Kumar, B. M. Sharma, *Synlett* **2018**, *29*, 1944–1956.
[65] M. P. Brochu, S. P. Brown, D. W. C. MacMillan, *J. Am. Chem. Soc.* **2004**, *126*, 4108–4109.
[66] J. Franzén, M. Marigo, D. Fielenbach, T. C. Wabnitz, A. Kjærsgaard, K. A. Jørgensen, *J. Am. Chem. Soc.* **2005**, *127*, 18296–18304.
[67] A. Job, C. F. Janeck, W. Bettray, R. Peters, D. Enders, *Tetrahedron* **2002**, *58*, 2253–2329.
[68] A. Hirao, S. Itsuno, S. Nakahama, N. Yamazaki, *J. Chem. Soc. Chem. Commun.* **1981**, 315–317.
[69] E. J. Corey, R. K. Bakshi, S. Shibata, *J. Am. Chem. Soc.* **1987**, *109*, 5551–5553.
[70] J. S. Baum, H. G. Viehe, *J. Org. Chem.* **1976**, *41*, 183–187.
[71] M. E. Jung, W. D. Vaccaro, K. R. Buszek, *Tetrahedron Lett.* **1989**, *30*, 1893–1896.
[72] M. Yamaguchi, T. Shiraishi, M. Hirama, *Angew. Chem. Int. Ed. Engl.* **1993**, *32*, 1176–1178.
[73] A. Kawara, T. Taguchi, *Tetrahedron Lett.* **1994**, *35*, 8805–8808.
[74] W. S. Jen, J. J. M. Wiener, D. W. C. MacMillan, *J. Am. Chem. Soc.* **2000**, *122*, 9874–9875.
[75] N. A. Paras, D. W. C. MacMillan, *J. Am. Chem. Soc.* **2001**, *123*, 4370–4371.
[76] N. A. Paras, D. W. C. MacMillan, *J. Am. Chem. Soc.* **2002**, *124*, 7894–7895.
[77] S. P. Brown, N. C. Goodwin, D. W. C. MacMillan, *J. Am. Chem. Soc.* **2003**, *125*, 1192–1194.
[78] M. Marigo, J. Franzén, T. B. Poulsen, W. Zhuang, K. A. Jørgensen, *J. Am. Chem. Soc.* **2005**, *127*, 6964–6965.
[79] M. Leven, J. M. Neudörfl, B. Goldfuss, *Beilstein J. Org. Chem.* **2013**, *9*, 155–165.
[80] Wöhler, Liebig, *Ann. Pharm.* **1832**, *3*, 249–282.
[81] T. Ukai, R. Tanaka, T. Dokawa, *Pharm. Soc. Jpn.* **1943**, *63*, 296–300.
[82] S. Mizuhara, P. Handler, *J. Am. Chem. Soc.* **1954**, *76*, 571–573.
[83] R. Breslow, *J. Am. Chem. Soc.* **1958**, *80*, 3719–3726.
[84] A. J. I. Arduengo, R. L. Harlow, M. Kline, *J. Am. Chem. Soc.* **1991**, *113*, 361–363.
[85] H. Stetter, *Angew. Chem. Int. Ed. Engl.* **1976**, *15*, 639–647.
[86] D. Enders, K. Breuer, G. Raabe, J. Runsink, J. H. Teles, J.-P. Melder, K. Ebel, S. Brode, *Angew. Chem. Int. Ed. Engl.* **1995**, *34*, 1021–1023.
[87] J. Henrique Teles, J.-P. Melder, K. Ebel, R. Schneider, E. Gehrer, W. Harder, S. Brode, D. Enders, K. Breuer, G. Raabe, *Helv. Chim. Acta* **1996**, *79*, 61–83.
[88] D. Enders, K. Breuer, J. H. Teles, *Helv. Chim. Acta* **1996**, *79*, 1217–1221.
[89] R. L. Knight, F. J. Leeper, *Tetrahedron Lett.* **1997**, *38*, 3611–3614.
[90] M. S. Kerr, J. Read de Alaniz, T. Rovis, *J. Am. Chem. Soc.* **2002**, *124*, 10298–10299.
[91] S. S. Sohn, E. L. Rosen, J. W. Bode, *J. Am. Chem. Soc.* **2004**, *126*, 14370–14371.
[92] C. Burstein, F. Glorius, *Angew. Chem. Int. Ed.* **2004**, *43*, 6205–6208.
[93] M. T. Berry, D. Castrejon, J. E. Hein, *Org. Lett.* **2014**, *16*, 3676–3679.
[94] M. Mahlau, B. List, *Angew. Chem. Int. Ed.* **2013**, *52*, 518–533.

[95] T. Hashimoto, K. Maruoka, *Chem. Rev.* **2007**, *107*, 5656–5682.
[96] U. H. Dolling, P. Davis, E. J. J. Grabowski, *J. Am. Chem. Soc.* **1984**, *106*, 446–447.
[97] S. Mayer, B. List, *Angew. Chem. Int. Ed.* **2006**, *45*, 4193–4195.
[98] K. Brak, E. N. Jacobsen, *Angew. Chem. Int. Ed.* **2013**, *52*, 534–561.
[99] M. S. Taylor, E. N. Jacobsen, *J. Am. Chem. Soc.* **2004**, *126*, 10558–10559.
[100] S. E. Reisman, A. G. Doyle, E. N. Jacobsen, *J. Am. Chem. Soc.* **2008**, *130*, 7198–7199.
[101] D. J. Cram, G. D. Y. Sogah, *J. Chem. Soc. Chem. Commun.* **1981**, 625–628.
[102] R. He, C. Ding, K. Maruoka, *Angew. Chem. Int. Ed.* **2009**, *48*, 4559–4561.
[103] D. Nakashima, H. Yamamoto, *J. Am. Chem. Soc.* **2006**, *128*, 9626–9627.
[104] M. S. Taylor, E. N. Jacobsen, *Angew. Chem. Int. Ed.* **2006**, *45*, 1520–1543.
[105] T. Steiner, *Angew. Chem. Int. Ed.* **2002**, *41*, 48–76.
[106] G. A. Jeffrey, *An Introduction to Hydrogen Bonding*, Oxford University Press, **1997**.
[107] K. Morokuma, *Acc. Chem. Res.* **1977**, *10*, 294–300.
[108] T. Steiner, *Angew. Chem.* **2002**, *114*, 50–80.
[109] J. E. Lennard-Jones, *Proc. Phys. Soc.* **1931**, *43*, 461.
[110] D. S. Coombes, S. L. Price, D. J. Willock, M. Leslie, *J. Phys. Chem.* **1996**, *100*, 7352–7360.
[111] J. Hine, K. Ahn, J. C. Gallucci, S. M. Linden, *J. Am. Chem. Soc.* **1984**, *106*, 7980–7981.
[112] M. C. Etter, T. W. Panunto, *J. Am. Chem. Soc.* **1988**, *110*, 5896–5897.
[113] M. C. Etter, *Acc. Chem. Res.* **1990**, *23*, 120–126.
[114] M. C. Etter, Z. Urbanczyk-Lipkowska, M. Zia-Ebrahimi, T. W. Panunto, *J. Am. Chem. Soc.* **1990**, *112*, 8415–8426.
[115] T. R. Kelly, P. Meghani, V. S. Ekkundi, *Tetrahedron Lett.* **1990**, *31*, 3381–3384.
[116] D. P. Curran, L. H. Kuo, *J. Org. Chem.* **1994**, *59*, 3259–3261.
[117] M. S. Sigman, E. N. Jacobsen, *J. Am. Chem. Soc.* **1998**, *120*, 4901–4902.
[118] P. Vachal, E. N. Jacobsen, *Org. Lett.* **2000**, *2*, 867–870.
[119] P. Vachal, E. N. Jacobsen, *J. Am. Chem. Soc.* **2002**, *124*, 10012–10014.
[120] A. G. Wenzel, E. N. Jacobsen, *J. Am. Chem. Soc.* **2002**, *124*, 12964–12965.
[121] P. R. Schreiner, A. Wittkopp, *Org. Lett.* **2002**, *4*, 217–220.
[122] A. Wittkopp, P. R. Schreiner, *Chem. – Eur. J.* **2003**, *9*, 407–414.
[123] G. Jakab, C. Tancon, Z. Zhang, K. M. Lippert, P. R. Schreiner, *Org. Lett.* **2012**, *14*, 1724–1727.
[124] C. Nieuwland, C. Fonseca Guerra, *Chem. – Eur. J.* **2022**, *28*, e202200755.
[125] T. Okino, Y. Hoashi, Y. Takemoto, *J. Am. Chem. Soc.* **2003**, *125*, 12672–12673.
[126] Y. Sohtome, A. Tanatani, Y. Hashimoto, K. Nagasawa, *Tetrahedron Lett.* **2004**, *45*, 5589–5592.
[127] R. P. Herrera, V. Sgarzani, L. Bernardi, A. Ricci, *Angew. Chem. Int. Ed.* **2005**, *44*, 6576–6579.
[128] B. Vakulya, S. Varga, A. Csámpai, T. Soós, *Org. Lett.* **2005**, *7*, 1967–1969.
[129] A. Berkessel, K. Roland, J. M. Neudörfl, *Org. Lett.* **2006**, *8*, 4195–4198.
[130] Y.-Q. Fang, E. N. Jacobsen, *J. Am. Chem. Soc.* **2008**, *130*, 5660–5661.

[131] W.-Y. Han, Z.-J. Wu, X.-M. Zhang, W.-C. Yuan, *Org. Lett.* **2012**, *14*, 976–979.
[132] J. P. Malerich, K. Hagihara, V. H. Rawal, *J. Am. Chem. Soc.* **2008**, *130*, 14416–14417.
[133] J. Alemán, A. Parra, H. Jiang, K. A. Jørgensen, *Chem. – Eur. J.* **2011**, *17*, 6890–6899.
[134] D. Quiñonero, A. Frontera, P. Ballester, P. M. Deyà, *Tetrahedron Lett.* **2000**, *41*, 2001–2005.
[135] C. Rotger, B. Soberats, D. Quiñonero, A. Frontera, P. Ballester, J. Benet-Buchholz, P. M. Deyà, A. Costa, *Eur. J. Org. Chem.* **2008**, *2008*, 1864–1868.
[136] T. Okino, Y. Hoashi, T. Furukawa, X. Xu, Y. Takemoto, *J. Am. Chem. Soc.* **2005**, *127*, 119–125.
[137] X. Li, H. Deng, B. Zhang, J. Li, L. Zhang, S. Luo, J.-P. Cheng, *Chem. – Eur. J.* **2010**, *16*, 450–455.
[138] X. Ni, X. Li, Z. Wang, J.-P. Cheng, *Org. Lett.* **2014**, *16*, 1786–1789.
[139] D. Zhou, Z. Huang, X. Yu, Y. Wang, J. Li, W. Wang, H. Xie, *Org. Lett.* **2015**, *17*, 5554–5557.
[140] J. V. Alegre-Requena, E. Marqués-López, R. P. Herrera, *Adv. Synth. Catal.* **2016**, *358*, 1801–1809.
[141] Q. Huang, L. Zhang, Y. Cheng, P. Li, W. Li, *Adv. Synth. Catal.* **2018**, *360*, 3266–3270.
[142] A. A. Rodriguez, H. Yoo, J. W. Ziller, K. J. Shea, *Tetrahedron Lett.* **2009**, *50*, 6830–6833.
[143] A. Borovika, P.-I. Tang, S. Klapman, P. Nagorny, *Angew. Chem. Int. Ed.* **2013**, *52*, 13424–13428.
[144] Y.-L. Liu, F. Zhou, J.-J. Cao, C.-B. Ji, M. Ding, J. Zhou, *Org. Biomol. Chem.* **2010**, *8*, 3847–3850.
[145] R. Wu, X. Chang, A. Lu, Y. Wang, G. Wu, H. Song, Z. Zhou, C. Tang, *Chem. Commun.* **2011**, *47*, 5034–5036.
[146] N. Melnyk, M. R. Garcia, C. Trujillo, *ACS Catal.* **2023**, *13*, 15505–15515.
[147] T. Brinck, J. S. Murray, P. Politzer, *Int. J. Quantum Chem.* **1993**, *48*, 73–88.
[148] J. S. Murray, K. Paulsen, P. Politzer, *Proc. Indian Acad. Sci. - Chem. Sci.* **1994**, *106*, 267–275.
[149] G. R. Desiraju, P. S. Ho, L. Kloo, A. C. Legon, R. Marquardt, P. Metrangolo, P. Politzer, G. Resnati, K. Rissanen, *Pure Appl. Chem.* **2013**, *85*, 1711–1713.
[150] B. Mallada, A. Gallardo, M. Lamanec, B. de la Torre, V. Špirko, P. Hobza, P. Jelinek, *Science* **2021**, *374*, 863–867.
[151] A. Bruckmann, M. A. Pena, C. Bolm, *Synlett* **2008**, *2008*, 900–902.
[152] S. M. Walter, F. Kniep, E. Herdtweck, S. M. Huber, *Angew. Chem. Int. Ed.* **2011**, *50*, 7187–7191.
[153] S. Guha, I. Kazi, A. Nandy, G. Sekar, *Eur. J. Org. Chem.* **2017**, *2017*, 5497–5518.
[154] F. Kniep, S. H. Jungbauer, Q. Zhang, S. M. Walter, S. Schindler, I. Schnapperelle, E. Herdtweck, S. M. Huber, *Angew. Chem. Int. Ed.* **2013**, *52*, 7028–7032.
[155] S. H. Jungbauer, S. M. Huber, *J. Am. Chem. Soc.* **2015**, *137*, 12110–12120.

[156] L. Zong, X. Ban, C. W. Kee, C.-H. Tan, *Angew. Chem.* **2014**, *126*, 12043–12047.
[157] M. Saito, N. Tsuji, Y. Kobayashi, Y. Takemoto, *Org. Lett.* **2015**, *17*, 3000–3003.
[158] S. H. Jungbauer, S. M. Walter, S. Schindler, L. Rout, F. Kniep, S. M. Huber, *Chem. Commun.* **2014**, *50*, 6281–6284.
[159] Y. Takeda, D. Hisakuni, C.-H. Lin, S. Minakata, *Org. Lett.* **2015**, *17*, 318–321.
[160] J.-P. Gliese, S. H. Jungbauer, S. M. Huber, *Chem. Commun.* **2017**, *53*, 12052–12055.
[161] S. Kuwano, T. Suzuki, M. Yamanaka, R. Tsutsumi, T. Arai, *Angew. Chem. Int. Ed.* **2019**, *58*, 10220–10224.
[162] M. Ahmad, T. Nawaz, I. Hussain, X. Chen, M. Imran, R. Hussain, M. A. Assiri, S. Ali, Z. Wu, *ACS Omega* **2022**, *7*, 28694–28707.
[163] H. Rose, *Ann. Pharm.* **1834**, *11*, 129–139.
[164] J. Liebig, F. Wohler, *Ann. Pharm.* **1834**, *11*, 139–150.
[165] A. Michaelis, G. Schroeter, *Berichte Dtsch. Chem. Ges.* **1894**, *27*, 490–497.
[166] P. Chandrasekaran, J. T. Mague, M. S. Balakrishna, *Eur. J. Inorg. Chem.* **2011**, *2011*, 2264–2272.
[167] D. F. Moser, L. Grocholl, L. Stahl, R. J. Staples, *Dalton Trans.* **2003**, 1402–1410.
[168] R. Keat, in *Inorg. Ring Syst.*, Springer, Berlin, Heidelberg, **1982**, pp. 89–116.
[169] I. Silaghi-Dumitrescu, I. Haiduc, *Phosphorus Sulfur Silicon Relat. Elem.* **1994**, *91*, 21–36.
[170] H. J. Chen, R. C. Haltiwanger, T. G. Hill, M. L. Thompson, D. E. Coons, A. D. Norman, *Inorg. Chem.* **1985**, *24*, 4725–4730.
[171] L. Stahl, *Coord. Chem. Rev.* **2000**, *210*, 203–250.
[172] R. R. Holmes, *J. Am. Chem. Soc.* **1961**, *83*, 1334–1336.
[173] R. R. Holmes, J. A. Forstner, *Inorg. Chem.* **1963**, *2*, 380–384.
[174] K. W. Muir, J. F. Nixon, *J. Chem. Soc. Chem. Commun.* **1971**, 1405–1406.
[175] A. Michaelis, *Justus Liebigs Ann. Chem.* **1903**, *326*, 129–258.
[176] A. Michaelis, *Justus Liebigs Ann. Chem.* **1915**, *407*, 290–332.
[177] M. Green, R. N. Haszeldine, G. S. A. Hopkins, *J. Chem. Soc. Inorg. Phys. Theor.* **1966**, 1766–1769.
[178] R. A. Shaw, E. H. M. Ibrahim, *Angew. Chem. Int. Ed. Engl.* **1967**, *6*, 556–556.
[179] J. D. Healy, R. A. Shaw, M. Woods, *Phosphorus Sulfur Relat. Elem.* **1978**, *5*, 239–243.
[180] H. Klare, J. M. Neudörfl, B. Goldfuss, *Beilstein J. Org. Chem.* **2014**, *10*, 224–236.
[181] R. Keat, L. Manojlović-Muir, K. W. Muir, *Angew. Chem. Int. Ed. Engl.* **1973**, *12*, 311–312.
[182] O. J. Scherer, G. Schnabl, *Chem. Ber.* **1976**, *109*, 2996–3004.
[183] W. Zeiß, C. Feldt, J. Weis, G. Dunkel, *Chem. Ber.* **1978**, *111*, 1180–1194.
[184] R. Keat, D. G. Thompson, *J. Chem. Soc. Dalton Trans.* **1980**, 928–936.
[185] M. S. Balakrishna, V. S. Reddy, S. S. Krishnamurthy, J. F. Nixon, J. C. T. R. B. St. Laurent, *Coord. Chem. Rev.* **1994**, *129*, 1–90.
[186] G. G. Briand, T. Chivers, M. Krahn, *Coord. Chem. Rev.* **2002**, *233–234*, 237–254.
[187] A. Nordheider, T. Chivers, R. Thirumoorthi, I. Vargas-Baca, J. D. Woollins,

Chem. Commun. **2012**, *48*, 6346–6348.
[188] A. Nordheider, K. Hüll, K. S. A. Arachchige, A. M. Z. Slawin, J. D. Woollins, R. Thirumoorthi, T. Chivers, *Dalton Trans.* **2015**, *44*, 5338–5346.
[189] M. S. Balakrishna, *Dalton Trans.* **2016**, *45*, 12252–12282.
[190] A. J. Plajer, R. García-Rodríguez, C. G. M. Benson, P. D. Matthews, A. D. Bond, S. Singh, L. H. Gade, D. S. Wright, *Angew. Chem. Int. Ed.* **2017**, *56*, 9087–9090.
[191] L. Grocholl, L. Stahl, R. J. Staples, *Chem. Commun.* **1997**, 1465–1466.
[192] M. S. Balakrishna, D. J. Eisler, T. Chivers, *Chem. Soc. Rev.* **2007**, *36*, 650–664.
[193] A. Nordheider, A. M. Z. Slawin, J. D. Woollins, T. Chivers, *Z. Für Anorg. Allg. Chem.* **2015**, *641*, 405–407.
[194] K. V. Axenov, M. Klinga, M. Leskelä, V. Kotov, T. Repo, *Eur. J. Inorg. Chem.* **2004**, *2004*, 4702–4709.
[195] K. V. Axenov, V. V. Kotov, M. Klinga, M. Leskelä, T. Repo, *Eur. J. Inorg. Chem.* **2004**, *2004*, 695–706.
[196] K. V. Axenov, M. Klinga, M. Leskelä, T. Repo, *Organometallics* **2005**, *24*, 1336–1343.
[197] K. V. Axenov, M. Leskelä, T. Repo, *J. Catal.* **2006**, *238*, 196–205.
[198] M. S. Balakrishna, D. Suresh, J. T. Mague, *Inorganica Chim. Acta* **2011**, *372*, 259–265.
[199] T. Roth, H. Wadepohl, D. S. Wright, L. H. Gade, *Chem. – Eur. J.* **2013**, *19*, 13823–13837.
[200] H. Klare, S. Hanft, J. M. Neudörfl, N. E. Schlörer, A. Griesbeck, B. Goldfuss, *Chem. – Eur. J.* **2014**, *20*, 11847–11855.
[201] F. F. Wolf, J.-M. Neudörfl, B. Goldfuss, *New J. Chem.* **2018**, *42*, 4854–4870.
[202] T. Komnenos, *Justus Liebigs Ann. Chem.* **1883**, *218*, 145–167.
[203] A. Michael, *J. Für Prakt. Chem.* **1887**, *35*, 349–356.
[204] B. D. Mather, K. Viswanathan, K. M. Miller, T. E. Long, *Prog. Polym. Sci.* **2006**, *31*, 487–531.
[205] K. Zheng, X. Liu, X. Feng, *Chem. Rev.* **2018**, *118*, 7586–7656.
[206] Y. Zhang, W. Wang, *Catal. Sci. Technol.* **2011**, *2*, 42–53.
[207] S. D. Pasuparthy, B. Maiti, *ChemistrySelect* **2022**, *7*, e202104261.
[208] J. Clayden, N. Greeves, S. Warren, *Organic Chemistry*, OUP Oxford, **2012**.
[209] J. H. Sinfelt, in *Adv. Chem. Eng.* (Eds.: T.B. Drew, J.W. Hoopes, T. Vermeulen, G.R. Cokelet), Academic Press, **1964**, pp. 37–74.
[210] O. V. Serdyuk, C. M. Heckel, S. B. Tsogoeva, *Org. Biomol. Chem.* **2013**, *11*, 7051–7071.
[211] A. Hamza, G. Schubert, T. Soós, I. Pápai, *J. Am. Chem. Soc.* **2006**, *128*, 13151–13160.
[212] J.-L. Zhu, Y. Zhang, C. Liu, A.-M. Zheng, W. Wang, *J. Org. Chem.* **2012**, *77*, 9813–9825.
[213] B. Kótai, G. Kardos, A. Hamza, V. Farkas, I. Pápai, T. Soós, *Chem. – Eur. J.* **2014**, *20*, 5631–5639.
[214] C.-L. Cao, M.-C. Ye, X.-L. Sun, Y. Tang, *Org. Lett.* **2006**, *8*, 2901–2904.
[215] P. Vinayagam, M. Vishwanath, V. Kesavan, *Tetrahedron Asymmetry* **2014**, *25*, 568–577.

[216] H. Jin, S. T. Kim, G.-S. Hwang, D. H. Ryu, *J. Org. Chem.* **2016**, *81*, 3263–3274.
[217] H. Jin, S. M. Cho, G.-S. Hwang, D. H. Ryu, *Adv. Synth. Catal.* **2017**, *359*, 163–167.
[218] J. Vargas-Caporali, C. Cruz-Hernández, E. Juaristi, *Heterocycles* **2012**, *86*, 1275–1300.
[219] H. Jin, S. M. Cho, J. Lee, D. H. Ryu, *Org. Lett.* **2017**, *19*, 2434–2437.
[220] O. Mitsunobu, M. Yamada, *Bull. Chem. Soc. Jpn.* **1967**, *40*, 2380–2382.
[221] B. Lal, B. N. Pramanik, M. S. Manhas, A. K. Bose, *Tetrahedron Lett.* **1977**, *18*, 1977–1980.
[222] N. Yamagiwa, S. Watanuki, T. Nishina, Y. Suto, G. Iwasaki, *Chem. Lett.* **2016**, *45*, 54–56.
[223] D. L. Hughes, *Org. Prep. Proced. Int.* **1996**, *28*, 127–164.
[224] A. Dondoni, B. Richichi, A. Marra, D. Perrone, *Synlett* **2004**, *2004*, 1711–1714.
[225] A. Cochi, B. Burger, C. Navarro, D. G. Pardo, J. Cossy, Y. Zhao, T. Cohen, *Synlett* **2009**, *2009*, 2157–2161.
[226] R. C. Fuson, C. L. Zirkle, *J. Am. Chem. Soc.* **1948**, *70*, 2760–2762.
[227] S. Rioton, A. Orliac, Z. Antoun, R. Bidault, D. Gomez Pardo, J. Cossy, *Org. Lett.* **2015**, *17*, 2916–2919.
[228] W. R. Zheng, J. L. Xu, T. Huang, Q. Yang, Z. C. Chen, *Res. Chem. Intermed.* **2011**, *37*, 31–45.
[229] H. Klare, J. M. Neudörfl, B. Goldfuss, *Beilstein J. Org. Chem.* **2014**, *10*, 224–236.
[230] O. M. Berner, L. Tedeschi, D. Enders, *Eur. J. Org. Chem.* **2002**, *2002*, 1877–1894.
[231] G. Suez, V. Bloch, G. Nisnevich, M. Gandelman, *Eur. J. Org. Chem.* **2012**, *2012*, 2118–2122.
[232] H. Klare, Entwicklung Phosphorbasierter Umpolungs- und Wasserstoffbrücken-Katalysatoren, Doctoral dissertation, University of Cologne, **2015**.
[233] V. K. Yadav, K. G. Babu, *Eur. J. Org. Chem.* **2005**, *2005*, 452–456.
[234] A. Bashall, E. L. Doyle, C. Tubb, S. J. Kidd, M. McPartlin, A. D. Woods, D. S. Wright, *Chem. Commun.* **2001**, 2542–2543.
[235] R. Jefferson, J. F. Nixon, T. M. Painter, R. Keat, L. Stobbs, *J. Chem. Soc. Dalton Trans.* **1973**, 1414–1419.
[236] N. Burford, T. S. Cameron, K. D. Conroy, B. Ellis, C. L. Macdonald, R. Ovans, A. D. Phillips, P. J. Ragogna, D. Walsh, *Can. J. Chem.* **2002**, *80*, 1404–1409.
[237] M. Piccart, M. Rozencweig, R. Abele, E. Cumps, P. Dodion, D. Dupont, D. Kisner, Y. Kenis, *Eur. J. Cancer Clin. Oncol.* **1981**, *17*, 775–779.
[238] J. William Lown, *Pharmacol. Ther.* **1993**, *60*, 185–214.
[239] L. J. Scott, D. P. Figgitt, *CNS Drugs* **2004**, *18*, 379–396.
[240] A. D. Patil, A. J. Freyer, D. S. Eggleston, R. C. Haltiwanger, M. F. Bean, P. B. Taylor, M. J. Caranfa, A. L. Breen, H. R. Bartus, *J. Med. Chem.* **1993**, *36*, 4131–4138.
[241] E. B. B. Ong, N. Watanabe, A. Saito, Y. Futamura, K. H. Abd El Galil, A. Koito, N. Najimudin, H. Osada, *J. Biol. Chem.* **2011**, *286*, 14049–14056.
[242] L. Verotta, E. Lovaglio, G. Vidari, P. V. Finzi, M. G. Neri, A. Raimondi, S.

Parapini, D. Taramelli, A. Riva, E. Bombardelli, *Phytochemistry* **2004**, *65*, 2867–2879.
[243] R. Argotte-Ramos, G. Ramírez-Avila, M. del C. Rodríguez-Gutiérrez, M. Ovilla-Muñoz, H. Lanz-Mendoza, M. H. Rodríguez, M. González-Cortazar, L. Alvarez, *J. Nat. Prod.* **2006**, *69*, 1442–1444.
[244] R. A. O'Reilly, *N. Engl. J. Med.* **1976**, *295*, 354–357.
[245] F. F. Wolf, H. Klare, B. Goldfuss, *J. Org. Chem.* **2016**, *81*, 1762–1768.
[246] E. Dündar, C. Tanyeli, *Tetrahedron Lett.* **2021**, *73*, 153153.
[247] P. M. Nowak, F. Sagan, M. P. Mitoraj, *J. Phys. Chem. B* **2017**, *121*, 4554–4561.
[248] R. C. da Silva, G. P. da Silva, D. P. Sangi, J. G. de M. Pontes, A. G. Ferreira, A. G. Corrêa, M. W. Paixão, *Tetrahedron* **2013**, *69*, 9007–9012.
[249] A. Quintavalla, F. Lanza, E. Montroni, M. Lombardo, C. Trombini, *J. Org. Chem.* **2013**, *78*, 12049–12064.
[250] M. Yamato, K. Hashigaki, Y. Yasumoto, J. Sakai, R. F. Luduena, A. Banerjee, S. Tsukagoshi, T. Tashiro, T. Tsuruo, *J. Med. Chem.* **1987**, *30*, 1897–1900.
[251] J. Alverson, *J. Invertebr. Pathol.* **2003**, *83*, 60–62.
[252] Y. Higa, M. Kawabe, K. Nabae, Y. Toda, S. Kitamoto, T. Hara, N. Tanaka, K. Kariya, M. Takahashi, *J. Toxicol. Sci.* **2007**, *32*, 143–159.
[253] A. Fassihi, D. Abedi, L. Saghaie, R. Sabet, H. Fazeli, G. Bostaki, O. Deilami, H. Sadinpour, *Eur. J. Med. Chem.* **2009**, *44*, 2145–2157.
[254] A. S. Kucherenko, A. A. Kostenko, A. N. Komogortsev, B. V. Lichitsky, M. Yu. Fedotov, S. G. Zlotin, *J. Org. Chem.* **2019**, *84*, 4304–4311.
[255] C. V. Credille, B. L. Dick, C. N. Morrison, R. W. Stokes, R. N. Adamek, N. C. Wu, I. A. Wilson, S. M. Cohen, *J. Med. Chem.* **2018**, *61*, 10206–10217.
[256] J. Jacques, A. Collet, S. H. Wilen, *Enantiomers, Racemates, and Resolutions*, Wiley, New York, **1981**.
[257] H. McNab, *Chem. Soc. Rev.* **1978**, *7*, 345–358.
[258] O. Bassas, J. Huuskonen, K. Rissanen, A. M. P. Koskinen, *Eur. J. Org. Chem.* **2009**, *2009*, 1340–1351.
[259] J. Bejjani, F. Chemla, M. Audouin, *J. Org. Chem.* **2003**, *68*, 9747–9752.
[260] D. J. Foley, R. G. Doveston, I. Churcher, A. Nelson, S. P. Marsden, *Chem. Commun.* **2015**, *51*, 11174–11177.
[259] Y. Zhao, Progessing of the DIBAL Adduct if a Proline-Derived Ester to Generate a Single Diastereomer of an Allyl Alcohol for Use in a Novel Synthetic Method for Pyrrolizidines, Master thesis, University of Pittsburgh, **2006**.
[262] X. Jiang, C. K. Tan, L. Zhou, Y.-Y. Yeung, *Angew. Chem. Int. Ed.* **2012**, *51*, 7771–7775.
[263] J. Cossy, C. Dumas, D. G. Pardo, *Eur. J. Org. Chem.* **1999**, *1999*, 1693–1699.
[259] E. A. Braude, F. C. Nachod, *Determination of Organic Structures by Physical Methods*, Academic Press, **1955**.
[265] H. K. Jr. Hall, *J. Am. Chem. Soc.* **1957**, *79*, 5441–5444.
[266] E. Chinnaraja, R. Arunachalam, K. Samanta, R. Natarajan, P. S. Subramanian, *Adv. Synth. Catal.* **2020**, *362*, 1144–1155.
[267] B. V. S. Reddy, S. M. Reddy, M. Swain, *RSC Adv.* **2012**, *3*, 930–936.
[268] L. N. Gautam, Y. Su, N. G. Akhmedov, J. L. Petersen, X. Shi, *Org. Biomol.*

Chem. **2014**, *12*, 6384–6388.
[269] V. A. Jones, S. Sriprang, M. Thornton-Pett, T. P. Kee, *J. Organomet. Chem.* **1998**, *567*, 199–218.
[270] N. R. Amarasinghe, P. Turner, M. H. Todd, *Adv. Synth. Catal.* **2012**, *354*, 2954–2958.
[271] A. Arizpe, F. J. Sayago, A. I. Jiménez, M. Ordóñez, C. Cativiela, *Eur. J. Org. Chem.* **2011**, *2011*, 3074–3081.
[272] W.-M. Zhou, H. Liu, D.-M. Du, *Org. Lett.* **2008**, *10*, 2817–2820.
[273] A. S. Kucherenko, A. A. Kostenko, A. N. Komogortsev, B. V. Lichitsky, M. Yu. Fedotov, S. G. Zlotin, *J. Org. Chem.* **2019**, *84*, 4304–4311.
[274] J. C. Anderson, A. S. Kalogirou, G. J. Tizzard, *Tetrahedron* **2014**, *70*, 9337–9351.

7 Appendix

7. 1 Abbreviations

Ac	acetyl
ACDC	Asymmetric Counteranion−Directed Catalysis
AIBN	azobisisobutyronitrile
aq	aqueous
Ar	argon
BINAP	2,2′-bis(diphenylphosphino)-1,1′-binaphthyl
BINOL	1,1′-Bi-2-naphthol
Bn	benzyl
Boc	*tert*-butoxycarbonyl
BuLi	butyllithium
calc.	calculated
Cat.	catalyst
CF_3	trifluoromethyl
CH_3	methyl
conc.	concentrated
DEAD	diethyl azodicarboxylate
DFT	density functional theory
DIAD	diisopropyl azodicarboxylate
Dipp	diisopropylphenyl
DMF	dimethylformamid
DMSO	dimethyl sulfoxide
DPPA	diphenylphosphoryl azide
ee	enantiomeric excess
eq.	equivalent
Et	ethyl
EWGs	electron withdrawing groups
h	hour(s)
H−bond(ing)	hydrogen bond(ing)
HOMO	highest occupied molecular orbital
LUMO	lowest unoccupied molecular orbital
MAO	methylaluminoxane
Me	methyl
min	minute(s)
MTBE	methyl *tert*-butyl ether
NMR	nuclear magnetic resonance
Nu	nucleophile

OH	hydroxy
Ph	phenyl
rac	racemic
RT	room temperature
t-Bu	*tert*-butyl
TFA	trifluoroacetic acid
TFAA	trifluoroacetic anhydride
THF	tetrahydrofuran
TLC	thin layer chromatography
TMSCN	trimethylsilyl cyanide
Tr	trityl
vs.	versus
XB	halogen bond

7.2 X−ray structure data

7.2.1 *cis*-2,4-dichloro-1,3-bis(2,6-diisopropylphenyl)-1,3,2,4-diazadiphosphetidine

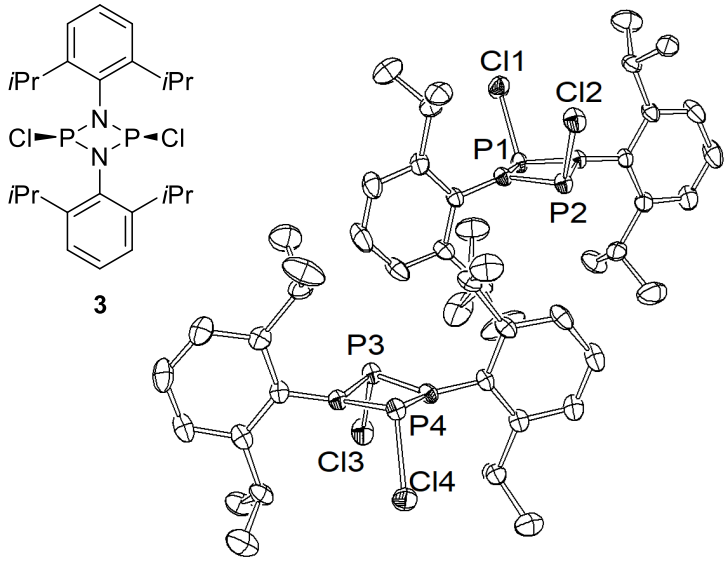

Table 7.2.1: Crystal data and structure refinement for **3**.

Empirical formula	C24 H34 Cl2 N2 P2	
Moiety formula	C24 H34 Cl2 N2 P2	
Formula weight	483.37	
Temperature	100(2) K	
Wavelength	1.54178 Å	
Crystal system	Monoclinic	
Space group	$P2_1/c$	
Unit cell dimensions	a = 25.3806(13) Å	a= 90°.
	b = 9.7883(5) Å	b= 116.547(2)°.
	c = 23.5644(12) Å	g = 90°.
Volume	5237.0(5) $Å^3$	
Z	8	
Density (calculated)	1.226 Mg/m^3	
Absorption coefficient	3.478 mm^{-1}	
F(000)	2048	
Crystal size	0.100 x 0.070 x 0.050 mm^3	
Theta range for data collection	1.946 to 72.591°.	

Index ranges	-31<=h<=31, -12<=k<=12, -29<=l<=29
Reflections collected	141812
Independent reflections	9893 [R(int) = 0.2247]
Completeness to theta = 67.679°	95.8 %
Absorption correction	Semi-empirical from equivalents
Max. and min. transmission	0.7437 and 0.5718
Refinement method	Full-matrix least-squares on F^2
Data / restraints / parameters	9893 / 0 / 557
Goodness-of-fit on F^2	1.044
Final R indices [I>2sigma(I)]	R1 = 0.0541, wR2 = 0.1218
R indices (all data)	R1 = 0.0756, wR2 = 0.1283
Extinction coefficient	n/a
Largest diff. peak and hole	1.318 and -0.556 e.$Å^{-3}$

7.2.2 1,3-di-*tert*-butyl-2,4-bis(((1*R*,2*R*)-2-(dimethylamino)cyclohexyl)amino)-1,3,2,4-diazadiphosphetidine 2,4-dioxide

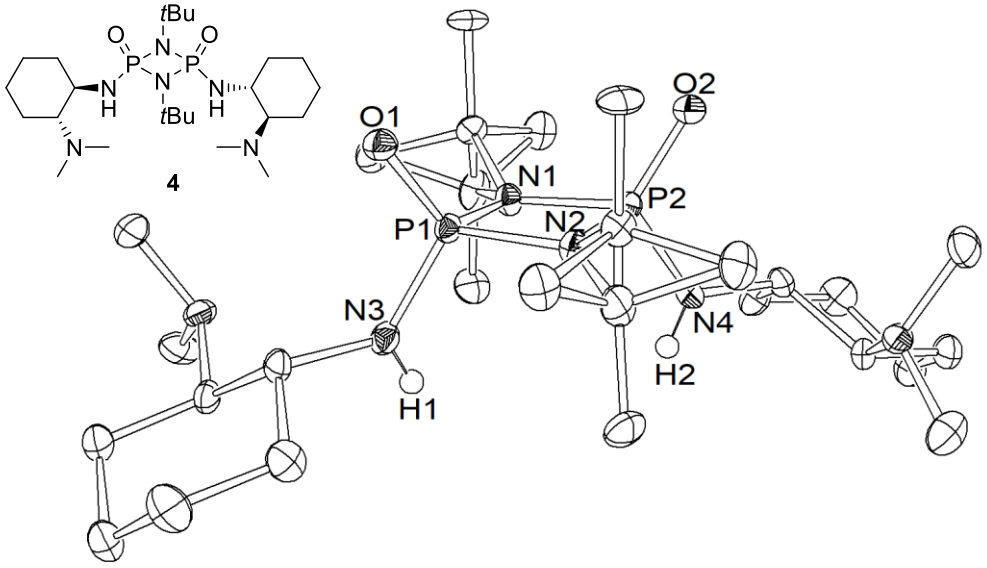

Table 7.2.2: Crystal data and structure refinement for **4**.

Empirical formula	C24 H52 N6 O2 P2

Moiety formula	C24 H52 N6 O2 P2	
Formula weight	518.65	
Temperature	100(2) K	
Wavelength	1.54178 Å	
Crystal system	Orthorhombic	
Space group	$P2_12_12$	
Unit cell dimensions	a = 11.0312(5) Å	a= 90°.
	b = 22.8278(10) Å	b= 90°.
	c = 5.6953(3) Å	g = 90°.
Volume	1434.18(12) $Å^3$	
Z	2	
Density (calculated)	1.201 Mg/m^3	
Absorption coefficient	1.617 mm^{-1}	
F(000)	568	
Crystal size	0.100 x 0.070 x 0.030 mm^3	
Theta range for data collection	3.873 to 72.012°.	
Index ranges	-12<=h<=13, -28<=k<=28, -6<=l<=7	
Reflections collected	11769	
Independent reflections	2736 [R(int) = 0.0486]	
Completeness to theta = 67.679°	97.5 %	
Absorption correction	Semi-empirical from equivalents	
Max. and min. transmission	0.7536 and 0.5571	
Refinement method	Full-matrix least-squares on F^2	
Data / restraints / parameters	2736 / 0 / 180	
Goodness-of-fit on F^2	1.238	
Final R indices [I>2sigma(I)]	R1 = 0.0588, wR2 = 0.1512	
R indices (all data)	R1 = 0.0593, wR2 = 0.1514	
Absolute structure parameter	0.190(11)	
Extinction coefficient	n/a	
Largest diff. peak and hole	0.452 and -0.525 $e.Å^{-3}$	

7.2.3 1,3-di-*tert*-butyl-2-(((1*R*,2*R*)-2-(dimethylamino)cyclohexyl)amino)-4-(phenylamino)-1,3,2,4-diazadiphosphetidine 2,4-dioxide

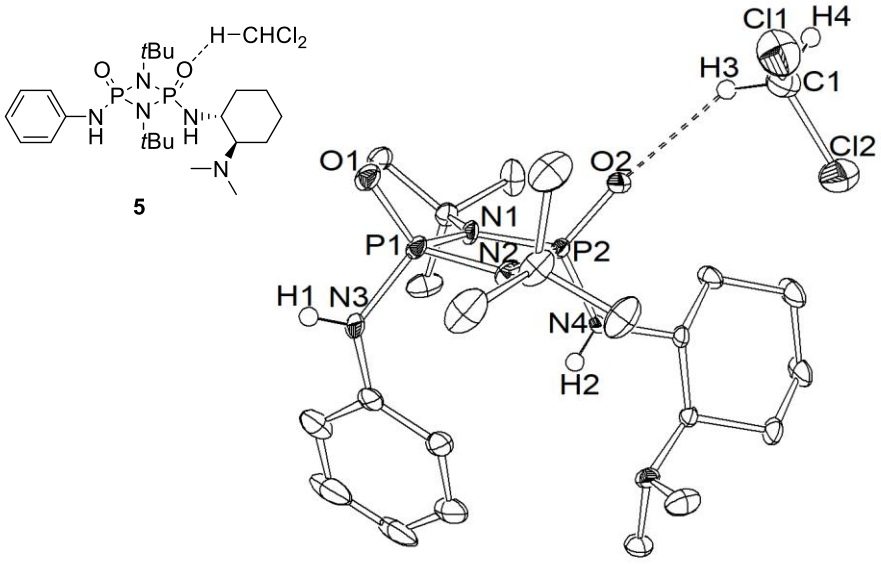

Table 7.2.3: Crystal data and structure refinement for **5**.

Empirical formula	C45 H84 Cl2 N10 O4 P4	
Moiety formula	2(C22 H41 N5 O2 P2), C H2 Cl2	
Formula weight	1024.00	
Temperature	100(2) K	
Wavelength	1.54178 Å	
Crystal system	Monoclinic	
Space group	C2	
Unit cell dimensions	a = 16.6986(4) Å	a= 90°.
	b = 9.7579(2) Å	b= 99.6310(10)°.
	c = 17.0133(4) Å	g = 90°.
Volume	2733.13(11) $Å^3$	
Z	2	
Density (calculated)	1.244 Mg/m^3	
Absorption coefficient	2.565 mm^{-1}	
F(000)	1100	
Crystal size	0.100 x 0.070 x 0.050 mm^3	
Theta range for data collection	5.274 to 68.337°.	
Index ranges	-20<=h<=20, -11<=k<=11, -20<=l<=20	
Reflections collected	17286	

Independent reflections	4937 [R(int) = 0.0385]
Completeness to theta = 67.679°	99.9 %
Absorption correction	Semi-empirical from equivalents
Max. and min. transmission	0.7531 and 0.5555
Refinement method	Full-matrix least-squares on F^2
Data / restraints / parameters	4937 / 1 / 310
Goodness-of-fit on F^2	1.045
Final R indices [I>2sigma(I)]	R1 = 0.0261, wR2 = 0.0645
R indices (all data)	R1 = 0.0272, wR2 = 0.0651
Absolute structure parameter	0.039(6)
Extinction coefficient	n/a
Largest diff. peak and hole	0.205 and -0.293 e.Å^{-3}

7.2.4 2-((3,5-bis(trifluoromethyl)phenyl)amino)-1,3-di-*tert*-butyl-4-(((1*R*,2*R*)-2-(dimethylamino)cyclohexyl)amino)-1,3,2,4-diazadiphosphetidine 2,4-dioxide

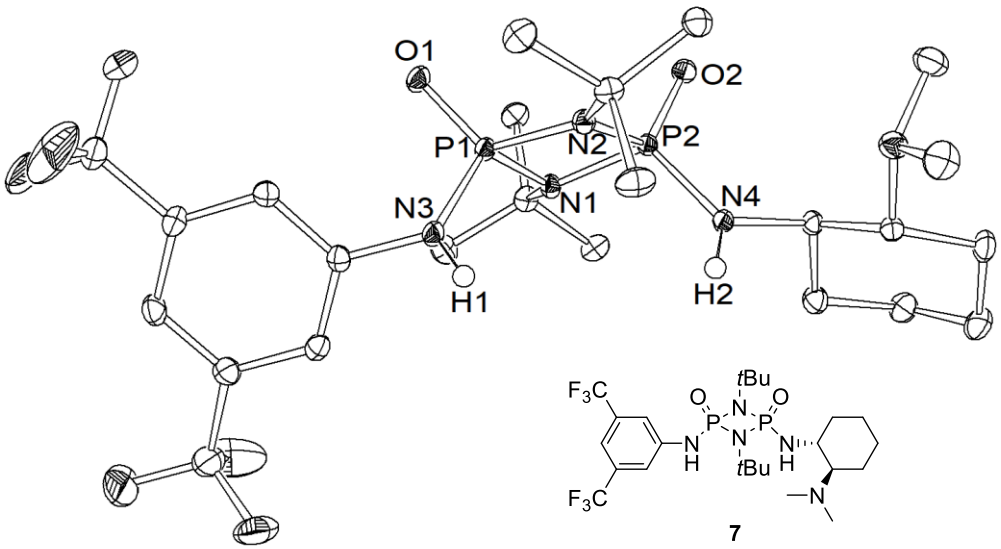

Table 7.2.4: Crystal data and structure refinement for **7**.

Empirical formula	C24 H39 F6 N5 O2 P2
Moiety formula	C24 H39 F6 N5 O2 P2

Formula weight	605.54	
Temperature	100(2) K	
Wavelength	1.54178 Å	
Crystal system	Orthorhombic	
Space group	$P2_12_12_1$	
Unit cell dimensions	a = 5.62290(10) Å	a= 90°.
	b = 22.0708(5) Å	b= 90°.
	c = 23.1679(5) Å	g = 90°.
Volume	2875.18(10) $Å^3$	
Z	4	
Density (calculated)	1.399 Mg/m^3	
Absorption coefficient	2.004 mm^{-1}	
F(000)	1272	
Crystal size	0.100 x 0.070 x 0.050 mm^3	
Theta range for data collection	2.765 to 72.140°.	
Index ranges	-6<=h<=6, -27<=k<=27, -28<=l<=28	
Reflections collected	150525	
Independent reflections	5639 [R(int) = 0.0587]	
Completeness to theta = 67.679°	100.0 %	
Absorption correction	Semi-empirical from equivalents	
Max. and min. transmission	0.7536 and 0.5903	
Refinement method	Full-matrix least-squares on F^2	
Data / restraints / parameters	5639 / 0 / 369	
Goodness-of-fit on F^2	1.054	
Final R indices [I>2sigma(I)]	R1 = 0.0251, wR2 = 0.0644	
R indices (all data)	R1 = 0.0256, wR2 = 0.0646	
Absolute structure parameter	0.036(3)	
Extinction coefficient	n/a	
Largest diff. peak and hole	0.357 and -0.367 e.$Å^{-3}$	

7.2.5 1,3-di-*tert*-butyl-2-(((1*R*,2*R*)-2-(dimethylamino)cyclohexyl)amino)-4-((3,5-dimethylphenyl)amino)-1,3,2,4-diazadiphosphetidine 2,4-disulfide

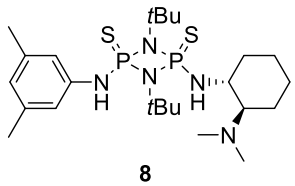

8

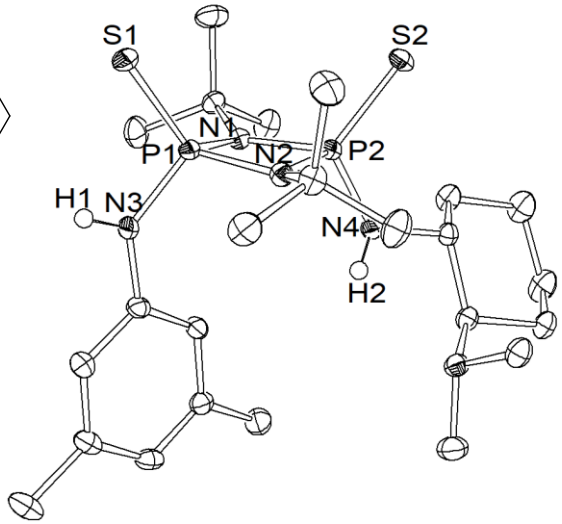

Table 7.2.5: Crystal data and structure refinement for **8**.

Empirical formula	C24 H45 N5 P2 S2	
Moiety formula	C24 H45 N5 P2 S2	
Formula weight	529.71	
Temperature	100(2) K	
Wavelength	1.54178 Å	
Crystal system	Orthorhombic	
Space group	$P2_12_12_1$	
Unit cell dimensions	a = 11.2095(8) Å	a= 90°.
	b = 15.4530(10) Å	b= 90°.
	c = 16.8670(11) Å	g = 90°.
Volume	2921.7(3) $Å^3$	
Z	4	
Density (calculated)	1.204 Mg/m^3	
Absorption coefficient	2.841 mm^{-1}	
F(000)	1144	
Crystal size	0.100 x 0.100 x 0.030 mm^3	
Theta range for data collection	3.879 to 72.496°.	
Index ranges	-13<=h<=13, -19<=k<=19, -20<=l<=20	

Reflections collected	83400
Independent reflections	5776 [R(int) = 0.0517]
Completeness to theta = 67.679°	100.0 %
Absorption correction	Semi-empirical from equivalents
Max. and min. transmission	0.7536 and 0.6105
Refinement method	Full-matrix least-squares on F^2
Data / restraints / parameters	5776 / 0 / 316
Goodness-of-fit on F^2	1.036
Final R indices [I>2sigma(I)]	R1 = 0.0205, wR2 = 0.0544
R indices (all data)	R1 = 0.0208, wR2 = 0.0545
Absolute structure parameter	0.011(4)
Extinction coefficient	n/a
Largest diff. peak and hole	0.228 and -0.207 e.$Å^{-3}$

7.2.6 1,3-di-*tert*-butyl-2-(((1*R*,2*R*)-2-(dimethylamino)cyclohexyl)amino)-4-((3,5-dimethylphenyl)amino)-1,3,2,4-diazadiphosphetidine 2,4-disulfide

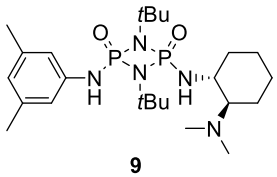

9

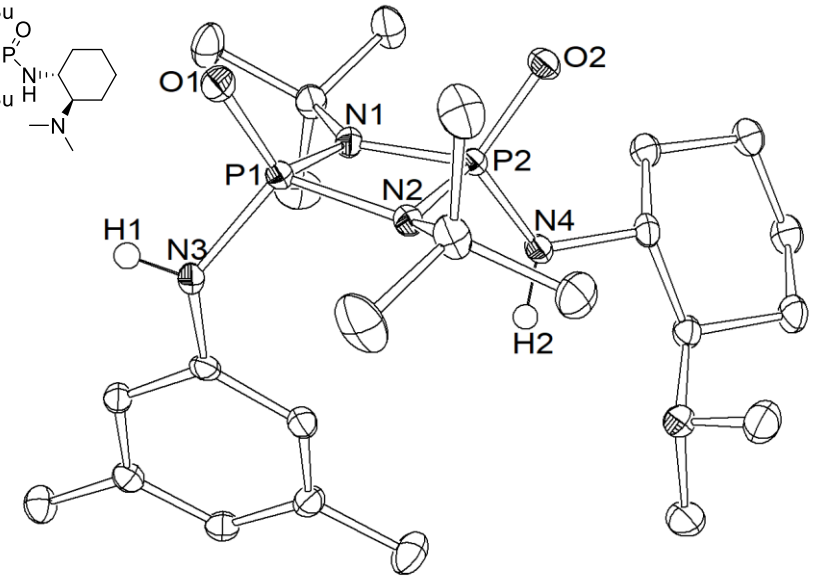

Table 7.2.6: Crystal data and structure refinement for **9**.

Empirical formula	C24 H45 N5 O2 P2	
Moiety formula	C24 H45 N5 O2 P2	
Formula weight	497.59	
Temperature	100(2) K	
Wavelength	1.54178 Å	
Crystal system	Orthorhombic	
Space group	$P2_12_12_1$	
Unit cell dimensions	a = 8.9326(2) Å	a= 90°.
	b = 13.6264(3) Å	b= 90°.
	c = 22.5490(4) Å	g = 90°.
Volume	2744.65(10) $Å^3$	
Z	4	
Density (calculated)	1.204 Mg/m^3	
Absorption coefficient	1.664 mm^{-1}	
F(000)	1080	
Crystal size	0.100 x 0.100 x 0.020 mm^3	
Theta range for data collection	3.790 to 72.146°.	
Index ranges	-11<=h<=11, -16<=k<=16, -27<=l<=27	
Reflections collected	89445	
Independent reflections	5381 [R(int) = 0.0880]	
Completeness to theta = 67.679°	100.0 %	
Absorption correction	Semi-empirical from equivalents	
Max. and min. transmission	0.7536 and 0.6091	
Refinement method	Full-matrix least-squares on F^2	
Data / restraints / parameters	5381 / 0 / 316	
Goodness-of-fit on F^2	1.080	
Final R indices [I>2sigma(I)]	R1 = 0.0258, wR2 = 0.0656	
R indices (all data)	R1 = 0.0272, wR2 = 0.0662	
Absolute structure parameter	0.009(6)	
Extinction coefficient	n/a	
Largest diff. peak and hole	0.195 and -0.267 $e.Å^{-3}$	

7.2.7 (*S*)-2-((*R*)-azido(phenyl)methyl)-1-tritylpyrrolidine

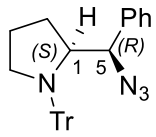

(*S*,*R*)-44

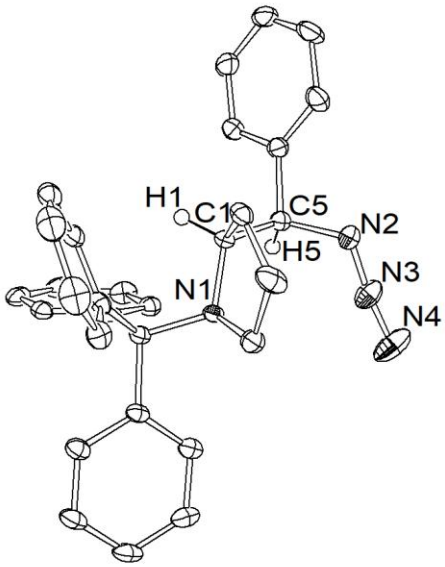

Table 7.2.7: Crystal data and structure refinement for **(*S*,*R*)-44**.

Empirical formula	C30 H28 N4	
Moiety formula	C30 H28 N4	
Formula weight	444.56	
Temperature	100(2) K	
Wavelength	1.54178 Å	
Crystal system	Orthorhombic	
Space group	$P2_12_12_1$	
Unit cell dimensions	a = 11.1159(3) Å	a= 90°.
	b = 13.4012(4) Å	b= 90°.
	c = 16.0151(5) Å	g = 90°.
Volume	2385.71(12) $Å^3$	
Z	4	
Density (calculated)	1.238 Mg/m^3	
Absorption coefficient	0.571 mm^{-1}	
F(000)	944	
Crystal size	0.300 x 0.100 x 0.100 mm^3	
Theta range for data collection	4.302 to 72.170°.	
Index ranges	-10<=h<=13, -16<=k<=14, -19<=l<=18	
Reflections collected	18246	
Independent reflections	4691 [R(int) = 0.0433]	
Completeness to theta = 67.679°	99.9 %	
Absorption correction	Semi-empirical from equivalents	

Max. and min. transmission	0.7536 and 0.6097
Refinement method	Full-matrix least-squares on F^2
Data / restraints / parameters	4691 / 0 / 307
Goodness-of-fit on F^2	1.113
Final R indices [I>2sigma(I)]	R1 = 0.0349, wR2 = 0.0837
R indices (all data)	R1 = 0.0385, wR2 = 0.0863
Absolute structure parameter	-0.07(18)
Extinction coefficient	n/a
Largest diff. peak and hole	0.176 and -0.200 e.$Å^{-3}$

7.3 Chiral HPLC spectra

7.3.1 (1*R*,2*R*)-cyclohexane-1,2-diamine

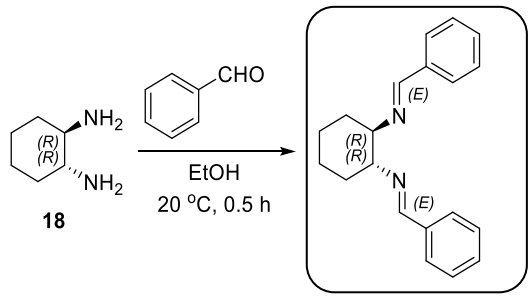

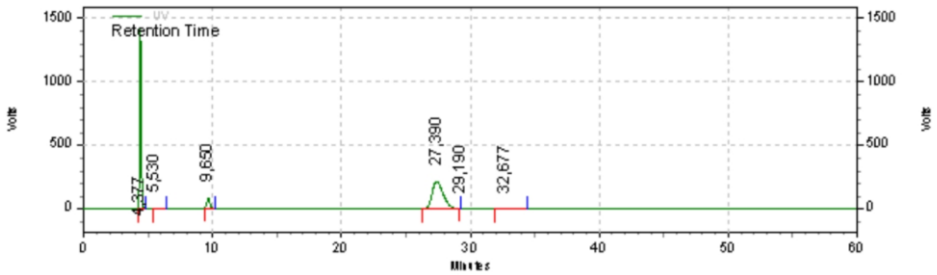

UV Results

Retention Time	Area	Area %	Height	Height %
4,377	51143523	46,49	5651440	82,39
5,530	124164	0,11	10970	0,16
9,650	6272870	5,70	337683	4,92
27,390	52438162	47,67	857368	12,50
29,190	4	0,00	0	0,00
32,677	10123	0,01	123	0,00
60,003	20013	0,02	1588	0,02
Totals	110008859	100,00	6859172	100,00

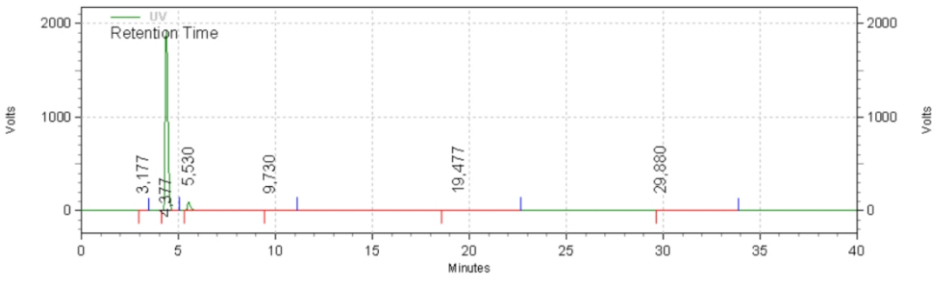

UV Results

Retention Time	Area	Area %	Height	Height %
3,177	58566	0,07	6410	0,08
4,377	73975362	92,45	7704665	95,49
5,530	5784048	7,23	350629	4,35
9,730	127562	0,16	6341	0,08
19,477	58507	0,07	822	0,01
29,880	16006	0,02	92	0,00
Totals	80020051	100,00	8068959	100,00

7.3.2 (*S*)-2-hydroxy-3-(2-nitro-1-phenylethyl)naphthalene-1,4-dione

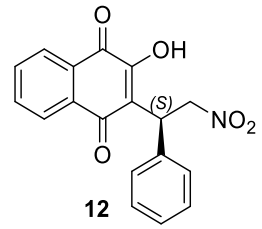

12

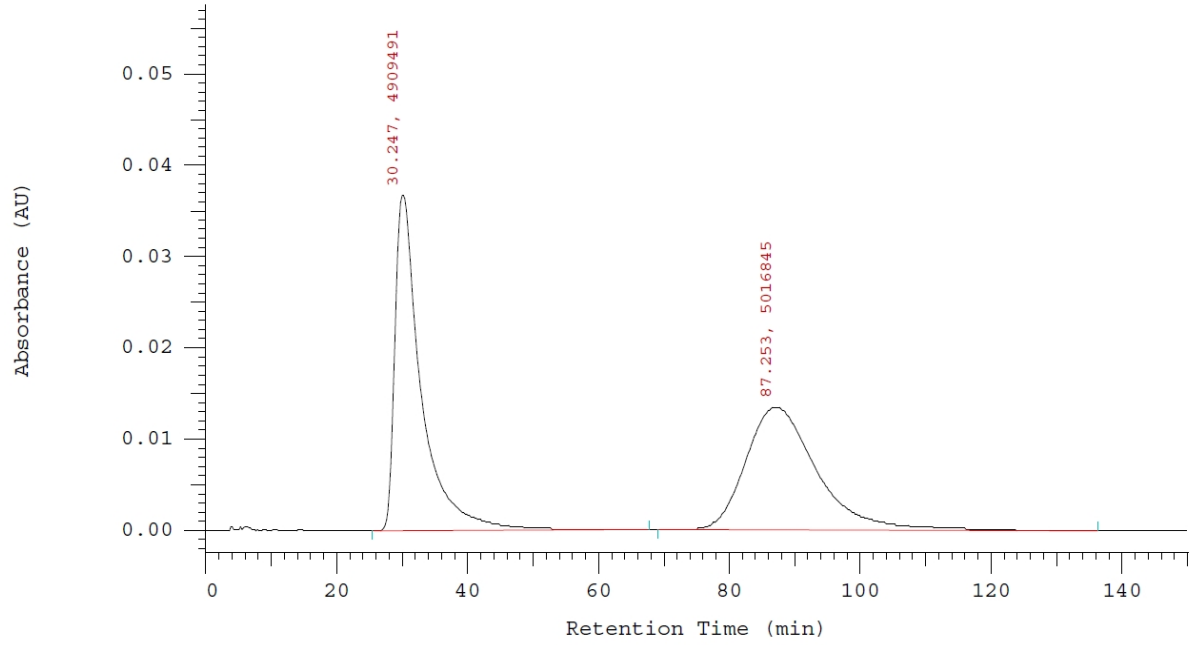

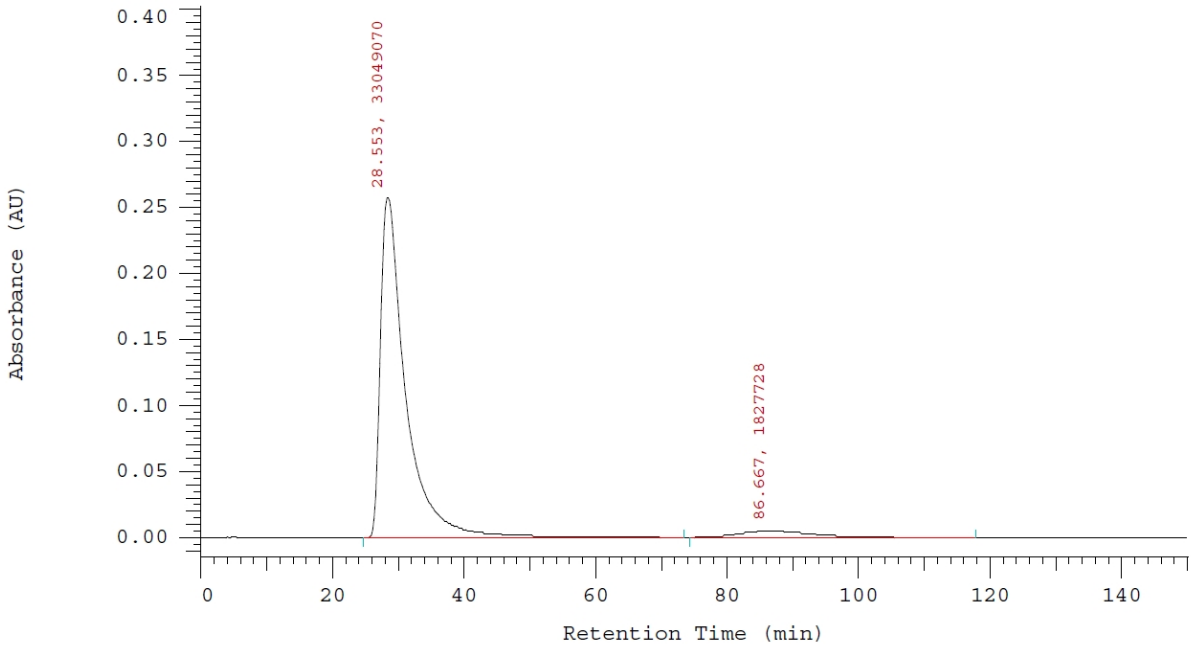

7.3.3 (*S*)-4-hydroxy-3-(2-nitro-1-phenylethyl)-2H-chromen-2-one

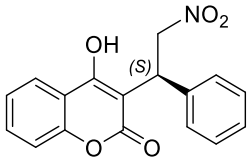

28

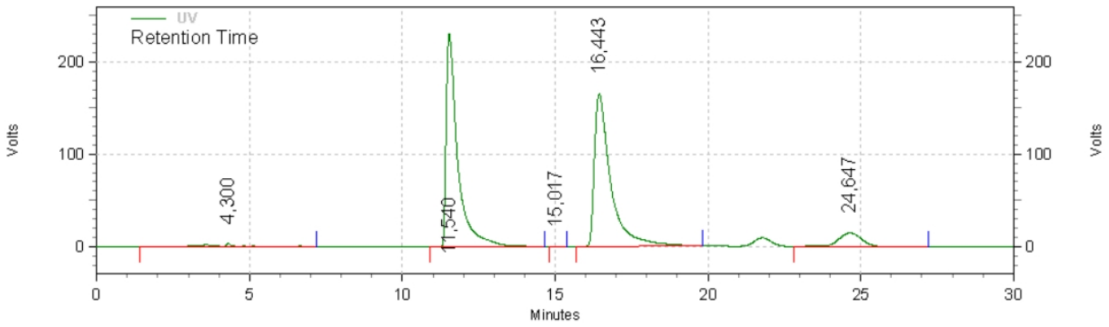

UV Results

Retention Time	Area	Area %	Height	Height %
4,300	827193	1,55	17068	1,03
11,540	24440926	45,82	921790	55,48
15,017	16618	0,03	954	0,06
16,443	24668138	46,24	661117	39,79
24,647	3392290	6,36	60423	3,64

Totals	53345165	100,00	1661352	100,00

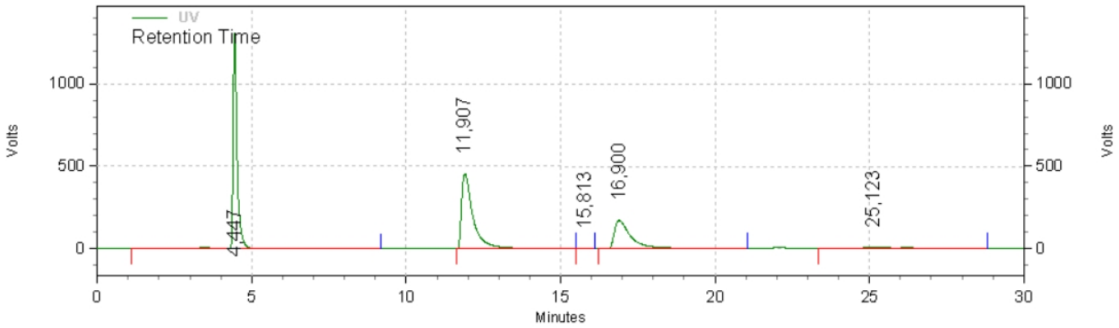

UV Results

Retention Time	Area	Area %	Height	Height %
4,447	48197000	38,08	5212014	67,11
11,907	47730608	37,72	1816041	23,38
15,813	12446	0,01	601	0,01
16,900	26568960	20,99	689557	8,88
25,123	4046603	3,20	47693	0,61

Totals	126555617	100,00	7765906	100,00

7.3.4 (*S*)-6-(chloromethyl)-3-hydroxy-2-(2-nitro-1-phenylethyl)-4H-pyran-4-one

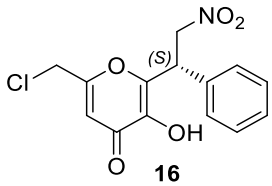

16

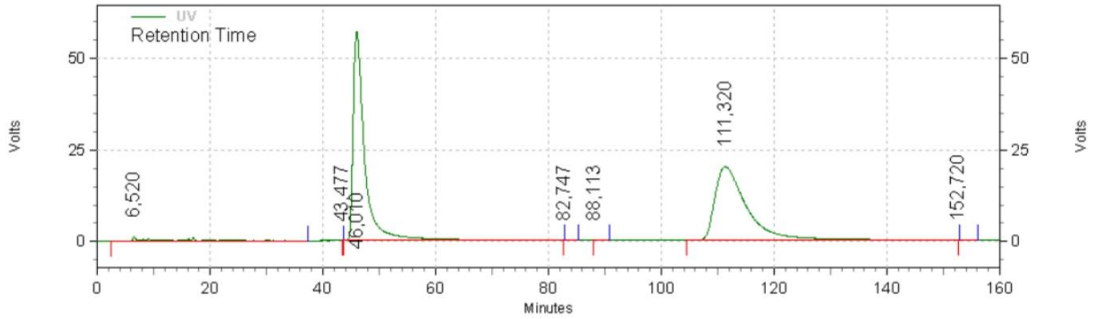

UV Results

Retention Time	Area	Area %	Height	Height %
6,520	1658650	2,48	5564	1,77
43,477	221	0,00	43	0,01
46,010	32781708	49,09	227803	72,52
82,747	17	0,00	9	0,00
88,113	9509	0,01	88	0,03
111,320	32323453	48,41	80580	25,65
152,720	219	0,00	48	0,02
Totals	66773777	100,00	314135	100,00

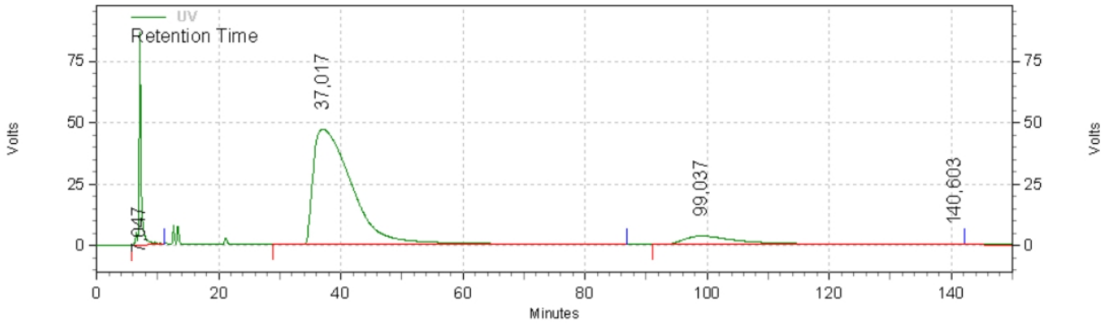

UV Results

Retention Time	Area	Area %	Height	Height %
7,047	8633174	8,52	345334	63,21
37,017	83229140	82,15	187060	34,24
99,037	8994205	8,88	13926	2,55
140,603	453126	0,45	49	0,01
Totals	101309645	100,00	546369	100,00

7.3.5 (*S*)-2,2-dimethyl-5-(2-nitro-1-phenylethyl)-1,3-dioxane-4,6-dione

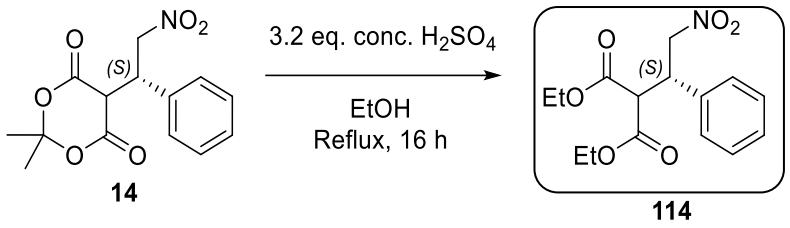

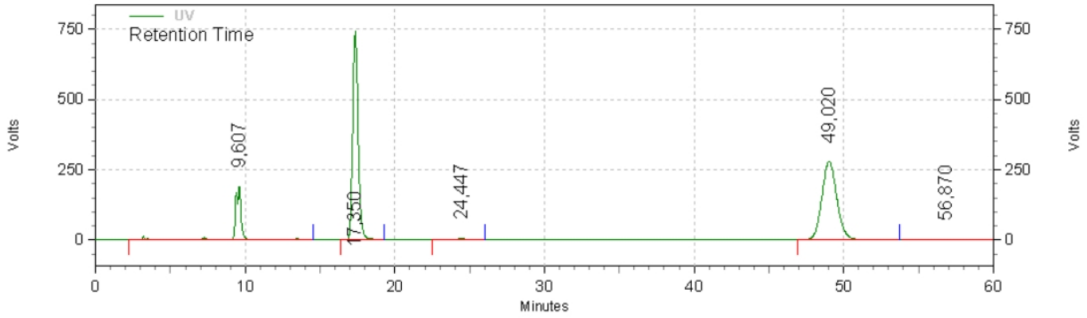

UV Results

Retention Time	Area	Area %	Height	Height %
9,607	20310733	11,70	751934	15,51
17,350	74543831	42,94	2963552	61,13
24,447	782659	0,45	15107	0,31
49,020	76564791	44,10	1112989	22,96
56,870	1395078	0,80	4139	0,09
Totals	173597092	100,00	4847721	100,00

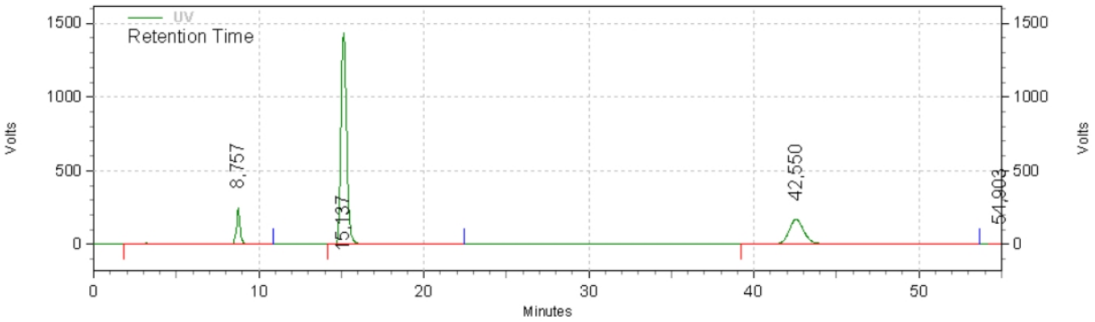

UV Results

Retention Time	Area	Area %	Height	Height %
8,757	16153568	8,27	992569	13,42
15,137	138206225	70,77	5721989	77,39
42,550	40447292	20,71	661269	8,94
54,903	485162	0,25	18068	0,24
Totals	195292247	100,00	7393895	100,00

8 Publication

X.Wang, B. Goldfuss, D. Sartakov, *Synthesis.* **2025**, *57*, 3334–3340.